UNIVERSDIDADE DE SÃO PAULO
INSTITUTO DE BIOCIÊNCIAS
PROGRAMA DE PÓS-GRADUAÇÃO EM CIÊNCIAS BIOLÓGICAS (BOTÂNICA)

Renata Callegari Ferrari

FOTOSSÍNTESE C_4 E METABOLISMO ÁCIDO DAS CRASSULÁCEAS (CAM) EM UMA MESMA FOLHA: ELUCIDANDO OS COMPONENTES, A PLASTICIDADE E A SINALIZAÇÃO POR TRÁS DE UMA RARA ADAPTAÇÃO FOTOSSINTÉTICA

C_4 and crassulacean acid metabolism (CAM) within a single leaf: elucidating the components, plasticity and signaling behind a rare photosynthetic adaptation

São Paulo
2021

Renata Callegari Ferrari

FOTOSSÍNTESE C_4 E METABOLISMO ÁCIDO DAS CRASSULÁCEAS (CAM) EM UMA MESMA FOLHA: ELUCIDANDO OS COMPONENTES, A PLASTICIDADE E A SINALIZAÇÃO POR TRÁS DE UMA RARA ADAPTAÇÃO FOTOSSINTÉTICA

C_4 and crassulacean acid metabolism (CAM) within a single leaf: elucidating the components, plasticity and signaling behind a rare photosynthetic adaptation

Tese apresentada ao Instituto de Biociências da Universidade de São Paulo, para a obtenção de Título de Doutor em Ciências (Área Botânica)

Orientador: Luciano Freschi
Co-orientador: James Hartwell

São Paulo

2021

Ficha Catalográfica

Ferrari, Renata Callegari

Fotossíntese C_4 e metabolismo ácido das crassuláceas (CAM) em uma mesma folha: elucidando os componentes, a plasticidade e a sinalização por trás de uma rara adaptação fotossintética / Renata Callegari Ferrari ; orientador Luciano Freschi ; coorientador James Hartwell -- São Paulo, 2021.
217 p.

Tese (Doutorado) -- Instituto de Biociências da Universidade de São Paulo. Programa de Pós-Graduação em Botânica.

1. estresse hídrico. 2. mecanismos concentradores de carbono. 3. Portulaca oleracea. 4. CAM facultativo. 5. ácido absísico. I. Freschi, Luciano, orient. II. Hartwell, James, coorient. III. Título.

Comissão Julgadora:

Prof(a). Dr(a).

Prof(a). Dr(a).

Prof(a). Dr(a).

Dedico esta tese à minha família e ao meu marido.
Se meu trabalho foi bem sucedido,
foi por conta do apoio e incentivo constantes de vocês.

Agradecimentos

Esta tese é fruto do meu trabalho e dedicação, mas o resultado não teria sido possível sem uma série de pessoas que me ajudaram muito. Portanto, agradeço:

À Fundação de Amparo à Pesquisa do Estado de São Paulo (FAPESP) pelo apoio financeiro recebido na forma de bolsa e reserva técnica (processo n° 2016/04755-4), o que não só possibilitou a execução do meu trabalho como me permitiu participar de conferências e eventos científicos, engrandecendo minha formação como pesquisadora;

À The Royal Society UK, pelo apoio financeiro fornecido ao meu orientador Dr. Luciano Freschi e co-orientador Dr. James Hartwell, possibilitando a execução de experimentos e cursos no exterior e ampliando minha rede de contatos e experiências no mundo acadêmico;

Ao meu orientador Dr. Luciano Freschi, por ter acreditado que eu era capaz e me incentivado desde o começo. Também pelo estoque de paciência e bom humor infinitos, por estar sempre presente, pela orientação riquíssima e pelas oportunidades valiosas que me proporcionou. Sua dedicação, ética, profissionalismo e genialidade foram inspiradores para minha carreira;

I would like to thank Dr. James Hartwell, along with colleagues and technicians from the University of Liverpool, but most importantly Dr. Susanna Boxall, Dr. Louisa Denver and Nirja Kadu, for welcoming me in their lab and providing amazing guidance and support. This was an invaluable opportunity and contributed massively to my development as a scientist;

A todos os colegas de laboratório que me instruíram, ajudaram e proporcionaram uma troca de conhecimentos fundamental para nosso desenvolvimento científico, principalmente Priscila, Grilo, Fred, Perdigão, Filipe, Paulo, Dani, Paula. Destaque especial à Auri, que foi essencial no começo da minha jornada;

Aos técnicos da Fisiologia Vegetal, Ana Maria, Aline Bertinatto e Willian, dentre aqueles que ficaram menos tempo ou são de outros laboratórios (Silvia, Tati e Waldir), pelo trabalho e amizade que foram essenciais;

Aos queridos amigos que fiz ao longo destes cinco anos por conta do doutorado. Felizmente a lista é grande, mas alguns deles merecem destaque especial

por tantos momentos importantes que vivenciamos: Marta, Patrícia, Marcos, Nana-sensei, Sara, Valéria, Antônio, Dêvisson, Letícia, Scarlet, Rafael, Maria, Larissa;

Aos alunos que tive oportunidade de orientar no laboratório (Aline, Bruna, Elisa e Thalyson), na disciplina de Forma e Função para a graduação e no curso Botânica no Inverno, pois vocês contribuíram muito não só para meu doutorado como também para o meu desenvolvimento como profissional;

A todos os professores do Instituto de Biociências da USP, pelas aulas, colaborações e ensinamentos valiosos;

A todos os funcionários do Departamento de Botânica e do IB, cujo trabalho é essencial para o andamento da ciência;

Aos meus amigos e familiares de maneira geral, pelo incentivo e paciência quando eu contava sobre meus experimentos bem ou mal sucedidos;

À Priscila e ao Junior pelo carinho, generosidade e apoio constantes ao longo da minha trajetória, e em especial à Gi, por ser uma *flatmate* incrível;

Aos meus pais e irmã, pelo maior amor do mundo, sem o qual eu não teria chegado até aqui;

Ao meu marido Vinícius, por ser meu porto seguro, me dar a mão nos momentos mais sombrios, vibrar comigo a cada alegria e conquista, e ainda atuar como bioinformata particular. Te amo infinitamente.

Muito obrigada a todos!

Summary

Resumo

O ciclo C_4 e o metabolismo ácido das Crassuláceas (CAM) são dois mecanismos concentradores de carbono (CCM) prevalentes em plantas vasculares. Apresentam semelhanças bioquímicas, mas representam adaptações ecológicas bem diferentes, resultado de diferenças evolutivas, regulatórias e estruturais. Acreditava-se que seriam incompatíveis entre si, porém o gênero *Portulaca* desafia esta definição, visto que apresenta espécies C_3-C_4 intermediárias e C_4 capazes de alternar para CAM de acordo com a disponibilidade hídrica. Os mecanismos genéticos e regulatórios que possibilitam a ocorrência desta rara adaptação fotossintética são pouco conhecidos. Portanto, o objetivo desta tese de doutorado foi investigar a transição C_4 para CAM em *P. oleracea* do ponto de vista fisiológico e molecular. Após uma introdução geral ao tema, o capítulo I contextualiza e propõe a espécie como modelo de estudo da transição C_4-CAM. O capítulo II caracteriza a maquinaria genética básica envolvida em ambos os CCMs em *P. oleracea* a partir de dados de transcriptoma associados a análises filogenéticas e fisiológicas. O capítulo III explora a plasticidade morfo-fisiológica da espécie, caracterizando o CAM em diferentes subespécies provenientes de diferentes lugares do mundo. O capítulo IV discute as melhores estratégias e protocolos moleculares para explorar *P. oleracea* como um modelo C_4-CAM. Finalmente, o capítulo V caracteriza a sinalização molecular e hormonal durante a transição do C_4 para o CAM e sua reversão, bem como a influência do relógio circadiano sobre o funcionamento de ambos CCMs. No contexto de mudanças climáticas, este trabalho visou ressaltar que C_4 e CAM não representam apenas interessantes adaptações fisiológicas do ponto de vista funcional ou evolutivo, mas também são mecanismos importantes para o desenvolvimento da sociedade, por ocorrerem separadamente em cultivares utilizados na produção de alimentos e biocombustíveis. Desse modo, este trabalho trouxe informações que possibilitam explorar a complexidade de *Portulaca* como um mapa genético para o desenvolvimento futuro via engenharia genética de cultivares que possam intercalar C_4 e CAM em um mesmo organismo, conforme a disponibilidade de recursos no ambiente.

Abstract

The C_4 cycle and crassulacean acid metabolism (CAM) are two common carbon concentrating mechanisms (CCM) in vascular plants. They have biochemical similarities, but represent very different ecological adaptations, as a result of evolutionary, regulatory and structural differences. It was believed they were incompatible to occur in a single organism, but the genus *Portulaca* challenges this assumption, as it presents intermediate C_3-C_4 and C_4 species capable of switching to CAM according to water availability. However, the genetic and regulatory mechanisms that enable this rare photosynthetic adaptation to occur are still poorly understood. Therefore, the aim of this doctoral thesis was to investigate the C_4 to CAM transition in *P. oleracea* from a physiological and molecular point of view. After a brief introduction to the subject, chapter I contextualizes and proposes the species as a model for studying the C_4-CAM transition. Chapter II characterized the central genetic machinery involved in both CCMs in *P. oleracea* using transcriptome data associated with phylogenetic and physiological analyses. Chapter III explored the morphophysiological plasticity of the species, characterizing CAM in different subspecies originated in different parts of the world. Chapter IV discusses the best optimized molecular strategies and protocols enabling the use of *P. oleracea* as a C_4-CAM model. Finally, Chapter V characterizes the molecular and hormonal signaling during the C_4-to-CAM transition and reversion and brings insights into the influence of the circadian clock on both CCMs' functioning. In general, and most importantly in the global context of climate change, this work aimed to emphasize that C_4 and CAM not only represent interesting physiological adaptations from both a functional and evolutionary point of view, but are also important mechanisms for the development of society, as they occur separately in cultivars used in food production and biofuels. Thus, this work provides information that makes it possible to explore the complexity of *Portulaca* as a blueprint for future development via genetic engineering of cultivars that can intercalate C_4 and CAM in a single organism according to the availability of resources in the environment.

Scientific Background

"Botany – the science of the vegetable kingdom, is one of the most attractive, most useful, and most extensive departments of human knowledge. It is, above every other, the science of beauty."

Joseph Paxton

Initial considerations

Six carbon assimilation pathways are currently described across living organisms, but the reductive phosphate pentose cycle (*i.e.* Calvin-Benson Cycle) is the most important in higher plants (BERG, 2011). Ribulose-1,5-bisphosphate carboxylase/oxygenase (Rubisco) has a major role as the first carboxylation enzyme in this cycle (TABITA et al., 2008), but not without caveats. Rubisco is prone to oxygenase activity since molecular oxygen can interact with the intermediate form of ribulose-1,5-biphosphate (RuBP), that is the acceptor for carbon dioxide (MORONEY et al., 2013). Overall, there is a 25% chance of Rubisco binding oxygen instead of carbon dioxide, what may vary according to the concentration of these compounds in the vicinity of the enzyme (BAUWE; HAGEMANN; FERNIE, 2010; ZABALETA; MARTIN; BRAUN, 2012). Resulting from the binding of RuBP and molecular oxygen is the formation of 3-phosphoglycerate (3PGA) and 2-phosphoglycolate (2PG) molecules, the latter being harmful to the plant since it inhibits photosynthesis (ZABALETA; MARTIN; BRAUN, 2012).

In order to recover CO_2 and eliminate toxicity, 2PG undergoes the photorespiration pathway. This pathway takes place in the presence of light, involving chloroplasts, peroxisomes and mitochondria, and recovering around 75% CO_2 in the form of 3PGA, despite being energetically dispendious (BAUWE; HAGEMANN; FERNIE, 2010; EISENHUT et al., 2008; TCHERKEZ; FARQUHAR; ANDREWS, 2006). To avoid photorespiration, CCMs have evolved in various plant lineages and consist of different strategies to minimize the oxygenase activity of Rubisco (MORONEY et al., 2013).

C_4 photosynthesis and crassulacean acid metabolism (CAM) are the most common CCMs in eudicots (KEELEY; RUNDEL, 2003). As they may require multiple traits to function, both can be referred to as syndromes. Their basic mechanisms are very similar, involving the incorporation of CO_2 molecules into organic acid skeletons that will be decarboxylated close to Rubisco (SAGE, 2002). To do this, the biochemical machinery employed by each CCM is quite similar, involving a common set of enzymes, such as: carbonic anhydrases (CA), phospho*enol*pyruvate carboxylase (PPC), PPC kinase (PPCK), NAD(P)–malate dehydrogenases (MDH), malic enzymes (ME), and phospho*enol*pyruvate carboxykinase (PEPCK), pyruvate, orthophosphate dikinase (PPDK) and PPDK regulatory protein (PPDKPR) (EDWARDS; OGBURN, 2012; KANAI; EDWARDS, 1999; WINTER; SMITH, 1996).

Although their basic biochemistry is similar, C_4 works as a spatial specialization, while CAM relies less on the tissue structure and more on temporal regulation. Nevertheless, due to this crucial difference, different transporters and regulatory steps have evolved for each CCM (SAGE, 2002).

C_4 photosynthesis

A remarkable, but not essential, feature of C_4 plants is the structural arrangement of two types of cells in the mesophyll, named Kranz anatomy, in which mesophyll cells (MCs) are reduced and surround the well-developed bundle sheath cells (BSCs) (SAGE, 2004; VOZNESENSKAYA et al., 2001). In this type of photosynthesis, MCs perform the first carboxylation step by PPC activity and form 4-carbon acids to store CO_2. Acids are then transported to the bundle sheath BSCs to be decarboxylated, redeeming CO_2 to the Calvin Cycle (KANAI; EDWARDS, 1999; SAGE, 2004).

In MCs, there is an increase in levels of CA and PPC in the cytoplasm for CO_2 fixation, and PPDK in the chloroplasts for phosphoenolpyruvate (PEP) regeneration (KANAI; EDWARDS, 1999). On the other hand, Rubisco levels in chloroplasts and glycine decarboxylation enzymes in mitochondria are low. BSCs, in its turn, concentrate Rubisco and glycine decarboxylase (GDC) activities. This assures the decarboxylation step to occur in BSCs and restricts photorespiration to these cells, promoting a CO_2 pump mechanism to enhance Rubisco activity (SAGE, 2004).

After CA equilibrates CO_2 and HCO_3^- in MCs, PPC forms oxaloacetate (OAA), which is converted to a tetracarboxylic acid to be transported to the BSCs. Kanai and Edwards (1999) describe in detail three types of C_4 photosynthesis according to the decarboxylation step in BSCs: NAD-malic (NAD-ME), NADP-malic (NADP-ME) and PEPCK types.

NADP-ME type plants use NADP-malate dehydrogenase to form malate (the remaining OAA forming aspartate), which is then transferred probably via plasmodesmata to the BSC and decarboxylated by NADP-ME feeding CO_2 and NADP to the Calvin Cycle. The product of this reaction is pyruvate, that is transported back to MC, where PPDK regenerates PEP.

NAD-ME type plants may form aspartate by aspartate aminotransferase in MCs, that is transported to the BSC mitochondria do be deaminated by aspartate aminotransferase. They may also form OAA, which is reduced to malate by NAD-malate dehydrogenase and decarboxylated by NAD-ME in BSCs, feeding CO_2 to the Calvin Cycle. The remaining pyruvate is converted to alanine and transported back to MCs to regenerate PEP by alanine aminotransferases.

In PEPCK type plants, aspartate formed via aspartate aminotransferase in MC and is transported to BSCs. Aspartate is deaminated and decarboxylated by PEPCK, redeeming CO_2, and the resulting pyruvate may return to MC as alanine or PEP. The formation of PEP at this step may result in reduced PPDK activity in PEPCK-type plants.

In particular, the NAD(P)-MDH and PPDK enzymes are prone to light regulation (KANAI; EDWARDS, 1999). Kanai and Edwards (1999) also explain that chloroplasts differ

from type to type, having a centrifugal position relative to the vascular bundle and thylakoid with reduced grana in NADP-ME. In NAD-ME and PEPCK types, thylakoids have well-developed grana stacking, but chloroplasts and mitochondria have a centripetal position in NAD-ME type, and chloroplasts are evenly or centrifugally distributed in PEPCK-type.

C_4 representatives are widespread over 19 families of angiosperms, comprising around 8,100 species, of which 80% are monocots (SAGE, 2017). Most representatives of C_4 flora show an herbaceous habit and are distributed in dry regions, where photorespiration would be favored by low stomatal aperture and warm temperatures (SAGE; LI; MONSON, 1999). As reviewed by Sage (2017), the evolution of C_4 lineages probably dates to between 30 and 35 million years ago, a period when CO_2 atmospheric levels decreased and temperatures increased, resulting in intense selective pressure. When it comes to economic use and applicability of C_4 plants, maize, sugarcane and sorghum are among the leading row crops, in addition to forage crops and a large portion of weed and invase species (SAGE, 2017).

In the molecular context, C_4 evolved independently, with the resulting gene product being the same in different plant lineages (MONSON, 1999). The evolution of C_4 involved the recruitment and duplication of C_3 non-photosynthetic genes, besides tuning the regulation of these genes in different mesophyll cell layers (KEELEY; RUNDEL, 2003; MONSON, 1999).

One interesting feature of C_4 photosynthesis was the discovery of single-cell C_4 (Voznesenskaya et al. 2001). Up to date, four members of the family Chenopodiaceae family *(Bienertia cycloptera, B. sinuspersici, B. kavirense and Suaeda aralocaspica)* were found to perform the entire biochemical cycle, commonly divided into two types of cells (MCs and BSCs), in one large, polarized chlorenchyma cell (FREITAG; STICHLER, 2000; LEISNER et al., 2010; PARK; OKITA; EDWARDS, 2009; VOZNESENSKAYA et al., 2002). There is a central, large vacuole that separates the proximal portion of the cell, with few chloroplasts, from a distal part, connected to the vascular bundle and possessing a high density of chloroplasts, and it promotes a high diffusive resistance between these two halves of the cell (VOZNESENSKAYA et al., 2001).

Crassulacean acid metabolism (CAM)

In a nutshell, CAM involves diel fluctuation of acidity in photosynthetic cells, and the whole process can be divided into four phases over the day/night cycle (TING, 1985), as clearly described by Winter and Smith (1996). The first phase takes place at night, when stomata remain open and PPC promotes the assimilation of CO_2 into four-carbon organic acids, that are stored inside MC vacuoles. The second phase starts at dawn, when PPC is deactivated and Rubisco is activated, and there can still be some CO_2 assimilation at this

stage in weak CAM-performing plants. During the third phase, in the light period, stomata remain closed and organic acids are mobilized from the vacuole to the chloroplasts to be decarboxylated, releasing CO_2 in the vicinity of Rubisco. In the fourth phase, at dusk, levels of PPC and Rubisco are inverted again, preceding the nocturnal CO_2 assimilation. Biochemically, there can be NADP-, NAD-ME and PEPCK decarboxylation systems in CAM performing plants as reported for C_4. In addition, as reviewed in Schiller and Bräutigam (2021), CAM plants usually mobilize the phosphorolytic starch degradation pathway instead of the hydrolytic pathway commonly used in C_3 plants.

CAM is usually associated with increased water use efficiency (WUE) when compared to C_3 and C_4 species, being widespread in plants from arid environments (CUSHMAN, 2001), but also occurring in other less obvious habitats, including the epiphytic flora of tropical forests and even certain aquatic plants (WINTER; SMITH, 1996). This syndrome has already been described in at least 16,800 species of 35 plant families (SILVERA et al., 2010). In economic terms, CAM is present in food crops such as pineapple, *Agave* and *Opuntia*, the two latter are also being largely used for biomass production and showing potential as biofuel (YANG et al., 2015).

Ontogenetic and/or environmental features can influence CAM expression, characterizing either the constitutive or facultative forms of CAM (WINTER; SMITH, 1996). Constitutive CAM (also referred to as obligatory or ontogenetic CAM) is developed as the plant matures independently of environmental conditions, and this is usually connected to a strong form of CAM. As such, the intensity of CAM is defined by the total carbon assimilation contribution of dark CO_2 fixation to the overall carbon metabolism of the plant (WINTER, 2019). On the other hand, in facultative CAM plants, the expression of the CAM machinery can be highly variable according to the environmental context, especially with varying light, temperature and water availability conditions (DODD et al., 2002; SILVERA et al., 2010). Among these environmental factors, water availability has been shown to modulate CAM expression in most CAM facultative species analyzed so far. Facultative CAM is usually, but not exclusively, associated with a weak form of CAM, where CO_2 assimilated by PPC corresponds to less than 5% of total carbon gain (WINTER, 2019).

Another subdivision in types of CAM can be defined according to their diel gas exchange and acid accumulation patterns. Plants performing constitutive CAM restrict stomatal opening to the dark period, which results in intense nocturnal acidification and CO_2 assimilation. CAM-cycling and CAM-idling, on the other hand, both show lower nocturnal acidification resulting from reutilizing respiratory CO_2, and both differ in diel CO_2 assimilation pattern. While CAM-cycling is characterized by closed stomata during the dark period and diurnal CO_2 assimilation usually restricted to bursts of assimilation in phase 2 (WINTER; HOLTUM, 2014), plants performing CAM-idling present no net CO_2 exchange

over the entire diel cycle (TING, 1985). CAM-idling is a survival and temporary mechanism when the plant is severely stressed, and occurs as the plant reutilizes respiratory CO_2 to maintain an active but low CAM metabolism (WINTER, 2019).

Signaling events controlling the facultative CAM cycle

In facultative CAM systems, the alternation of C_3 to CAM requires changes in the circadian system, carbohydrate partitioning, intracellular transport of metabolites, osmotic adjustment and the synchronization between two competing carboxylation systems (PPC and Rubisco). These changes occur inside the same cell and are triggered within a time frame that may vary from a few hours to several weeks (FRESCHI; MERCIER, 2012). Consequently, a series of adjustments aiming to keep homeostasis during these changes involve transcriptional, translational, and post-translational regulatory processes (CUSHMAN; BOHNERT, 2000). Therefore, based on the physiological complexity and high responsiveness to environmental stimuli, it is plausible to expect the existence of equally complicated signaling routes controlling C_3-CAM or C_4-CAM transitions.

Distinct lines of evidence indicate that abscisic acid (ABA) acts as one of the major stimulatory signals for CAM expression (TAYBI; CUSHMAN, 2002). Studies conduced on distinct CAM plants, including ice plant (*Mesembryanthemum crystallinum*), *Kalanchöe blossfeldiana* and pineapple (*Ananas comosus*), have demonstrated that exogenous ABA can trigger increases in activity and/or transcript accumulation of CAM-related enzymes either when applied to intact plants or directly supplied to detached leaves. The ABA-induced up-regulation of CAM enzymes is followed by an initiation, or up-regulation, of functional CAM, leading to levels of night-time acid accumulation equivalent to those observed in water-stressed plants (reviewed by Freschi and Mercier 2012).

In parallel to the positive regulation of ABA, which induces CAM expression, the existence of negative endogenous signals that would repress CAM in reversible facultative plants is somewhat expected. Based on available data, cytokinins (CKs) are the best candidates to fulfil a role as negative root-derived signals responsible for inhibiting CAM expression in leaves of well-watered plants (SCHMITT; PIEPENBROCK, 1992). Among the evidence supporting this view, considerable decreases in endogenous CKs have been observed during the water stress-induced up-regulation of CAM in excised ice plant leaves (PETERS et al., 1997) and intact pineapple young plants (FRESCHI et al., 2010). In addition, supplying exogenous CKs has suppressed CAM initiation triggered by stress conditions (DAI et al., 1994; FRESCHI et al., 2010; PETERS et al., 1997). Compared to ABA and CKs, significantly less information is currently available regarding the involvement of other plant hormones in the modulation of CAM expression.

Bioengineering C_4 and CAM into crops to improve drought stress resistance

Climate change is a major concern, possibly causing the aridification of tropical regions, an increase in temperature of temperate areas, and changes in sea levels and ocean currents. When combined, these global changes can result in a loss of arable land and immediately impact agriculture (FAO 2020). Amidst such pessimistic scenarios, food and fuel demands will continue to grow (BORLAND et al., 2009). Therefore, sustainable and green technologies coupled with responsible land management that maximize yield in reduced arable land have never been as crucial as now (FAO 2020).

Another approach in this scenario is to search broadly into the plant's metabolism and physiology, aiming at finding out clever strategies to improving the agricultural performance of crops and other species of interest (FURBANK; QUICK; SIRAULT, 2015; YANG et al., 2015; SCHILLER; BRÄUTIGAM, 2021). In this context, CCMs have evolved as a strategy to reduce carbon loss caused by the oxygenase activity of Rubisco and resulted in plant lineages that express CAM and C_4 photosynthesis, which very frequently colonize habitats characterized by persistent or recurrent abiotic stress events. These two mechanisms have recruited enzymes that already exist in the C_3 metabolism to perform different roles, resulting in a neofunctionalization of the plant primary C_3 metabolism (EDWARDS; OGBURN, 2012; HEYDUK et al., 2019). Hence, although the molecular machinery and regulation of each CCM are still not completely dissected, CCMs represent flexible adaptations, which ensure photosynthetic yield under high irradiance (C_4) and strong tolerance to drought under arid conditions (CAM).

Consequently, it may be promising to investigate the possibility of combining the different aspects of C_4 and CAM into crops (BORLAND et al., 2009; VON CAEMMERER; QUICK; FURBANK, 2012), as an attempt to increase abiotic stress tolerance ensuring plant productivity or its survival when under unfavorable environmental conditions (YANG et al., 2015). Although the journey is long and challenging when it comes to engineering CCMs, two ongoing initiatives stand out: the C_4 Rice project, which has focused on introducing C_4 into a C_3 plant (ERMAKOVA et al., 2020; FURBANK, 2016); and the CAM Biodesign, that seeks to express CAM in Arabidopsis and poplar, also C_3 plants (DEPAOLI et al., 2014; LIU et al., 2018). Even the C_2 metabolism, another variation of CCM which acts as a C_3-C_4 intermediate, has also been discussed as a possible target for bioengineering of crops (LUNDGREN, 2020), but it will not be discussed here. The two mentioned projects deal with CCM-C_3 engineering alone, but another approach would be bioengineering a facultative CAM system into C_4-crop plants.

<u>Portulaca</u> phylogeny and evolution

Multiple plant lineages include both C_4 species and facultative or constitutive CAM representatives, while the occurrence of both C_4 and CAM within a single species is rare, considering each CCM followed distinct and exclusive evolutionary pathways (SAGE, 2002). C_4 evolution favors a well-developed bundle sheath, whereas CAM favors succulence and tight mesophyll packing (SAGE, 2004; SILVERA et al., 2010). The evolution of these contrasting anatomical features is favored by different selective pressures, preconditioning the evolution of either C_4 or CAM, while limiting the chances of both pathways to evolve in a single individual. Hence, C_4 and CAM evolved a differential regulation in enzyme activation of carboxylation and decarboxylation steps, different metabolite transport dynamics, and specialized structural arrangements for each syndrome (SAGE, 2002).

Nevertheless, it may also have been simply a matter of not having enough time to evolve the two syndromes in one single organism. There are a few extreme examples of CCM connectivity, such as the *Portulaca* species in Caryophyllales (SAGE, 2002; WINTER, 2019). In fact, Caryophyllales concentrates many independent and parallel origins of CCMs, being considered a hotspot for CCM evolution (GOOLSBY et al., 2018; EDWARDS; OGBURN, 2012).

Portulacaceae (Caryophyllales) is a monotypic family and comprises ca. 100 species distributed worldwide (APG III, 2009; OCAMPO; COLUMBUS, 2012). The genus probably diverged around 23 million years ago somewhere in the southern hemisphere and became widely distributed probably via long-distance dispersal, but its exact place of origin is still uncertain (OCAMPO; COLUMBUS, 2012). Centers of diversity for the family are South America, Africa, and Australia (OCAMPO; COLUMBUS, 2012). The clade is a member of the Portulacineae (Caryophyllales), which includes well-known CAM lineages such as the cacti and Didiereaceae (SILVERA et al., 2010).

The family is divided into two main lineages: the opposite-leaved clade (OL), comprising fewer species and distributed in Africa, Asia and Australia; and the alternate-leaved clade (AL), more widespread and including most of the species (OCAMPO; COLUMBUS, 2012). Within the AL clade are: *P. cryptopetala*, identified as a C_3-C_4 intermediate (VOZNESENSKAYA et al., 2010), and three groups: the Oleracea, Umbraticola and Pilosa clades (OCAMPO; COLUMBUS, 2012). There still remains considerable uncertainty about species relationships within these groups, and the species that is best known physiologically (*P. oleracea*) is not monophyletic (OCAMPO; COLUMBUS, 2012).

Except for *P. cryptopetala*, all taxa show C_4 leaves and C_3 stems (LAETSCH, 1974; SAGE; CHRISTIN; EDWARDS, 2011; VOZNESENSKAYA et al., 2010, 2016). Different types of Kranz anatomy were reported in representatives of the family, as were NADP-ME and NAD-ME-type species (KU et al., 1981; VOZNESENSKAYA et al., 2010). While Ocampo et al. (2013) preferred the interpretation of a single inferred origin of C_4 at the base

of *Portulaca* with an evolutionary reversion to C_3-C_4, there is an alternative hypothesis of multiple, parallel evolutionary shifts to C_4 (CHRISTIN et al., 2014). There are various lines of evidence to support this. First, each of the three major C_4 clades presents a distinct C_4 leaf anatomical configuration, and second, different clades have recruited different decarboxylating enzymes to release CO_2 in the BSCs (VOZNESENSKAYA et al., 2010). Third, *Portulaca* has recruited a novel, recently duplicated homolog of one gene encoding PPC (*PPC1E1a')* in its C_4 cycle. Codon model tests strongly favored independent adaptive evolution of *PPC1E1a'* in each of the three clades (Oleracea, Umbraticola and Pilosa), with each AL clade presenting a unique suite of amino acid substitutions known to show selection for C_4 function (CHRISTIN et al., 2014). This supports the scenario that selection of *PPC1E1a'* for C_4 function occurred in each lineage separately, after they diverged from their common ancestor.

Moreover, the *Portulaca* genus is remarkable, since all C_4 and C_3-C_4 intermediate species studied up to date undergo CAM induction upon water deficit (GURALNICK; JACKSON, 2001; HOLTUM et al., 2017; KOCH; KENNEDY, 1980, 1982; KRAYBILL; MARTIN, 1996; KU et al., 1981; WINTER et al., 2019). The most studied species, *P. oleracea,* provides us with the blueprint, refined over millions of years of evolution, for developing this group as a new workhorse of CCM-based crop improvement and genetic engineering. Also, studying facultative CAM systems can provide good insight into CAM regulation and signal transduction cascades, since the ontogenetic factor of constitutive CAM species are not present (WINTER; HOLTUM, 2014).

Portulaca oleracea L. as a model system to study C_4-CAM compatibility

Commonly known as purslane, *P. oleracea* is an annual cosmopolite usually found growing in human-disturbed areas as gardens, field crops, lawns and sidewalks, or as a pioneer species (VENGRIS; DUNN; STACEWICZ-SAPUNCAKIS, 1972). It has succulent leaves and stems, solitary flowers, a self-fertilization system and a pronounced seed production (VENGRIS; DUNN; STACEWICZ-SAPUNCAKIS, 1972; ZIMMERMAN, 1977). Adding to the remarkable photosynthetic plasticity of *Portulaca* species, *P. oleracea* also presents extreme tolerance to drought (JIN et al., 2015; REN et al., 2011), salinity (YAZICI et al., 2007), as well as variations in temperature, photoperiod, soil and light intensity (ZIMMERMAN, 1976). When combined, all these factors may help to explain the wide distribution of this species, its weedy propagation in agricultural systems and a wide morphologic diversification (DANIN; DOMINA; RAIMONDO, 2008; OCAMPO; COLUMBUS, 2012; WALTER; VEKSLYARSKA; DOBEŠ, 2015).

Even though it is considered one of the ten most noxious weeds on the planet (SINGH; SINGH, 1967), *P. oleracea* has many uses for different cultures. For example, it

exhibits pharmacological effects and has been used in traditional Chinese medicine for thousands of years (CHAN et al., 2000; CHEN; SHI; LIU, 2003; GONNELLA et al., 2010; HABTEMARIAM; HARVEY; WATERMAN, 1993; KARIMI; HOSSEINZADEH; ETTEHAD, 2004; RADHAKRISHNAN et al., 2001; RASHED; AFIFI; DISI, 2003). It is also considered a neglected crop by the Food and Health Organization, rich in vitamins, antioxidants, and omega 3-fatty acids, and is widely consumed in African and Asian countries either in salads or soups (EGEA-GILABERT et al., 2014; GONNELLA et al., 2010; HERNÁNDEZ-BERMEJO; LEÓN, 1994; LIM; QUAH, 2007; OBIED; MOHAMOUD; MOHAMED, 2003).

However, *P. oleracea* has unresolved taxonomic issues. On the one hand, it is considered an aggregate of subspecies or microspecies (DANIN; BAKER; BAKER, 1978; DANIN; RAUS, 2012), also sometimes referred to as different species (DANIN; DOMINA; RAIMONDO, 2008; DANIN; REYES BETANCORT, 2006; RICCERI; ARRIGONI, 2000). The most recent taxonomic reports list 19 microspecies distinguished according to their seed size and seed coat ornaments (DANIN; RAUS, 2012). On the other hand, *P. oleracea* can be referred to as a complex, being considered a polymorphic species that, due to its cosmopolitan distribution and high adaptability, is expected to present high variability in morphological and physiological traits among populations, even forming a continuum (GORSKE; RHODES; HOPEN, 1979; MATTHEWS; KETRON; ZANE, 1993; WALTER; VEKSLYARSKA; DOBEŠ, 2015). In this sense, seed size and ornamentation are not considered enough to define the different subspecies, as there should be more noticeable morphological differences associated with allopatric populations (MATTHEWS; KETRON; ZANE, 1993; WALTER; VEKSLYARSKA; DOBEŠ, 2015).

The leaves of *P. oleracea* have three types of cells: (1) water storage cells (WSCs), whose contribution to overall carbon gain may be minimal due to their small number of chloroplasts; (2) photosynthetically active cells usually referred to as MCs; and (3) and BSCs that surround the vascular bundles forming the Kranz anatomy (which is atriplicoid type) (VOZNESENSKAYA et al., 2010). This species is a NAD-malic enzyme (NAD-ME) type of C_4 plant (KENNEDY; LAETSCH, 1973; KENNEDY, 1976), accumulating malate and aspartate as a means of transferring assimilated CO_2 from MCs to BSCs for decarboxylation and Rubisco carboxylation (LARA; DRINCOVICH; ANDREO, 2004). Due to the presence of photosynthetically active cells and no apparent Kranz anatomy, *P. oleracea* stems are considered C_3 under well-watered conditions (KOCH; KENNEDY, 1980; MAZEN, 1996; VOZNESENSKAYA et al., 2010).

P. oleracea leaves have been shown to increase nocturnal acidity and perform a low level of CO_2 assimilation in the dark after prolonged periods of water deprivation (KOCH; KENNEDY, 1982a, 1980; KRAYBILL; MARTIN, 1996; LARA et al., 2003; LARA;

DRINCOVICH; ANDREO, 2004; MAZEN, 1996, 2000; WINTER; HOLTUM, 2014). After this discovery, Lara et al. (2004) developed a first hypothetical model of C_4-CAM compatibility in *P. oleracea*, and provided preliminary evidence that PPC may be up-regulated in WSCs when plants were droughted. In this model, malate generated from CAM in WSCs and MCs is shuttled to BSCs for decarboxylation.

A potential breakthrough occurred when Christin et al. (2014) analyzed the transcriptome of two individuals of *P. oleracea* grown under well-watered and droughted conditions and identified two genes possibly responsible for encoding two different isoforms of PPC, each one involved in one photosynthetic behavior. While *PPC1E1c* was highly expressed during the night in droughted plants, *PPC1E1a'* was predominantly expressed during the day and in well-watered samples (CHRISTIN et al., 2014). This finding is correlated with the different properties and activity of PPC in well-watered and droughted *P. oleracea* plants (LARA et al., 2003; MAZEN, 1996, 2000).

Despite the remarkably impressive photosynthetic plasticity observed within *P. oleracea*, very limited information is currently available on the biochemical, physiological and genetic regulation of CAM expression in this fascinating genus. Therefore, *P. oleracea*, whose leaves can present both C_4 and CAM and whose stems can perform either C_3 or CAM, represents a precious model for exploring the molecular, biochemical and signaling mechanisms responsible for allowing the occurrence of these distinct photosynthetic modes within a single individual.

Given such promising system for photosynthetic plasticity studies, *P. oleracea* was chosen as the target species for exploring the connectivity between the C_4 and the CAM cycles in this work. Gene recruiting for either CO_2 concentration mechanisms (CCMs), the plasticity inside the *Portulaca oleracea* complex, and the signaling events controlling the up- and down-regulation of either CCM cycles, were the object of study in this thesis.

References

APG III. An update of the Angiosperm Phylogeny Group classification for the ordens and families of flowering plants: APG III. **Botanical Journal of the Linnean Society**, v. 161, p. 105–121, 2009. DOI: 10.1046/j.1095-8339.2003.t01-1-00158.x.

BAUWE, H.; HAGEMANN, M.; FERNIE, A. R. Photorespiration: players, partners and origin. **Trends in Plant Science**, 2010. DOI: 10.1016/j.tplants.2010.03.006.

BERG, I. A. Ecological aspects of the distribution of different autotrophic CO_2 fixation pathways. **Applied and Environmental Microbiology**, 2011. DOI: 10.1128/AEM.02473-10.

BORLAND, A. M.; GRIFFITHS, H.; HARTWELL, J.; SMITH, J. A. C. Exploiting the potential of plants with crassulacean acid metabolism for bioenergy production on marginal lands. **Journal of Experimental Botany**, v. 60, n. 10, p. 2879–2896, 2009. DOI: 10.1093/jxb/erp118.

CHAN, K.; ISLAM, M. W.; KAMIL, M.; RADHAKRISHNAN, R. The analgesic and anti-inflammatory effects of *Portulaca oleracea* L *subsp sativa* (Haw) Celak. **Journal of Ethnopharmacology 73**, v. 73, p. 445–451, 2000.

CHEN, J.; SHI, Y.; LIU, J. Determination of noradrenaline and dopamine in Chinese herbal extracts from *Portulaca oleracea* L by high-performance liquid chromatography. **Journal of Chromatography**, v. 1003, p. 127–132, 2003.

CHOLLET, R.; VIDAL, J.; O'LEARY, M. H. Phosphoenolpyruvate carboxylase: A ubiquitous, highly regulated enzyme in plants. **Annual Review of Plant Physiology and Plant Molecular Biology**, v. 47, n. 1, p. 273–298, 1996. DOI: 10.1146/annurev.arplant.47.1.273.

CHRISTIN, P. et al. Shared origins of a key enzyme during the evolution of C_4 and CAM metabolism. **Journal of experimental botany**, v. 65, n. 13, p. 3609–3621, 2014. a. DOI: 10.1093/jxb/eru087.

CUSHMAN, J. C. Crassulacean acid metabolism: s plastic photosynthetic adaptation to arid environments. **Plant Physiology**, 2001. DOI: 10.1104/pp.010818.

CUSHMAN, J. C.; BOHNERT, H. J. Genomic approaches to plant stress tolerance. **Current Opinion in Plant Biology**, 2000. DOI: 10.1016/S1369-5266(99)00052-7.

DAI, Z.; KU, M. S. B.; ZHANG, D.; EDWARDS, G. E. Effects of growth regulators on the induction of Crassulacean acid metabolism in the facultative halophyte *Mesembryanthemum crystallinum* L. **Planta**, v. 192, n. 3, p. 287–294, 1994. DOI: 10.1007/BF00198562.

DANIN, A.; BAKER, I.; BAKER, H. G. Cytogeography and taxonomy of the *Portulaca oleracea* L. polyploid complex. **Israel Journal of Botany**, 1978.

DANIN, A.; DOMINA, G.; RAIMONDO, F. M. Microspecies of the *Portulaca oleracea* aggregate found on major Mediterranean islands (Sicily, Cyprus, Crete, Rhodes). **Flora Mediterranea**, , v. 18, p. 89–107, 2008.

DANIN, A.; RAUS, T. A key to 19 microspecies of the *Portulaca oleracea* aggregate. *In*: CARYOPHYLLALES SIMPOSIUM 2012, Moskov. **Anals**. Moskov: Lomonosov State University, 2012. p. 70–83.

DANIN, A.; REYES BETANCORT, J. The status of *Portulaca oleraceal* in Tenerife, the Canary Islands. **Lagascalia**, , v. 26, n. 1, p. 71–81, 2006.

DEPAOLI, H. C.; BORLAND, A. M.; TUSKAN, G. A.; CUSHMAN, J. C.; YANG, X. Synthetic biology as it relates to CAM photosynthesis: Challenges and opportunities. **Journal of Experimental Botany**, v. 65, n. 13, p. 3381–3393, 2014. DOI: 10.1093/jxb/eru038.

DODD, A. N.; BORLAND, A. M.; HASLAM, R. P.; GRIFFITHS, H.; MAXWELL, K. Crassulacean acid metabolism: plastic, fantastic Antony. **Journal of Experimental Botany**, v. 53, n. 369, p. 569–580, 2002. DOI: 10.1201/9780203910344.ch10.

EDWARDS, E. J.; OGBURN, M. R. Angiosperm responses to a low-CO_2 world: CAM and C_4 photosynthesis as parallel evolutionary trajectories. **International Journal of Plant Sciences**, v. 173, n. 6, p. 724–733, 2012. DOI: 10.1086/666098.

EGEA-GILABERT, C.; RUIZ-HERNÁNDEZ, M. V.; PARRA, M. Á.; FERNÁNDEZ, J. A. Characterization of purslane (*Portulaca oleracea* L.) accessions: suitability as ready-to-eat product. **Scientia Horticulturae**, v. 172, p. 73–81, 2014. DOI: 10.1016/j.scienta.2014.03.051.

EISENHUT, M.; RUTH, W.; HAIMOVICH, M.; BAUWE, H.; KAPLAN, A.; HAGEMANN, M. The photorespiratory glycolate metabolism is essential for cyanobacteria and might have been conveyed endosymbiontically to plants. **PNAS**, v. 105, n. 44, 2008.

ERMAKOVA, M.; DANILA, F. R.; FURBANK, R. T.; CAEMMERER, S. V.. On the road to C_4 rice: advances and perspectives. **The Plant Journal**, v. 101, p. 940–950, 2020. DOI: 10.1111/tpj.14562.

FAO (the state of food and agriculture). Overcoming water challenges in agriculture. Rome. **https://doi.org/10.4060/cb1447en.** 2020

FREITAG, H.; STICHLER, W. A remarkable new leaf type with unusual photosynthetic tissue in a central asiatic genus of Chenopodiaceae. **Plant Biology**, v. 2, n. 2, p. 154–160, 2000. DOI: 10.1055/s-2000-9462.

FRESCHI, L.; MERCIER, H. Connecting environmental stimuli and crassulacean acid metabolism expression: phytohormones and other signaling molecules. *In*: Progress in Botany 73, v. 73, p. 231–255. DOI: 10.1007/978-3-642-22746-2_9.

FRESCHI, Luciano; RODRIGUES, Maria Aurineide; DOMINGUES, Douglas Silva; PURGATTO, Eduardo; SLUYS, Marie-anne Van; MAGALHAES, Jose Ronaldo; KAISER, Werner M.; MERCIER, Helenice. Nitric Oxide Mediates the Hormonal Control of Crassulacean Acid Metabolism Expression in Young Pineapple plants. **Plant Physiology**, v. 152, p. 1971–1985, 2010. DOI: 10.1104/pp.109.151613.

FURBANK, R. T. Walking the C_4 pathway: past, present, and future. **Journal of Experimental Botany**, 2016. DOI: 10.1093/jxb/erw161.

FURBANK, R. T.; QUICK, W. P.; SIRAULT, X. R. R. Improving photosynthesis and yield potential in cereal crops by targeted genetic manipulation: prospects, progress and challenges. **Field Crops Research**, v. 182, p. 19–29, 2015. DOI: 10.1016/j.fcr.2015.04.009.

GONNELLA, M.; CHARFEDDINE, M.; CONVERSA, G.; SANTAMARIA, P. Purslane: a review of its potential for health and agricultural aspects. **The European Journal of Plant Science and Biotechnology**, v. 4, p. 131–136, 2010.

GOOLSBY, Eric W.; MOORE, A. J.; HANCOCK, L. .. P.; DE VOZ, J. M.; EDWARDS, E. J. Molecular evolution of key metabolic genes during transitions to C 4 and CAM photosynthesis. **American Journal of Botany**, v. 105, n. 3, p. 602–613, 2018. DOI: 10.1002/ajb2.1051.

GORSKE, S. F.; RHODES, A. M.; HOPEN, H. J.A numerical taxonomic study of *Portulaca oleracea*. **Weed Science**, v. 27, n. 1, p. 96–102, 1979. DOI: 10.1017/s0043174500043575.

GURALNICK, L. J.; JACKSON, M. D. the occurrence and phylogenetics of crassulacean acid metabolism in the Portulacaceae. **International Journal of Plant Science**, v. 162, n. 2, p. 257–262, 2001. DOI: 10.1086/657678.

HABTEMARIAM, S.; HARVEY, A. L.; WATERMAN, P. G. The muscle relaxant properties of *Portulaca oleracea* are associated with high concentrations of potassium ions. **Journal of Ethnopharmacology**, v. 40, n. 3, p. 195–200, 1993. DOI: 10.1016/0378-8741(93)90068-G.

HERNÁNDEZ-BERMEJO, J. E.; LEÓN, J. **Neglected Crops - 1492 from a different perspective**. FAO Plant Production and Protection Series, n. 26, 1994. DOI: 10.1017/CBO9781107415324.004.

HEYDUK, K.; MORENO-VILLENA, J. J.; GILMAN, I. S.; CHRISTIN, P.; EDWARDS, E. J. The genetics of convergent evolution: insights from plant photosynthesis. **Nature Reviews Genetics**, v. 20, n. 8, p. 485–493, 2019. DOI: 10.1038/s41576-019-0107-5.

HOLTUM, J. A. M.; HANCOCK, L. P.; EDWARDS, E. J.; WINTER, K. Optional use of CAM photosynthesis in two C_4 species, *Portulaca cyclophylla* and *Portulaca digyna*.

Journal of Plant Physiology, v. 214, p. 91–96, 2017. DOI: 10.1016/j.jplph.2017.01.010.

IZUI, K.; MATSUMURA, H.; FURUMOTO, T.; KAI, Y. Phosphoenolpyruvate carboxylase: A new era of structural biology. **Annual Review of Plant Biology**, 2004. DOI: 10.1146/annurev.arplant.55.031903.141619.

JIN, R.; SHI, H.; HAN, C.; ZHONG, B.; WANG, Q.; CHAN, Z. Physiological changes of purslane (*Portulaca oleracea* L.) after progressive drought stress and rehydration. **Scientia Horticulturae**, v. 194, p. 215–221, 2015. DOI: 10.1016/j.scienta.2015.08.023.

KANAI, R.; EDWARDS, G. E. The Biochemistry of C_4 photosynthesis. *In*: SAGE, R. F.; MONSON, R. K. (org.). **C_4 Plant Biology**. San Diego: Academic Press, 1999. p. 49–87.

KARIMI, G.; HOSSEINZADEH, H.; ETTEHAD, N. Evaluation of the gastric antiulcerogenic effects of *Portulaca oleracea* L. extracts in mice. **Phytotherapy Research**, v. 18, n. 6, p. 484–487, 2004. DOI: 10.1002/ptr.1463.

KEELEY, J. E.; RUNDEL, P. W. Evolution of CAM and C_4 carbon-concentrating mechanisms. **International Journal Plant Science**, v. 164, p. S55–S77, 2003.

KENNEDY, R. A.; LAETSCH, W. M. Relationship between leaf development and primary photosynthetic products in the C_4 plant *Portulaca oleracea* L. **Planta**, v. 115, n. 2, p. 113–124, 1973. DOI: 10.1007/BF00387777.

KENNEDY, R. A. Relationship between leaf development, carboxylase enzyme activities and photorespiration in the C_4-plant *Portulaca oleracea* L. **Planta,** v. 128, p. 149–154, 1976.

KOCH, K. E.; KENNEDY, R. A. Crassulacean acid metabolism in the succulent C_4 dicot, *Portulaca oleracea* L. under natural environmental conditions. **Plant Physiology**, v. 69, n. 4, p. 757–761, 1982. DOI: 10.1104/pp.69.4.757.

KOCH, K.; KENNEDY, R. A. characteristics of crassulacean acid metabolism in the succulent C_4 dicot, *Portulaca oleracea* L. **Plant Physiology**, v. 65, n. 2, p. 193–197, 1980. DOI: 10.1104/pp.65.2.193.

KRAYBILL, A. A.; MARTIN, C. E. Crassulacean acid metabolism in three species of the C_4 genus *Portulaca*. **International Journal of Plant Sciences**, v. 157, n. 1, p. 103–109, 1996. DOI: 10.1086/297325.

KU, S.; SHIEH, Y.; REGER, B. J.; BLACK, C. C. Photosynthetic characteristics of *Portulaca grandiflora* , a succulent C_4 dicot . **Plant Physiology**, v. 68, n. 5, p. 1073–1080, 1981. DOI: 10.1104/pp.68.5.1073.

LAETSCH, W. M. The C_4 Syndrome: a structural analysis. **Annual Review of Plant Physiology**, v. 25, n. 1, p. 27–52, 1974. DOI: 10.1146/annurev.pp.25.060174.000331.

LARA, M. V.; DISANTE, K. B.; PODESTÁ, F. E.; ANDREO, C. S.; DRINCOVICH, M. F. Induction of a crassulacean acid like metabolism in the C_4 succulent plant, *Portulaca oleracea* L.: physiological and morphological changes are accompanied by specific modifications in phosphoenolpyruvate carboxylase. **Photosynthesis Research**, v. 77, n. 2–3, p. 241–254, 2003. DOI: 10.1023/A:1025834120499.

LARA, M. V.; DRINCOVICH, M. F.; ANDREO, C. S. Induction of a crassulacean acid-like metabolism in the C_4 succulent plant, *Portulaca oleracea* L.: study of enzymes involved in carbon fixation and carbohydrate metabolism. **Plant and Cell Physiology**, v. 45, n. 5, p. 618–626, 2004. DOI: 10.1093/pcp/pch073.

LEISNER, C. P.; COUSINS, A. B.; OFFERMANN, S.; OKITA, T. W.; EDWARDS, G. E. The effects of salinity on photosynthesis and growth of the single-cell C_4 species *Bienertia sinuspersici* (Chenopodiaceae). **Photosynthesis Research**, v. 106, n. 3, p. 201–214, 2010. DOI: 10.1007/s11120-010-9595-z.

LEPINIEC, L.; VIDAL, J.; CHOLLET, R.; GADAL, P.; CRÉTINT, C. Phospho*enol*pyruvate carboxylase: structure, regulation and evolution. **Plant Science**, v. 99, 1994.

LIM, Y. Y.; QUAH, E. P. L. Antioxidant properties of different cultivars of *Portulaca oleracea*. **Food Chemistry.** v. 103, p. 734–740, 2007. DOI: 10.1016/j.foodchem.2006.09.025.

LIU, D. et al. Perspectives on the basic and applied aspects of crassulacean acid metabolism

(CAM) research. **Plant Science**, v. 274, p. 394–401, 2018. DOI: 10.1016/j.plantsci.2018.06.012.

LUNDGREN, Marjorie R. C_2 photosynthesis: a promising route towards crop improvement? **New Phytologist**, v. 228, n. 6, p. 1734–1740, 2020. DOI: 10.1111/nph.16494.

MATTHEWS, J. F.; KETRON, D. W.; ZANE, S. F. The biology and taxonomy of the *Portulaca oleracea* L. (Portulacaceae) complex in North America. **Rhodora**, v. 95, n. 882, p. 166–183, 1993.

MAZEN, A. M. A. Changes in levels of phosphoenolpyruvate carboxylase with induction of crassulacean acid metabolism (CAM)-like behavior in the C_4 plant *Portulaca oleracea*. **Physiologia Plantarum**, v. 98, n. 1, p. 111–116, 1996. DOI: 10.1111/j.1399-3054.1996.tb00681.x.

MAZEN, A. M. A. Changes in properties of phosphoenolpyruvate carboxylase with induction of crassulacean acid metabolism (cam) in the C_4 plant *Portulaca oleracea*. **Photosynthetica**, 2000. DOI: 10.1023/A:1010969419962.

MONSON, R. K. The origins of C_4 genes and evolutionary pattern in the C_4 metabolic phenotype. *In*: SAGE, R. F.; MONSON, R. K. (org.). **C_4 Plant Biology**. San Diego: Academic Press, 1999. p. 49–87.

MORONEY, J. V; JUNGNICK, N.; DIMARIO, R. J.; LONGSTRETH, D. J. Photorespiration and carbon concentrating mechanisms: two adaptations to high O_2 , low CO_2 conditions. Photosynth Research, n. 117, p. 121–131, 2013. DOI: 10.1007/s11120-013-9865-7.

NIMMO, H. G. The regulation of phospho*enol*pyruvate carboxylase in CAM plants. **Trends in Plant Science,** v. 5, n. 2, p. 75–80, 2000.

OBIED, W. A.; MOHAMOUD, E. N.; MOHAMED, O. S. A. *Portulaca oleracea* (purslane): nutritive composition and clinico-pathological effects on Nubian goats. **Small Ruminant Research,** v. 48, n. July 1994, p. 31–36, 2003.

OCAMPO, G.; COLUMBUS, J. T. Molecular phylogenetics, historical biogeography, and chromosome number evolution of *Portulaca* (Portulacaceae). **Molecular Phylogenetics and Evolution**, v. 63, n. 1, p. 97–112, 2012. DOI: 10.1016/j.ympev.2011.12.017.

OCAMPO, G.; KOTEYEVA, N. K.; VOZNESENSKAYA, E. V.; EDWARDS, G. E.; SAGE, T. L.; SAGE, R. F.; COLUMBUS, J. T. Evolution of leaf anatomy and photosynthetic pathways in Portulacaceae. **American Journal of Botany**, v. 100, n. 12, p. 2388–2402, 2013. DOI: 10.3732/ajb.1300094.

PARK, J.; OKITA, T. W.; EDWARDS, Ge. E. Salt tolerant mechanisms in single-cell C_4 species *Bienertia sinuspersici* and *Suaeda aralocaspica* (Chenopodiaceae). **Plant Science**, v. 176, n. 5, p. 616–626, 2009. DOI: 10.1016/j.plantsci.2009.01.014.

PETERS, W.; BECK, E.; PIEPENBROCK, M.; LENZ, B.; SCHMITT, J. M. Cytokinin as a negative effector of phosphoenolpyruvate carboxylase induction in *Mesembryanthemum crystallinum*. **Journal of Plant Physiology**, v. 151, n. 3, p. 362–367, 1997. DOI: 10.1016/S0176-1617(97)80266-0.

RADHAKRISHNAN, R.; ZAKARIA, M. N. M.; ISLAM, M. W.; CHEN, H. B.; KAMIL, M.; CHAN, K.; AL-ATTAS, A. Neuropharmacological actions of *Portulaca oleraceae* L v. sativa (Hawk). **Journal of Ethnopharmacology**, v. 76, n. 2, p. 171–176, 2001. DOI: 10.1016/S0378-8741(01)00230-6.

RASHED, A. N.; AFIFI, F. U.; DISI, A. M. Simple evaluation of the wound healing activity of a crude extract of *Portulaca oleracea* L. (growing in Jordan) in *Mus musculus* JVI-1. **Journal of Ethnopharmacology**, v. 88, n. 2–3, p. 131–136, 2003. DOI: 10.1016/S0378-8741(03)00194-6.

REN, S.; WEEDA, S.; AKANDE, O.; GUO, Y.; RUTTO, L.; MEBRAHTU, T.. Drought tolerance and AFLP-based genetic diversity in purslane (*Portulaca oleracea* L.). **Journal of Biotech Research**, v. 3, n. 1, p. 51–61, 2011.

RICCERI, C.; ARRIGONI, P. V. L'aggregato di *Portulaca oleracea* L. (Portulacaceae) in Italia. **Parlatorea**, v. 4, n. 1990, p. 91–97, 2000.

SAGE, R. F. Are crassulacean acid metabolism and C_4 photosynthesis incompatible?

Functional Plant Biology, v. 29, p. 775–785, 2002.

SAGE, R. F. The evolution of C_4 photosynthesis. **New Phytologist**, v. 161, p. 341–370, 2004. DOI: 10.1046/j.1469-8137.2004.00974.x.

SAGE, R. F. A portrait of the C_4 photosynthetic family on the 50th anniversary of its discovery: species number, evolutionary lineages, and Hall of Fame. **Journal of Experimental Botany**, v. 68, n. 2, p. e11–e28, 2017. DOI: 10.1093/jxb/erx005.

SAGE, R. F.; CHRISTIN, P.; EDWARDS, E. J. The C_4 plant lineages of planet Earth. **Journal of Experimental Botany.** v. 62, n. 9, p. 3155–3169, 2011. DOI: 10.1093/jxb/err048.

SAGE, R. F.; LI, M.; MONSON, R. K. The taxonomic distribution of C_4 photosynthesis. **C_4 Plant Biology**. San Diego: Academic Press, 1999, p. 551–584. DOI: 10.1016/b978-012614440-6/50017-3.

SCHILLER, K; BRÄUTIGAM, A. Engineering of crassulacean acid metabolism. **Annual Review of Plant Biology,** v. 72, p. 77–103, 2021.

SCHMITT, J. M.; PIEPENBROCK, M. Regulation of phospho*enol*pyruvate carboxylase and crassulacean acid metabolism induction in *Mesembryanthemum crystallinum* L. by Cytokinin. **New Phytologist**, v. 99, p. 1664–1669, 1992.

SILVERA, K. A.; NEUBIG, K. M.; WHITTEN, W. M.; WILLIAMS, N. H.; WINTER, K. C.; CUSHMAN, J. C. Evolution along the crassulacean acid metabolism continuum. **Functional Plant Biology**, v. 37, p. 995–1010, 2010. a.

SINGH, JS; SINGH, KP. Contibution to the ecology of ten noxious weeds. **The journal of the Indian Botanical Society**, v. 46, p. 440–451, 1967.

TABITA, F. R.; HANSON, T. E.; SATAGOPAN, S.; WITTE, B. H.; KREEL, N. E. Phylogenetic and evolutionary relationships of Rubisco and the Rubisco-like proteins and the functional lessons provided by diverse molecular forms. **Philosophical Transactions of the Royal Society**, v. 363, p. 2629–2640, 2008. DOI: 10.1098/rstb.2008.0023.

TAYBI, T.; CUSHMAN, J. C. Abscisic acid signaling and protein synthesis requirements for phosphoenolpyruvate carboxylase transcript induction in the common ice plant. **Journal of Plant Physiology**, v. 159, n. 11, p. 1235–1243, 2002. DOI: 10.1078/0176-1617-00834.

TCHERKEZ, G. G. B.; FARQUHAR, G. D.; ANDREWS, T. J. Despite slow catalysis and confused substrate specificity, all ribulose bisphosphate carboxylases may be nearly perfectly optimized. **PNAS,** v. 103, n. 19, p. 7246–7251, 2006.

TING, I. P. Crassulacean acid metabolism. **Annual Review of Plant Biology**, v. 36, p. 959–622, 1985. DOI: 10.1016/j.cub.2019.11.073.

VENGRIS, J.; DUNN, S.; STACEWICZ-SAPUNCAKIS, M. **L**ife history studies as related to weed control in the Northeast 7 - Common purslane. **Results Bulletin University of Massachusetts**, v. 46, n. 598, 2–45, 1972.

VON CAEMMERER, S.; QUICK, W. P.; FURBANK, R. T. The development of C_4 rice: current progress and future challenges. **Science**, v. 336, n. 6089, p. 1671–1672, 2012. DOI: 10.1126/science.1220177.

VOZNESENSKAYA, E. V.; KOTEYEVA, N. K.; EDWARDS, G. E.; OCAMPO, G. Revealing diversity in structural and biochemical forms of C_4 photosynthesis and a C_3-C_4 intermediate in genus *Portulaca* L. (Portulacaceae). **Journal of Experimental Botany**, v. 61, n. 13, p. 3647–3662, 2010. a. DOI: 10.1093/jxb/erq178.

VOZNESENSKAYA, E. V; FRANCESCHI, V. R.; KIIRATS, O.; ARTYUSHEVA, E. G.; FREITAG, H. Proof of C_4 photosynthesis without Kranz anatomy in *Bienertia cycloptera* (Chenopodiaceae). **The Plant Journal,** v. 31, n. 5, p. 649–662, 2002.

VOZNESENSKAYA, E. V; FRANCESCHI, V. R.; KIIRATS, O.; FREITAG, H.; EDWARDS, G. E. Kranz anatomy is not essential for terrestrial C_4 plant photosynthesis. **Nature**, v. 414, n. 6863, p. 543–546, 2001. DOI: 10.1038/35107073.

WALTER, J.; VEKSLYARSKA, T.; DOBEŠ, C. Flow cytometric, chromosomal and morphometric analyses challenge current taxonomic concepts in the *Portulaca oleracea* complex (Portulacaeae, Caryophyllales). **Botanical Journal of the Linnean**

Society, v. 179, n. 1, p. 144–156, 2015. DOI: 10.1111/boj.12309.

WINTER, K.; SMITH, J. A. C. An introduction to crassulacean acid metabolism. biochemical principles and ecological diversity. *In*: WINTER, K.; SMITH, J. A. C. (org.). **Crassulacean Acid Metabolism Biochemistry, Ecophysiology and Evolution**.: Springer-Verlag, 1996. p. 1–10.

WINTER, K. Ecophysiology of constitutive and facultative CAM photosynthesis. **Journal of Experimental Botany**, v. 70, n. 22, p. 6495–6508, 2019. DOI: 10.1093/jxb/erz002.

WINTER, K.; HOLTUM, J. A. M. Facultative crassulacean acid metabolism (CAM) plants: powerful tools for unravelling the functional elements of CAM photosynthesis. **Journal of Experimental Botany**, v. 65, p. 3425–3441, 2014. DOI: 10.1093/jxb/eru063.

WINTER, K.; SAGE, R. F.; EDWARDS, E. J.; VIRGO, A.; HOLTUM, J. A. M. Facultative crassulacean acid metabolism in a C_3–C_4 intermediate. **Journal of Experimental Botany**, v. 70, p. 6571–6579, 2019. DOI: 10.1093/jxb/erz085.

YANG, X. et al. A roadmap for research on crassulacean acid metabolism (CAM) to enhance sustainable food and bioenergy production in a hotter, drier world. **New Phytologist**, v. 207, p. 491–504, 2015.

YAZICI, I.; ISMAIL, T.; SEKMEN, A. H.; DEMIRAL, T. Salinity tolerance of purslane (*Portulaca oleracea* L.) is achieved by enhanced antioxidative system, lower level of lipid peroxidation and proline accumulation. **Environmental and Experimental Botany,** v. 61, p. 49–57, 2007. DOI: 10.1016/j.envexpbot.2007.02.010.

ZABALETA, E.; MARTIN, M. V.; BRAUN, H. P. A basal carbon concentrating mechanism in plants. **Plant Science**, 2012. DOI: 10.1016/j.plantsci.2012.02.001.

ZIMMERMAN, C. A. Growth characteristics of weediness in *Portulaca Oleracea* L. **Ecology**, v. 57, n. 5, p. 964–974, 1976. DOI: 10.2307/1941061.

ZIMMERMAN, C. A. A comparison of breeding systems and seed physiologies in three species of *Portulaca* L. **Ecology**, v. 58, n. 4, p. 860–868, 1977. DOI: 10.2307/1936221.

Hypothesis and goals

Three primary hypotheses tested here were:

1. The evolution of a C_4 cycle on top of a CAM-performing organism in *P. oleracea* might have required recruiting distinct genes encoding proteins specifically enrolled in each CCM cycle.

2. Due to its cosmopolite distribution, *P. oleracea* might possess high plasticity in CAM expression, particularly when comparing subspecies that have evolved under contrasting environmental conditions (*e.g.*, hot deserts *versus* cold mesic regions).

3. The alternation between C_4 and CAM might be differently regulated by endogenous signals in *P. oleracea* leaves, possibly involving different arrays of transcription factors and hormonal signals.

The overall goal was to significantly increase the understanding of molecular, biochemical, physiological and regulatory aspects of the photosynthetic plasticity in *P. oleracea*, which can be considered a photosynthetic marvel due to the presence of three photosynthetic pathways in a single organism (*i.e.* C_3 in stems, C_4 in leaves, and CAM in both organs). More specifically, the aims of this thesis were:

A. To utilize RNA-seq and RT-qPCR analysis to generate a global transcriptional profile and identify key components of the C_4 and CAM machineries involved in the complex photosynthetic transitions occurring in leaves and stems of *P. oleracea* under drought stress (to test **hypothesis 1**);

B. To evaluate C_4 and CAM plasticity within *P. oleracea* subspecies complex under well-watered and droughted conditions by using physiological and molecular approaches (to test **hypothesis 2**);

C. To explore the signaling events responsible for the up- and down-regulation of CAM expression in leaf tissues of *P. oleracea* plants subjected to contrasting water availability conditions using transcriptional profiling and network analysis data (to test **hypothesis 3**).

D. As an additional goal, we aimed to develop technical resources for promoting *P. oleracea* as a genetic model in the context of C_4-CAM photosynthesis, including the optimization of conditions for gene expression analysis and a stable genetic transformation protocol.

Chapter I

C_4/CAM facultative photosynthesis as a means to improve plant sustainable productivity under abiotic-stressed conditions: regulatory mechanisms and biotechnological implications

"What is a weed? A plant whose virtues have not yet been discovered."

Ralph Waldo Emerson

This chapter is organized as in the chapter published in the book "Plant Signaling Molecules" by Elsevier:

Ferrari, R. C; Freschi, L. C_4/CAM as a means to improve plant sustainable productivity under abiotic-stressed conditions: regulatory mechanisms and biotechnological implications. *In* Plant Signaling Molecules (eds Khan, M. I. R. et al.) 517–532 (Elsevier, Amsterdam, 2019). Doi: 10.1016/B978-0-12-816451-8.00032 -0.

Abstract

Crassulacean acid metabolism (CAM) and the C_4 pathway are photosynthetic adaptations that greatly improve plant water use efficiency. Both involve a prefixation of CO_2 into acids prior to the carbon fixation via Rubisco and require refined regulatory mechanisms to synchronize reactions and minimize energy waste. C_4 and CAM have been regarded as essentially incompatible, although the existence of C_4-CAM facultative species challenges this assumption. Considering the potential emergence of drier areas in many parts of the globe due to climate change, understanding the compatibility between C_4 and CAM holds enormous promise for future engineering of both photosynthetic adaptations in crop species. In this chapter, the major biochemical, anatomical and molecular features of C_4 and CAM are compared, and the stress signaling cascades controlling these syndromes are highlighted. The challenges and opportunities in combining the best of both photosynthetic adaptations into crops via genetic engineering approaches are also briefly discussed.

Keywords: abiotic stress, bioengineering, Crassulacean acid metabolism, *Portulaca*, stress signaling, water use efficiency

1. Initial considerations

When referring to carbon concentrating mechanisms (CCMs), it is important to take a first, brief overview of the selective pressures that lead to their evolution. Under low CO_2 availability, the oxygenase activity of Ribulose-1,5-biphosphate-carboxylase oxygenase (Rubisco) is favored, resulting in the production of 3-phosphoglyceric acid (PGA) and phosphoglycolate (PG), a toxic molecule capable of inhibiting photosynthesis, instead of PGA alone (Erb and Zarzycki, 2018; Miziorko and Lorimer, 1983). As a result, all plant lineages evolved the photorespiratory pathway, a complex mechanism that involves coordinated chemical reactions in chloroplasts, peroxisomes, and mitochondria. Photorespiration leads to the conversion of PG into less toxic products and yields back part of the CO_2 that would have been lost due to the formation of PG (Sage et al. 2012). For this reason, although energetically expensive, photorespiration is essential to photosynthetic organisms (Eisenhut et al. 2008).

Different methods for reconstructing atmospheric history converge in estimating that, for the last 40 million years until the present date, atmospheric CO_2 concentration has decreased from over 800 ppm to the current 390 ppm (Beerling and Royer, 2011; Zhang et al. 2013). In this scenario, photorespiration limits carbon fixation in plants performing C_3 photosynthesis, being intensified by high temperatures or stress conditions that promote stomatal closure and consequently lead to a decline in intercellular CO_2 levels (Keeley and Rundel, 2003). As atmospheric CO_2 levels dropped significantly, some photosynthetic organisms evolved CCMs, which are mechanisms capable of increasing inorganic carbon availability inside cells (Moroney et al. 2013; Raven et al. 2008). CCMs are responsible for a significant portion of Earth's inorganic carbon assimilation since they occur in a vast diversity of phylogenetic groups (Raven et al. 2008). These pathways have diversified among cyanobacteria (Badger et al. 1980; Badger et al. 2002), eukaryotic algae (Giordano et al. 2005; Meyer and Griffiths, 2013), basal embryophyte lineages (Raven et al. 2008), and flowering plants, either terrestrial or aquatic (Keeley and Rundel, 2003; Maberly and Madsen, 2002; Raven et al. 2008; Sage, 2004; Silvera et al. 2010). Among the distinct CCMs currently known, the C_4 photosynthesis and the Crassulacean acid metabolism (CAM) are particularly relevant for flowering plants; therefore, they will be the focus of this chapter. We do not intend to exhaustively review the biochemical, anatomical, regulatory and evolutionary similarities and differences between the C_4 and CAM systems, but instead we aim to discuss the compatibility between these two photosynthetic adaptations, the environmental regulation and signaling events controlling both syndromes and the potential biotechnological implications of engineering C_4 and CAM together into one crop species.

2. C_4 and CAM: similarities and differences

In the low CO_2 availability scenario, when increasing CO_2 assimilation involved higher transpiration losses, C_4 and CAM lineages evolved independently and irradiated, resulting in increased fitness under specific environmental conditions (Edwards and Ogburn, 2012; Ehleringer and Monson, 1993). These two pathways recruited existing genes, formerly involved in anaplerotic functions, to perform photosynthetic-related roles (Edwards and Ogburn, 2012). On their evolutionary trajectories, C_4 and CAM evolved from C_3 ancestors, and probably the first few characteristics opted lead to their final divergent phenotypes (Sage, 2002). CAM is considered to have arisen first, since it is present in basal lineages such as lycophytes, ferns, isoetids and cycads, whereas C_4 probably evolved more recently (Edwards and Ogburn, 2012; Ehleringer and Monson ,1993; Keely and Rundel, 2003; Silvera et al. 2010). C_4 is present in 19 angiosperm families, mostly grasses, representing roughly 3% of known species (Sage, 2017), while CAM is more widespread, occurring in 35 families (about 6% of total species number) (Silvera et al. 2010). C_4 and CAM can be considered as

photosynthetic syndromes, since both comprise a whole set of morphoanatomical and biochemical attributes, and may be associated with specific ecological niches.

2.1 Defining C_4 and CAM

Both pathways utilize organic four carbon (4-C) acids as temporary reservoirs of CO_2. C_4 photosynthesis, or dual-cell C_4, represents a spatial specialization, where CO_2 is prefixed into 4-C acids in mesophyll cells (MC) and transported to bundle sheath cells (BSC), the latter being the only cells containing Rubisco and performing the photosynthetic carbon reductive (PCR) cycle (Monson, 1999). On the other hand, CAM is a temporal specialization, with carbon prefixation into 4-C acids occurring at night, followed by day-time remobilization of acids to release CO_2 when the PCR cycle is active (Winter and Smith, 1996).

The steps involved in each mechanism can be described in a comparative manner, as similar biochemical modules are required in both these photosynthetic adaptations. As highlighted in recent next-generation sequencing (NGS) and biodesign studies (Borland et al. 2014; Schluter et al. 2016; Yang et al. 2015), both C_4 and CAM pathways require a coordinated series of reactions comprising distinct modules (*e.g.* 'carboxylation', 'decarboxylation', 'CO_2 acceptor regeneration', 'transfer acid generation', 'anatomy', 'stomatal control'), for which the participating enzymes and regulatory proteins have been identified over the years (Table 1). Despite efforts in dissecting the components of these modules, uncertainties remain, particularly regarding the role played by many transporters in both syndromes (Hibberd and Covshoff, 2010; Schluter et al. 2016).

2.2 Modules common to both C_4 and CAM plants

2.2.1 'Carboxylation' and 'decarboxylation' modules

A common set of enzymes and regulatory proteins are responsible for the 'carboxylation' and 'decarboxylation' modules in both syndromes (Fig. 1, Table 1). In C_4, the 'carboxylation' module is restricted to MC whereas the 'decarboxylation' module is confined to BSC, and both take place during day-time (Monson, 1999). In CAM, the 'carboxylation' and 'decarboxylation' modules occur in the same cells (Fig. 1), but during four distinct phases: carboxylation occurs at night when stomata are open (phase I); decarboxylation occurs during the day when stomata are closed (phase III); dawn and dusk are transition moments (phases II and IV, respectively), when phosphoenolpyruvate carboxylase (PEPC) activity declines and Rubisco initiates CO_2 assimilation (phase II), or vice-versa (phase IV) (Winter and Smith, 1996).

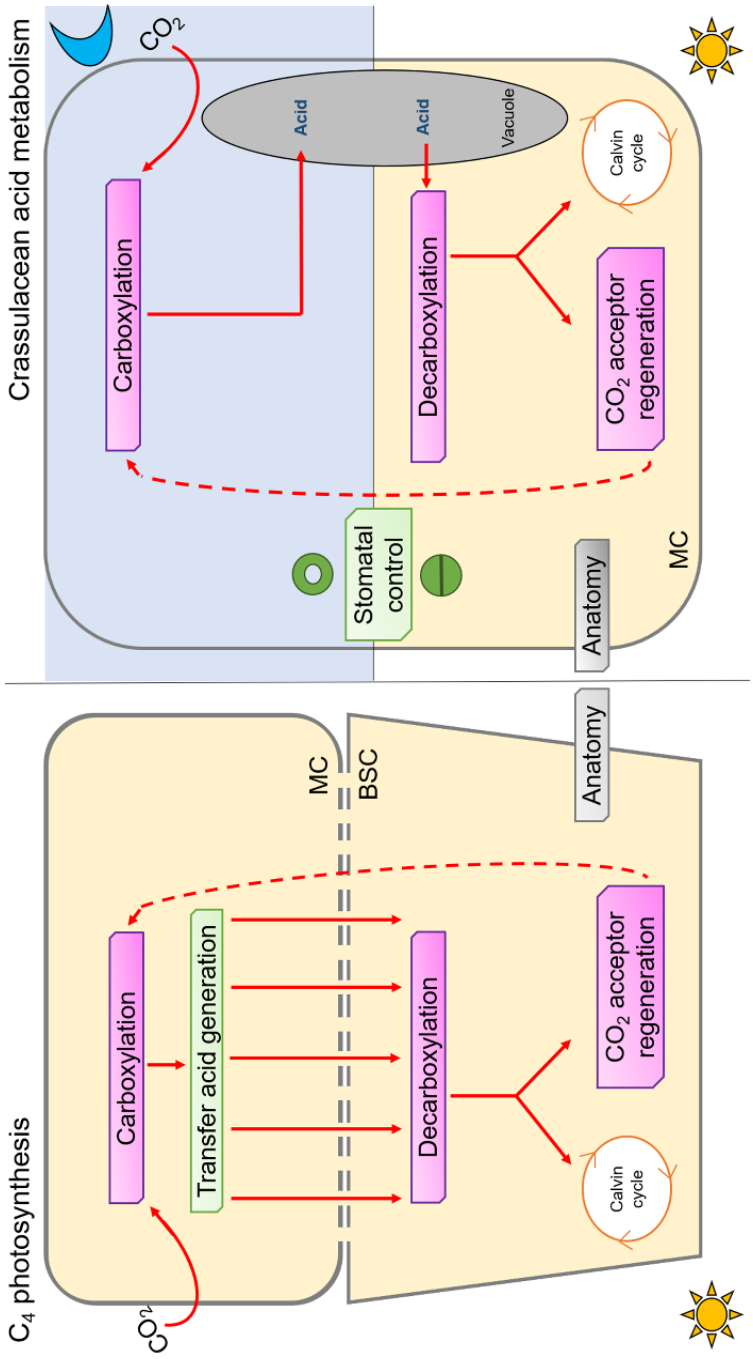

Figure 1: Comparative scheme between C_4 photosynthesis and Crassulacean acid metabolism. Boxes indicate modules composed of a set of genes. Exclusive modules are indicated in green boxes. Common modules are indicated in purple boxes. Grey boxes indicate modules that are different in composition but share a common theme. Red arrows indicate the carbon pathway inside the cells. MC = mesophyll cell; BSC = bundle sheath cell.

Table 1: Core candidate genes for C_4 and CAM syndromes based recent literature

Module	Gene	Type	Protein name	Reaction
Carboxylation		C_4/CAM		
	CA		Beta carbonic anhydrase	H_2CO_3 <=> CO_2 + H_2O
	PEPC		Phosphoenolpyruvate carboxylase	H_2O + phosphoenolpyruvate + HCO_3^- <=> phosphate + oxaloacetate
	V-ATPases		V-type proton ATPase	ATP + H_2O + H^+ (in) = ADP + phosphate + H^+ (out)
	ALMT		Aluminum-activated malate transporter	Presumably controlling malate influx and eflux in and out of the tonoplast
	VPPases		Pyrophosphate-energized vacuolar membrane proton pump	PP => 2 P
Decarboxylation		C_4/CAM		
	NADP-ME		NADP-dependent malic enzyme	Malate + $NADP^+$ <=> pyruvate + CO_2 + NADPH
	NAD-ME		NAD-dependent malic enzyme	Malate + NAD^+ <=> pyruvate + CO_2 + NADH
	PEPCK		Phosphoenolpyruvate carboxykinase	ATP + oxaloacetate <=> ADP + phosphoenolpyruvate + CO_2
	DiT2/DCT		Dicarboxylate transporter	Malate (out) + X => malate (in) + X
	DIC		Dicarboxylate carrier	Malate (out) + P or SO_4^- (in) => malate (in) + P or SO_4 (out)
	Pyruvate exporter		Unknown pyruvate exporter in mitochondria and chloroplasts	Pyruvate (in) + X => Pyruvate (out) + X
CO_2 acceptor regeneration[a]		C_4/CAM		
	PPDK		Pyruvate, phosphate dikinase	ATP + pyruvate + phosphate <=> AMP + phosphoenolpyruvate + diphosphate
	AMK		AMP kinase	AMP + ATP => 2 ADP
	PPase		Pyrophosphorylase	PP => 2 P
	BASS2		Sodium/pyruvate cotransporter BASS2	Pyruvate (out) + Na^+ (out) => pyruvate (in) + Na^+ (in)
	NHD		Na/H Antiporter	H^+ (out) + Na^+ (in) => H^+ (in) + Na^+ (out)
	PPT		Phosphoenolpyruvate transporter	PEP (in) + H^+ (in) + P (out) => PEP (out) + H^+ (out) + P (in)
	Proton pyruvate transporter		Unknown chloroplast pyruvate importer	Pyruvate (out) + H^+ (out) => pyruvate (in) + H^+ (in)
Transfer acid generation[b]		C_4		
	MDH		Malate dehydrogenase	Malate + $NAD(P)^+$ <=> oxaloacetate + NAD(P)H
	AlaAT		Alanine transaminase	Alanine + 2-oxoglutarate <=> pyruvate + glutamate

AspAT	Aspartate transaminase	Aspartate + 2-oxoglutarate <=> oxaloacetate + glutamate
DiT1/OMT	Dicarboxylate transporter 1	OAA (out) + malate (in) => malate (out) + OAA (in)
DiT2/DCT	Dicarboxylate transporter 2	OAA (out) + aspartate (in) => aspartate (out) + OAA (in)

[a] Although a PEP regeneration module has only been named separately for C_4, the reactions involved also occur in CAM and, for this work, it was considered here as part of the CO_2 acceptor regeneration module.

[b] The role played by many transporters is still unclear for both syndromes; therefore, we summarize the most probable candidate reported in the literature (Schluter et al. 2016).

The first carboxylation by PEPC is one of the key steps for both the C_4 and CAM photosynthesis (Fig. 1, Table 1). Because of its fundamental role, PEPC regulation has been widely studied and extensively reviewed (*e.g.* Chollet et al. 1996; Izui et al. 2004; Lepiniec et al. 1994; Nimmo et al. 2000). Allosteric regulation of PEPC involves effector molecules, being glucose-6-P (G-6-P) and triose-P positive effectors, and malate and aspartate negative regulators (Chollet et al. 1996). Different isoforms of PEPC are encountered in higher plants, involved both in photosynthetic and anaplerotic reactions. According to Christin et al. (2014), there are two major groups of PEPC genes in plants: *PPC-1* and *PPC-2*. The *PPC-1* group comprises all CAM- and C_4-related genes and was duplicated many times in different plant lineages, while *PPC-2* genes are related to C_3 housekeeping functions and are present in a single copy in plant genomes. The *PPC-1* lineage is divided in different groups: *PPC-1E2* and *PPC-1E1*, the latter containing the CAM and C_4 specific genes (Christin et al. 2014).

The most significant difference between PEPC isoforms is the substitution of an alanine for a serine residue near the N-terminal domain (Chollet et al. 1996). This serine can be phosphorylated, what is a critical step in the regulation of PEPC activity. A PEPC kinase is responsible for phosphorylating this serine residue, thus activating PEPC, whereas a typical mammalian-type protein phosphatase 2A (PP2A) converts PEPC back to its inactive form by dephosphorylating this residue (Nimmo, 2000). The activation of PEPC occurs in opposite moments of the diel cycle for C_4 and CAM (daytime and nighttime, respectively) and results in lower sensitivity to malate inhibition and higher sensitivity to G-6-P activation in both cases (Chollet et al. 1996).

Compared to the conserved role played by PEPC in all C_4 and CAM plants, distinct decarboxylation enzymes can be found among representatives of both syndromes. In fact, three types of C_4 photosynthesis can be defined according to the decarboxylation enzyme employed (*i.e.* NAD-ME, NADP-ME and PEPCK types), which are accompanied by ultrastructural differences involving chloroplast position in the BSC (Kanai and Edwards 1999). In the NADP-ME type, chloroplasts are arranged centrifugally and have reduced grana stackings; most oxaloacetate (OAA) is converted to malate, that is metabolized in MC and BSC chloroplasts. In NAD-ME type, chloroplasts and mitochondria are arranged centripetally and show developed grana stackings; most OAA is converted to aspartate in the cytoplasm, which is transferred to BSC mitochondria to be decarboxylated. While grana-rich chloroplasts are related to NADP and ATP production due to higher photosystem II activities and linear electron flow, lower grana content is related to ATP production and photosystem I-mediated cyclic electron flow (Edwards et al. 2004). In the PEPCK-type, chloroplasts also have developed grana stackings, and there may be a 30% contribution or more from NAD-ME decarboxylation (Bräutigam et al. 2014; Kanai and Edwards, 1999). Recently, this type has been questioned due to metabolite and energetic specific requirements that may be hard

to maintain in BSC (Wang et al. 2014). Overall, it is more probable that NAD- or NADP-ME act as the main decarboxylating enzyme and PEPCK act as a second decarboxylating enzyme instead of an exclusive PEPCK type (Bräutigam et al. 2014; Muhaidat et al. 2007; Wang et al. 2014).

The decarboxylation enzyme employed may also vary in CAM according to the species, and options are the same as employed by C_4. In addition, the transitory carbohydrate pool converted into phosphoenolpyruvate (PEP) for CO_2 assimilation can be starch or soluble sugars (Borland et al. 2016; Holtum et al. 2005), resulting in an array of combinations of transitory carbohydrate pool and decarboxylation system.

2.2.2 'Anatomy' module

Anatomical traits are encompassed in an 'anatomy' module, but although the theme is common, different attributes are involved for each syndrome (Fig. 1, Table 1). Most C_4 plants present Kranz anatomy, named after the well-developed layer of BSC surrounding vascular bundles and containing all Rubisco and glycine decarboxylase (GD) activity of the leaf (Hibberd and Covshoff, 2010; Sage, 2004). However, there are also a few examples of single-cell terrestrial C_4 photosynthesis, indicating that the presence of Kranz anatomy is not mandatory (Voznesenskaya et al. 2001). In these cases, dimorphic chloroplasts can be found inside a single MC, where there is asymmetrical distribution of C_4-related enzymes and organelles between the distal and proximal regions of the cytoplasm, as in *Borszczowia aralocaspica*, or between internal and external regions, as in *Bienertia cycloptera* (Edwards et al. 2004; Voznesenskaya et al. 2001, 2002).

Different types of Kranz anatomy can be found among dual-cell C_4 representatives based on the position of MC, BSC, vascular bundles and other tissues, also varying between eudicots and monocots (Dengler and Nelson, 1999; Edwards et al. 2004; Muhaidat et al. 2007). However, there is no well-specified correlation between specific anatomical and biochemical types (Muhaidat et al. 2007). Other important traits associated to Kranz anatomy, all aiming to provide short distances for metabolite diffusion but at the same time avoid CO_2 leakage, are: (1) low M:BSC ratio with numerous plasmodesmata connecting these two cell types, (2) increased vein density, (3) thin leaves, and (4) a diffusion barrier in or around BSC, with either suberization of cell walls or high concentration of organelles at peripheric regions (Dengler and Nelson, 1999; Edwards et al. 2004; Sage, 2004). Specific mesophyll and bundle sheath *trans* and *cis*-acting elements for core C_4 enzymes have been identified and some have already been tested successfully (Wang et al. 2017). Moreover, tissue specificity in C_4 leaves is guaranteed via epigenetic, transcriptional and post-transcriptional, translational and post-translational regulation (Fig. 2; Reeves et al. 2016).

In line with the need of accumulating large quantities of 4-C acids in vacuoles of MC overnight, the most frequent anatomical features related to CAM are (1) increased MC size, (2) reduced intercellular air space (IAS), (3) reduced mesophyll surface exposed to IAS (L_{mes}) per unit area, and (4) increased leaf thickness compared to C_3 and C_4 species (Nelson et al. 2005). This results in more succulent leaves and prevents CO_2 efflux during the day, although an increase in succulence itself is not related to higher CAM expression (Nelson and Sage, 2008).

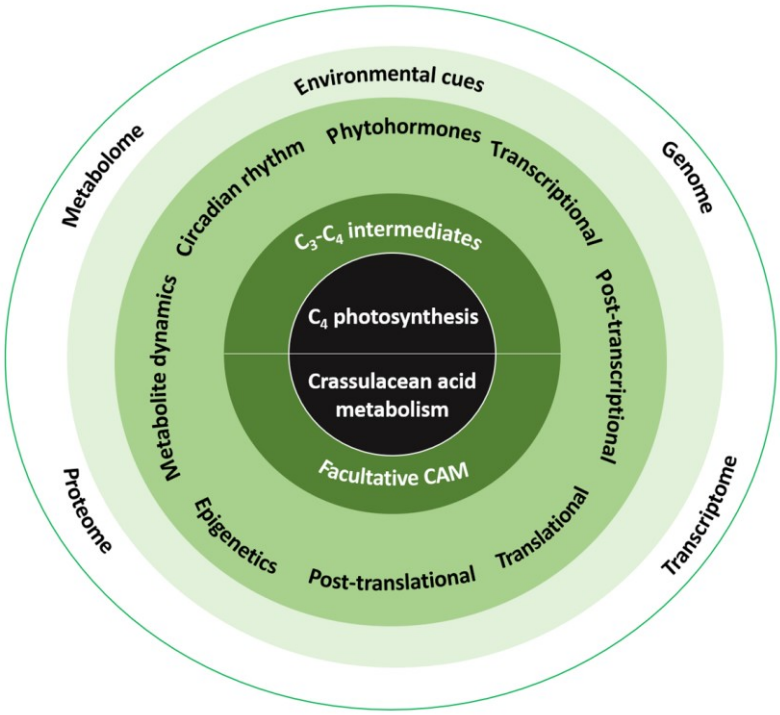

Figure 2: C_4 and CAM are both complex syndromes that are regulated in many different levels. The study of intermediary and facultative systems for C_4 and CAM, respectively, using 'omics'' technologies is very promising in understanding the regulatory processes. The two inner circles represent both photosynthetic metabolism types and its variations. The three outer circles represent the regulatory levels and 'omics' fields that can be used to explore them.

2.3 Exclusive modules: 'transfer acid generation' and 'stomatal control'

Lastly, there are two exclusive modules, one related to each syndrome alone. The 'transfer acid generation' module (Table 1) is very relevant for dual-cell C_4 representatives since metabolites must flow between two different cell types (*i.e.* MC and BSC) (Schluter et al. 2016). As the type of transfer acid formed in MC and the place of decarboxylation in BSC may vary, this module involves a variable number of genes depending on the species. Essentially, it comprises proteins responsible for transporting or generating metabolites in

different cell compartments such as mitochondria, chloroplasts and the cytosol (Kanai and Edwards, 1999; Schluter et al. 2016).

On the other hand, the so-called 'stomatal control' module is particularly relevant in CAM research. In C_3 and C_4, stomata remain open during the day and closed during the night. In contrast, in most CAM plants stomata remain closed during the day (phase III) probably due to the increase in partial CO_2 pressure (pCO_2) from daytime acid decarboxylation, followed by nocturnal stomata opening (Borland and Taybi, 2004; Hartwell, 2005). Stomata may also remain open during transitional phase II in some species, promoting a burst in CO_2 assimilation at the beginning of the light period (Winter and Holtum, 2014). In the CAM species *Agave americana*, several protein kinase-encoding genes, including *HIGH LEAF TEMPERATURE 1* (*HT1*), *OPEN STOMATA 1* (*OST*) and *SnRK2.10*, presented rescheduled expression compared to their orthologs in *Arabidopsis thaliana* (Abraham et al. 2016). Furthermore, *PHOTOTROPIN 2* (*PHOT2*), which encodes a blue light receptor, showed an inverted pattern of expression in the CAM plant model *Kalanchöe fedtschenkoi* compared to that observed in C_3 species (Yang et al. 2017). Also, genes related to ion channels in guard cells, such as *POTASSIUM TRANSPORTER 2/3* (*AKT2/3*) and *CHLORIDE CHANNEL FAMILY* (*CLC-c*), showed reciprocal expression behavior in *A. americana* compared to that described in *Arabidopsis* (Abraham et al. 2016). Therefore, these genes exemplify some of the promising candidates associated with the inverted stomatal control typically found in CAM plants (Abraham et al. 2016; Yang et al. 2017).

3. Environmental cues controlling C_4 and CAM

As stated by Lüttge (2004), environmental cues act as an input upon organisms, referred to as receivers, and this interacting network will result in an output at community and ecosystems level. The input affects genotypes and phenotypes of receivers, the latter including morphotype and physiotype. C_4 and CAM, both including genotypes and phenotypes components, represent two cases of parallel convergent evolution, where unrelated taxa from various phylogenetic backgrounds have evolved similar mechanisms in two independent ways (Christin et al. 2013, 2014; Muhaidat et al. 2007; Sage, 2017; Silvera et al. 2010). This makes the study of how representatives from both syndromes respond to the environment particularly interesting since a diverse array of strategies and different magnitudes of response has been observed.

In C_4 species such as the traditionally studied monocots maize (*Zea mays*) and sugarcane (*Saccharum officinarum*) or in CAM crops such as *Agave americana* or *Opuntia ficus-indica*, the CCM is constitutively expressed. Among CAM plants, there are also facultative species, whose CAM expression is highly influenced by environmental cues, thereby representing valuable tools for dissecting the regulatory mechanisms responsible for adjusting the CCM

expression in response to the surrounding environmental conditions (Winter et al. 2007; Winter and Holtum, 2014). In addition, increasing attention has been dedicated to the so-called C_3-C_4 intermediates, which may shed light on evolutionary paths leading to full C_4 expression (Christin et al. 2011).

An interesting strategy to understand how external cues affect organisms is to study these intermediate and facultative phenotypes, because the first may help to understand evolutionary paths, and in the latter, the timing and inducing factors can be controlled without developmental interference (Christin et al. 2011; Winter and Holtum, 2014; Winter et al. 2007).

3.1 Modulation of C_4 by environmental cues

The relationship between dual-cell C_4 and environmental cues can be traced in an evolutionary panorama or considering phenotypically plastic responses. Regarding the latter, a great description of environmental variables – such as light, water, nitrogen, and temperature – and how they modulate photosynthetic aspects of C_4 plants was made by Long (1999). When referring to the biochemical types of C_4, NAD-type grasses were able to enhance water use efficiency (WUE) at leaf level in a higher proportion than NADP-ME type grasses, what was probably related to stomatal adjustments (Ghannoum et al. 2002).

Dual-cell C_4 requires more specialized structural arrangements when compared to single-cell C_4, C_3 and CAM, and presents more restricted geographic distribution than the latter two types. This can be correlated to a reduced potential for phenotypic plasticity when compared to C_3 plants, as stated by Sage and McKown (2006). These authors highlight that acclimation processes must involve coordinated changes in the different tissues involved in C_4 to keep functional stoichiometries. Besides, when compared to C_3 plants, dual-cell C_4 representatives display restricted potential to modulate leaf thickness, due to the enlarged BSC, the costs associated with changes in vein density, and a limited capacity to modulate Rubisco content. However, there are exceptions to this assumption, since *Flaveria bidentis* and maize have been shown to exhibit plastic acclimation responses to low-light conditions (Pengelly et al. 2010; Bellasio and Griffiths, 2014), indicating that this subject needs further investigation. Plants exhibiting single-cell C_4 do not face such structural constraints since they can more easily modulate photosynthesis-related processes within a single photosynthetic cell (Edwards et al. 2004; Voznesenskaya et al. 2001). Perhaps, in this case, more plastic responses could be observed, but no experimental evidence has been reported yet.

Similarly, little is known about the phenotypic plasticity within C_3–C_4 intermediate species. This photosynthetic type is considered a transitional stage between ancestral C_3 and fully expressed C_4, as it presents biochemical and anatomical features of both photosynthetic types (Christin et al. 2011; Monson and Moore, 1989). In a different point of view, C_3–C_4 plants

can also be treated as a successful adaptive strategy, not merely as a transitional stage, as is the case for *Mollugo verticillata* and *M. nudicaulis*. These two species are weeds that show a cosmopolitan distribution, suggesting that the intermediate photosynthetic type may have contributed to their wide geographical distribution (Christin et al. 2011).

Differently from most C_4 and C_3-C_4 intermediates, the aquatic species *Eleocharis vivipara* stands out as a remarkable example of C_4 expression controlled by environmental circumstances (Ueno et al. 1988). *E. vivipara* produces C_3 photosynthetically active culms when underwater, but emerged C_3 culms wither away and new C_4 culms develop after a few days (Ueno et al. 1988; Ueno, 2001). The C_4 culms have already been characterized biochemically and anatomically (Ueno, 2001), and C_4-related gene expression is not strictly dependent on Kranz anatomy in the species (Uchino et al. 1998).

3.2 Modulation of CAM by environmental cues

It is increasingly accepted that a higher plasticity can be found between and within CAM plants than in most C_4 species (Edwards and Ogburn, 2012). Compared to the rare examples of C_3-C_4 facultative plants (*e.g. E. vivipara, E. baldwinii*), a significantly higher number of C_3-CAM facultative species are described in the literature (Silvera et al. 2010; Winter et al. 2015). Moreover, even obligate CAM species display some plasticity in CAM expression during early developmental stages (Freschi et al. 2010; Winter et al. 2007). In this sense, CAM has been considered a trait with continuous distribution oppositely to an all-or-nothing adaptive response (Silvera et al. 2010; Winter et al. 2015).

Besides the variation in plasticity (*i.e.* constitutive versus facultative CAM), differences in the magnitude of nighttime acid accumulation and the diel pattern of stomata opening also greatly vary among CAM, giving rise to the following CAM modes: (1) CAM-cycling, in which gas exchange is limited to daytime, with nocturnal acid production due to respiratory CO_2 recycling, and (2) CAM-idling, which is an emergency process triggered during periods of prolonged drought and heat. The latter state is characterized by the complete closure of stomata over the diel cycle associated with a small nocturnal acid production from respiratory CO_2 recycling (Cushman, 2001). Both these modes are considered weak versions of CAM as the amount of acids accumulated overnight is usually lower than in plants performing classical CAM.

Facultative plants frequently perform weak CAM for variable portions of their life cycles; therefore, the adaptive advantages of facultative CAM have been questioned (Herrera, 2009). However, even if a low level of CAM is induced, this may improve plant survival by increasing WUE, promoting a positive carbon balance, intensifying the photo-protection of the photosynthetic machinery, and, consequently, improving reproductive success (Herrera, 2009; Winter and Holtum, 2014).

Due to the absence of clear anatomical traits characterizing CAM and the fact that $\delta^{13}C$ values in facultative CAM species tend to be closer to C_3 plants, detailed physiological studies are required to properly identify facultative CAM (Silvera et al. 2010; Winter et al. 2015). This may contribute to an underestimation of the total number of facultative C_3-CAM species (Silvera et al. 2010). Nevertheless, confirmed facultative CAM species have been described in Bromeliaceae, Crassulaceae, Montiaceae, Piperaceae, Portulacaceae, Talinaceae and Clusiaceae families (Winter and Holtum 2014). In most facultative species, CAM expression can be induced or intensified by drought either alone or in combination with other environmental stresses such as nutrient availability and changes in temperature, light intensity and photoperiod (Silvera et al. 2010). In the halophyte *Mesembryanthemum crystallinum*, either drought or salt stress strongly induce CAM (Cushman et al. 1990; Herppich et al. 1992; Winter and Holtum, 2007), and although a great deal of physiological, signaling and molecular studies has been performed in this facultative model (Bohnert et al. 1988; Cushman et al. 1990; Cushman et al. 2008; Herppich et al. 1992; Holtum and Winter, 1982; Winter and Holtum, 2007), much still remains to be elucidated.

Besides *M. crystallinum*, constitutive and facultative CAM species belonging to the tropical genus *Clusia* have also been intensively studied over the years (Lüttge 1996; 2006). CAM induction may be under developmental control as in *C. rosea*, *C. alata* and *C. hilariana*; or under environmental control in a fully reversible manner as in *C. pratensis*; or even exhibit intermediary influences as in *C. minor* (Winter et al. 2007). Given the rapid, intense and completely reversible induction of CAM observed in *C. pratensis* in response to drought, this species has emerged as an interesting model for future studies on the regulation of facultative CAM (Winter and Holtum, 2014).

4. Stress signaling networks controlling C_4 and CAM

As presented so far, C_4 and CAM are both complex syndromes, involving multiple genes, complicated metabolite dynamics, biochemical adjustments, and sometimes anatomical specializations. This implies the existence of equally complex signaling routes, as stated by Freschi and Mercier (2012) for CAM signaling, and here extended to C_4. Intricate transcriptional, translational, post-translational, and metabolic regulatory changes are supposedly required to facilitate the establishment and functioning of either CCM in a given tissue (Fig. 2). This includes, but is not limited to, coarse changes in enzyme content/activity and the fine-tuned control of regulatory proteins (*e.g.* transcription factors, kinases, phosphatases) (Taybi et al. 2002).

Most of the studies regarding the establishment of the C_4 machinery has been based on the developmental gradient in leaves (*e.g.* Li et al. 2010; Pick et al. 2011), since C_4 induction upon environmental variables is rare, with a few exceptions in the *Eleocharis* genus (Ueno,

2001) as previously mentioned. In *E. vivipara* submerged plants, abscisic acid (ABA) was shown to induce Kranz anatomy formation and C_4-like biochemical traits (Ueno, 1998) whereas in the C_3-C_4 intermediate *E. baldwinii*, full C_4 was induced after ABA treatment causing auxin signaling and changes in the transcriptional profile of genes involved in the glycolytic pathway, ion and metabolite transporters, citrate metabolism, among other processes (Chen et al. 2014). Recent evidence also indicated that PEPC content and activity increased in light-exposed *Amaranthus hypochondriacus* leaf discs upon ABA treatment (Aloor et al. 2017), suggesting that it may be advantageous for C_4 plants to keep PEPC activated by ABA under drought stress conditions.

Although still fragmented, our current knowledge on the stress signaling cascades controlling CAM expression is relatively more detailed than for C_4 photosynthesis (Taybi et al. 2002; Freschi and Mercier, 2012). Most studies have been performed in the C_3-CAM halophyte *M. crystallinum*, but data is also available for other few CAM species including pineapple (*Ananas comosus*), and *K. blossfeldiana*. The signaling cascades controlling CAM expression in these species have been extensively reviewed first by Taybi et al. (2002) and later by Freschi and Mercier (2012); therefore, they are briefly discussed here.

Data indicate that ABA and cytokinins (Cks) play opposite roles in controlling CAM expression (Chu et al. 1990; Schmitt and Piepenbrock, 1992; Thomas and Bohnert, 1993; Thomas et al. 1992), which agrees to the contrasting impact of water availability on the biosynthesis of these two hormonal classes (Hare et al. 1997; Pospisilova et al. 2000; Pospisilova et al. 2005; Tanaka et al. 2006). Two major lines of evidence support a promotive role of ABA on CAM expression. First, exogenous ABA has been shown to increase the activity and/or mRNA levels of CAM-related enzymes both in detached leaves and intact plants (Chu et al. 1990; Dai et al. 1994; Forsthoefel et al. 1995a; Forsthoefel et al. 1995b; Freschi et al. 2010; Taybi et al. 1995; Taybi and Cushman, 1999; Taybi and Cushman, 2002; Tsiantis et al. 1996;). Second, stress-induced CAM expression is normally accompanied by an increment in endogenous ABA content (Freschi et al. 2010; Taybi et al. 1995; Taybi and Cushman, 2002). However, studies indicate that a parallel, non ABA-dependent, signaling route is also involved in controlling CAM expression in response to environmental stresses (Freschi et al. 2010; Taybi and Cushman, 2002).

In contrast, accumulating evidence implicates Cks as negative regulators of CAM expression in facultative CAM species as the stress-induced increase in CAM expression in facultative plants is usually accompanied by a reduction in endogenous Ck levels (Freschi et al. 2010; Peters et al. 1997), and exogenous Cks generally represses CAM induction in response to stress conditions (Freschi et al. 2010; Peters et al. 1997; Schmitt et al. 1996; Schmitt and Piepenbrock, 1992). Some studies also indicate that exogenous methyl jasmonate (MJA) can

limit CAM expression in droughted *M. crystallinum* plants (Dai et al. 1994; Schmitt et al. 1996), though the roles of endogenous MJA still remain elusive. More recently, gibberellin (GA) levels have been reported to decrease and not recover in *Aptenia cordifolia* plants exposed to successive drought stress, being thus connected to a drought stress memory response in CAM expression (Fleta-Soriano et al. 2015).

So far, only a few second messengers have been demonstrated to control CAM expression in facultative plants (Freschi et al. 2010; Taybi and Cushman, 1999; Taybi and Cushman, 2002; Taybi et al. 2002;). Among them, the influx of extracellular calcium (Ca^{2+}) has been identified as a key downstream event in both ABA-dependent and -independent signaling pathways leading to CAM expression (Freschi et al. 2010; Taybi et al. 2002). Data also indicate that inositol-1,4,5-triphosphate (IP3) and nitric oxide (NO) participate in the ABA-dependent signaling cascade promoting CAM expression (Taybi et al. 2002).

In addition to studies focused on specific signaling events, the generation of genomic and transcriptomic databases for both facultative and obligate CAM species has also recently opened a window of opportunities for more detailed characterization of the stress signaling cascades controlling CAM expression (Abraham et al. 2016; Brilhaus et al. 2016; Wai et al. 2017). In *Tallinum triangulare*, ABA-responsive transcription factors were among the most up-regulated transcription factors during the drought-triggered CAM induction (Brilhaus et al. 2016). In addition, studies also indicate that several families of miRNAs presumably target key CAM-related enzymes, and many of these miRNAs display a circadian pattern of expression in *Ananas comosus* (Wai et al. 2017). Cluster analysis of gene expression patterns leading to the generation of co-expression modules have also been increasingly employed to identify less obvious candidate genes potentially involved in controlling CAM expression. For example, *CONSTANS*-like genes and *REVEILLE* transcription factor-encoding genes have been grouped with PEPC and NADP-ME genes, thereby suggesting their potential involvement in controlling the CAM machinery in *K. fedtschenkoi* (Yang et al. 2017).

Metabolite fluctuation is also reported as an important layer of control in CAM plants (Borland and Taybi, 2004). In *Agave americana*, besides malic and fumaric acid nocturnal fluctuation, ascorbic acid was also shown to accumulate during the night, presumably providing anti-redox power against reactive oxygen species (ROS) in this CAM plant (Abraham et al. 2016). Glycolysis and carbohydrate metabolism-related transcripts have been highlighted as a very important step for CAM regulation (Brilhaus et al. 2016; Yang et al. 2017). Moreover, the transcript abundance of core CAM and starch degradation-related enzymes were drastically altered in a starch and CAM-deficient *M. crystallinum* mutant, thereby reinforcing the role of carbohydrates in CAM regulation (Taybi et al. 2017).

5. C_4 / CAM compatibility

C_4 and CAM have been considered incompatible syndromes for various reasons: (1) they show differential regulation of enzymes involved in the carboxylation and decarboxylation steps; (2) the metabolite transport dynamics of each syndrome is strikingly different; and (3) structural arrangements for each syndrome differ, favoring Kranz anatomy in C_4 and succulence in CAM (Sage, 2002). In addition to this list, Sage (2002) also highlights that the evolutionary pathways selecting for each of these photosynthetic behaviors appear to be exclusive. Thus, the simultaneous evolution of C_4 and CAM in a single organism would be unnecessary.

One of the most stunning cases, the order Caryophyllales, contains many C_4 and/or CAM origins including its intermediates variants (Kellogg, 1999), being considered a hotbed for these CCMs (Edwards and Ogburn, 2012). To illustrate the photosynthetic diversity of Caryophyllales, the following representatives of the order are here listed: *Borszczowia aralocaspica* and *Bienertia cycloptera* (Chenopodiaceae), the two species known to perform single-cell C_4 in a family of many dual-cell C_4 (Edwards et al. 2004); cacti (Cactaceae), traditionally known to be obligate CAM plants (Ocampo and Columbus, 2012); and the "Portullugo" clade, as referred to by Edwards and Ogburn (2012), comprising the sister-groups Molluginaceae and Portulacaceae, that each evolved C_4 independently (Christin et al. 2011, 2014). Both families contain C_3, C_4, and C_3–C_4 intermediates, and the latter, monogeneric, also includes C_4–CAM species (Edwards and Ogburn, 2012). Recently, Christin et al. (2015) studying C_4 evolution in Caryophyllales reinforced that genetic enablers were present in C_3 ancestors and genes were co-opted into C_4 when already expressed in a C_4-manner. However, the identity of the co-opted candidates varies in different lineages inside Caryophyllales, representing truly independent evolution events of C_4 photosynthesis.

The genus *Portulaca* is an exception to the C_4–CAM incompatibility assumption. *Portulaca* comprises about 60 species of C_4 annual weeds, of which many, if not all and including the C_3-C_4 intermediate species, can undergo CAM induction upon environmental stimuli (Guralnick and Jackson, 2001; Guralnick et al. 2002; Holtum et al. 2017; Koch and Kennedy, 1980, 1982; Ku et al. 1981; Winter and Holtum, 2017; Winter et al. 2019). This metabolic plasticity has been better studied in *P. grandiflora* and *P. oleracea* (Christin et al. 2014; Guralnick and Jackson, 2001; Guralnick et al. 2002; Mazen, 1996, 2000), revealing that both leaves and stems display the induction of CAM-like features under stress conditions (Guralnick et al 2002; Koch and Kennedy, 1980; 1982; Mazen, 1996; Voznesenskaya et al. 2010).

The first discovery was carried out in *P. oleracea,* when leaves were shown to increase nocturnal acidity and perform a low level of CO_2 assimilation in the dark after prolonged periods of water deprivation or under short-day conditions (Koch and Kennedy, 1982; 1980). Similar findings of a CAM-like behavior were made around the same time for *P. grandiflora*

(Ku et al. 1981), and after a decade, the records of CAM in these two species plus *P. pilosa* (previously known as *P. mundula*) were confirmed (Kraybill and Martin, 1996). Moreover, leaf PEPC content was shown to increase in *P. oleracea* as the drought period was prolonged, associated with opposite diel changes in PEPC kinetic properties characterized by a peak in PEPC activity during the day and higher malate sensitivity at night in well-watered plants, and the exact opposite pattern in drought-stressed individuals (Mazen, 1996, 2000).

In line with these findings, the comparison of the global transcriptional profile of well-watered and droughted *P. oleracea* plants lead to the identification of two PEPC-encoding genes differentially regulated under each condition: while *PoPPC1E1c* was highly expressed during the night in droughted plants, *PoPPC1E1a'* was predominantly expressed during the day and in well-watered samples (Christin et al. 2014). Therefore, *PoPPC1E1c* and *PoPPC1E1a'* were probably recruited by the CAM and C_4 pathways, respectively, which may have facilitated the evolution of regulatory mechanisms to allow the expression of both CCM in leaves of this plant species. According to the evolutionary history of PEPC genes and considering the existence of other CAM plants with close phylogenetic proximity, C_4 probably evolved on top of a CAM-performing organism (Christin et al. 2014), and the CAM pathway may have been lost in most species of the genus. In addition, the appearance of different types of C_4 in different *Portulaca* species (*e.g. P. oleracea* is NAD-ME type and *P. grandiflora* is NADP-type) reinforces this hypothesis, where C_4 would have evolved independently in each species (Voznesenskaya et al. 2010).

Based on immunoblot results, Lara et al. (2003, 2004) proposed a first hypothetical model of C_4–CAM compatibility in *P. oleracea.* Most *Portulaca* leaves have three types of cells: water storage cells (WSC), whose contribution to overall carbon gain may be minimal due to their small number of chloroplasts, and photosynthetically active MC and BSC (Lara et al 2003, 2004; Voznesenskaya et al. 2010). In the hypothetical model, malate generated from CAM at night in WSC and MC would be shuttled to BSC for decarboxylation during the day (Lara et al 2004).

The compatibility between C_4 and CAM observed in certain *Portulaca* species is much more than an evolutionary curiosity, as these species represent a particularly interesting model for exploring the molecular, biochemical and signaling mechanisms responsible for allowing the occurrence of these distinct photosynthetic modes within a single individual (Yang et al. 2015). Among the C_4-CAM facultative *Portulaca* species currently identified, *P. oleracea* display short size, rapid growth, flat leaves and abundant production of long-lived seed (Zimmerman, 1976), making this species a particularly attractive target for future research on C_4/CAM compatibility.

6. Engineering C_4 and CAM: challenges and possibilities

In a context of climate change, drier and warmer conditions are expected to occur in many important agricultural regions of the world (IPCC 2014). Given the significant adaptive advantages of C_4 and CAM pathways under hot and dry environments compared to C_3 photosynthesis, it is perhaps unsurprising that ambitious initiatives aiming to engineer either CCMs into C_3 crops have being initiated: the C_4 Rice project (von Caemmerer et al. 2012; von Caemmerer and Furbank, 2016; Furbank, 2016) and the CAM Biodesign project (Borland et al. 2014, 2015; Hartwell et al. 2016; Yang et al. 2015). Both initiatives are long-term endeavors (10 years or more) and agree on the intensive use of 'omics'' technologies to provide essential information on poorly understood aspects of both cycles. Moreover, since both syndromes involve hundreds or thousands of genes, considerable efforts have been done by both projects to develop new technologies to engineer plants for complex, multi-gene constructs (Czarnecki et al. 2016; Yang et al. 2015).

Though the engineering of functional C_4 into rice or any other species has not been achieved yet, many important accomplishments have been obtained in recent years, such as massive advances in understanding the components and regulatory processes responsible for the C_4 functioning and the successful increase of chloroplast, mitochondria and plasmodesmata number in rice BSC (Wang et al. 2017), among others. Similarly, the CAM Biodesign initiative has also lead to impressive advances in understanding CAM biology, including the development of 'omics'' dataset for several key CAM model species (Abraham et al. 2016; Yang et al. 2017) and key functional genomics data (Boxal et al. 2017; Dever et al. 2015). In addition to engineering CAM in C_3 crops, the CAM Biodesign initiative also aims to explore the photosynthetic plasticity of CAM plants for high biomass production in marginal lands and habitat restoration (Borland et al. 2011).

6.1 Engineering CAM into C_4

In addition to the current efforts to increase drought tolerance in C_4 crops (Lopes et al. 2011), another elusive possibility would be to engineer inducible CAM into C_4 crops. C_4 and CAM have been considered incompatible to occur in the same cells (Sage, 2002), but as is the case for some *Portulaca* species, stress-induced CAM has been shown to occur in C_4-performing organisms (Guralnick and Jackson, 2001; Guralnick et al. 2002; Holtum et al. 2017; Koch and Kennedy, 1980, 1982; Ku et al. 1981; Winter and Holtum, 2017). Although an obligate CAM pathway would maximize WUE, a partial commitment to CAM, specifically when abiotic stress conditions challenge the functioning of C_4, may prove to be beneficial by increasing the survival of the C_4 crops until favorable environmental conditions are restored (Borland et al. 2014). Therefore, C_4 and CAM would not necessarily co-occur in a given tissue, providing that the stress-induced CAM is preceded by the down-regulation of the C_4 pathway.

A strong CAM response would require, most of all, a compact mesophyll for storing large amounts of nocturnal organic acid, and inverted stomatal control. On the other hand, CAM cycling seems to be more plausible to engineer into a C_4 plant, as this mode of CAM do not require changes in the diel stomata pattern, nor much vacuolar space to accumulate the comparatively limited acids generated overnight (Borland et al. 2014). Although performing CAM cycling would only contribute with a small additional input in carbon supply, this could mean an increase in survival under dry seasons.

6.2 Parts list for CAM into C_4

Engineering CAM or C_4 in C_3 plants involves transferring genes directly involved in either machineries as many of the modules required for either syndromes are absent in C_3-performing species. In contrast, many genes and biochemical steps are common in both CCMs, so perhaps the most important and challenging task in engineering weak facultative CAM into C_4 plants would be to coordinate the timing of expression of components of each CCM depending on the environmental conditions. Therefore, understanding the transcriptional regulation of genes involved in the C_4 and CAM machineries is important to the future adjustments in their expression patterns via genome editing technologies. For example, the main players of the 'carboxylation' module required for CAM functioning are already present in the MC of C_4 plants, only functioning in a different moment of the diel cycle. Therefore, an important challenge to engineer the 'carboxylation' module of CAM in a C_4 species would be to invert the timing of PEPC expression and activation in the MC and guarantee available carbonic anhydrase (CA) activity. Adjustments to promote the nighttime accumulation of acids in the vacuoles and the subsequent transport of these molecules back to the cytosol during the day will also be necessary.

The 'decarboxylation" module in CAM plants also take place in MC, whereas in dual-cell C_4 species this module is in the BSC. *P. oleracea* plants under drought stress, it has been proposed that the acids accumulated overnight inside MC vacuoles are transferred to BSC during the day (Lara et al. 2004). Therefore, it seems tempting to propose that, with some adjustments, the acid transport mechanisms and decarboxylating enzymes already present in a C_4 plant would be enough to decarboxylate the acids accumulated overnight in a C_4-CAM engineered plant.

A hypothetical scheme of CAM cycling to be engineered into C_4 as a means to improve drought stress tolerance in crops is presented in Fig. 3, which is based on current knowledge available in C_4-CAM facultative plants (Lara et al. 2004). Although accomplishing this idea would take place in a more distant future compared to the other bioengineering initiatives, technological progress achieved through projects such as the C_4 Rice and the CAM Biodesign may shed light on this C_4–CAM engineering endeavor and bring it closer to realization. Our

discussion has not, by any means, exhausted such a rich and interesting research topic, which should be revisited as our current understanding on C_4 and CAM functioning and compatibility is increased.

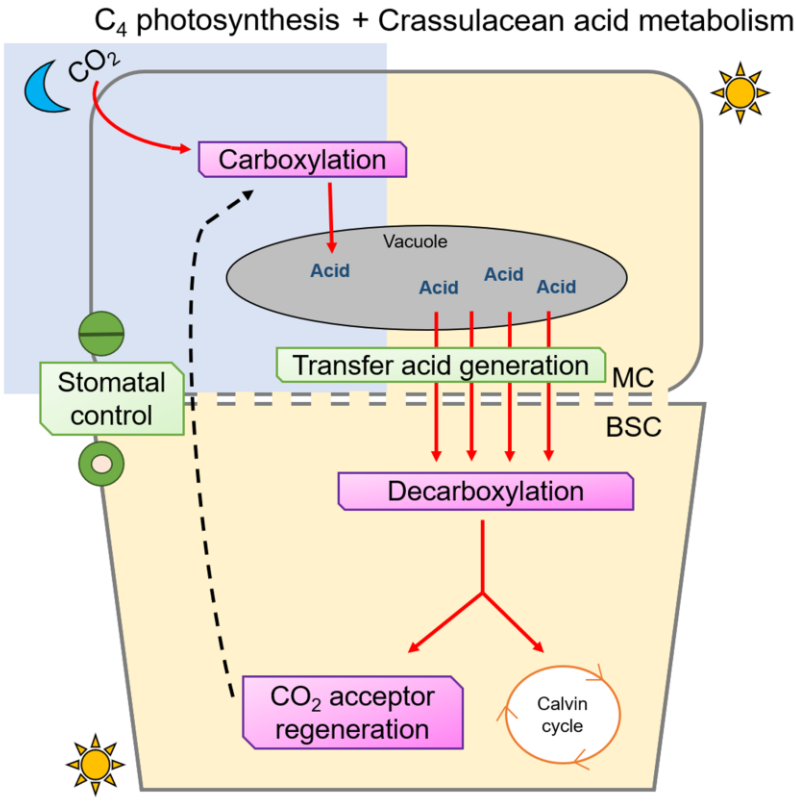

Figure 3: Hypothetical scheme of CAM cycling to be engineered into C_4 as a means to improve drought stress tolerance in crops, based on current knowledge available in C_4-CAM facultative plants (Lara et al. 2004). Respiratory CO_2 would be used in nocturnal acid formation on mesophyll cells. Acids stored overnight would then be transported to the bundle sheath cells to be decarboxylated during the day. Red arrows indicate the carbon pathway inside the cells. MC = mesophyll cell; BSC = bundle sheath cell.

7. Concluding remarks

In summary, there is still much room for improving our current knowledge on the complexity involving C_4 and CAM functioning and regulation, especially regarding metabolite transport, stomatal control, and molecular and hormonal events regulating the expression of these CCMs. Given the vast array of biochemical and anatomical variation found among C_4 and CAM plants, it seems plausible to anticipate that equally diverse regulatory mechanisms have evolved to control the distinct C_4 and CAM genotypes and physiotypes currently known. Therefore, generating and comparing data for different candidate species seems a valid

approach to provide a broad and more complete overview of the regulatory mechanisms controlling C_4 and CAM pathways. As both syndromes display higher WUE and lower crop water demand compared to C_3 plants, C_4 and CAM have been increasingly proposed as promising systems for bioengineering approaches in a context of climate change. A common initial step in these bioengineering initiatives is the use of 'omics'' approaches to unravel new candidate genes involved in both the core CCM pathway and the regulatory processes to produce a parts list for each syndrome. Besides exploring C_4 and CAM in obligate organisms, further attention should be devoted to the few known examples of C_4-CAM facultative plants, as they may help to explain how these syndromes interconnect, thereby holding a great value as a living blueprint for engineering CAM into C_4 crops.

Acknowledgements We thank the Royal Society (UK) through grant #NA140007 and the Sao Paulo State Foundation for Research Support (FAPESP, Brazil) through grant #2016/04755-4 for financial support.

References

Abraham, P.E., Yin, H., Borland, A.M., Weighill, D., Lim, S., Depaoli, H., Engle, N., Jones, P., Agh, R., Weston, D., Wullschleger, S.D., Tschaplinski, T., Jacobson, D., Cushman, J., Hettich, R., Tuskan, G., Yang, X., 2016. Transcript, protein, and metabolite temporal dynamics in the CAM plant *Agave*. Nat. Plants 2, 16178.

Aloor, B.P., Avasthi, U.K., Raghavendra, A.S., 2017. Stimulation by abscisic acid of the activity of phosphoenolpyruvate carboxylase in leaf disks of *Amaranthus hypochondriacus* L., C_4 plant: role of pH and protein levels. Protoplasma 254, 1973–1981. https://doi.org/10.1007/s00709-017-1091-2

Badger, M.R., Hanson, D., Price, G.D., 2002. Evolution and diversity of CO_2-concentrating mechanisms in cyanobacteria. Funct. Plant Biol. 29, 161–173. https://doi.org/Doi 10.1071/Pp01213

Badger, M.R., Kaplan, A., Berry, J.A., 1980. Internal inorganic carbon pool of *Chlamydomonas reinhardtii*: evidence for a carbon dioxide-concentrating mechanism. Plant Physiol. 66, 407–413. https://doi.org/10.1104/pp.66.3.407

Beerling, D.J., Royer, D.L., 2011. Convergent Cenozoic CO_2 history. Nat. Geosci. 4, 418–420. https://doi.org/10.1038/ngeo1186

Bellasio, C., Griffiths, H., 2014. Acclimation of C_4 metabolism to low light in mature maize leaves could limit energetic losses during progressive shading in a crop canopy. J. Exp. Bot. 65, 3725–3736. https://doi.org/10.1093/jxb/eru052

Bohnert, H.I., Ostrem, J.A., Cushman, J.C., Michalowski, C.B., Rickers, J., Meyer, G., DeRocher, E.J., Vernon, D.M., Krueger, M., Vazquez-Moreno, L., Velten, J., Hoefner, R., Schmitt, J.M., 1988. *Mesembryanthemum crystallinum*, a higher plant model for the study of environmentally induced changes in gene expression. Plant Mol. Biol. Report. 6, 10–28. https://doi.org/10.1007/BF02675305

Borland, A.M., Guo, H., Yang, X., Cushman, J.C., 2016. Orchestration of carbohydrate processing for crassulacean acid metabolism. Curr. Opin. Plant Biol. 31, 118–124.

Borland, A.M., Hartwell, J., Weston, D.J., Schlauch, K.A., Tschaplinski, T.J., Tuskan, G.A., Yang, X., Cushman, J.C., 2014. Engineering Crassulacean acid metabolism to improve water-use efficiency. Trends Plant Sci. 19, 327–338. https://doi.org/10.1016/j.tplants.2014.01.006

Borland, A.M., Taybi, T., 2004. Synchronization of metabolic processes in plants with Crassulacean acid metabolism. J. Exp. Bot. 55, 1255–1265.

https://doi.org/10.1093/jxb/erh105
Borland, A.M., Wullschleger, S.D., Weston, D.J., Hartwell, J., Tuskan, G.A., Yang, X., Cushman, J.C., 2015. Climate-resilient agroforestry: Physiological responses to climate change and engineering of crassulacean acid metabolism (CAM) as a mitigation strategy. Plant, Cell Environ. 38, 1833–1849. https://doi.org/10.1111/pce.12479
Borland, A.M., Zambrano, V.A.B., Ceusters, J., Shorrock, K., 2011. The photosynthetic plasticity of Crassulacean acid metabolism : an evolutionary innovation for sustainable productivity in a changing world 619–633.
Boxall, S.F., Dever, L. V, Kneřová, J., Gould, P.D., 2017. Phosphorylation of Phosphoenol pyruvate Carboxylase is essential for maximal and sustained dark CO_2 fixation and core circadian clock operation in the obligate Crassulacean acid metabolism species *Kalanchoë fedtschenkoi*. https://doi.org/10.1105/tpc.17.00301
Bräutigam, A., Schliesky, S., Külahoglu, C., Osborne, C.P., Weber, A.P.M., 2014. Towards an integrative model of C_4 photosynthetic subtypes: insights from comparative transcriptome analysis of NAD-ME, NADP-ME, and PEP-CK C_4 species. J. Exp. Bot. 65, 3579–3593. https://doi.org/10.1093/jxb/eru100
Brilhaus, D., Bräutigam, A., Mettler-Altmann, T., Winter, K., Weber, A.P.M., 2016. Reversible burst of transcriptional changes during induction of Crassulacean acid metabolism in *Talinum triangulare*, Plant Phys. https://doi.org/10.1104/pp.15.01076
Chen, T., Zhu, X.G., Lin, Y., 2014. Major alterations in transcript profiles between C_3-C_4 and C_4 photosynthesis of an amphibious species *Eleocharis baldwinii*. Plant Mol. Biol. 86, 93–110. https://doi.org/10.1007/s11103-014-0215-8
Chollet, R., Vidal, J., O'Leary, M.H., 1996. Phosphoenolpyruvate carboxylase: a ubiquitous, highly regulated enzyme in plants. Annu. Rev. Plant Physiol. Plant Mol. Biol. 47, 273–298. https://doi.org/10.1146/annurev.arplant.47.1.273
Christin, P.A., Arakaki, M., Osborne, C.P., Bräutigam, A., Sage, R.F., Hibberd, J.M., Kelly, S., Covshoff, S., Wong, G.K.S., Hancock, L., Edwards, E.J., 2014. Shared origins of a key enzyme during the evolution of C_4 and CAM metabolism. J. Exp. Bot. 65, 3609–3621. https://doi.org/10.1093/jxb/eru087
Christin, P.A., Arakaki, M., Osborne, C.P., Edwards, E.J., 2015. Genetic enablers underlying the clustered evolutionary origins of C_4 photosynthesis in angiosperms. Mol. Biol. Evol. 32, 846–858. https://doi.org/10.1093/molbev/msu410
Christin, P.A., Boxall, S.F., Gregory, R., Edwards, E.J., Hartwell, J., Osborne, C.P., 2013. Parallel recruitment of multiple genes into C_4 photosynthesis. Genome Biol. Evol. 5, 2174–2187. https://doi.org/10.1093/gbe/evt168
Christin, P.A., Sage, T.L., Edwards, E.J., Ogburn, R.M., Khoshravesh, R., Sage, R.F., 2011. Complex evolutionary transitions and the significance of C_3-C_4 intermediate forms of photosynthesis in Molluginaceae. Evolution 65, 643–660. https://doi.org/10.1111/j.1558-5646.2010.01168.x
Chu, C., Dai Z.Y., Ku, M.S.B., Edwards, G.E., 1990. Induction of Crassulacean acid metabolism in the facultative halophyte *Mesembryanthemum crystallinum* by abscisic acid. Plant Physiol
93:1253–1260. https://doi.org/10.1104/pp.93.3.1253
Cockburn, W., 1983. Stomatal mechanism as the basis of the evolution of CAM and C_4 photosynthesis. Plant. Cell Environ. 6, 275–279. https://doi.org/10.1111/1365-3040.ep11611925
Cushman, J.C., 2001. Crassulacean acid metabolism. a plastic photosynthetic adaptation to arid environments. Plant Physiol. 127, 1439–1448. https://doi.org/10.1104/pp.010818.plants
Cushman, J.C., Michalowski, C.B., Bohnert, H.J., 1990. Developmental control of Crassulacean acid metabolism inducibility by salt stress in the common ice plant. Plant Physiol. 94, 1137–1142. https://doi.org/10.1104/pp.94.3.1137
Cushman, J.C., Tillett, R.L., Wood, J.A., Branco, J.M., Schlauch, K.A., 2008. Large-scale mRNA expression profiling in the common ice plant, *Mesembryanthemum crystallinum*, performing C_3 photosynthesis and Crassulacean acid metabolism (CAM). J. Exp. Bot.

59, 1875–1894. https://doi.org/10.1093/jxb/ern008
Czarnecki, O., Bryan, A.C., Jawdy, S.S., Yang, X., Cheng, Z., Chen J., Tuskan, G.A., 2016. Simultaneous knockdown of six non-family genes using a single synthetic RNAi fragment in *Arabidopsis thaliana*. Plant Methods 12:16 .https://doi.org/10.1186/s13007-016-0116-8
Dai, Z., Ku, M.S.B., Zhang, D.Z., Edwards, G.E., 1994. Effects of growth regulators on the induction of Crassulacean acid metabolism in the facultative halophyte *Mesembryanthemum crystallinum* L.. Planta 192:287–294. https://doi/10.1007/BF00198562
Dengler, N.G., Nelson, T., 1999. Leaf structure and development in C_4 plants, in: Sage, R., Monson, R. (Eds.), C_4 Plant Biology. Academic Press, San Diego, pp. 133–172.
Dever, L. V., Boxall, S.F., Kneřová, J., Hartwell, J., 2015. Transgenic perturbation of the decarboxylation phase of Crassulacean acid metabolism alters physiology and metabolism but has only a small effect on growth. Plant Physiol. 167, 44–59. https://doi.org/10.1104/pp.114.251827
Edwards, E.J., Ogburn, R.M., 2012. Angiosperm responses to a low-CO_2 world: CAM and C_4 photosynthesis as parallel evolutionary trajectories. Int. J. Plant Sci. 173, 724–733. https://doi.org/10.1086/666098
Edwards, G.E., Franceschi, V.R., Voznesenskaya, E. V., 2004. Single-cell C_4 photosynthesis versus the dual-cell (Kranz) paradigm. Annu. Rev. Plant Biol. 55, 173–196. https://doi.org/10.1146/annurev.arplant.55.031903.141725
Ehleringer, J.R., Monson, R.K., 1993. Evolutionary and ecological aspects of photosynthetic pathway variation. Annu. Rev. Ecol. Syst. 24, 411–439. https://doi.org/10.1146/annurev.es.24.110193.002211
Eisenhut, M., Ruth, W., Haimovich, M., Bauwe, H., Kaplan, A., Hagemann, M., 2008. The photorespiratory glycolate metabolism is essential for cyanobacteria and might have been conveyed endosymbiontically to plants. Proc. Natl. Acad. Sci. 105, 17199–17204. https://doi.org/10.1073/pnas.0807043105
Erb, T.J., Zarzycki, J., 2018. A short history of RubisCO: the rise and fall (?) of Nature's predominant CO_2 fixing enzyme. Curr. Opin. Biotechnol. 49, 100–107. https://doi.org/10.1016/j.copbio.2017.07.017
Fleta-Soriano, E., Pintó-Marijuan, M., Munné-Bosch, S., 2015. Evidence of drought stress memory in the facultative CAM, *Aptenia cordifolia*: Possible role of phytohormones. PLoS One 10, 1–12. https://doi.org/10.1371/journal.pone.0135391
Forsthoefel, N.R., Cushman, M.A.F., Cushman, J.C., 1995a. Post-transcriptional and post-translational control of enolase expression in the facultative Crassulacean acid metabolism plant *Mesembryanthemum crystallinum* L. Plant Physiol 108:1185–1195. https://doi.org/10.1104/pp.108.3.1185
Forsthoefel, N.R., Vernon, D.M., Cushman, J.C., 1995b. A salinity-induced gene from the halophyte *M. crystallinum* encodes a glycolytic enzyme, cofactor-independent phosphoglyceromutase. Plant Mol. Biol. 29:213–226. https://doi.10.1007/BF00043647
Freschi, L., Mercier, H., 2012. Connecting environmental stimuli and Crassulacean acid metabolism expression: Phytohormones and other signaling molecules. Prog. Bot. 73, 231–255. https://doi.org/10.1007/978-3-319-08807-5
Freschi, L., Rodrigues, M,A,, Domingues, D.S., Purgatto, E., Van Sluys, M.A., Magalhaes, J.R., Kaiser, W.M., Mercier, H., 2010. Nitric oxide mediates the hormonal control of Crassulacean acid metabolism expression in young pineapple plants. Plant Physiol. 152(4):1971–1985. https://doi: 10.1104/pp.109.151613
Furbank, R.T., 2016. Walking the C_4 pathway: past, present, and future. J. Exp. Bot. 68, 4057–4066. https://doi.org/10.1093/jxb/erx006
Ghannoum, O., Von Caemmerer, S., Conroy, J.P., 2002. The effect of drought on plant water use efficiency of nine NAD-ME and nine NADP-ME Australian C_4 grasses. Funct. Plant Biol. 29, 1337–1348. https://doi.org/10.1071/FP02056
Giordano, M., Beardall, J., Raven, J.A., 2005. CO_2 concentrating mechanisms in algae: mechanisms, environmental modulation, and evolution. Annu. Rev. Plant Biol. 56, 99–

131. https://doi.org/10.1146/annurev.arplant.56.032604.144052
Guralnick, L.J., Edwards, G., Ku, M.S.B., B, B.H., Franceschi, V.R., 2002. Photosynthetic and anatomical characteristics in the C_4–crassulacean acid metabolism-cycling plant, *Portulaca grandiflora*. Funct. Plant Biol. 29, 763–773.
Guralnick, L.J., Jackson, M.D., 2001. The occurrence and phylogenetics of crassulacean acid metabolism in the Portulacaceae. Int. J. Plant Sci. 162, 257–262.
Hare PD, Cress WA, van Staden J (1997) The involvement of cytokinins in plant responses to environmental stress. Plant Growth. Regul. 23:79-103.
Hartwell, J., 2005. The co-ordination of central plant metabolism by the circadian clock. Biochem. Soc. Trans. 33, 945–948. https://doi.org/10.1042/BST20050945
Hartwell, J., Dever, L. V., Boxall, S.F., 2016. Emerging model systems for functional genomics analysis of Crassulacean acid metabolism. Curr. Opin. Plant Biol. 31, 100–108. https://doi.org/10.1016/j.pbi.2016.03.019
Herppich, W., Herppich, M., Willert, D. Von, 1992. The irreversible C_3 to CAM shift in well-watered and salt-stressed plants of *Mesembryanthemum crystallinum* is under strict ontogenetic control. Botanica Acta 105, 34–40.
Herrera, A., 2009. Crassulacean acid metabolism and fitness under water deficit stress: if not for carbon gain, what is facultative CAM good for? Ann. Bot. 103, 645–653. https://doi.org/10.1093/aob/mcn145
Hibberd, J.M., Covshoff, S., 2010. The regulation of gene expression required for C_4 photosynthesis. Annu. Rev. Plant Biol. 61, 181–207. https://doi.org/10.1146/annurev-arplant-042809-112238
Holtum, J.A.M., Hancock, L.P., Edwards, E.J., Winter, K., 2017. Optional use of CAM photosynthesis in two C_4 species, *Portulaca cyclophylla* and *Portulaca digyna*. J. Plant Physiol. https://doi.org/10.1016/j.jplph.2017.01.010
Holtum, J.A.M., Winter, K., 1982. Activity of enzymes of carbon metabolism during the induction of Crassulacean acid metabolism in *Mesembryanthemum crystallinum* L. Planta 155, 8–16. https://doi.org/10.1007/BF00402925
Holtum, J.A.M., Smith, J.A.C., Neuhaus, H.E., 2005. Intracellular transport and pathways of carbon flow in plants with Crassulacean acid metabolism. Funct. Plant Biol. 32, 429. https://doi.org/10.1071/FP04189
IPCC, 2014. Climate Change 2014: Synthesis Report., in: Pachauri, R.K., Meyer, L.A. (Eds.) Climate Change 2014: Synthesis Report - Contribution of Working Groups I, II and III to the Fifth Assessment Report of the Intergovernmental Panel on Climate Change. IPCC, Geneva.
Izui, K., Matsumura, H., Furumoto, T., Kai, Y., 2004. Phosphoenolpyruvate carboxylate: A new era of structural biology. Annu. Rev. Plant Biol. 55, 69–84. https://doi.org/10.1146/annurev.arplant.55.031903.141619
Kanai, R., Edwards, G.E., 1999. The biochemistry of photosynthesis, in: Sage, R., Monson, R. (Eds.), C_4 Plant Biology. Academic Press, San Diego, pp. 49–87.
Keeley, J.E., Rundel, P.W., 2003. Evolution of CAM and C_4 carbon-concentrating mechanisms. Int. J. Plant Sci. 164, S55–S77. https://doi.org/10.1086/374192
Kellogg, E.A., 1999. Phylogenetic aspects of the evolution of C_4 photosynthesis, in: Sage, R., Monson, R. (Eds.), C_4 Plant Biology. Academic Press, San Diego, pp. 411–444.
Koch, K.E., Kennedy, R.A., 1982. Crassulacean acid metabolism in the succulent C_4 dicot, *Portulaca oleracea* L under natural environmental conditions. Plant Physiol. 69, 757–761.
Koch, K.E., Kennedy, R.A., 1980. Characteristics of Crassulacean acid metabolism in the succulent C_4 dicot, *Portulaca oleracea* L. Plant Physiol. 65, 193–197. https://doi.org/10.1104/pp.69.4.757
Kraybill, A.A., Martin, C.E., 1996. Crassulacean acid metabolism in three species of the C_4 genus *Portulaca*. Int. J. Plant Sci. 157, 103–109.
Ku, S.B., Shieh, Y.J., Reger, B.J., Black, C.C., 1981. Photosynthetic characteristics of *Portulaca grandiflora*, a succulent C_4 dicot. Plant Physiol. 68, 1073–1080. https://doi.org/10.1104/pp.68.5.1073

Lara, M., Disante, K.B., Podestá, F.P., Andreo, C.S., Drincovich, M.F., 2003. Induction of a Crassulacean acid like metabolism in the C_4 succulent plant, *Portulaca oleracea* L.: physiological and morphological changes are accompanied by specific modifications in phosphoenolpyruvate carboxylase. Photosynth. Res. 77, 241–254. https://doi.org/10.1023/A:1025834120499

Lara, M. V., Drincovich, M.F., Andreo, C.S., 2004. Induction of a Crassulacean acid-like metabolism in the C_4 succulent plant, *Portulaca oleracea* L.: Study of enzymes involved in carbon fixation and carbohydrate metabolism. Plant Cell Physiol. 45, 618–626. https://doi.org/10.1093/pcp/pch073

Lepiniec, L., Vidal, J., Chollet, R., Gadal, P., Crétin, C., 1994. Phosphoenolpyruvate carboxylase: structure, regulation and evolution. Plant Sci. 99, 111–124. https://doi.org/10.1016/0168-9452(94)90168-6

Li, P., Ponnala, L., Gandotra, N., Wang, L., Si, Y., Tausta, S.L., Kebrom, T.H., Provart, N., Patel, R.., Myers, C.R., Reidel, C.J.,, Turgeon, R., Liu, P., Sun, Q., Nelson, T., Brutnell, T.P., 2010. The developmental dynamics of the maize leaf transcriptome. Nature Genetics 42 1060–1067. https://doi:10.1038/ng.703

Long, S.P., 1999. Environmental Responses, in: Sage, R., Monson, R. (Eds.), C_4 Plant Biology. Academic Press, San Diego, pp. 215–249.b

Lopes, M.S., Araus, J.L., Van Heerden, P.D.R., Foyer, C.H., 2011. Enhancing drought tolerance in C_4 crops. J. Exp. Bot. 62, 3135–3153. https://doi.org/10.1093/jxb/err105

Lüttge, U., 1996. *Clusia*: plasticity and diversity in a genus of C_3/CAM intermediate tropical trees, in: Winter, K., Smith, J. (Eds.), Crassulacean acid metabolism. Springer-Verlag Berlin, pp. 296–311.

Lüttge, U., 2004. Ecophysiology of Crassulacean acid metabolism (CAM). Ann. Bot. 93, 629–652. https://doi.org/10.1093/aob/mch087

Lüttge, U., 2006. Photosynthetic flexibility and ecophysiological plasticity: Questions and lessons from *Clusia*, the only CAM tree, in the neotropics. New Phytol. 171, 7–25. https://doi.org/10.1111/j.1469-8137.2006.01755.x

Maberly, S.C., Madsen, T.V., 2002. Freshwater angiosperm carbon concentrating mechanisms: processes and patterns. Funct. Plant Biol. 29(3), 393–405.

Mazen, A.M.A., 2000. Changes in properties of phosphoenolpyruvate carboxylase with induction of Crassulacean Acid Metabolism (CAM) in the C_4 plant *Portulaca oleracea*. Photosynthetica. https://doi.org/10.1023/A:1010969419962

Mazen, A.M.A., 1996. Changes in levels of phosphoenolpyruvate carboxylase with induction of Crassulacean acid metabolism (CAM)-like behavior in the C_4 plant *Portulaca oleracea*. Physiol. Plant. 98, 111–116. https://doi.org/10.1111/j.1399-3054.1996.tb00681.x

McElwain, E.F., Bohnert, H.J., Thomas, J.C., 1992. Light moderates the induction of phosphoenolpyruvate carboxylase by NaCl and abscisic acid in *Mesembryanthemum crystallinum*. Plant Physiol 99:1261–1264

Meyer, M., Griffiths, H., 2013. Origins and diversity of eukaryotic CO_2-concentrating mechanisms: Lessons for the future. J. Exp. Bot. 64, 769–786. https://doi.org/10.1093/jxb/ers390S

Miziorko, H.M., Lorimer, G.H., 1983. Ribulose-1,5-biphosphate carboxylase-oxygenase. Ann. Rev. Biochem. 52, 507–535.

Monson, R.K., 1999. The origins of C_4 genes and evolutionary pattern in the C_4 metabolic phenotype, in: Sage, R., Monson, R. (Eds.), C_4 Plant Biology. Academic Press, San Diego, pp. 377–410. http://dx.doi.org/10.1016/B978-012614440-6/50012-4

Moroney, J.V., Jungnick, N., DiMario, R.J., Longstreth, D.J., 2013. Photorespiration and carbon concentrating mechanisms: two adaptations to high O_2, low CO_2 conditions. Photosynth. Res. 117:121–131. https://doi.org/10.1007/s11120-013-9865-7

Monson, R.K., Moore, B. d., 1989. On the significance of C_3-C_4 intermediate photosynthesis to the evolution of C_4 photosynthesis. Plant. Cell Environ. 12, 689–699. https://doi.org/10.1111/j.1365-3040.1989.tb01629.x

Muhaidat, R.I.M., Sage, R.F., Denglres, N.G., 2007. Diversity of Kranz anatomy and

biochemistry in C_4 eudicots. Am. J. Bot. 94, 362–381.
Nelson, E.A., Sage, R.F., 2008. Functional constraints of CAM leaf anatomy: Tight cell packing is associated with increased CAM function across a gradient of CAM expression. J. Exp. Bot. 59, 1841–1850. https://doi.org/10.1093/jxb/erm346
Nelson, E.A., Sage, T.L., Sage, R.F., 2005. Functional leaf anatomy of plants with Crassulacean acid metabolism. Funct. Plant Biol. 32, 409–419. https://doi.org/10.1071/FP04195
Nimmo, H.G., 2000. The regulation of phosphoenolpyruvate carboxylase. Trends Plant Sci 5, 75–80.
Ocampo, G., Columbus, J.T., 2012. Molecular phylogenetics, historical biogeography, and chromosome number evolution of *Portulaca* (Portulacaceae). Mol. Phylogenet. Evol. 63, 97–112. https://doi.org/10.1016/j.ympev.2011.12.017
Pospisilova J, Synkova H, Rulcova J (2000) Cytokinins and water stress. Biol. Plantarum 43:321-328. https://doi.org/10.1023/A:1026754404857
Pospisilova J, Vagner M, Malbeck J, Travniakova A, Batkova P (2005) Interactions between abscisic acid and cytokinins during water stress and subsequent rehydration. Biol. Plantarum 49:533-540. https://doi.org/10.1007/s10535-005-0047-0
Peters W, Beck E, Piepenbrock M, Lenz B, Schmitt JM (1997) Cytokinin as a negative effector of phosphoenolpyruvate carboxylase induction in *Mesembryanthemum crystallinum*. J Plant Physiol 151:362–367. https://doi.org/10.1016/S0176-1617(97)80266-0
Pengelly, J.J.L., Sirault, X.R.R., Tazoe, Y., Evans, J.R., Furbank, R.T., Von Caemmerer, S., 2010. Growth of the C_4 dicot *Flaveria bidentis*: Photosynthetic acclimation to low light through shifts in leaf anatomy and biochemistry. J. Exp. Bot. 61, 4109–4122. https://doi.org/10.1093/jxb/erq226
Pick, T.R., Bräutigam, A., Schlüter, U., Denton, A.k., Colmsee, C., Scholz, U., Fahnenstich, H., Pieruschka, R., Rascher, U., Sonnewald, U., Weber, A.P.M., 2011. Systems Analysis of a maize leaf developmental gradient redefines the current C_4 model and provides candidates for regulation. Plant Cell 23: 4208–4220. https://doi.org/10.1105/tpc.111.090324
Raven, J.A., Cockell, C.S., De La Rocha, C.L., 2008. The evolution of inorganic carbon concentrating mechanisms in photosynthesis. Philos. Trans. R. Soc. B Biol. Sci. 363, 2641–2650. https://doi.org/10.1098/rstb.2008.0020
Reeves, G., Grangé-guermente, M.J., Hibberd, J.M., 2016. Regulatory gateways for cell-specific gene expression in C_4 leaves with Kranz anatomy. https://doi.org/10.1093/jxb/erw438
Sage, R.F., 2017. A portrait of the C_4 photosynthetic family on the 50th anniversary of its discovery: species number, evolutionary lineages, and Hall of Fame. J. Exp. Bot. 68, e11–e28. https://doi.org/10.1093/jxb/erx005
Sage, R.F., 2004. The evolution of C_4 photosynthesis. New Phytol. 161, 341–370. https://doi.org/10.1046/j.1469-8137.2004.00974.x
Sage, R.F., 2002. Are crassulacean acid metabolism and C_4 photosynthesis incompatible? Funct. Plant Biol. 29, 775–785.
Sage, R.F., McKown, A.D., 2006. Is C_4 photosynthesis less phenotypically plastic than C_3 photosynthesis? J. Exp. Bot. 57, 303–317. https://doi.org/10.1093/jxb/erj040
Sage, R.F., Sage, T.L., Kocacinar, F., 2012. Photorespiration and the evolution of C_4 photosynthesis. Annu. Rev. Plant Biol. 63, 19–47. https://doi.org/10.1146/annurev-arplant-042811-105511
Schluter, U., Denton, A.K., Bräutigam, A., 2016. Understanding metabolite transport and metabolism in C_4 plants through RNA-seq 31. https://doi.org/10.1016/j.pbi.2016.03.007
Schmitt, J.M., Piepenbrock, M., 1992. Regulation of phosphoenolpyruvate carboxylase and Crassulacean acid metabolism induction in *Mesembryanthemum crystallinum* L. by cytokinin. Modulation of leaf gene expression by roots? Plant Physiol 99:1664–1669. https://doi.org/10.1104/pp.99.4.1664
Silvera, K., Neubig, K.M., Whitten, W.M., Williams, N.H., Winter, K., Cushman, J.C., 2010.

Evolution along the Crassulacean acid metabolism continuum. Funct. Plant Biol. 37, 995–1010. https://doi.org/10.1071/FP10084

Tanaka Y, Sano T, Tamaoki M, Nakajima N, Kondo N, Hasezawa S (2006) Cytokinin and auxin inhibit abscisic acid-induced stomatal closure by enhancing ethylene production in *Arabidopsis*. J. Exp. Bot. 57:2259-2266

Taybi, T., Cushman, J.C., Borland, A.M., 2002. Environmental, hormonal and circadian regulation of Crassulacean acid metabolism expression. Funct. Plant Biol. 29, 669–678. https://doi.org/10.1071/PP01244

Taybi, T., Sotta, B., Gehrig, H., Guclu, S., Kluge, M., Brulfert, J., 1995. Differential effects of abscisic acid on phosphoenolpyruvate carboxylase and CAM operation in *Kalanchoe¨ blossfeldiana*. Bot. Acta 108:240–246. https:// doi/10.1111/j.1438-8677.1995.tb00856.x/abstract

Thomas, J.C., Bohnert, H.J., 1993. Salt stress perception and plant growth regulators in the halophyte *Mesembryanthemum crystallinum*. Plant Physiol. 103:1299–1304. https://doi.org/10.1104/pp.103.4.1299. https://doi.org/10.1104/pp.103.4.1299

Thomas, J.C., Mcelwain, E.F., Bohnert, H.J., 1992 Convergent induction of osmotic stress responses. Abscisic acid, cytokinin, and the effects of NaCl. Plant Physiol 100:416–423. https://doi.org/10.1104/pp.100.1.416

Tsiantis, M.S., Bartholomew, D.M., Smith, J.A.C., 1996. Salt regulation of transcript levels for the c subunit of a leaf vacuolar H^+-ATPase in the halophyte *Mesembryanthemum crystallinum*. Plant J 9:729–736. https:// doi/10.1046/j.1365-313X.1996.9050729.x/abstract

Uchino, A., Sentoku, N., Nemoto, K., Ishii, R., Samejima, M., Matsuoka, M., 1998. C_4-type gene expression is not directly dependent on Kranz anatomy in an amphibious sedge *Eleocharis vivipara* Link. Plant J. 14, 565–572. https://doi.org/10.1046/j.1365-313X.1998.00155.x

Ueno, O., 2001. Update on C_4 Photosynthesis Environmental Regulation of C_3 and C_4 Differentiation in the Amphibious Sedge *Eleocharis vivipara*. Plant Physiol. 127, 1524–1532. https://doi.org/10.1104/pp.010704.1524

Ueno, O., 1998. Induction of Kranz anatomy and C_4-like biochemical characteristics in a submerged amphibious plant by abscisic acid. Plant Cell 10, 571–583. https://doi.org/10.1105/tpc.10.4.571

Ueno, O., Samejima, M., Muto, S., Miyachi, S., 1988. Photosynthetic characteristics of an amphibious plant, *Eleocharis vivipara*: Expression of C_4 and C_3 modes in contrasting environments. Proc. Natl. Acad. Sci. U. S. A. 85, 6733–6737. https://doi.org/10.1073/pnas.85.18.6733

von Caemmerer, S., Furbank, R.T., 2016. Strategies for improving C_4 photosynthesis. Curr. Opin. Plant Biol. 31, 125–134.

von Caemmerer, S., Quick, W.P., Furbank, R.T., 2012. The development of C_4 rice: Current progress and future challenges. Science 336, 1671–1672. https://doi.org/10.1126/science.1220177

Voznesenskaya, E. V., Koteyeva, N.K., Edwards, G.E., Ocampo, G., 2010. Revealing diversity in structural and biochemical forms of C_4 photosynthesis and a C_3-C_4 intermediate in genus *Portulaca* L. (Portulacaceae). J. Exp. Bot. 61, 3647–3662. https://doi.org/10.1093/jxb/erq178

Voznesenskaya, E. V, Franceschi, V.R., Kiirats, O., Artyusheva, E.G., Freitag, H., Edwards, G.E., 2002. Proof of C_4 photosynthesis without Kranz anatomy in *Bienertia cycloptera* (Chenopodiaceae). Plant J. 31, 649–662. https://doi.org/10.1046/j.1365-313X.2002.01385.x

Voznesenskaya, E. V, Franceschi, V.R., Kiirats, O., Freitag, H., Edwards, G.E., 2001. Kranz anatomy is not essential for terrestrial C_4 plant photosynthesis. Nature 414, 543–546. https://doi.org/10.1038/35107073

Wai, C.M., VanBuren, R., Zhang, J., Huang, L., Miao, W., Edger, P.P., Yim, W.C., Priest, H.D., Meyers, B.C., Mockler, T., Smith, J.A.C., Cushman, J.C., Ming, R., 2017. Temporal and spatial transcriptomic and microRNA dynamics of CAM photosynthesis

in pineapple. Plant J. 92, 19–30. https://doi.org/10.1111/tpj.13630
Wang, P., Khoshravesh, R., Karki, S., Furbank, R., Sage, T.L., Langdale, J.A., Wang, P., Khoshravesh, R., Karki, S., Tapia, R., Balahadia, C.P., 2017. Re-creation of a Key Step in the Evolutionary Switch from C_3 to C_4 Leaf Anatomy Article Re-creation of a Key Step in the Ann. Bot. 93, 629–652. https://doi.org/10.1093/aob/mch087
Wang, Y., Bräutigam, A., Weber, A.P.M., Zhu, X.G., 2014. Three distinct biochemical subtypes of C_4 photosynthesis? A modelling analysis, J. Exp. Bot. 65, 3567–3578. https://doi.org/10.1093/jxb/eru058
Winter, K., Holtum, J.A.M., 2017. Facultative crassulacean acid metabolism (CAM) in four small C_3 and C_4 leaf-succulents. Aust. J. Bot. https://doi.org/10.1071/BT16015
Winter, K., Sage, R. F., Edwards, E. J., Virgo, A., Holtum, J. A. M. 2019. Facultative crassulacean acid metabolism in a C_3–C_4 intermediate. J. Exp. Bot. 70, 6571–6579, 2019. https://doi.org/10.1093/jxb/erz085.
Winter, K., Holtum, J.A.M., 2014. Facultative crassulacean acid metabolism (CAM) plants: Powerful tools for unravelling the functional elements of CAM photosynthesis. J. Exp. Bot. 65, 3425–3441. https://doi.org/10.1093/jxb/eru063
Winter, K., Holtum, J.A.M., 2007. Environment or development? Lifetime net CO_2 exchange and control of the expression of Crassulacean acid metabolism in *Mesembryanthemum crystallinum*. Plant Physiol. 143, 98–107. https://doi.org/10.1104/pp.106.088922
Winter, K., Holtum, J.A.M., Smith, J.A.C., 2015. Crassulacean acid metabolism: a continuous or discrete trait? New Phytol. 208, 73–8. https://doi.org/10.1111/nph.13446
Winter, K., Smith, J.A.C., 1996. An introduction to Crassulacean acid metabolism. Biochemical principles and ecological diversity, in: Winter, K., Smith, J. (Eds.), Crassulacean Acid Metabolism. Springer-Verlag Berlin, pp. 1–13.
Yang, X., Cushman, J.C., Borland, A.M., Edwards, E.J., Wullschleger, S.D., Tuskan, G.A., Owen, N.A., Griffiths, H., Smith, J.A.C., De Paoli, H.C., Weston, D.J., Cottingham, R., Hartwell, J., Davis, S.C., Silvera, K., Ming, R., Schlauch, K., Abraham, P., Stewart, J.R., Guo, H.B., Albion, R., Ha, J., Lim, S.D., Wone, B.W.M., Yim, W.C., Garcia, T., Mayer, J.A., Petereit, J., Nair, S.S., Casey, E., Hettich, R.L., Ceusters, J., Ranjan, P., Palla, K.J., Yin, H., Reyes-García, C., Andrade, J.L., Freschi, L., Beltrán, J.D., Dever, L. V., Boxall, S.F., Waller, J., Davies, J., Bupphada, P., Kadu, N., Winter, K., Sage, R.F., Aguilar, C.N., Schmutz, J., Jenkins, J., Holtum, J.A.M., 2015. A roadmap for research on Crassulacean acid metabolism (CAM) to enhance sustainable food and bioenergy production in a hotter, drier world. New Phytol. 207, 491–504. https://doi.org/10.1111/nph.13393
Yang, X., Hu, R., Yin, H., Jenkins, J., Shu, S., Tang, H., Liu, D., Weighill, D.A., Cheol Yim, W., Ha, J., Heyduk, K., Goodstein, D.M., Guo, H.-B., Moseley, R.C., Fitzek, E., Jawdy, S., Zhang, Z., Xie, M., Hartwell, J., Grimwood, J., Abraham, P.E., Mewalal, R., Beltrán, J.D., Boxall, S.F., Dever, L. V., Palla, K.J., Albion, R., Garcia, T., Mayer, J.A., Don Lim, S., Man Wai, C., Peluso, P., Van Buren, R., De Paoli, H.C., Borland, A.M., Guo, H., Chen, J.-G., Muchero, W., Yin, Y., Jacobson, D.A., Tschaplinski, T.J., Hettich, R.L., Ming, R., Winter, K., Leebens-Mack, J.H., Smith, J.A.C., Cushman, J.C., Schmutz, J., Tuskan, G.A., 2017. The *Kalanchoë* genome provides insights into convergent evolution and building blocks of Crassulacean acid metabolism. Nat. Commun. 8, 1899. https://doi.org/10.1038/s41467-017-01491-7
Zhang, Y.G., Pagani, M., Liu, Z., Bohaty, S.M., Deconto, R., A, P.T.R.S., 2013. A 40-million-year history of atmospheric CO_2 A 40-million-year history of atmospheric CO_2. Philos. Trans. R. Soc. https://doi.org/10.1098/rsta.2013.0096
Zimmerman, C.A., 1976. Growth Characteristics of Weediness in *Portulaca oleracea* L.. Ecology 57(5),.964–974

Chapter II

C_4 and crassulacean acid metabolism within a single leaf: deciphering key components behind a rare photosynthetic adaptation

"A weed is but an unloved flower."

Ella Wheeler Wilcox

This chapter is organized as published in the journal New Phytologist:

Ferrari R.C.; Bittencourt P.P.; Rodrigues M.A.; Moreno-Villena J.J.; Frederico R.R.; Gastaldi V.D.; Boxall S.F.; Dever L.V.; Demarco D.S.C.; Edwards E.J., Hartwell J., Freschi L. (2020) C_4 and crassulacean acid metabolism within a single leaf: deciphering key components behind a rare photosynthetic adaptation. *New Phytologist* 225, 1699–1714, 2020. Doi:10.1111/nph.16265

Supplementary information is available for this paper at https://nph.onlinelibrary.wiley.com/doi/full/10.1111/nph.16265.

SUMMARY

- Though biochemically related, C_4 and crassulacean acid metabolism (CAM) pathways are expected to be incompatible. However, *Portulaca* species, including *P. oleracea*, operate C_4 and CAM within a single leaf, and the mechanisms behind this unique photosynthetic arrangement are still largely unknown.
- Here, we employed RNA-seq to identify candidate genes involved exclusively or shared by C_4 or CAM, and provided an in-depth characterization of their transcript abundance patterns during the drought-induced photosynthetic transitions in *P. oleracea*. Data revealed fewer candidate CAM-specific genes than those recruited to function in C_4. The putative CAM-specific genes were predominantly involved in nighttime primary carboxylation reactions and malate movement across the tonoplast. Analysis of gene transcript-level regulation and photosynthetic physiology indicated that C_4 and CAM co-exist within a single *P. oleracea* leaf under mild drought conditions.
- Developmental and environmental cues were shown to regulate CAM expression in stems, whereas the shift from C_4 to C_4-CAM hybrid photosynthesis in leaves was strictly under environmental control. Moreover, efficient starch turnover was identified as part of the metabolic adjustments required for CAM operation in both organs.
- These findings provide insights into C_4/CAM connectivity and compatibility, contributing to a deeper understanding of alternative ways to engineer CAM into C_4 crop species.

Keywords: C_4 photosynthesis, crassulacean acid metabolism, drought stress, facultative CAM, *Portulaca oleracea*, RNA-seq, transcriptome.

INTRODUCTION

C_4 photosynthesis and crassulacean acid metabolism (CAM) are two major carbon concentrating mechanisms (CCMs) in higher plants (Hatch 1987; Griffiths 1989; Keeley & Rundel, 2003). C_4 occurs in ca. 19 families, mostly distributed in hot and high-light environments (Sage, 2017). It relies on the spatial separation between primary CO_2 assimilation by phosho*enol*pyruvate carboxylase (PPC) in mesophyll cells (MCs) and secondary refixation by ribulose 1,5-biphosphate carboxylase/oxygenase (RuBisCO) in bundle sheath cells (BSCs) (Laetsch, 1968; Kanai & Edwards, 1999), being usually associated with Kranz anatomy (Voznesenskaya *et al.,* 2001, 2002). Besides increasing photosynthetic rates and suppressing photorespiration, C_4 can increase water use efficiency (WUE) relative to C_3 as lower stomatal conductance is required for a given assimilation rate (Taylor *et al.,* 2014).

CAM is found in at least 35 families mainly distributed in arid environments (Winter, 2019), and is also commonly, but not exclusively, associated with higher leaf succulence (Nelson *et al.,* 2005; Silvera *et al.,* 2010; Edwards 2019). In contrast to C_4, CAM occurs in each individual MC and relies on temporal coordination of primary and secondary CO_2 fixation by the circadian clock (Hartwell, 2006). In strong CAM plants, stomatal opening and consequently atmospheric CO_2 uptake and C_4 acid formation are rescheduled to the dark period, when transpiration rates are lower, whereas stomata close for much of the light period, preventing water loss and increasing WUE (Osmond, 1978; Borland *et al*., 2009). The dark CO_2 fixation by PPC and the daytime refixation of CO_2 by RuBisCO characterize CAM phases I and III, respectively, with additional transitional phases at dawn and dusk (phases II and IV, respectively) where stomata can also be open allowing direct fixation of atmospheric CO_2 by RuBisCO (Winter & Smith, 1996). CAM also differs from C_4 in its variability of expression, as many facultative plants operate CAM under stress (e.g., drought), but perform C_3 photosynthesis whenever conditions allow (Winter & Holtum, 2014). CAM is weakly expressed in many facultative species as nocturnal CO_2 fixation under stress conditions contributes less than 5% compared with daytime CO_2 fixation via C_3 under optimal growth conditions (Winter, 2019).

A set of biochemical reactions are shared by C_4 and CAM, including many involved in carboxylation and decarboxylation steps (Bräutigam *et al*., 2017), since both CCMs depend on the formation of four-carbon organic acids to store, transport and release CO_2 in the vicinity of RuBisCO (Edwards & Ogburn, 2012).). Post-translational regulatory steps are also shared in C_4 and CAM species, including the phosphorylation-dependent control of PPC and PPDK (pyruvate, orthophosphate dikinase) activities by PPC kinase (PPCK) and PPDK-regulatory protein (PPDKRP), respectively (Nimmo *et al*., 2001; Chastain & Chollet, 2003;

Dever *et al.,* 2015). However, while C_4 requires specific metabolites, transporters and decarboxylases (Kanai & Edwards, 1999; Schluter *et al.,* 2016), CAM relies on strict temporal coordination of primary and secondary CO_2 fixation and appropriate transporters for acid import and export from the vacuole (Winter & Smith, 1996; Hartwell *et al*., 2016). Differently from C_4 species, a dedicated pool of carbohydrates (starch or soluble sugars, depending on the species) is converted into PEP via glycolysis each night to sustain PPC activity in CAM (Black *et al.,* 1996; Weise *et al.,* 2011). Moreover, a change from the hydrolytic to the phosphorolytic starch breakdown pathway is usually observed during CAM induction in facultative species (Borland *et al*., 2016).

C_4 and CAM are believed to be incompatible to occur in the same cell, as each CCM requires potentially conflicting regulatory processes, metabolic fluxes and structural arrangements (Sage, 2002). However, the occurrence of both CCMs within a single leaf is rare, but possible, as observed in *Portulaca* species (Sage, 2002; Winter, 2019). Species from all main *Portulaca* lineages have been reported to induce CAM in response to drought (Koch & Kennedy, 1980, 1982; Ku *et al.,* 1981; Guralnick & Jackson, 2001; Holtum *et al.,* 2017; Winter & Holtum, 2017; Winter *et al.,* 2019). Among them, *P. oleracea* L. displays rapid growth, high seed production (up to 200,000 seeds/plant), a cosmopolitan distribution, and it is economically important as food and medicine (Zimmerman, 1976; Miyanishi & Cavers, 1980; Gonnella *et al.,* 2010). *P. oleracea*, therefore, represents an attractive model for the study of the C_4-CAM compatibility in leaves (Hartwell *et al*., 2016; Ferrari & Freschi, 2019). Moreover, stems are also photosynthetic in this species, and can accumulate acids overnight under drought (Koch & Kennedy, 1980), but are devoid of C_4 anatomical attributes (Voznesenskaya *et al.,* 2010).

Both C_4 and CAM are relevant targets for forward genetic engineering into C_3 crop species due to their natural ability to outperform C_3 plants in hotter and drier environments. Attempts are underway to engineer the C_4 pathway into rice, such as the C_4 Rice Initiative (Kajala *et al.,* 2011; Covshoff & Hibberd, 2012), and to transfer CAM into C_3 food and bioenergy crops (Borland *et al.,* 2009, Yang *et al.,* 2015; Hartwell *et al.,* 2016). From this perspective, *P. oleracea* provides a potentially unique genetic blueprint of how C_4 and CAM can occur within a single leaf. As such, unraveling the components behind this rare photosynthetic adaptation may provide valuable insights that can guide and inform the challenge of bioengineering facultative CAM into C_4 crops, combining high productivity under optimum growth conditions and increased survival during intermittent drought events (Ferrari & Freschi, 2019).

In this study, we report the gene transcript level and metabolic changes associated with the modulation of C_4 and CAM expression in *P. oleracea* plants challenged by alterations in water availability. We focused on the identification of components that were either exclusive

to or shared by C_4 and/ or CAM pathways. Our results revealed that inducible CAM in *P. oleracea* requires the up-regulation of relatively few CCM genes, and that the induction of these genes can be controlled either by the environment (drought) or by developmental cues, depending on the organ (leaves or stems). Simultaneous C_4 and CAM functioning were observed soon after drought exposure, indicating that both CCMs can co-exist within a single leaf. Novel insights are also provided into the additional metabolic adjustments (e.g., sugar metabolism rewiring) and regulatory mechanisms (e.g., transcriptional regulation of key genes) involved in this remarkable photosynthetic adaptation.

MATERIAL AND METHODS

Plant material, growth conditions and sampling

Plants were grown in 300-ml square pots containing commercial substrate and vermiculite at a photosynthetic flux density (PFD) at plant height of 250-300 μmol m^{-2} s^{-1}, 12h photoperiod, temperature of 27 ± 1ºC day and 22 ± 1ºC night, and air humidity of 60 ± 10% day and 80 ± 10% night. After 20-30 days of initial growth, plants were separated into three experimental groups, each one submitted to a different watering regime as follows: (1) plants watered daily (well-watered), (2) plants subjected to water withholding until soil volumetric water content (SVWC) reached 10-20% and subsequently maintained at this level until sampling (drought-stressed), (3) plants irrigated to field capacity after 22 and 34 days of drought (re-watered). SVWC was continuously monitored (every 30 minutes) using Decagon soil moisture meter EC-5 coupled to the Em5b datalogger (Decagon Devices, Pullman, WA, USA).

Sampling of leaves and stems took place after 0, 10, 22 and 34 days of drought treatment (D0, D1, D2 and D3, respectively), and also 4-days after re-watering events that were initiated at D2 and D3 (R1 and R2, respectively). Samples were harvested one hour after the onset of illumination (dawn samples) and one hour before the end of the light period (dusk samples). At D3, leaf and stem samples were also harvested every four hours over a light/dark cycle starting two hours after the onset of the light period (8h, 12h, 16h, 20h, 24h, 4h, 8h). Three to four biological replicates, each composed of at least three individual plants per replicate, were harvested at each sampling time. All fully-expanded and non-senescent leaves (leaf samples) and whole stems (stem samples) were frozen in liquid N_2, powdered and stored at -80°C until use.

Leaf gas exchange, chlorophyll *a* fluorescence and metabolite analysis

Net CO_2 uptake (*A*), stomatal conductance (*gs*) and transpiration rate (*E*) were determined for the third fully expanded leaf (counting from the top) of at least three individuals using an infrared gas analyzer (Li 6400XT, Li-Color, Lincoln, USA). Measurements were performed between the 2^{nd} and the 5^{th} hour after the onset of illumination, under controlled conditions of

CO_2 concentration (380 ppm CO_2), PFD approx. 300 µmol m^{-2} s^{-1} and chamber temperature of 25ºC. Whenever relevant, continuous monitoring of net CO_2 uptake and transpiration rate over the 24h cycle was also performed as described in Boxall *et al.* (2019). Chlorophyll *a* fluorescence parameters were measured using a portable Pulse Amplitude Modulation fluorometer (PAM-2500, Walz, Germany) following the protocols and equations described by Alves *et al.* (2016). Values of minimal (F_o) and maximal (F_m) fluorescence were obtained from leaves dark-adapted for 30 min before receiving a saturating pulse of light (3000 µmol photons m^{-2} s^{-1} for 1 s).

Tissues osmotic potential (Ψ_s)

Leaf and stem sap samples were extracted two hours after the onset of illumination by subjecting the leaves to overpressure in the pressure pump and Ψ_s was measured (10µl) by using a vapor pressure osmometer model VAPRO 5520 (Wescor, Logan, UT, USA). Osmolarity was measured in mmol kg^{-1} and transformed into MPa using the Van't Hoff equation, where MPa = mmol kg^{-1} x 2.58 x 10^{-3}.

Titratable acidity analysis and organic acid and soluble carbohydrate profiling

For metabolite analysis, frozen leaf and stem samples (200 mg fresh weight – FW) were extracted in 1 ml 80 % (v/v) methanol for 15 min at 80°C, and the supernatants were recovered by centrifugation (15,000 *g*, 15 min, 25ºC). The pellets were re-extracted five times, and all supernatants were combined before the analysis. For the titratable acidity analysis, 50µl aliquots of the supernatant fraction were titrated with 2 mM NaOH to pH 8.0 using phenolphthalein as an indicator.

For the organic acid and soluble carbohydrate profiling, methanol extracts (~ 1 ml) were reduced to dryness under vacuum and resuspended in 25 µl pyridine. Samples were derivatized 1 h at 60°C with 25 µl of N,O-*bis*(trimethylsilyl) trifluoroacetamide with 1% (v/v) trimethylchlorosilane for sugar profiling, and 1 h at 92°C with 25 µl of *N*-tert-butyldimethylsilyl-N-methyltrifluoroacetamide with 1% (v/v) *tert*-butyldimethyl-chlorosilane for organic acid profiling. The derivatized extracts were analyzed by GC-MS (model GCMS-QP2010 SE, Shimadzu, Japan), and the total ion current spectra were recorded in the mass range of 50–700 atomic mass units in scanning mode. The chromatograph was equipped with a fused-silica capillary column DB-5 MS stationary phase using helium as the carrier gas at a flow rate of 4.5 ml min^{-1}. The initial running conditions were 100°C for 5 min, followed by a gradient up to 320°C at 8°C min^{-1}. Endogenous metabolite concentrations were obtained by comparing the peak areas of the chromatograms against commercial standards.

Whenever applicable, malate content was also quantified enzymatically as described in Boxall *et al.* (2019). Starch content was determined from dried pellets as described in Amaral *et al.* (2007).

Anatomical analyses

Leaf and stem samples from well-watered plants were fixed in FAA (formalin, acid acetic and ethanol 50% 9:1:1) for 24h and stocked in ethanol 70% (v/v), dehydrated, embedded in historesin (Leica®) and serial sectioned at 12 µm thickness on a Leica RM2145 rotary microtome (Leica Microsystems, Wetzlar, Germany). Transverse sections of leaves and stems were stained with toluidine blue solution and analyzed by light microscopy (Leica Microsystems, Wetzlar, Germany). Leaf and stem samples were also dehydrated in an ethanol dilution series before being critically point-dried with CO_2, sputter-coated with gold (SCD-050 sputter coater, Bal-Tec AG, Balzers, Liechtenstein) and examined by scanning electron microscopy (Sigma VP - Zeiss, Oberkochen, Germany). To determine chloroplast distribution within tissues, transversal leaf and stem cryosections were prepared using Leica KS34 cryomicrotome (Leica Microsystems) immediately analyzed using a UV epifluorescence microscope (DMLB; Leica) equipped with a Leica H3 filter (excitement at 420 nm and emission at 495 nm).

Total RNA extraction, cDNA synthesis and RT-qPCR analysis

Total RNA was extracted (~ 80 mg FW) using ReliaPrep™ RNA Tissue Miniprep System (Promega) for fibrous tissues. Additional homogenization steps by pipetting up and down multiple times were performed between each added solvent to disrupt the formed mucilage. RNA purity and concentration were assessed using a microvolume spectrophotometer (NanoDrop™ 8000, Thermo Scientific™, Wilmington, DE). Sufficient purity was considered 260/280 nm and 260/230 nm ratios between 1.8–2.2 and 1.6–2.2, respectively.

Total RNA was treated with DNase (DNase I Amplification Grade, Thermo Fisher Scientific) for 10 min at room temperature. For the diel gene expression profiling and RNA-seq validation, cDNA was synthesized using QuantiTect Reverse Transcription kit (Quiagen) and qPCR reactions were performed using the LightCycler® 480 Instrument II (Roche Life Science) with a 10 µl mix reaction composed of 5 µl SensiFAST™ SYBR kit (Bioline Reagents Ltd), 1 µl cDNA sample and 300 nM of forward and 300 nM of reverse primers. The amplification program consisted of 5 min initial step at 95°C, followed by 40 cycles with 5 s - 95°C, 15 s - 63°C and 15 s - 72°C. For the remaining gene expression analysis, cDNA was synthesized using SuperScript® IV Reverse Transcriptase kit (Thermo Fisher Scientific) and qPCR reactions were performed in a StepOnePlus™ Real-Time PCR System (Applied Biosystems) using 10 µl mix reaction composed of 5 µl Power SYBR green 2X (Thermo

Fisher Scientific), 2 µl cDNA sample and 300 nM of forward and 300 nM of reverse primers. The amplification program consisted of 10 min initial step at 95°C, followed by 40 cycles with 15 s 95°C, 30 s 60°C and 30 s 72°C. In all cases, the melting curve was analyzed to detect unspecific amplification and primer dimerization. The relative transcript abundance was calculated by applying the $2^{-\Delta\Delta CT}$ method (Livak & Schmittgen, 2001). Expression values were normalized against the geometric mean of two reference genes, *UBIQUITIN-TRANSFERASE (UPL7* - At3g53090*)* and *CLATHRIN ADAPTOR COMPLEX SUBUNIT* (*AP2M* - At5g46630), chosen after different reference genes were tested for stability in *P. oleracea* based on the listing made by Czechowski *et al.,* (2005). Absolute fluorescence data were analyzed using the LinRegPCR program (http://linregpcr.nl/) to obtain primer efficiency. All reactions were performed with two technical replicates and three to four biological replicates.

RNA-seq generation, assembly, annotation and analysis

Total RNA was extracted as described above from leaf and stem samples harvested in biological triplicates from well-watered and drought-stressed plants at D3 (8h, 16h and 24h, corresponding to 2h and 10h after the onset of light, and 6h into the 12 h dark period, respectively). The quality of the RNA isolated from leaves and stems at D3 was assessed using the Agilent 2100 Bioanalyzer (Agilent Technologies, Santa Clara, CA). Samples were treated with DNase I and the Ribo-Zero™ Plant Leaf Kit (Illumina, Inc.) and cDNA libraries were obtained with the NEBNext® Ultra™ Directional RNA Library Prep Kit for Illumina® (New England Biolabs, Inc.). Paired-end sequences (2 x 150bp) of the 36 indexed RNA-seq libraries were multiplexed across a total of 3 lanes of the Illumina HiSeq4000 platform, using V4 chemistry and generating more than 280 M clusters per lane. Fastq sequence files were deposited at NCBI under BioProject PRJNA576481.

Reads were filtered using Seqyclean (v. 1.9.10) (https://github.com/ibest/seqyclean), with average 24 Phred quality, and 65 bp as the minimum length for filtered reads. UniVec (https://www.ncbi.nlm.nih.gov/tools/vecscreen/univec/) database was used to identify contaminants and vector sequences. Only high-quality paired-end sequences were used for further analyses and over 90% of the total raw read count was kept. *De novo* transcriptome assembly was performed by Trinity (v. 2.3.2) (Grabherr *et al.,* 2013) using one of the three biological replicates, with a minimal contig length selection of 300bp and using the "normalize_by_kmer" flag. Trinity uses three softwares, Inchworm, Chrysalis and Butterfly, to assemble the reads based on k-mer graphs, build de Bruijn graphs by checking for shared k-mers, and finally build compact paths among the graphs, respectively, resulting in linear sequences for each spliced form (Grabherr *et al.,* 2013). This software provides contigs with an ID and report sequence similarities between contigs using a system of three levels:

component, gene and isoform. After generating the *de novo* assembly, ORFs were identified using TransDecoder (v. 3.0.0 – available at https://github.com/TransDecoder/TransDecoder /wiki) and contigs were then clustered and filtered using CD-HIT (v.4.6.6) (Li & Godzik, 2006) with the clustering threshold set to 95% to reduce redundancy. The homology between the assembled transcriptome and sequences from the SwissProt database (The UniProt Consortium, 2019) was evaluated using the BLASTX program (Camacho *et al.,* 2009) with e-value threshold $1e^{-6}$. SwissProt was chosen because it includes sequences from multiple C_3, C_4 and CAM organisms. Reads were mapped to the assembly using bowtie2 (version 2.3.1) (Langmead & Salzberg, 2012). Seeking to further reduce redundancy, contigs with the same ID and annotation were filtered for the longest isoform at gene level, as defined by Trinity, using a homemade R script.

Pairwise differential expression (DE) analysis using Trimmed mean of M values (TMM) normalization and counts per million (CPM) filtering was conducted using edgeR package (version 3.7) for Bioconductor (Robinson *et al.,* 2010; McCarthy *et al.,* 2012). We compared well-watered and droughted leaves or stems for all three-time points across the diel cycle, and also compared leaves and stems in well-watered or droughted conditions at all sampling points. Heatmaps were generated using Morpheus tool (https://software.broadinstitute.org/ morpheus). Venn diagrams for DE gene lists were generated using http://bioinformatics.psb.ugent.be/webtools/Venn/. Enrichment analysis for GO terms in DE lists was performed on Blast2GO software (Götz et *al.,* 2008) using Fisher's test with False Discovery Rate (FDR) at 0.08.

Phylogenetic annotation of *P. oleracea* CDS into homologs and co-orthologs encoding CCM related enzymes

The generated transcriptome was annotated as in Christin *et al.* (2014), Christin *et al.* (2015), Moreno-Villena *et al.* (2017) with modifications. To generate a dataset with homologs from publicly available, well-annotated genomes, we used a set of genomic sequences for each C_4 related genes from Moreno-Villena *et al.* (2017). For enzymes with not previously delimited eudicots gene lineages, selected *P. oleracea* transcripts were used to retrieve highly similar sequences from gene bank, and those were used as the starting dataset to retrieve homologs from the reference genomes.

These served as query to BLAST searches (Camacho et al., 2009) to retrieve homologous CDS (primary transcript only). Blast hits with a minimal e-value of 0.01 and minimal mapping length of 300 bp were retrieved and added to the data set from the genomes of four monocots (*Oryza sativa, Setaria italica, Sorghum bicolor, Zea mays*) seven eudicots (*Arabidopsis thaliana, Brassica rapa, Daucus carota, Glycine max, Kalanchöe laxiflora, Populus trichocarpa, Solanum tuberosum*) and 3 Caryophyllales (*Amaranthus*

hypochondriacus, Beta vulgaris, Chenopodium quinoa). The final genomic dataset was used into a new BLAST search in our *P. oleracea* transcriptome, with the same BLAST parameters. Genomic and transcriptomic sequences were aligned using MUSCLE v3.8.425 (Edgar 2004). Alignments were visually inspected in AliView version 1.23 (Larsson 2004) to remove potential chimeras and sequences of ambiguous homology (false positives). The remaining sequences were re-aligned as codons, manually refined for truncated non-aligning ends. Maximum likelihood phylogenetic trees were inferred for each alignment using IQ-TREE multicore version 1.6.6 PhyML (Guindon & Gascuel 2003) combining ModelFinder, 1000 ultrafast bootstrap iterations, and the SH-aLRT test to search for the best-fit tree. when possible, sequences from previous studies were added to the alignments prior to the tree inference to accurately circumscribe new *P. oleracea* transcripts into the different Caryophyllales gene lineages. For PPC, sequences from Christin *et al.* (2014), whereas for ASPAT, NADMDH, NADPME, PPDK, PPA, PPDKRP and DIC, sequences were retrieved from Christin *et al.* (2015).

Carbohydrate metabolism-related genes lineages were named after the most similar homolog in the Arabidopsis transcriptome (Araport11 Official Release dataset, available at The Arabidopsis Information Resource (TAIR), https://www.arabidopsis.org/download/index-auto.jsp?dir=/download_files/Sequences, on 05/03/2019, Berardini et al., 2015), identified by sequence similarity analysis using BLASTX with e-value = 10^{-6} and the -max_hsps = 1 flag.

Statistical analyses

All remaining statistical analyses were performed using R statistics software (version 3.4.0) provided by the CRAN project via RStudio (version 1.0.136). Data were checked for normality using the Shapiro-Wilk test (p-value > 0.05), and for homogeneity of variances using the Levene test (p-value < 0.05). When appropriate, mean differences were compared using either a two-sample t-test (normal, equal variances), Welch's t-test (normal, unequal variance), the Mann-Whitney test (non-normal, equal variances), or square-root transformed and fitted into one of the other conditions (non-normal, unequal variances).

RESULTS

Assessing CAM induction in *P. oleracea* leaves and stems during progressive drought treatment

Well-watered *P. oleracea* leaves showed atriplicoid-type anatomy, high daytime CO_2 uptake rates, and did not accumulate acids overnight (Fig. 1), confirming the use of C_4 whenever water was not limiting. In contrast, 34 days of water withholding promoted significant leaf nocturnal malic acid accumulation (ΔH^+) as detected via either enzymatic (Fig. 1b) or chromatographic (Fig. S1a) malate quantification and titratable acidity analysis (Fig. S1b),

which was associated with no diel leaf gas exchange (Fig. 1c), thereby characterizing a CAM idling state (Winter, 2019). CAM expression was up-regulated rather than induced in *P. oleracea* stems in response to drought, likely relying on internal refixation of respiratory CO_2 as the stems lacked stomata (Fig. S2c-d). Kranz anatomy traits were absent in stems, in which ΔH^+ detected under well-watered conditions was significantly intensified upon drought (Fig. 1a-b), and chloroplasts are mainly distributed in cells of the inner cortex (Fig. S2g-h).

Global transcriptional changes in response to drought

To gain insight into the transcriptional changes associated with C_4 and CAM functioning in *P. oleracea*, RNA-seq was performed using leaf and stem RNA samples isolated from well-watered and drought-stressed plants harvested at 8h, 16h and 24h. A total of 1,061,191,351 reads were obtained from all 36 libraries. Our *de novo* assembly for *P. oleracea* yielded 452,522 contigs, of which 84,494 were kept after ORF identification and redundancy elimination (Table S2). 52,514 contigs were successfully annotated against the UniProt database and 80.35% of trimmed reads of all samples were mapped against our *de novo* assembly. Only the longest isoform for each annotated contig was kept (see Methods for details), resulting in a total of 32,306 contigs.

Differentially expressed (DE) contigs in response to drought were identified at each sampling time-point, revealing that approximately 6 and 14% of the whole transcriptome were down-regulated upon drought in leaves and stems, respectively (Fig. S3a; Table S3). Enrichment analysis for gene ontology (GO) terms revealed that photosynthesis and sugar metabolism-related terms were particularly down-regulated in drought-stressed leaves (Table S4), which agrees with the negative influence of drought on leaf CO_2 assimilation (Fig. 1c).

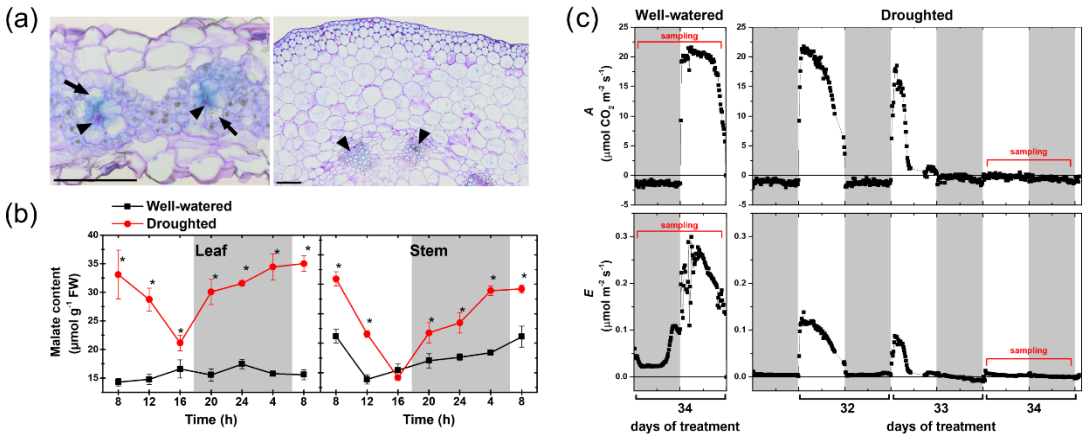

Figure 1 Drought promotes CAM induction in C_4 leaves and intensifies CAM expression in stems of *Portulaca oleracea*. (a) Leaf (left) and stem (right) cross-sections of well-watered plants. Black arrows and arrowheads indicate bundle sheath cells and vascular bundles, respectively. Bars = 250μm. (b) Diel fluctuation of malate content in leaf and stem from plants exposed to 34 days of well-watered or drought treatments. Malate was determined via enzymatic assays. In (b), data are means (±SE) of at least three biological replicates and asterisks indicate significant difference ($P < 0.05$). (c) Diel net CO_2

assimilation (*A*) and transpiration (*E*) in leaves of plants exposed to well-watered or drought treatments. In (c), data are normalized against the leaf area. In (b-c), the shaded areas indicate the dark period.

Photosynthesis- and carbohydrate metabolism-related GO terms were also enriched in well-watered leaves compared to well-watered stems (Table S4), reinforcing that, although photosynthetically active, *P. oleracea* stems play a minor role in the overall shoot carbon fixation compared to the leaves.

The mean correlation coefficients obtained by comparing $\log_2$ fold-change (logFC) values from RNA-seq and $\log_2$ ratio of mRNA relative abundance from qPCR analysis revealed adequate correspondence between RNA-seq and qPCR data in both leaf and stem samples (Fig. S4).

Using transcriptomic data to identify CCM-related genes

Multiple approaches were employed to identify key candidate genes involved in *P. oleracea* CCM reactions. First, genes encoding major C_4/CAM-related genes were filtered according to annotation (Table S5), and the most representative contig for each gene was selected based on transcript abundance and logFC (Figs. 2-3, S5-S6). Second, gene nomenclature was established according to Christin *et al.* (2014), based on phylogenetic trees inferred using data from C_3, C_4 and CAM plants. Groups of co-orthologs for selected CCM genes (Figs. S7, S8) matched those previously identified for *Portulaca* (Christin *et al.,* 2014, 2015). Third, CCM genes differentially regulated by drought were further analyzed via qPCR for a detailed characterization of their diel cycles of transcript abundance (Figs. 3, 5).

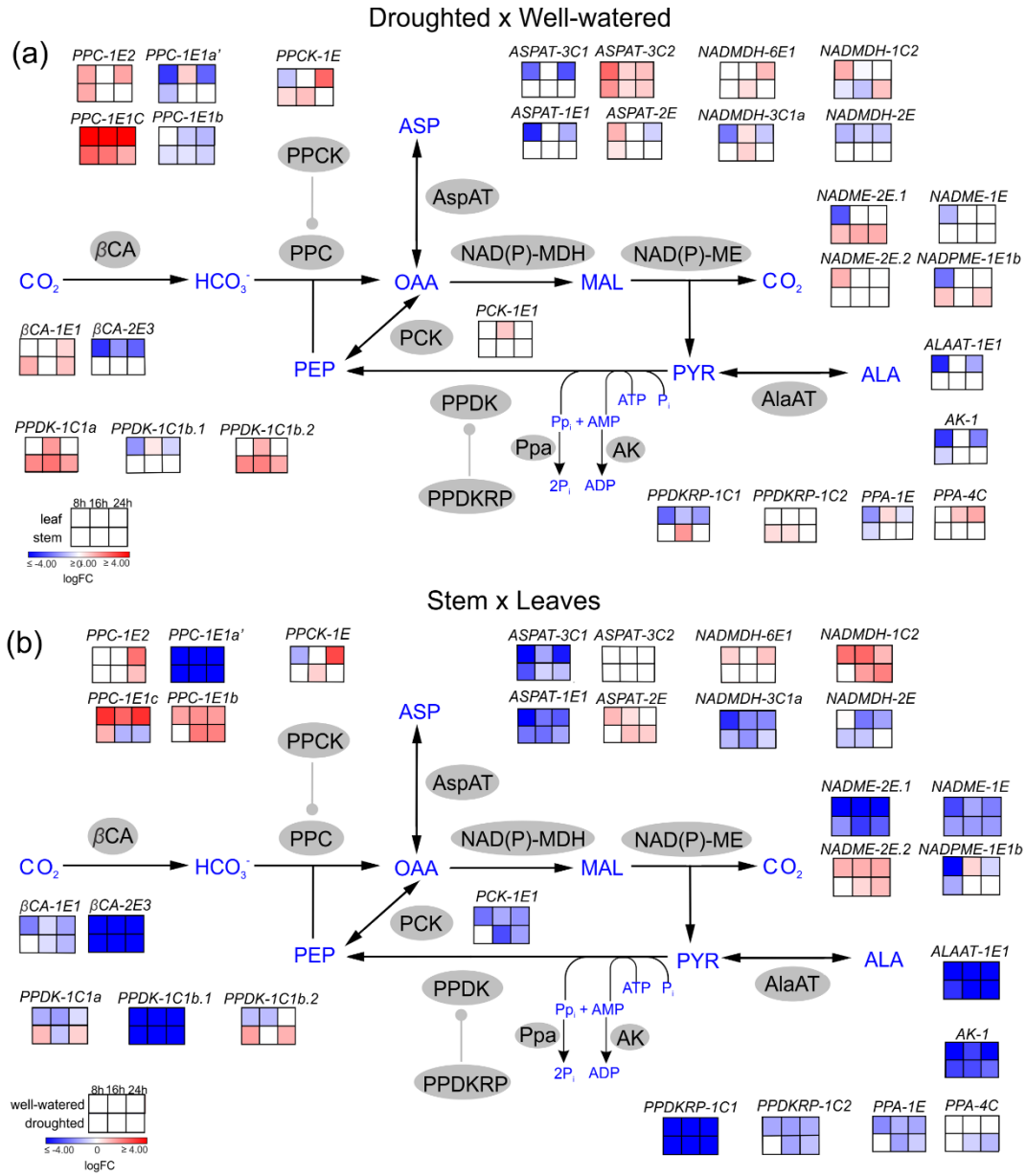

Figure 2 Drought-induced changes in transcriptional profile reveal key components of the C_4/CAM machineries in *Portulaca oleracea*. Leaf and stem samples were harvested from plants maintained for 34 days under well-watered or droughted conditions. (a) Heatmaps indicate $\log_2$-fold change of droughted samples compared to well-watered samples. (b) Heatmaps indicate $\log_2$-fold change of stem samples compared to leaf samples. Black arrows indicate core reactions in both C_4 and CAM biosynthetic pathways whereas gray lines terminated by a closed circle indicate regulatory interactions. Intermediate reactions are omitted. Biosynthetic enzymes and metabolites are represented with gray ovals and blue letters, respectively. TMM and $\log_2$-fold change values for genes shown in the heatmaps are presented in Table S5 and Fig. S5, and their phylogenetic relationship is presented in Fig. S7. Statistically significant differences in comparison with well-watered (a) or leaf (b) samples are represented as colored squares (adjusted p-value<0.05). Data are means (±SE) of at least three replicates. Metabolites: ALA, alanine; ASP, aspartate; OAA, oxaloacetate; MAL, malate; PEP, phospho*enol*pyruvate; Ppa, inorganic pyrophosphatase; PYR, pyruvate. Enzymes: AK, adenylate kinase; ALAAT, ALA aminotransferase; ASPAT, ASP aminotransferase; βCA, beta-carbonic anhydrase; NAD(P)-ME, NAD(P)-malic enzyme; NADMDH, NAD-malate dehydrogenase; PCK, PEP carboxykinase; PPC, PEP carboxylase; PPCK, PPC kinase; PPDK, PYR orthophosphate dikinase; PPDKRP, PPDK regulatory protein.

A typical C_4-like transcript abundance pattern was observed for CCM genes down-regulated by drought (Fig. 2a), as they were more abundant in leaves (Fig. 2b) and accumulated overnight reaching a peak level phased to dawn (Fig. 3a), thereby preceding the start of C_4 reactions. In contrast, fewer CCM genes were significantly up-regulated following drought in both organs (Fig. 2a) and peaked in the dark (Fig. 3b), coinciding with the nocturnal acid accumulation promoted by drought in *P. oleracea* leaves and stems (Fig. 1b).

In both CCMs, CO_2 can be converted to HCO_3^- passively or enzymatically by a beta-carbonic anhydrase (βCA). HCO_3^- is combined with phospho*enol*pyruvate (PEP) by PPC to generate oxaloacetate (OAA) (Hatch, 1987). Although shared by both CCMs, these reactions occur at different times over the 24 h light/ dark cycle in C_4 and CAM, namely in the light and the dark, respectively. Among *P. oleracea* βCA- and PPC-encoding genes, *βCA-2E3* and *PPC-1E1a'* exhibited a C_4-like expression pattern, whereas *βCA-1E1* and *PPC-1E1c* were expressed in a CAM-like fashion (Fig. 2), reinforcing previous evidence that specific gene family members may have been recruited to fulfill the C_4 and CAM carboxylation reactions according to the prevailing environmental conditions (Christin *et al.,* 2014).

PPCK is induced by high-light in C_4 leaves (Carter *et al*., 1991). In contrast, *PPCK* expression is mainly controlled by the endogenous circadian clock in CAM species, leading to a dark phased peak of PPCK activity, which promotes PPC phosphorylation and consequently increases the K_i of PPC for feedback inhibition by L-malate (Hartwell *et al.,* 1996; Hartwell *et al*., 1999). In *P. oleracea*, RNA-seq data revealed a single *PPCK* ortholog (*PPCK-1E*), which showed transcript levels that peaked 2 h into the 12-h-light period (08:00) in C_4-performing leaves and peaked 16 h later (at 24:00) in CAM-performing leaves and stems (Figs. 3c, S5).

C_4 species can use either NAD-malic enzyme (NAD-ME) or NADP-ME as primary decarboxylation enzymes with or without the additional involvement of PEP carboxykinase (PCK) (Furbank, 2011). *P. oleracea* has been classified as a NAD-ME-type species (Lara *et al*., 2004; Voznesenskaya *et al*., 2010), implying that most CO_2 incorporated as OAA in this species is converted to aspartate (ASP) in MCs via aspartate aminotransferase (AspAT) activity. The ASP formed diffuses to BSCs via plasmodesmata and enters the mitochondria, where AspAT reverts ASP to OAA, and NAD-malate dehydrogenase (MDH) converts OAA to malate, which is decarboxylated by NAD-ME (Kanai & Edwards, 1999). To sustain these reactions, ASP and malate movements across mitochondria are facilitated by Uncoupling protein 2 (UCP2) and Dicarboxylate transport 1 (DIC1) proteins, respectively (Vozza *et al.,*

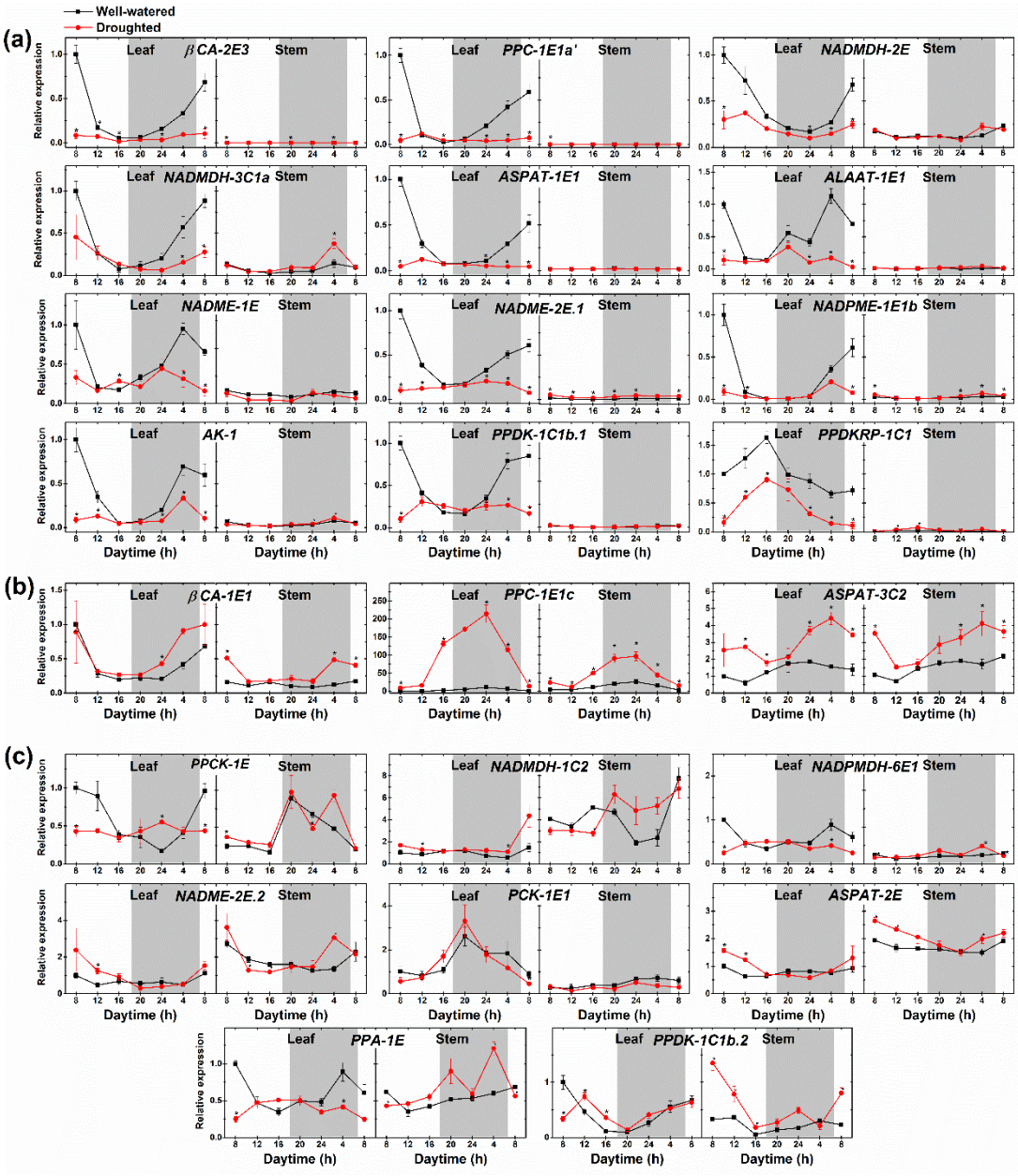

Figure 3 Drought induces changes in diel transcript abundance of key C_4/CAM genes in *Portulaca oleracea*. (a) qPCR data of genes exhibiting C_4-like expression patterns. (b) qPCR data of genes exhibiting CAM-like expression patterns. (c) qPCR data of other CCM genes. Mean relative expression in leaf and stem samples was normalized against the first time point (8h) of well-watered leaf samples. The shaded areas indicate the dark period, and asterisks indicate significant difference ($P<0.05$). Data are means (±SE) of at least three replicates. AK, adenylate kinase protein; ALAAT, alanine aminotransferase; ASPAT, aspartate aminotransferase; βCA, beta-carbonic anhydrase; NAD(P)-ME, NAD(P)-malic enzyme; NADMDH, NAD-malate dehydrogenase; PCK, phospho*enol*pyruvate carboxykinase; Ppa, inorganic pyrophosphatase; PPC, phospho*enol*pyruvate carboxylase; PPCK, PPC kinase; PPDK, pyruvate orthophosphate dikinase; PPDKRP, PPDK regulatory protein.

2014; Monné *et al.,* 2018; Palmieri *et al.,* 2008). Transcripts encoding enzymes and transporters characteristic of NAD-ME-type photosynthesis (*ASPAT-1E1*, *NADMDH-2E*, *NADMDH-3C1a*, *NADME-1E, NADME-2E.1*, *UCP-2* and *DIC-1.2*) were abundant in well-watered leaves and exhibited C_4-like diel regulation, with peak levels phased to 08:00, 2h into the 12-h-light period (Figs. 2-5). In contrast, *ASPAT-3C2* was up-regulated significantly by drought in both leaves and stems, with a transcript peak phased to the second half of the dark period (Fig. 3b). However, ASP to OAA interconversion via AspAT is not part of the canonical CAM cycle, and *ASPAT-3C2* is phylogenetically closest to Arabidopsis *ASP3* (AT5G11520) (Fig. S7), which encodes a peroxisomal and chloroplastic protein implicated in photorespiration and senescence processes (Fukao *et al.,* 2002, Schultz & Coruzzi 1995; Wilkie & Warren 1998). Therefore, it seems unlikely that *ASPAT-3C2*-encoded protein is directly involved in *P. oleracea* CAM machinery.

Other genes, including *NADMDH-1C2*, *NADMDH-6E1* and *NADME-2E.2*, could be either shared by both CCMs or responsible for anaplerotic reactions since they did not show a clear pattern of modulation by drought (Figs. 3c, S5). Transcripts of a NADP-ME-encoding gene (*NADPME-1E1b*) were abundant in both C_4- and CAM-performing tissues (Fig. S5), but *NADPME-1E1b* is phylogenetically closest to Arabidopsis *NADP-ME4* (AT1G79750) (Fig. S7), which is implicated in fatty acids biosynthesis (Wheeler *et al.,* 2005). The only PCK-encoding gene identified (*PCK-1E1*) was a low abundance transcript compared to other decarboxylases (Fig. S5), suggesting a limited, if any, contribution of PCK for decarboxylation reactions in this species.

In C_4 plants such as *P. oleracea*, after CO_2 is released by NAD-ME, the residual pyruvate (PYR) is transported to the cytosol by an unknown transporter, converted to alanine (ALA) by ALA aminotransferase (AlaAT) to flow back to MCs and be reverted to PYR again finally entering the chloroplast (Kanai & Edwards, 1999). PYR is imported into the chloroplast in exchange of sodium by the Bile acid:sodium symporter family protein (BASS), functioning in concert with the sodium:hydrogen antiporter (NHD) (Furumoto *et al.,* 2011). PEP supply is restored via PPDK, releasing pyrophosphate (PPi) and adenosine monophosphate (AMP), which are further metabolized via pyrophosphorylase (PPa) and AMP kinase (AK) activities, respectively (Matsuoka, 1995). PEP is then exported to the cytosol by PEP/phosphate translocator (PPT) (Thompson *et al.,* 1987). Genes encoding this suite of enzymes (*ALAAT-1E1, PPDK-1C1b.1, PPA-1E, AK-1*) and transporters (*BASS-1* and *PPT-1E2*) were abundant transcripts that displayed a C_4-like temporal pattern in well-watered leaves (Figs. 2-5). In response to drought, *BASS-1*, *PPT-1E2*, *ALAAT-1E1* and *AK-1* were down-regulated in leaves, whereas *PPA-4C* was upregulated by drought in leaves (Fig 2a) and *PPA-1E* and *PPDK-1C1b.2* were up-regulated by drought in stems (Fig. 3c). As PPDK activity is required at daytime in both C_4 and CAM systems (Chastain *et al.,* 2002; Dever *et al.,* 2015), the

PPDKRP-1C1 transcript peak detected at the end of the light period (Fig. 3a) is consistent with the fact that PPDK needs to be activated in the light and inactivated in the dark in both C_4 and CAM. Similar diel transcript abundance patterns have also been reported previously for *PPDKRP*-encoding genes in C_4 and CAM species (Chastain & Chollet, 2003; Dever *et al.,* 2015).

In CAM plants, malate accumulates as vacuolar malic acid due to nocturnal CO_2 fixation, and is subsequently released from the vacuole in the light period. The most likely candidates for nocturnal voltage-gated uptake of malate are the tonoplast-localized aluminum-activated malate transporters (ALMT) (Kovermann *et al.,* 2007; Borland *et al*., 2009). Also, the tonoplast dicarboxylate transporter (tDT) may function in the transport of malate out of the vacuole for decarboxylation in the light period (Borland *et al*., 2009). In *P. oleracea*, *ALMT-12E.1* and *ALMT-9E* were up-regulated by drought in both leaf and stem tissues, whereas the opposite was observed for *ALMT-12E.2*, which was most abundant at the start of the light period in leaves under well-watered conditions (Figs. 4-5, S6). Among *ALMT* genes, *ALMT-9E* is closely related to Arabidopsis *ALMT9* (AT3G18440), a voltage-gated chloride channel in the tonoplast of guard cells (Zhang *et al.,* 2013), that has also been reported to act as a vacuolar malate channel in MCs (Kovermann *et al.,* 2007; De Angeli *et al.,* 2012). In addition to *ALMT* genes, *TDT-1E* was markedly up-regulated by drought in stems, with a peak phased to 2 h before dawn (Figs. 3, S6), which may suggest involvement in CAM.

Malate import into vacuoles in the dark period during CAM is mediated by a voltage-gated, inward-rectifying anion channel (Hafke *et al*., 2003). The membrane potential difference across the tonoplast membrane that energizes this import is generated by the V-ATPase (also known as Vacuolar-type proton ATPase – VHA) and/ or the VPPase (Pyrophosphate-energized membrane proton pump – AVP) (Smith *et al.,* 1996). Drought promoted up- and down-regulation of *VHAB2-1E1* and *AVP1-2E*, respectively (Figs. 4-5), and slightly increased transcript abundance for a range of other VHA subunit genes, including *VHAA3-3E*, *VHAF-1E* and *VHAG1-1E* (Fig. S6). Taken together, these results suggest a preference for VHA over AVP for the nocturnal accumulation of protons in the vacuole, which in turn energize nocturnal malate import via the putative tonoplast ALMT in CAM-performing *P. oleracea* tissues. It was noteworthy that *VHAB2-1E1* transcripts peaked in the middle of the night in drought-stressed leaves of *P. oleracea* (Fig. 3c), consistent with the proposed regulation of V-ATPase activity via the level of the transcript abundance of the associated subunit genes (Chen *et al*., 2012).

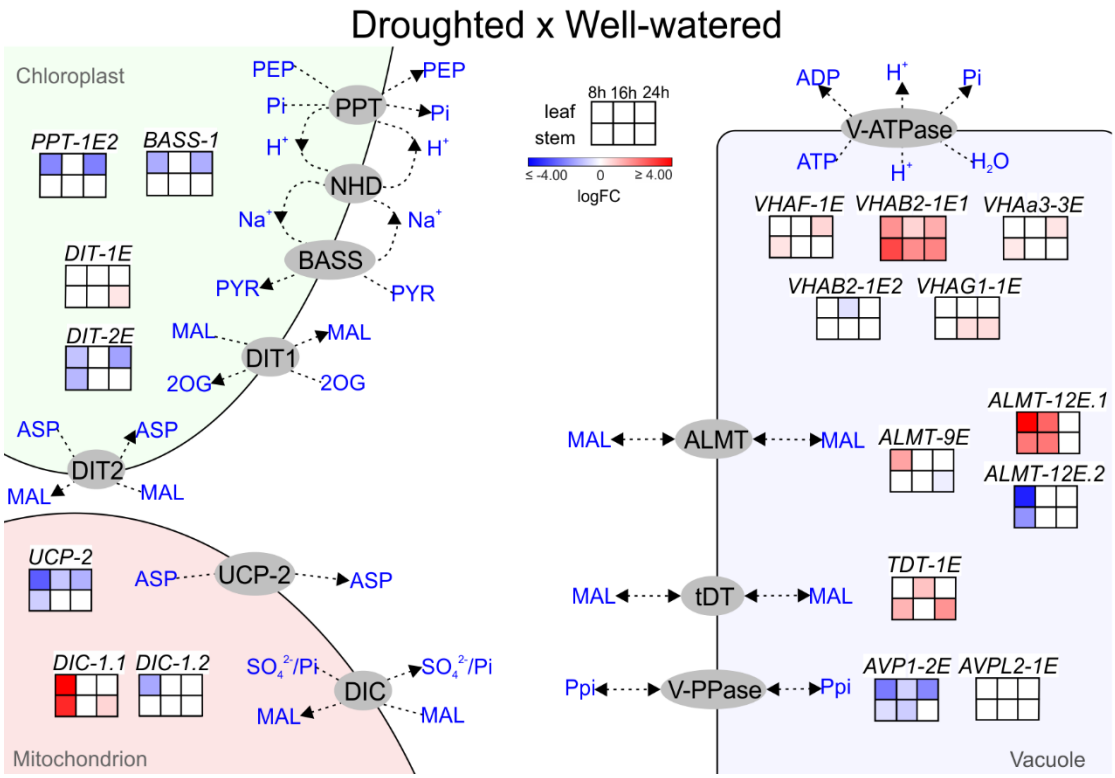

Figure 4 Drought modulates the transcriptional profile of genes encoding CCM-related transporters and pumps in *Portulaca oleracea*. Leaf and stem samples were harvested from plants maintained for 34 days under well-watered or droughted conditions. Schematic representation illustrating the putative intracellular localization of C_4/CAM-related transporters and pumps, which are represented with gray ovals. Heatmaps indicate log_2-fold change of droughted samples compared to well-watered samples. TMM and log_2-fold change values for genes shown in the heatmaps are presented in Fig. S6 and Tables S5 and S6, and their phylogenetic relationship are presented in Fig. S8. Statistically significant differences in comparison with well-watered samples are represented as colored squares (adjusted p-value<0.05). Data are means (±SE) of at least three replicates. Metabolites: 2OG, 2-oxoglutarate; ASP, aspartate; MAL, malate; OAA, oxaloacetate; PEP, phospho*enol*pyruvate; PPi, inorganic phosphate. Transporters and pumps: ALMT, aluminum-activated malate transporter; BASS, sodium bile acid symporter family; DIC, dicarboxylate carrier; DIT, dicarboxylate transporter; PPT, PEP/phosphate translocator; PYR, pyruvate; tDT, tonoplast MAL/fumarate transporter; UCP-2, mitochondrial uncoupling protein 2; V-ATPase/VHA, V-type proton ATPase; V-PPase/AVP, pyrophosphate-energized membrane proton pump.

Temporal dynamics of photosynthetic transitions in response to water availability

Following the identification of signature C_4 and CAM genes (Figs. 2-5), we next performed comprehensive analysis of their temporal expression dynamics, aiming to determine (1) whether C_4 and CAM co-occur as drought conditions intensify, and (2) whether CAM is reverted after re-watering events applied at distinct points of the drought treatment. Therefore, transcript abundance of CCM-marker genes (Table S6), fluctuations in Ψ_s, ΔH^+, leaf gas exchange and chlorophyll *a* fluorescence were monitored in samples harvested after 0-, 10-, 22- and 34-days of drought treatment (named D0, D1, D2 and D3, respectively) and

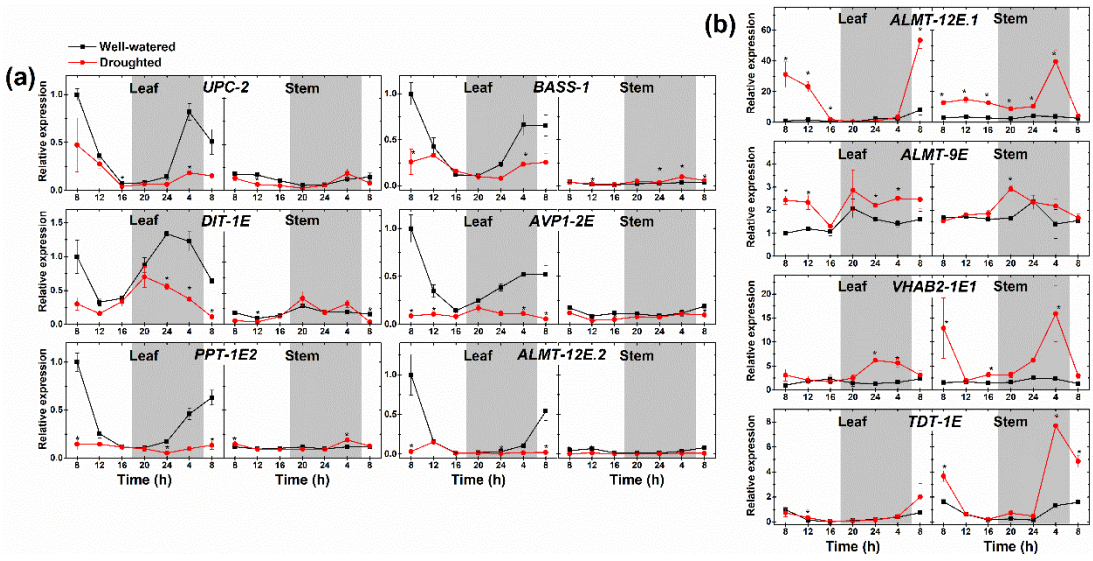

Figure 5 Diel transcript fluctuation of genes encoding CCM-related transporters and pumps is altered by drought in *Portulaca oleracea*. (a) qPCR data of genes exhibiting C_4-like expression patterns. (b) qPCR data of genes exhibiting CAM-like expression patterns. Mean relative expression in leaf and stem samples was normalized against the first time point (8h) of well-watered leaf samples. The shaded areas indicate the dark period and asterisks indicate significant difference ($P<0.05$). Data are means (±SE) of at least three replicates. ALMT, aluminum-activated malate transporter; BASS, sodium bile acid symporter family; DIT, dicarboxylate transporter; PPT, phosphoenolpyruvatephosphate translocator; tDT, tonoplast malate/fumarate transporter; UCP-2, mitochondrial uncoupling protein 2; VHA, V-type proton ATPase; AVP, pyrophosphate-energized membrane proton pump.

during re-watering events initiated after 22- and 34-days of drought (R1 and R2, respectively).

Drought reduced plant growth, resulting in shorter shoots with fewer branches in comparison to well-watered plants (Fig. 6a). The prolonged maintenance of SVWC below 20% field capacity (Fig. 6b) resulted in a significant decrease in both leaf and stem Ψ_s (Fig. 6c), which was associated with the reduction of A, g_s and E values close to or below zero, the latter signifying the respiratory loss of CO_2 from the leaf (Fig. 6d). In agreement, leaf mRNA levels of genes encoding RuBisCO small subunit (*RBCS*), RuBisCO activase (*RCA*) and most photorespiration-related enzymes (Table S7), which were named according to phylogenetic analysis (Fig. S9), declined progressively in response to lengthening drought (Fig. S10).

Leaf transcript abundance of C_4-marker genes and daytime CO_2 uptake were progressively reduced as drought intensified over time, whereas CAM-marker genes and ΔH^+ exhibited the opposite trend (Figs. 6e-h, S11), indicating a gradual, rather than abrupt, intensification of CAM in leaves. Consequently, both physiological and gene transcript abundance data suggested that both CCMs may co-exist in *P. oleracea* leaves under mild water deficit (D1). Furthermore, transcript levels of C_4-related genes in leaves were still detected at about 10 to 40% of their original abundance when maximum CAM expression had already been achieved (D2).

In contrast, drought-induced ΔH^+ and CAM-related transcript accumulation were rapidly and completely reversed upon re-watering (Fig. 6), regardless of the duration of the preceding drought treatment (R1 and R2). Within 1 and 2 days after re-watering, leaf Ψ_s, daytime CO_2 uptake and C_4-related gene expression were fully re-established to levels similar to well-watered plants (Fig. 6). Therefore, CAM seems to be entirely replaced by C_4 in leaves of *P. oleracea* soon after the water supply is re-established. In contrast, stems showed a progressive increase in both ΔH^+ and *PPC-1E1c* mRNA levels during plant growth under well-watered conditions, which was intensified by drought (Fig. 6e,g), reinforcing that CAM expression in stem tissues is under both ontogenetic and environmental regulation.

The progressive decline in *A*, *gs*, *E* and transcript levels of *RBCS*, *RCA* and C_4-signature genes in *P. oleracea* droughted leaves was not accompanied by significant changes in chlorophyll *a* fluorescence parameters such F_v/F_m, Fq′/Fm, ETR and NPQ (Fig. S12). This suggests that linear electron transport within chloroplasts may have been maintained despite the drought-induced decline in atmospheric CO_2 uptake (Fig. 1c).

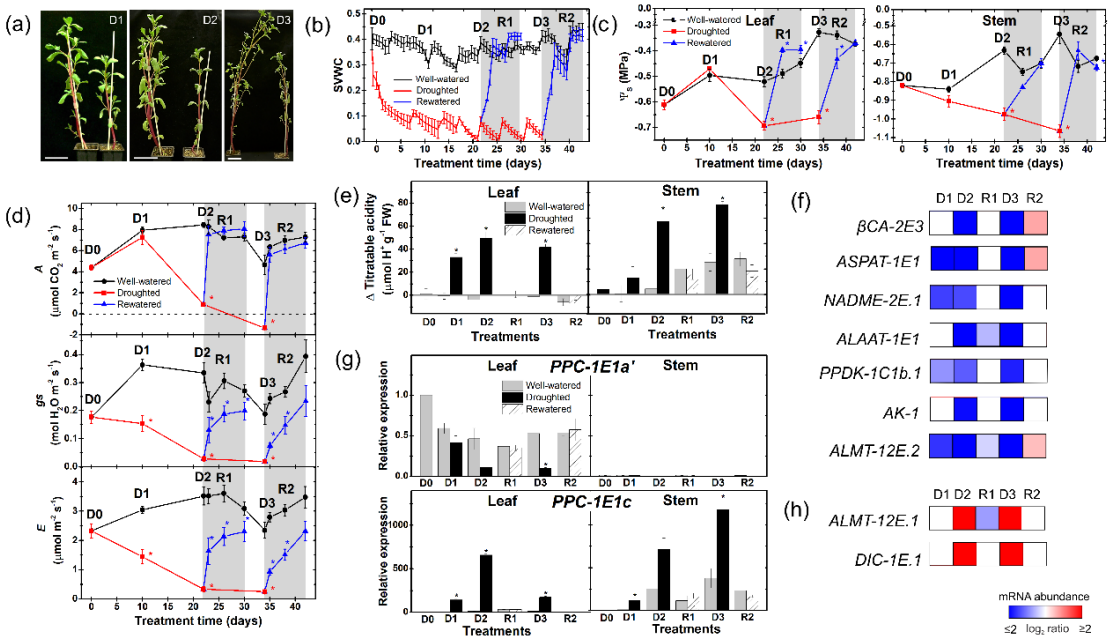

Figure 6 Changes in water availability promotes completely reversible photosynthetic transitions in *Portulaca oleracea*. Plants were sampled after 0, 10, 22 and 34 days of drought treatment (D0, D1, D2 and D3, respectively) and during rewatering events initiated after 22 and 34 days of drought (R1 and R2, respectively). (a) Overall morphological aspects of well-watered (left) and droughted (right) plants. Bars: 7 cm. (b) Soil volumetric water content (SVWC) during the treatments. (c) Leaf and stem osmotic potential (Ψs). (d) Net CO_2 uptake (*A*), stomatal conductance (*gs*) and transpiration (*E*) in leaves. (e) Titratable acidity in leaf and stem tissues. ΔH^+ indicates dawn-dusk differences. In (e), standard error of the dawn-dusk difference = $\sqrt{((\text{standard error}_{dawn})^2 + (\text{standard error}_{dusk})^2)}$. (f) Heatmaps indicate $\log_2$-fold change of well-watered compared to drought/rewatered leaves for C_4-signature genes (qPCR data presented in Fig. S11). (g) Transcript abundance of phospho*enol*pyruvate carboxylase (PPC)-encoding genes normalized against D0 leaf samples. (h) Heatmaps indicate $\log_2$-fold change of well-watered compared to drought/rewatered leaves for CAM-signature genes (qPCR data presented in Fig. S11). In (c-e, g), asterisks indicate significant difference ($P < 0.05$). In (f,h), statistically significant differences are represented as colored squares (adjusted p-value<0.05). In (b-d),

gray areas indicate rewatering events. Data are means (±SE) of at least three replicates. AK, adenylate kinase; ALAAT, alanine aminotransferase; ALMT, aluminum-activated malate transporter; ASPAT, aspartate aminotransferase; βCA, beta-carbonic anhydrase; DIC, dicarboxylate carrier; NAD-ME, NAD-malic enzyme; PPC, phosphoenolpyruvate carboxylase; PPCK, PPC kinase; PPDK, pyruvate orthophosphate dikinase.

Starch turnover intensified during CAM in *P. oleracea*

Transitory leaf starch metabolism is not as important for C_4 as it is for starch-storing CAM species, which require a sufficient pool size of starch at the start of each night in order to supply PEP to PPC throughout the dark period (Weise *et al*., 2011). In line with these differential metabolic demands, a significant rewiring of carbohydrate-associated metabolism was observed during CAM induction and intensification in *P. oleracea* leaves and stems, respectively (Fig. 7; Table S8). Drought-promoted diel fluctuation in starch levels was exclusively observed in stem tissues, achieving levels up to 2-fold higher in drought-stressed compared to well-watered plants at the end of the light period, and declining to similar levels in both watering conditions during the first half of the dark period (Fig. 7a). Consequently, the drought-triggered increment in stem ΔH^+ coincided with an intensification in diel starch fluctuation. CAM induction in leaves was instead associated with lower starch accumulation in leaves, which correlates with the progressive reduction in leaf photosynthetic carbon assimilation caused by drought-induced stomatal closure (Figs. 1b, 6d).

Transcript levels of contigs encoding both the small (*ADG1* and *ADG2*) and large (*APL3*) subunits of ADP-glucose pyrophosphorylase (AGPase), the first committed step in starch biosynthesis, as well as Granule-bound starch synthase (*GBSS1*), responsible for amylose synthesis, peaked at 2 h into the light period, regardless of the tissue or watering condition (Fig. S13; Table S8). At this temporal peak, drought promoted transcript accumulation of *ADG1*, *APL3* and *GBSS1* in stems, but not in leaves (Figs 7b, S13). Transcript abundance of genes encoding enzymes involved in both the hydrolytic (amylolytic) and the phosphorolytic pathways of transitory starch degradation, including Isoamylase 3 (*ISA3*), Limit Dextrinase or Pullulase (*LDA*), Disproportionating enzyme 1 (*DPE1*) and Alpha-glucan water dikinase dikinase (*GWD*) were up-regulated in both organs in response to drought (Fig. 7b; Table S8). Moreover, genes encoding enzymes associated with hydrolytic starch degradation – Phosphoglucan phosphatase (*SEX4*), Alpha-amylase (*AMY3*) and Beta-amylase (*BAM1*) – as well as those required for the phosphorolytic pathway – Starch phosphorylase1 (*PHS1*) – were also up-regulated upon drought (Figs. 7b, S13). Besides, chloroplast maltose exporter-encoding gene *MEX1* was predominantly down-regulated upon drought, whereas *GPT2.2*, which encodes a G6P/phosphate translocator, was up-regulated in both organs in response to drought (Fig. 7b, S14).

Maltose can be converted to glucose via cytosolic Disproportionating enzyme 2 (*DPE2*), Starch phosphorylase 2 (*PHS2*) and Phosphoglucomutase 2 (*PGM2*) (Brilhaus *et al.,* 2016). Transcripts encoding these three cytosolic enzymes remained unchanged or were down-regulated in response to drought, whereas *PGM1*, which encodes a chloroplastic PGM, was up-regulated by drought at dawn in both leaves and stems (Fig. 7b, S13). The abundance of transcripts encoding cytosolic Hexokinase 2 (HXK2), responsible for catalyzing the conversion of glucose to G6P (Brilhaus *et al.,* 2016), remained unchanged, whereas other *HXK* genes, such as *HXK1* (AT4G29130, nuclear localization) and *HXK3* (AT1G47840, chloroplastic) were only slightly modulated by drought. Glucose-6-phosphate isomerase (PGI) can be either chloroplastic (*PGI1*) or cytosolic (*SIS.1* and *SIS.2*) and only the cytosolic forms were slightly up-regulated in our transcriptome.

Despite the significant reduction in leaf and stem soluble sugar content following drought (Fig. 7a), genes encoding tonoplast sugar transporters, such as Tonoplast monosaccharide transporters (*TMT*), Early responsive to dehydration-like 6 (*ERDL6*) and *SWEET* (Sugars will eventually be exported transporters), were predominantly up-regulated upon drought, with the exception of *TMT1* and *SWEET16*. Variable transcript abundance patterns were also observed for genes encoding enzymes involved in glycolytic PEP production, with Phosphofructokinase (*PFK6*), Fructose-bisphosphate aldolase (*FBA6*) and Triosephosphate isomerase (*TPI.1*) up-regulated significantly in drought-stressed leaves 2 h before dusk (16:00) and in the middle of the dark period (24:00) (Figs. 7b, S13; Table S8).

DISCUSSION

Species across the Caryophyllales comprise a hot-spot for CCM evolution, including C_3, C_3-C_4 intermediates, variations of C_4 or CAM and even C_4-CAM facultative species, the latter occurring exclusively in *Portulaca* (Edwards & Ogburn, 2012). In *Portulaca,* CAM is believed to be ancestral to C_4 considering its position relative to CAM-performing clades (e.g., cacti, *Ancampseros* and *Talinum*), and the evolution of biochemically and anatomically distinct C_4 sub-types within the lineage (Voznesenskaya *et al.,* 2010; Christin *et al.,* 2014). Previous reports for *P. oleracea*, (Koch & Kennedy, 1980, Mazen 1996, Lara *et al.,* 2003), as well as our current data, indicate that well-watered leaves perform C_4, whereas weak CAM is induced in both leaves and stems in response to drought.

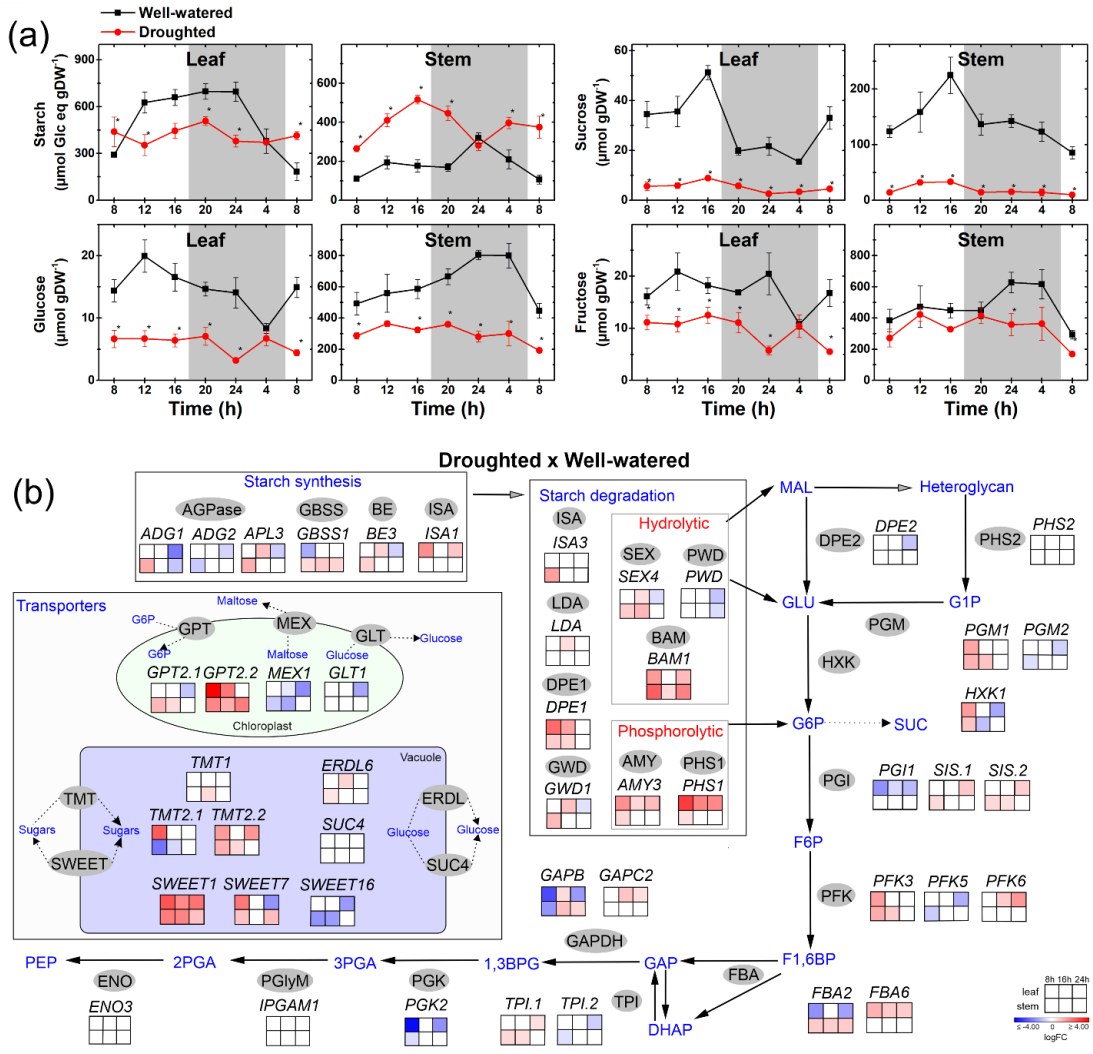

Figure 7 Coordinated changes in sugar metabolism accompany the drought-induced photosynthetic transitions of leaves and stems of *Portulaca oleracea*. Leaf and stem samples were harvested from plants maintained for 34 days under well-watered or drought conditions. (a) Diel fluctuations in starch, sucrose, glucose and fructose content. The shaded areas indicate the dark period and asterisks indicate significant difference ($P<0.05$). (b) Schematic representation of sugar metabolic reactions, with heatmaps indicating $\log_2$-fold change of droughted samples compared to well-watered samples for leaves and stems. Biosynthetic enzymes and transporters are represented with gray ovals and intermediate reactions are omitted. Statistically significant differences are represented as colored squares (adjusted p-value<0.05). Gene names were assigned based on Arabidopsis closest homolog according to sequence similarity (see Methods). TMM and $\log_2$-fold change values for genes shown in heatmaps are presented in Table S8. Data are means (±SE) of at least three replicates. Metabolites: 1,3-BPG, 1,3-Bisphosphoglycerate; 2-PGA, 2-phosphoglycerate; 3-PGA, 3-phosphoglycerate; DHAP, dihydroxyacetone phosphate; F1,6BP, fructose-1,6-bisphosphate; F6P, fructose-6-phosphate; G1P, Glucose-1-phosphate; G6P, Glucose-6-phosphate; GAP, glyceraldehyde 3-phosphate; GLU, Glucose; MAL, maltose; PEP, phospho*enol*pyruvate; SUC, sucrose. Enzymes: AGPase, G1P adenylyltransferase; ADG, AGPase small subunit; APL, AGPase large subunit; AMY, amylase; BAM, Beta-amylase; BE, Starch branching enzyme; DPE, disproportionating enzyme; ENO, enolase; ERDL, vacuolar ERD6-like 6 glucose transporter; FBA, fructose-bisphosphate aldolase; GAPDH, GAP dehydrogenase; GBSS, granule-bound starch synthase; GLT, plastidic glucose transporter; GPT, G6P/phosphate translocator; GWD, alpha-glucan water dikinase; HXK, hexokinase; ISA, isoamylase; LDA, limit dextrinase; MEX, maltose exporter; PFK, 6-phosphofructokinase; PGI/SIS, G6P isomerase; PGK, phosphoglycerate kinase-2; PGlyM/IPGAM, phosphoglycerate mutase; PGM, phosphoglucomutase; PHS, starch phosphorylase; PWD, Phosphoglucan water dikinase; SEX,

phosphoglucan phosphatase; SUC4, sucrose transport protein 4; SWEET, bidirectional sugar transporter; TMT, monosaccharide sensing protein; TPI, triosephosphate isomerase.

Adding to the identification of two *P. oleracea PPC* genes recruited to function in the C_4 and CAM cycles (Christin *et al.,* 2014), here we demonstrated contrasting diel cycling of transcript abundance for *PPC-1E1a'* compared to *PPC-1E1c*. Hence, the light/dark synchronization of the PPC-mediated primary carboxylation reactions in C_4- and CAM-performing leaves may, at least partially, rely on the opposite diel transcriptional regulation of these two *PPC* genes (Fig. 3). However, PPC is also post-translationally regulated, with PPCK-mediated PPC phosphorylation during daytime (C_4) or nighttime (CAM) adjusting the enzyme's sensitivity to its allosteric inhibitor L-malate over the diel cycle (Nimmo *et al*., 2001; Hibberd & Covshoff, 2010; Boxall *et al.,* 2017). Previously published results demonstrated that PPC kinetic properties, including its sensitivity to feedback inhibition by malate, activation by G6P, and affinity for PEP, were inverted relative to one another within the diel cycle as C_4 was replaced by CAM in *P. oleracea* leaves (Mazen 1996, 2000). Our findings revealed that a single PPCK-encoding gene is shared by both CCMs, since *PPCK-1E1* mRNA accumulation coincided with C_4 *PPC-1E1a'* accumulation in well-watered and with CAM *PPC-1E1c* accumulation in droughted leaves.

Putative C_4 signature genes were identified, including those implicated in carboxylation (*βCA-2E3*, *PPC-1E1a'*), acid formation (*ASPAT-1E1, NADMDH-2E, NADMDH-3C1a, ALAAT-1E1*), decarboxylation (*NADME-2E.1)*, and PEP regeneration reactions (*AK-1, PPDK-1C1b.1)*, as well as in the transport of PEP, ASP and PYR between sub-cellular compartments (*UCP-2, BASS-1, PPT-1E2*). Most reactions and processes associated with CAM functioning in *P. oleracea*, except nocturnal carboxylation reactions (*PPC-1E1c*, *βCA-1E1)* and malate transport across the tonoplast (*ALMT-9E*, *VHAB2-1E1, TDT-1E*), were able to utilize genes shared by both CCMs. Since drought-stressed *P. oleracea* display low-level diel acid fluctuation (weak CAM; Winter 2019), it probably demands reduced steady-state levels of dedicated enzymes to fulfill decarboxylation, PEP regeneration and other CAM cycle-related reactions.

The connectivity between C_4 and CAM pathways in *P. oleracea* remains enigmatic and poorly investigated (Lara *et al.*, 2004; Christin *et al.,* 2014; Ferrari & Freschi, 2019). At one extreme, C_4 and CAM pathways could be disconnected, never occurring at the same time and/or region of the mesophyll. Alternatively, an interconnected C_4/CAM hybrid system may exist, in which several components and reactions would be shared between both CCMs. Within these extremes, any level of C_4/CAM interconnection seems to be possible. Our findings support the temporal coexistence of both CCMs within *P. oleracea* leaves whenever water supply is restricted. We demonstrated that prolonged drought exposure promoted a

gradual, rather than abrupt, down- and up-regulation of leaf C_4 and CAM central components, respectively. Significant ΔH^+ and mRNA levels of CAM marker genes were observed as early as 10 d after water withholding, when diurnal CO_2 uptake and C_4 gene expression were only slightly reduced. Moreover, mRNA levels of C_4 signature genes were still detectable when daytime gas exchange had ceased.

However, gathering reliable information about the tissue, cell type and sub-cellular distribution of C_4 and CAM machineries within the *P. oleracea* leaf mesophyll remains critical for a full understanding of the interconnections between both CCMs. Therefore, the identification of CAM and C_4 signature genes provided by this study provides a comprehensive set of candidates for future *in situ* hybridization and immunolocalization studies. Only one *in situ* immunolocalization study has been performed on drought-stressed *P. oleracea* leaves, which revealed that both RuBisCO and NAD-ME were localized to the BSCs, whereas PPC was found in MCs and water storage cells (WSCs) (Lara *et al.*, 2004). Thus, instead of all CAM-reactions taking place within a single cell (Winter & Smith 1996), an alternative two-cell C_4/CAM hybrid system has been proposed to operate in droughted *P. oleracea*. This hypothetical model proposes that malate accumulated overnight in vacuoles of MCs and WSCs would be transferred to BSCs during the light period for decarboxylation, providing CO_2 to sustain RuBisCO activity behind closed stomata (Lara *et al.*, 2004).

Although malate is typically transported from MCs to BSCs via plasmodesmata in C_4 (Kanai & Edwards 1999), the C_4/CAM hybrid system would implicate additional metabolic fluxes, including the daily transport of malate stored at MCs, and possibly WSCs, to BSCs (Lara *et al.*, 2004). Interestingly, drought stress significantly impacted the transcript abundance of *P. oleracea ALMT-12E.1* and *ALMT-12E.2*, both closely related to Arabidopsis *ALMT12*, which encodes a plasma membrane malate transporter predominantly found in guard cells (Meyer *et al.,* 2010). As *P. oleracea* stems are devoid of stomata, the predominance of *ALMT-12E.2* transcripts in leaves suggests a functionally conserved role for this gene in controlling stomatal movements (Meyer *et al.,* 2010). In contrast, *ALMT-12E.2* transcripts were equally abundant in tissues containing or lacking stomata (leaves and stems, respectively), which may indicate functional divergence compared to Arabidopsis *ALMT12*. As *ALMT-12E.1* was highly induced by drought, it could suggest their involvement in the daytime transport of malate between WSCs, MCs and BSCs in *P. oleracea* leaves engaged in the C_4/CAM hybrid system.

Our data revealed completely reversible and environmentally-controlled CAM in *P. oleracea* leaves, which agrees with previous findings for the species (D'Andrea *et al.,* 2014, Winter & Holtum, 2014). As no ΔH^+ or CAM-marker transcript accumulation was observed after re-watering events applied following different lengths of the drought period, the ability of *P. oleracea* to revert from the C_4/CAM hybrid system to C_4 was not influenced by the intensity

or duration of CAM prior to re-watering. By contrast, both developmental and environmental cues were shown to regulate the occurrence and intensity of CAM in stems. As a consequence, multiple photosynthetic CO_2 fixation systems were detected in *P. oleracea*, including: (1) C_3 stems and C_4 leaves in young, well-watered plants, (2) CAM stems and C_4 leaves in adult well-watered and re-watered plants, and (3) CAM stems and C_4/CAM hybrid leaves in adult, drought-stressed plants.

As stems represent up to 50% of *P. oleracea* total biomass (Zimmerman 1976) and display ΔH^+ values as high as those found in droughted leaves (Fig. 6e), the presence of CAM in stem tissues may facilitate recycling the nighttime respiratory CO_2 produced by its large chlorenchymatous cells. On the other hand, the adaptive value of facultative CAM in leaves is presumably similar for both C_4-CAM and C_3-CAM facultative plants. As other weak CAM facultative species, dark CO_2 fixation in drought-stressed, CAM-performing *P. oleracea* plants is negligible compared to daytime C_4-mediated CO_2 assimilation under well-watered conditions (Winter and Holtum, 2014; Winter 2019). Instead of contributing to carbon gain, weak and inducible CAM may promote plant fitness by offering other adaptive advantages (reviewed by Herrera, 2009). Our findings connect CAM induction to a photoprotective role in *P. oleracea* as the daytime CO_2 release from organic acids behind closed stomata may have supported linear electron transport within chloroplasts, maintaining the integrity of the photosynthetic apparatus under extreme drought as evidenced by chlorophyll *a* fluorescence data (Fig. S12). The rapid recovery of photosynthetic rates once sufficient water supply becomes available may also be seen as an indicator of this photoprotective role of weak CAM (Adams & Osmond, 1988; Herrera, 2009).

Compared to CAM plants, PEP generation represents a much less significant sink for carbohydrates in C_4 plants due to the continuous daytime conversion of PYR to PEP by PPDK or its direct generation via PCK (Weise *et al*., 2011; Borland *et al*., 2016). In *Mesembryanthemum crystallinum*, where ΔH^+ contributes to plant carbon gain under stressful conditions (Bohnert & Cushman, 2000), incremental accumulation of starch during the C_3-to-CAM switch seems essential for the supply of PEP (Haider *et al.,* 2012, Cushman *et al.,* 2008). In contrast, leaf starch levels either remained unchanged, or were slightly reduced, upon drought in weak CAM facultative species such as *Tallinum triangulare* (Brilhaus *et al.,* 2016) and *P. oleracea* (Fig. 7, D'Andrea *et al.,* 2014), accompanied by lower soluble sugar content, particularly sucrose and glucose, in both cases. In *P. oleracea* leaves, CAM induction was accompanied by the up-regulation of most, but not all, starch metabolism genes (*ADG1, APL3, GBSS1, BE3, ISA3, GWD1, SEX4* and *BAM1*), as also observed for both *M. crystallinum* and *T. triangulare* (Cushman *et al.,* 2008; Brilhaus *et al.,* 2016). Therefore, an increased starch turnover, rather than a higher accumulation of this carbohydrate, seems to be sufficient to sustain the dark CO_2 fixation and ΔH^+ observed in *P. oleracea*.

It has been hypothesized that a transition to phosphorolytic starch turnover favors the energetic balance for the nocturnal production of PEP from starch, requiring increased levels of *GPT2*, which transports G6P across the chloroplast envelope in exchange for P_i (Neuhaus & Schulte, 1996; Cushman *et al.,* 2008; Borland *et al*., 2009; Weise *et al*., 2011). In *P. oleracea*, an overall increment in transcript abundance of *GPT2* as well as genes encoding enzymes either shared by both (*LDA*, *DPE1*, *GWD1*), or exclusively involved in the hydrolytic (*SEX4, BAM1*) and phosphorylytic (*PHS1*) starch degradation pathways was observed in response to drought. Therefore, both pathways seem to contribute to starch degradation in CAM-performing *P. oleracea* tissues. Additionally, the up-regulation of *GPT2.2* may connect with the up-regulation of cytosolic *SIS.1* and *SIS.2*, by transporting cytosolic G6P formed by SISs into the chloroplast to increase PEP regeneration via starch formation (Wai *et al.,* 2019).

Overall, our findings provide novel insights into the gene transcript level and metabolic adjustments required to accommodate both the C_4 and CAM cycles within a single leaf. In particular, our work builds on previous findings by identifying transcripts that are likely to play an exclusive role in drought-induced CAM reactions, as well as components that are shared by both the C_4 and CAM. By demonstrating that the C_4 and CAM machineries co-exist within *P. oleracea* leaves under mild drought conditions, we open up a new window of opportunity for investigating the biochemical and regulatory mechanisms underpinning the co-occurrence of these two CCMs. Knowledge generated using C_4/CAM facultative species such as *P. oleracea* may shed new light on alternative biochemical arrangements for future bioengineering initiatives aiming to combine the high productivity of C_4 and the stress-resistance traits offered by CAM into target crop species.

ACKNOWLEDGMENTS

This work was supported in part by the São Paulo Research Foundation (FAPESP - grant no. # 2016/04755-4 awarded to R.C.F.), by a Newton Advanced Fellowship funded by the Royal Society, UK (grant no. #NA140007 awarded to L.F. and J.H.) and by the US National Science Foundation (grant no. IOS-1754662 awarded to E.J.E). This study was financed in part by the Coordenação de Aperfeiçoamento de Pessoal de Nível Superior - Brasil (CAPES) - Finance Code 001. We also thank Nirja Kadu, Richard Eccles and Steve Paterson for the support given during the work at the Institute of Integrative Biology (University of Liverpool, UK), the members of the Centre for Genomic Research at the University of Liverpool that carried out the RNA-seq library production and Illumina sequencing, Emerson Alves da Silva (Instituto de Botânica de São Paulo) for support during osmotic potential measurements, and Luiz Lehmann Coutinho for granting access to the ESALQ Genomics Center Computer Cluster.

AUTHOR CONTRIBUTIONS:

LF and JH conceived the project and supervised the experiments, RCF and PPB conducted most of the experiments; MAR, LF, FRRA, DD, SFB, LVD, and JH conducted part of the experiments; SCSA conducted most bioinformatics analysis; VDG assisted the bioinformatic and statistical analysis; JJMV and EJE performed the phylogenetic analyses; RCF, LF and JH wrote the article with contributions from other authors.

REFERENCES

Adams WW, Osmond CB. **1988**. Internal CO_2 supply during photosynthesis of sun and shade grown CAM plants in relation to photoinhibition *Fv/Fm*. *Plant Physiology* **86**: 117–123.

Alves FRR, Melo HC, Crispim-Filho AJ, Costa AC, Nascimento KJT, Carvalho RF. 2016. Physiological and biochemical responses of photomorphogenic tomato mutants (cv. Micro-Tom) under water withholding. *Acta Physiologiae Plantarum* **38**: 155.

Amaral LIV do, Gaspar M, Costa PMF, Aidar MPM, Buckeridge MS. **2007**. Novo método enzimático rápido e sensível de extração e dosagem de amido em materiais vegetais. *Hoehnea* **34**: 425–431.

Berardini TZ, Reiser L, Li D, Mezheritsky Y, Muller R, Strait E, Huala E. 2015. The Arabidopsis information resource: making and mining the "gold standard" annotated reference plant genome. *Genesis* **53**: 474–485.

Black CC, Chen JQ, Doong RL, Angelov MN, Sung SJS. 1996. Alternative carbohydrate reserves used in the daily cycle of crassulacean acid metabolism. *In*: Winter K, Smith J, eds. *Crassulacean Acid Metabolism*. Heidelberg, Germany: Springer–Verlag Berlin, 31–45.

Bohnert HJ, Cushman JC. **2000**. The ice plant cometh: lessons in abiotic stress tolerance. *Journal of Plant Growth Regulation* **19**: 334–346.

Borland AM, Griffiths H, Hartwell J, Smith JAC. **2009**. Exploiting the potential of plants with crassulacean acid metabolism for bioenergy production on marginal lands. *Journal of Experimental Botany* **60**: 2879–2896.

Borland AM, Guo HB, Yang X, Cushman JC. **2016**. Orchestration of carbohydrate processing for crassulacean acid metabolism. *Current Opinion in Plant Biology* **31**: 118–124.

Boxall SF, Dever LV, Kneřová J, Gould PD, Hartwell J. 2017. Phosphorylation of phospho*enol*pyruvate carboxylase is essential for maximal and sustained dark CO_2 fixation and core circadian clock operation in the obligate crassulacean acid metabolism species *Kalanchoë fedtschenkoi*. *The Plant Cell* **29**: 2519–2536.

Boxall SF, Kadu N, Dever LV, Kneřová J, Waller JL, Gould PJD, Hartwell J. 2019. Silencing *PHOSPHOENOLPYRUVATE CARBOXYLASE1* in the obligate crassulacean acid

metabolism species *Kalanchoë laxiflora* causes reversion to C_3-like metabolism and amplifies rhythmicity in a subset of core circadian clock genes. *bioRxiv* 684050; doi: https://doi.org/10.1101/684050

Bräutigam A, Schlüter U, Eisenhut M, Gowik U. 2017. On the Evolutionary Origin of CAM Photosynthesis. *Plant Physiology* **174**: 473–477.

Brilhaus D, Bräutigam A, Mettler–Altmann T, Winter K, Weber APM. **2016**. Reversible burst of transcriptional changes during induction of crassulacean acid metabolism in *Talinum triangulare*. *Plant Physiology* **170**: 102–122.

Camacho C, Coulouris G, Avagyan V, Ma N, Papadopoulos J, Bealer K, Madden TL. **2009**. BLAST +: architecture and applications. *BMC Bioinformatics* **9**: 1–9.

Carter PJ, Nimmo HG, Fewson CA, Wilkins MB. 1991. Circadian rhythms in the activity of a plant protein kinase. *EMBO Journal* **10**: 2063–2068.

Chastain CJ, Chollet R. **2003**. Regulation of pyruvate, orthophosphate dikinase by ADP–/Pi–dependent reversible phosphorylation in C_3 and C_4 plants. *Plant Physiology and Biochemistry* **41**: 523–532.

Chastain CJ, Fries JP, Vogel JA, Randklev CL, Vossen AP, Dittmer SK, Watkins EE, Fiedler LJ, Wacker SA, Meinhover KC, *et al.* 2002. Pyruvate, orthophosphate dikinase in leaves and chloroplasts of C_3 Plants undergoes light–/dark–induced reversible phosphorylation. *Plant Physiology* **128**: 1368–1378.

Chen Z, Hills A, Bätz U, Amtmann A, Lew VL, Blatt MR. 2012. Systems dynamic modeling of the stomatal guard cell predicts emergent behaviors in transport, signaling, and volume control. *Plant Physiology* **159**: 1235–1251.

Christin PA, Arakaki M, Osborne CP, Bräutigam A, Sage RF, Hibberd JM, Kelly S, Covshoff S, Wong GKS, Hancock L, *et al.* 2014. Shared origins of a key enzyme during the evolution of C_4 and CAM metabolism. *Journal of Experimental Botany* **65**: 3609–3621.

Christin PA, Arakaki M, Osborne CP, Edwards EJ. **2015**. Genetic enablers underlying the clustered evolutionary origins of C_4 photosynthesis in angiosperms. *Molecular Biology and Evolution* **32**: 846–858.

Covshoff S, Hibberd JM. **2012**. Integrating C_4 photosynthesis into C_3 crops to increase yield potential. *Current Opinion in Biotechnology* **23**: 209–214.

Cruz AB, Bianchetti RE, Alves FRR, Purgatto E, Peres LEP, Rossi M, Freschi L. **2018**. Light, ethylene and auxin signaling interaction regulates carotenoid biosynthesis during tomato fruit ripening. *Frontiers in Plant Science* **9**: 1–16.

Cushman JC, Tillett RL, Wood JA, Branco JM, Schlauch KA. **2008**. Large–scale mRNA expression profiling in the common ice plant, *Mesembryanthemum crystallinum*, performing C_3 photosynthesis and crassulacean acid metabolism (CAM). *Journal of Experimental Botany* **59**: 1875–1894.

Czechowski T, Stitt M, Altmann T, Udvardi MK, Scheible W-R. 2005. Genome-wide identification and testing of superior reference genes for transcript normalization in Arabidopsis. *Plant physiology* **139:** 5–17.

D'Andrea RM, Andreo CS, Lara MV. **2014**. Deciphering the mechanisms involved in *Portulaca oleracea* (C_4) response to drought: metabolic changes including crassulacean acid–like metabolism induction and reversal upon re–watering. *Physiologia Plantarum* **152**: 414–430.

De Angeli A, Zhang J, Meyer S, Martinoia E. **2013**. *AtALMT9* is a malate-activated vacuolar chloride channel required for stomatal opening in Arabidopsis. *Nature Communications* **4**: 1–10.

Dever LV, Boxall SF, Kneřová J, Hartwell J. **2015**. Transgenic perturbation of the decarboxylation phase of crassulacean acid metabolism alters physiology and metabolism but has only a small effect on growth. *Plant Physiology* **167**: 44–59.

Edgar RC. 2004. MUSCLE: multiple sequence alignment with high accuracy and high throughput. *Nucleic Acids Research* **32**: 1792–1797.

Edwards EL. 2019. Evolutionary trajectories, accessibility and other metaphors: the case of C_4 and CAM photosynthesis. *New Phytologist.* doi: 10.1111/nph.15851

Edwards EJ, Ogburn RM. **2012**. Angiosperm responses to a low–CO_2 world: CAM and C_4 photosynthesis as parallel evolutionary trajectories. *International Journal of Plant Sciences* **173**: 724–733.

Ferrari RC, Freschi L. 2019. C_4/CAM facultative photosynthesis as a means to improve plant sustainable productivity under abiotic–stressed conditions: regulatory mechanisms and biotechnological implications. *In*: Khan MIR, Reddy PS, Ferrante A, Khan NA, eds. *Plant Signaling Molecules*, Chennai, India: Woodhead Publishing, 517–532.

Freschi L, Rodrigues MA, Tiné MAS, Mercier H. **2010**. Correlation between citric acid and nitrate metabolisms during CAM cycle in the atmospheric bromeliad *Tillandsia pohliana*. *Journal of Plant Physiology* **167**: 1577–1583.

Fukao Y, Hayashi M, Nishimura M. 2002. Proteomic analysis of leaf peroxisomal proteins in greening cotyledons of *Arabidopsis thaliana*. *Plant Cell Physiol*ogy **43:** 689–696.

Furbank RT. **2011**. Evolution of the C_4 photosynthetic mechanism: are there really three C_4 acid decarboxylation types? *Journal of Experimental Botany* **62**: 3103–3108.

Furumoto T, Yamaguchi T, Ohshima–Ichie Y, Nakamura M, Tsuchida–Iwata Y, Shimamura M, Ohnishi J, Hata S, Gowik U, Westhoff P, *et al.* 2011. A plastidial sodium–dependent pyruvate transporter. *Nature* **476**: 472–476.

Gonnella M, Charfeddine M, Conversa G, Santamaria P. **2010**. Purslane: a review of its potential for health and agricultural aspects. *The European Journal of Plant Science and Biotechnology* **4**: 131–136.

Götz S, García-Gómez JM, Terol J, Williams TD, Nagaraj SH, Nueda MJ, Robles M, Talón M, Dopazo J, Conesa A. 2008. High-throughput functional annotation and data mining with the Blast2GO suite. *Nucleic Acids Research* **36:** 3420–3435.

Grabherr MG, Haas BJ, Yassour M, Levin JZ, Thompson DA, Amit I, Adiconis X, Fan L, Raychowdhury R, Zeng Q, Chen Z, Mauceli E, *et al.* 2013. Trinity: reconstructing a full-length transcriptome without a genome from RNA-Seq data. *Nature Biotechnology* **29**: 644–652.

Guindon S, Gascuel O. 2003. A simple, fast, and accurate algorithm to estimate large phylogenies by maximum likelihood. *Systematic Biology* **52**: 696–704.

Griffiths H. 1989. Carbon dioxide concentrating mechanisms and the evolution of CAM in vascular epiphytes. *In:* Lüttge, U, ed. *Vascular Plants as Epiphytes: Evolution and Ecophysiology*. Berlin: Springer-Verlag, 42-86.

Guralnick LJ, Jackson MD. **2001**. The occurrence and phylogenetics of crassulacean acid metabolism in the Portulacaceae. *International Journal of Plant Sciences* **162**: 257–262.

Hafke JB, Hafke Y, Smith JAC, Lüttge UE, Thiel G. 2003. Vacuolar malate uptake is mediated by an anion-selective inward rectifier. *The Plant Journal* 35, 116–128.

Haider MS, Barnes JD, Cushman JC, Borland AM. **2012**. A CAM– and starch–deficient mutant of the facultative CAM species *Mesembryanthemum crystallinum* reconciles sink demands by repartitioning carbon during acclimation to salinity. *Journal of Experimental Botany* **63**: 1985–1996.

Hartwell J, Smith LH, Wilkins MB, Jenkins GI, Nimmo HG. 1996. Higher plant phosphoenolpyruvate carboxylase kinase is regulated at the level of translatable mRNA in response to light or a circadian rhythm. *Plant Journal* **10**: 1071–1078.

Hartwell J, Gill A, Nimmo GA, Wilkins MB, Jenkins GI, Nimmo HG. 1999. Phosphoenolpyruvate carboxylase kinase is a novel protein kinase regulated at the level of expression. *Plant Journal* **20**: 333–342.

Hartwell J. 2006. The circadian clock in CAM plants. *In*: Hall AJ, McWatters H, eds. *Annual Plant Reviews Volume 21: Endogenous Plant Rhythms*. Kundli, India: Blackwell Publishing, 211–236.

Hartwell J, Dever L V, Boxall SF. **2016**. Emerging model systems for functional genomics analysis of crassulacean acid metabolism. *Current Opinion in Plant Biology* **31**: 100–108.

Hatch MD. **1987**. C_4 photosynthesis: a unique blend of modified biochemistry, anatomy and ultrastructure. *Bioehimica et Biophysica Acta* **895**: 81–106.

Herrera A. **2009**. Crassulacean acid metabolism and fitness under water deficit stress: if not for carbon gain, what is facultative CAM good for? *Annals of Botany* **103**: 645–653.

Hibberd JM, Covshoff S. **2010**. The Regulation of gene expression required for C_4 photosynthesis. *Annual Review of Plant Biology* **61**: 181–207.

Holtum JAM, Hancock LP, Edwards EJ, Winter K. **2017**. Optional use of CAM photosynthesis in two C_4 species, *Portulaca cyclophylla* and *Portulaca digyna*. *Journal of Plant Physiology* **214**: 91–96

Kajala K, Covshoff S, Karki S, Woodfield H, Tolley BJ, Dionora MJA, Mogul RT, Mabilangan AE, Danila FR, Hibberd JM, *et al.* 2011. Strategies for engineering a two–celled C_4 photosynthetic pathway into rice. *Journal of Experimental Botany* **62**: 3001–3010.

Kanai R, Edwards GE. **1999**. The biochemistry of photosynthesis. *In*: Sage R, Monson R, eds. *C_4 Plant Biology*. San Diego: Academic Press, 49–87.

Keeley JE, Rundel PW. **2013**. Evolution of CAM and C_4 carbon - concentrating mechanisms. *International Journal of Plant Sciences* **164**: 54–77.

Koch KE, Kennedy RA. **1980**. Characteristics of crassulacean acid metabolism in the succulent C_4 dicot, *Portulaca oleracea* L. *Plant Physiology* **65**: 193–197.

Koch KE, Kennedy RA. **1982**. Crassulacean acid metabolism in the succulent C_4 dicot, *Portulaca oleracea* L under natural environmental conditions. *Plant Physiology* **69**: 757–761.

Kovermann P, Meyer S, Hörtensteiner S, Picco C, Scholz–Starke J, Ravera S, Lee Y, Martinoia E. **2007**. The Arabidopsis vacuolar malate channel is a member of the ALMT family. *Plant Journal* **52**: 1169–1180.

Ku SB, Shieh YJ, Reger BJ, Black CC. **1981**. Photosynthetic characteristics of *Portulaca grandiflora*, a succulent C_4 dicot. *Plant physiology* **68**: 1073–1080.

Laetsch WM. 1968. Chloroplast specialization in dicotyledons possessing the C_4-dicarboxylic acid pathway of photosynthetic CO_2 fixation. *American Journal of Botany* **55**: 875-883.

Langmead B, Salzberg SL. **2012**. Fast gapped-read alignment with Bowtie 2. *Nature Methods* **9**: 357–359.

Larsson A. 2004. AliView: a fast and lightweight alignment viewer and editor for large datasets. *Bioinformatics* **30**: 3276-3278.

Lara M, Disante KB, Podestá FP, Andreo CS, Drincovich MF. **2003**. Induction of a crassulacean acid like metabolism in the C_4 succulent plant, *Portulaca oleracea* L.: physiological and morphological changes are accompanied by specific modifications in phosphoenolpyruvate carboxylase. *Photosynthesis Research* **77**: 241–254.

Lara M V, Drincovich MF, Andreo CS. **2004**. Induction of a crassulacean acid–like metabolism in the C_4 succulent plant, *Portulaca oleracea* L.: study of enzymes involved in carbon fixation and carbohydrate metabolism. *Plant and Cell Physiology* **45**: 618–626.

Li W, Godzik A. **2006**. Cd-hit: a fast program for clustering and comparing large sets of protein or nucleotide sequences. *Bioinformatics* **22**: 1658–1659.

Livak KJ, Schmittgen TD. **2001**. Analysis of relative gene expression data using real-time quantitative PCR and the $2^{-\Delta\Delta CT}$ method. *Methods* **25**: 402–408.

Matsuoka M. **1995**. The gene for pyruvate,orthophosphate dikinase in C_4 plants: structure, regulation and evolution. *Plant and Cell Physiology* **36**: 937–943.

Mazen AMA. **1996**. Changes in levels of phosphoenolpyruvate carboxylase with induction of crassulacean acid metabolism (CAM)–like behavior in the C_4 plant *Portulaca oleracea*. *Physiologia Plantarum* **98**: 111–116.

Mazen AMA. **2000**. Changes in properties of phosphoenolpyruvate carboxylase with induction of crassulacean acid metabolism (CAM) in the C_4 plant *Portulaca oleracea*. *Photosynthetica* **38**: 385–391.

Mccarthy DJ, Chen Y, Smyth GK. **2012**. Differential expression analysis of multifactor RNA-Seq experiments with respect to biological variation. *Nucleic Acids Research* **40**: 4288–4297.

Meyer S, Mumm P, Imes D, Endler A, Weder B, Al-Rasheid KAS, Geiger D, Marten I, Martinoia E, Hedrich R. **2010**. *AtALMT12* represents an R-type anion channel required for stomatal movement in Arabidopsis guard cells. *Plant Journal* **63**: 1054–1062.

Miyanishi K, Cavers PB. **1980**. The biology of canadian weeds. *Canadian Journal of Plant Science* **60**: 953–963.

Monné M, Daddabbo L, Gagneul D, Obata T, Hielscher B, Palmieri L, Miniero DV, Fernie AR, Weber APM, Palmieri F. **2018**. Uncoupling proteins 1 and 2 (*UCP1* and *UCP2*) from *Arabidopsis thaliana* are mitochondrial transporters of aspartate, glutamate, and dicarboxylates. *Journal of Biological Chemistry* **293**: 4213–4227.

Monroe JD, Storm AR. **2018**. Review: the Arabidopsis β–amylase (BAM) gene family: diversity of form and function. *Plant Science* **276**: 163–170.

Moreno–Villena JJ, Dunning LT, Osborne CP, Christin PA. **2017**. Highly expressed genes are preferentially co–opted for C_4 photosynthesis. *Molecular Biology and Evolution* **35**: 94–106.

Nelson EA, Sage TL, Sage RF. **2005**. Functional leaf anatomy of plants with crassulacean acid metabolism. *Functional Plant Biology* **32**: 409–419.

Neuhaus HE, Schulte N. 1996. Starch degradation in chloroplasts isolated from C_3 or CAM (crassulacean acid metabolism)–induced *Mesembryanthemum crystallinum* L. *Biochemical Journal* **318**: 945–953.

Nimmo HG, Fontaine V, Hartwell J, Jenkins GI, Nimmo GA, Wilkins MB. 2001. PEP carboxylase kinase is a novel protein kinase controlled at the level of expression. *New Phytologist.* **151**: 91–97.

Osmond CB. 1978. Crassulacean acid metabolism: a curiosity in context. *Annual Review of Plant Physiology* **29**: 379–414.

Palmieri L, Picault N, Arrigoni R, Besin E, Palmieri F, Hodges M. **2008**. Molecular identification of three *Arabidopsis thaliana* mitochondrial dicarboxylate carrier isoforms:

organ distribution, bacterial expression, reconstitution into liposomes and functional characterization. *Biochemical Journal* **410**: 621–629.

Robinson MD, Mccarthy DJ, Smyth GK. **2010**. edgeR: a Bioconductor package for differential expression analysis of digital gene expression data. *Bioinformatics* **26**: 139–140.

Sage RF. **2002**. Are crassulacean acid metabolism and C_4 photosynthesis incompatible? *Functional Plant Biology* **29**: 775–785.

Sage RF. **2017**. A portrait of the C_4 photosynthetic family on the 50^{th} anniversary of its discovery: species number, evolutionary lineages, and hall of fame. *Journal of Experimental Botany* **68**: e11–e28.

Smith JAC, Ingram J, Tsiantis MS, Barkla BI, Bartholomew DM, Bettey M. 1996. Transport across the vacuolar membrane in CAM plants. *In*: Winter K, Smith J, eds. *Crassulacean Acid Metabolism*. Heidelberg, Germany: Springer–Verlag Berlin, 53–71.

Schluter U, Denton AK, Bräutigam A. **2016**. Understanding metabolite transport and metabolism in C_4 plants through RNA–seq. *Current Opinion in Plant Biology* **31:** 83–90.

Schultz CJ, Coruzzi GM. **1995**. The aspartate aminotransferase gene family of Arabidopsis encodes isoenzymes localized to three distinct subcellular compartments. *The Plant Journal*: 61–75.

Silvera K, Neubig KM, Whitten WM, Williams NH, Winter K, Cushman JC. **2010**. Evolution along the crassulacean acid metabolism continuum. *Functional Plant Biology* **37**: 995–1010.

Taylor SH, Ripley BS, Martin T, De–Wet LA, Woodward FI, Osborne CP. **2014**. Physiological advantages of C_4 grasses in the field: a comparative experiment demonstrating the importance of drought. *Global Change Biology* **20**: 1992–2003.

The UniProt Consortium. **2019**. UniProt: a worldwide hub of protein knowledge. *Nucleic Acids Research* **47**: 506–515.

Thompson JD, Higgins DG, Gibson TJ. 1994. CLUSTAL W: improving the sensitivity of progressive multiple sequence alignment through sequence weighting, position- specific gap penalties and weight matrix choice. *Nucleic Acids Research* **22**: 4673–4680.

Thompson AG, Brailsford MA, Beechey RB. **1987**. Identification of the phosphate translocator from maize mesophyll chloroplasts. *Biochemical and Biophysical Research Communications* **143**: 164–169.

Voznesenskaya EV, Franceschi VR, Kiirats O, Freitag H, Edwards GE. **2001**. Kranz anatomy is not essential for terrestrial C_4 plant photosynthesis. *Nature* **414**: 543–546.

Voznesenskaya EV, Franceschi VR, Kiirats O, Artyusheva EG, Freitag H, Edwards GE. **2002**. Proof of C_4 photosynthesis without Kranz anatomy in *Bienertia cycloptera* (Chenopodiaceae). *Plant Journal* **31**: 649–662.

Voznesenskaya EV, Koteyeva NK, Edwards GE, Ocampo G. **2010**. Revealing diversity in

structural and biochemical forms of C_4 photosynthesis and a C_3–C_4 intermediate in genus *Portulaca* L. (Portulacaceae). *Journal of Experimental Botany* **61**: 3647–3662.

Vozza A, Parisi G, De Leonardis F, Lasorsa FM, Castegna A, Amorese D, Marmo R, Calcagnile VM, Palmieri L, Ricquier D, *et al.* 2014. *UCP2* transports C_4 metabolites out of mitochondria, regulating glucose and glutamine oxidation. *Proceedings of the National Academy of Sciences* **111**: 960–965.

Wai CM, Weise SE, Ozersky P, Mockler TC, MichaelI TP, VanBuren R. 2019. Time of day and network reprogramming during drought induced CAM photosynthesis in *Sedum album*. *PLOS Genetics*. doi: 10.1371/journal.pgen.1008209

Weise SE, Van Wijk KJ, Sharkey TD. **2011**. The role of transitory starch in C_3, CAM, and C_4 metabolism and opportunities for engineering leaf starch accumulation. *Journal of Experimental Botany* **62**: 3109–3118.

Wilkie SE, Warren MJ. **1998**. Recombinant expression, purification, and characterization of three isoenzymes of aspartate aminotransferase from Arabidopsis thaliana. *Protein Expression and Purification* **12**: 381–389.

Winter K. 2019. Ecophysiology of constitutive and facultative CAM photosynthesis. *Journal of Experimental Botany*. doi: 10.1093/jxb/erz002.

Winter K, Smith J. 1996. Crassulacean acid metabolism: current status and perspectives. *In*: Winter K, Smith J, eds. *Crassulacean Acid Metabolism*. Heidelberg, Germany: Springer–Verlag Berlin, 1–13.

Winter K, Holtum JAM. **2014**. Facultative crassulacean acid metabolism (CAM) plants: powerful tools for unravelling the functional elements of CAM photosynthesis. *Journal of Experimental Botany* **65**: 3425–3441.

Winter K, Holtum JAM. **2017**. Facultative crassulacean acid metabolism (CAM) in four small C_3 and C_4 leaf–succulents. *Australian Journal of Botany* **65**: 3425–3441.

Winter K, Sage RF, Edwards EJ, Virgo A, Holtum JAM. 2019. Facultative crassulacean acid metabolism in a C_3–C_4 intermediate. *Journal of Experimental Botany.* doi:10.1093/jxb/erz085

Wheeler MCG, Tronconi MA, Drincovich MF, Andreo CS, Flügge U, Maurino VG. 2005.
A comprehensive analysis of the NADP-malic enzyme gene family of Arabidopsis. *Plant Physiology* **139**: 39–51.

Yang X, Cushman JC, Borland AM, Edwards EJ, Wullschleger SD, Tuskan GA, Owen NA, Griffiths H, Smith JAC, De Paoli HC, *et al.* 2015. A roadmap for research on crassulacean acid metabolism (CAM) to enhance sustainable food and bioenergy production in a hotter, drier world. *New Phytologist* **207**: 491–504.

Zhang J, Baetz U, Krugel U, Martinoia E, De Angeli A. **2013**. Identification of a probable

pore-forming domain in the multimeric vacuolar anion channel *AtALMT9*. *Plant Physiology* **163**: 830–843.

Zimmerman CA. **1976**. Growth characteristics of weediness in *Portulaca Oleracea* L. *Ecology* **57**: 964–974.

Supporting Information

(Supplementary Figs. S7-S9 and tables are all available at https://doi.org/10.1111/nph.16265)

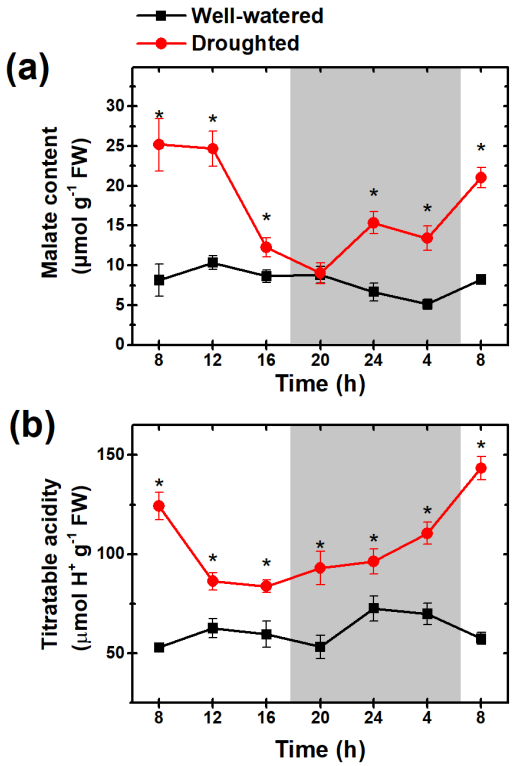

Fig. S1 Diel leaf acid fluctuation in well-watered and droughted plants. Samples were harvested from plants maintained for 34 days under well-watered or drought conditions. (a) Malate levels measured via CG-MS. (b) Titratable acidity. Data are means (±SE) of at least three biological replicates, and asterisks indicate significant difference ($P < 0.05$). The shaded areas indicate the dark period.

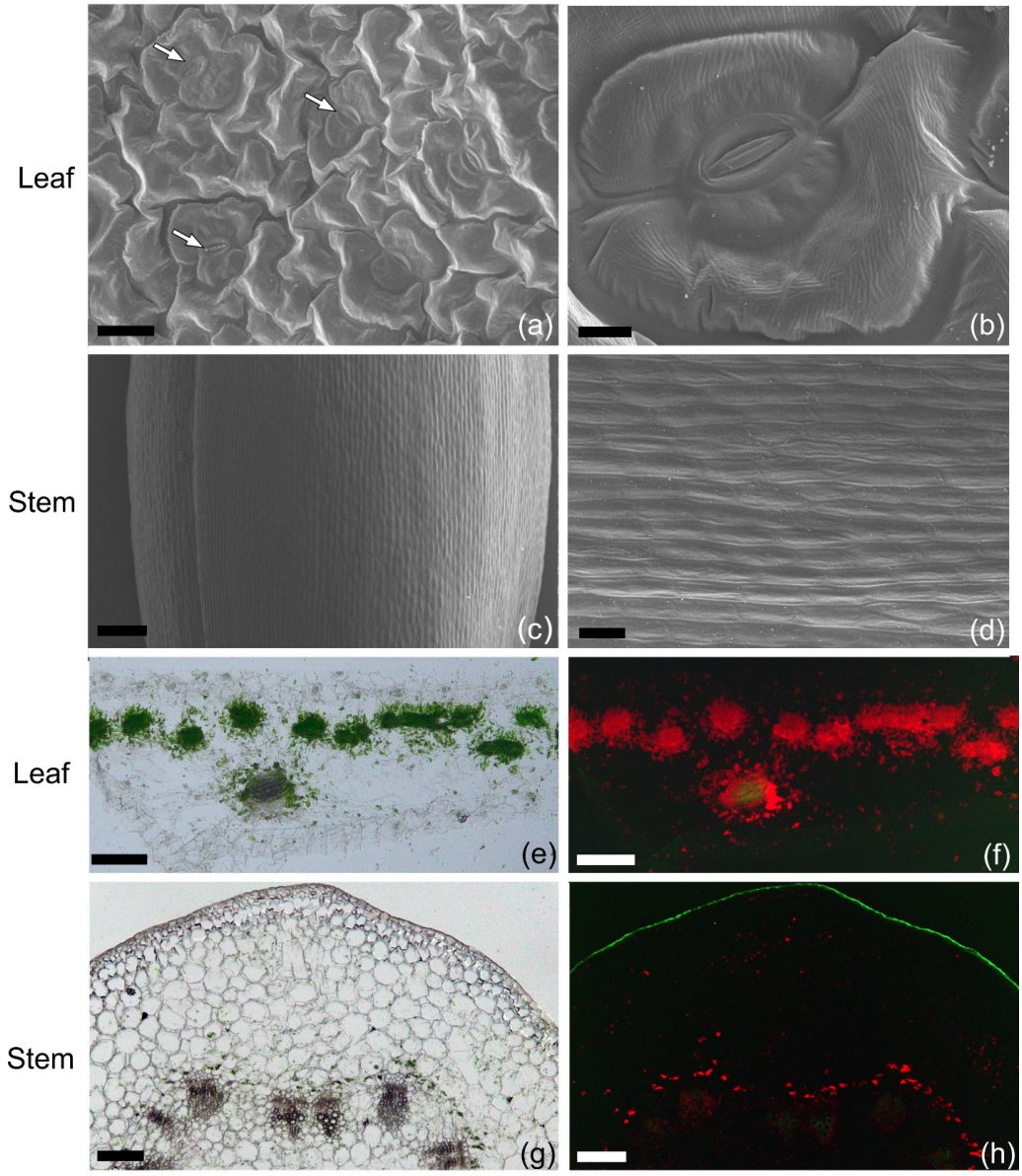

Fig. S2 Surface view and fluorescence microscopy of *P. oleracea* leaves and stems. (a-d) Surface view of *P. oleracea* leaf (a-b) and stem (c-d) under a scanning electron microscope (SEM). Representative SEM images for each organ (a, c) and details of the epidermal cells (b, d) are shown. White arrows indicate stomata. (e-h) Bright-field (e,g) and fluorescence microscopy (f,h) of leaf (e-f) and stem (g-h) sections. Red color represents chlorophyll autofluorescence under blue light. Scale bar = 40 µm in (a), 10 µm in (b), 400 µm in (c), 100 µm in (d) and 250 µm in (e-h).

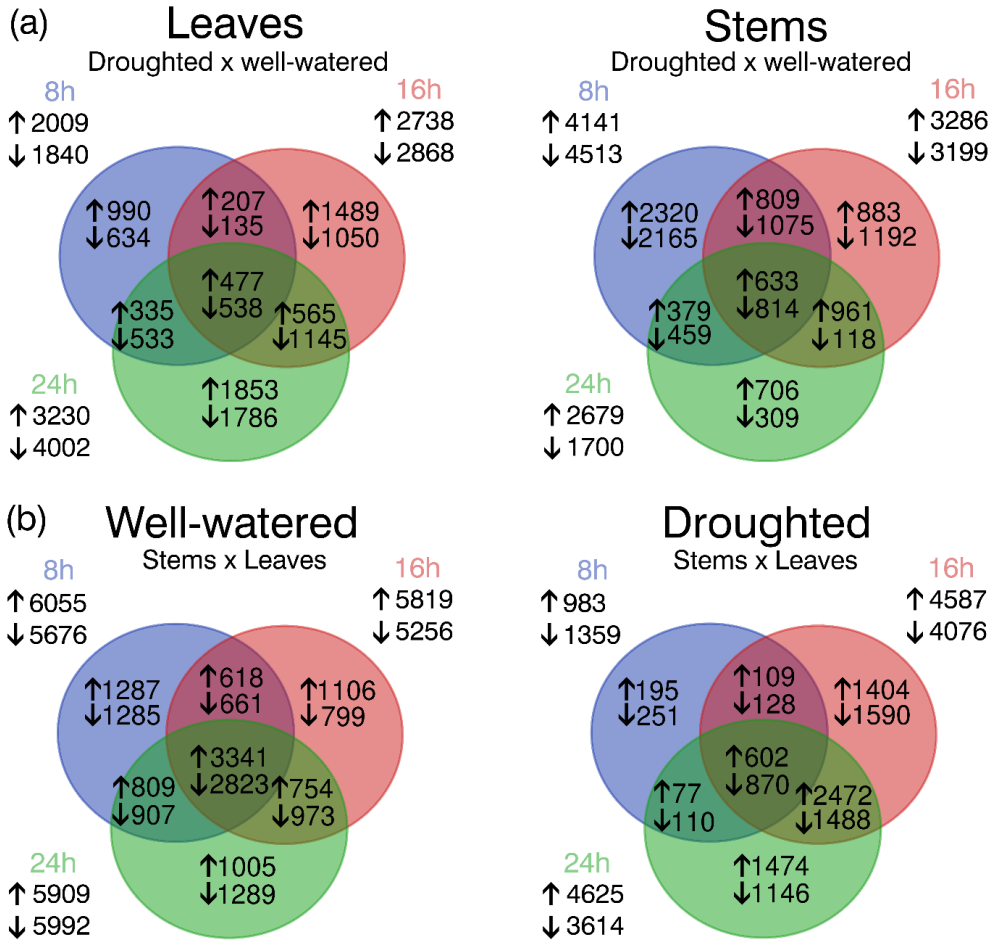

Fig. S3 Differentially expressed genes (DEGs) in pairwise comparisons of *P. oleracea* transcriptome, including leaves and stems under well-watered and droughted conditions. (a) Venn diagrams comparing droughted and well-watered samples of each organ analyzed. In (a), down-regulated DEGs in stems can be interpreted as up-regulated in leaves. (b) Venn diagrams comparing stem and leaf samples at each watering condition. In (b), down-regulated DEGs in droughted tissues can be interpreted as up-regulated in well-watered tissues. Numbers represent overlapping changes among DEGs (↑ up-regulated with log FC > 2; ↓ down-regulated with logFC < -2) (adjusted p-value < 0.01).

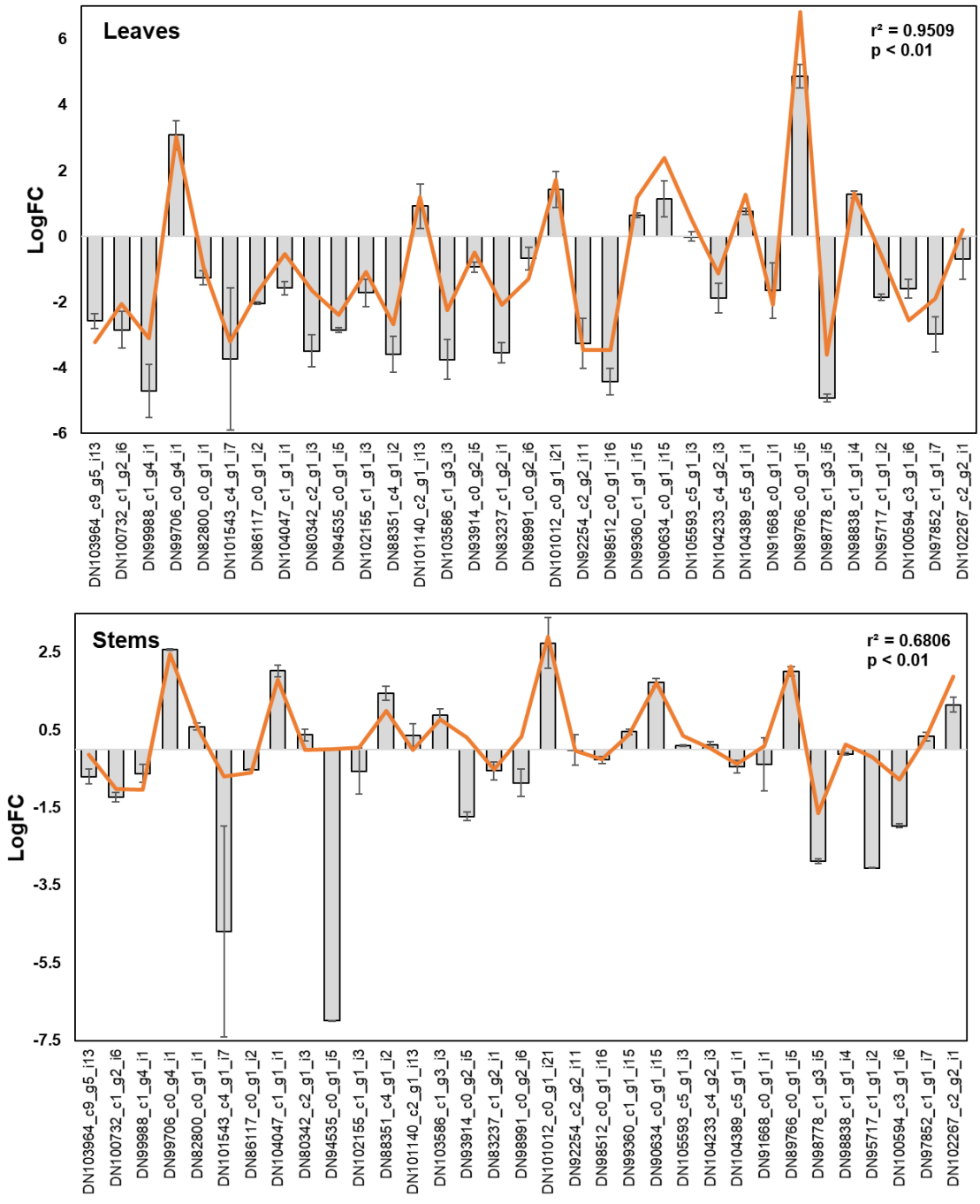

Fig. S4 Validation of RNA-seq data via qPCR, performed for 33 contigs comparing well-watered and droughted leaf and stem samples harvested at early morning (8h). Bars represent mean $\log_2$ relative transcript abundances calculated using the $2^{-\Delta\Delta CT}$ method with error bar (±SD). Lines represent mean $\log_2$ expression ratios calculated by pairwise differential expression analysis using edgeR. Primers used for the analyzed genes are included in Table S1. Pearson correlation was calculated for each comparison and R^2 and p-values are given in each figure.

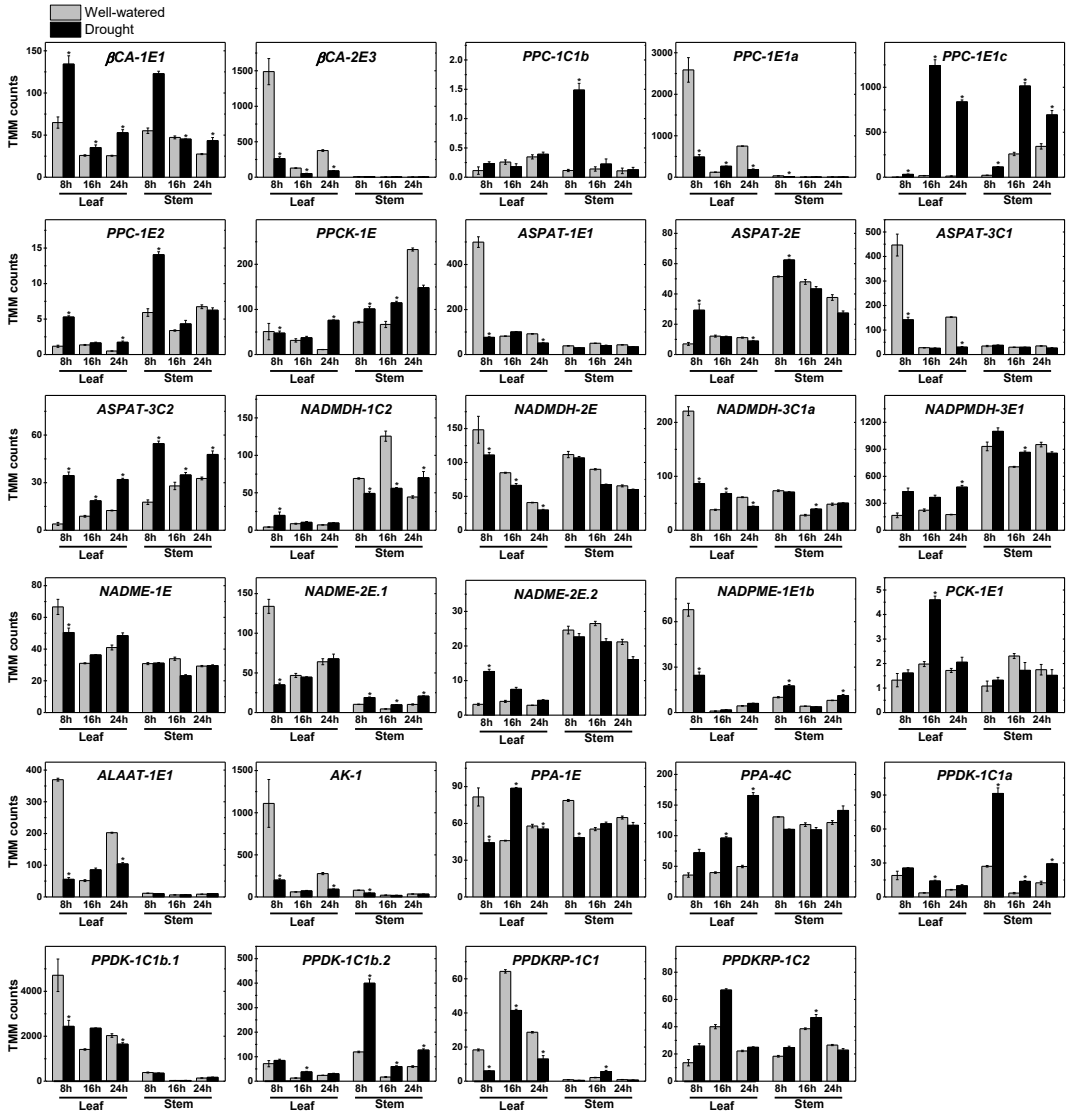

Fig. S5 Mean TMM values for contigs of genes encoding enzymes involved in CCM core reactions. Leaf and stem samples were harvested from plants maintained for 34 days under well-watered or drought conditions. TMM values are presented in Table S5 and their phylogenetic relationship is presented in Fig. S7. Data are means (±SE) of at least three replicates. Asterisks indicate significant difference (adjusted p-value<0.05) between well-watered and droughted samples. Abbreviations are explained in the text and/ or in Table S5 (see Material and Methods and for details).

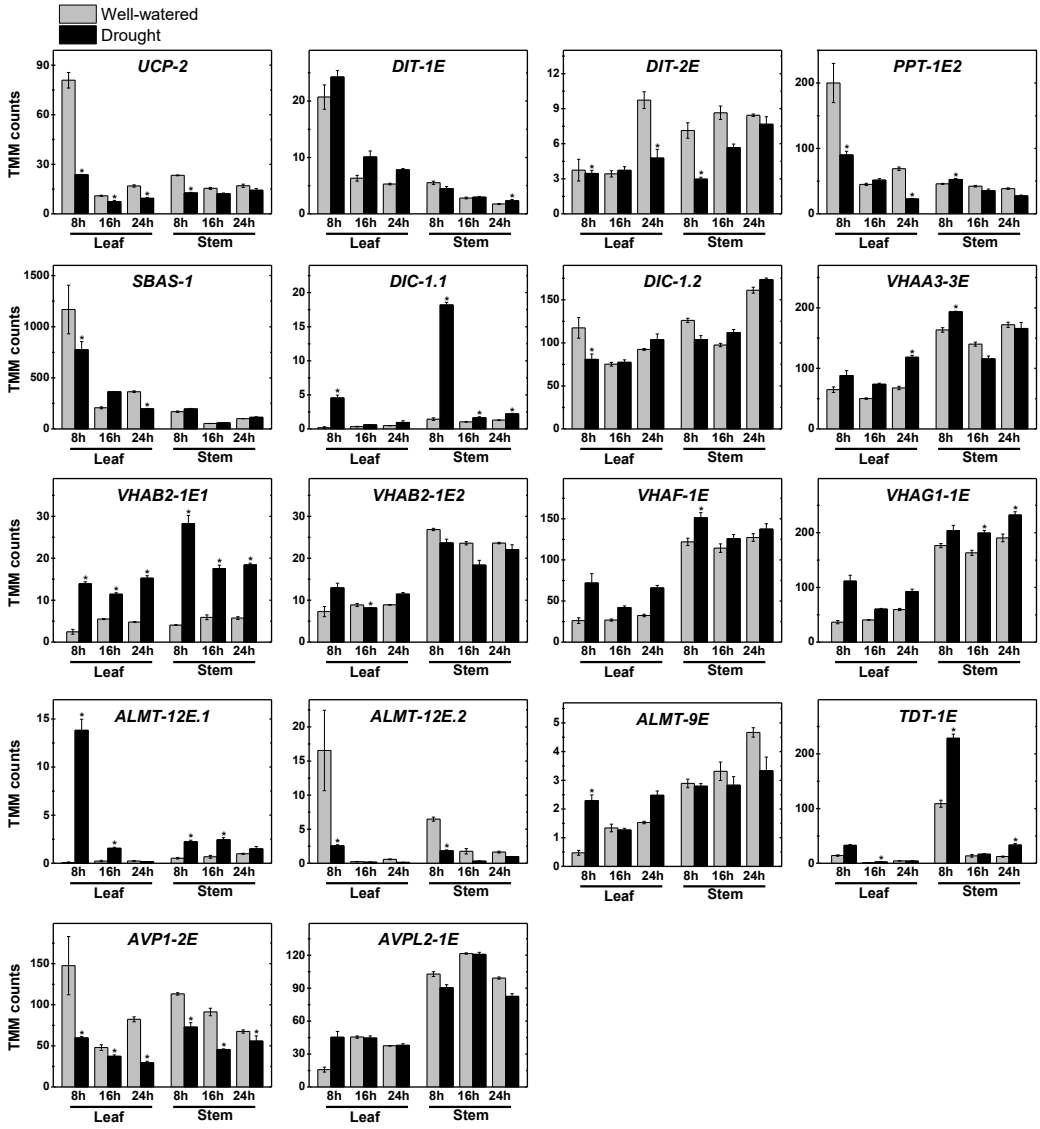

Fig. S6 Mean TMM values for contigs of genes encoding CCM-related transporters. Leaf and stem samples were harvested from plants maintained for 34 days under well-watered or drought conditions. TMM values are presented in Table S5 and their phylogenetic relationship is presented in Fig. S8. Data are means (±SE) of at least three replicates. Asterisks indicate significant difference ($P<0.05$, according to the False Discovery Rate analysis) between well-watered and droughted samples. Abbreviations are explained in the text and/ or in Table S5 (see Material and Methods and for details).

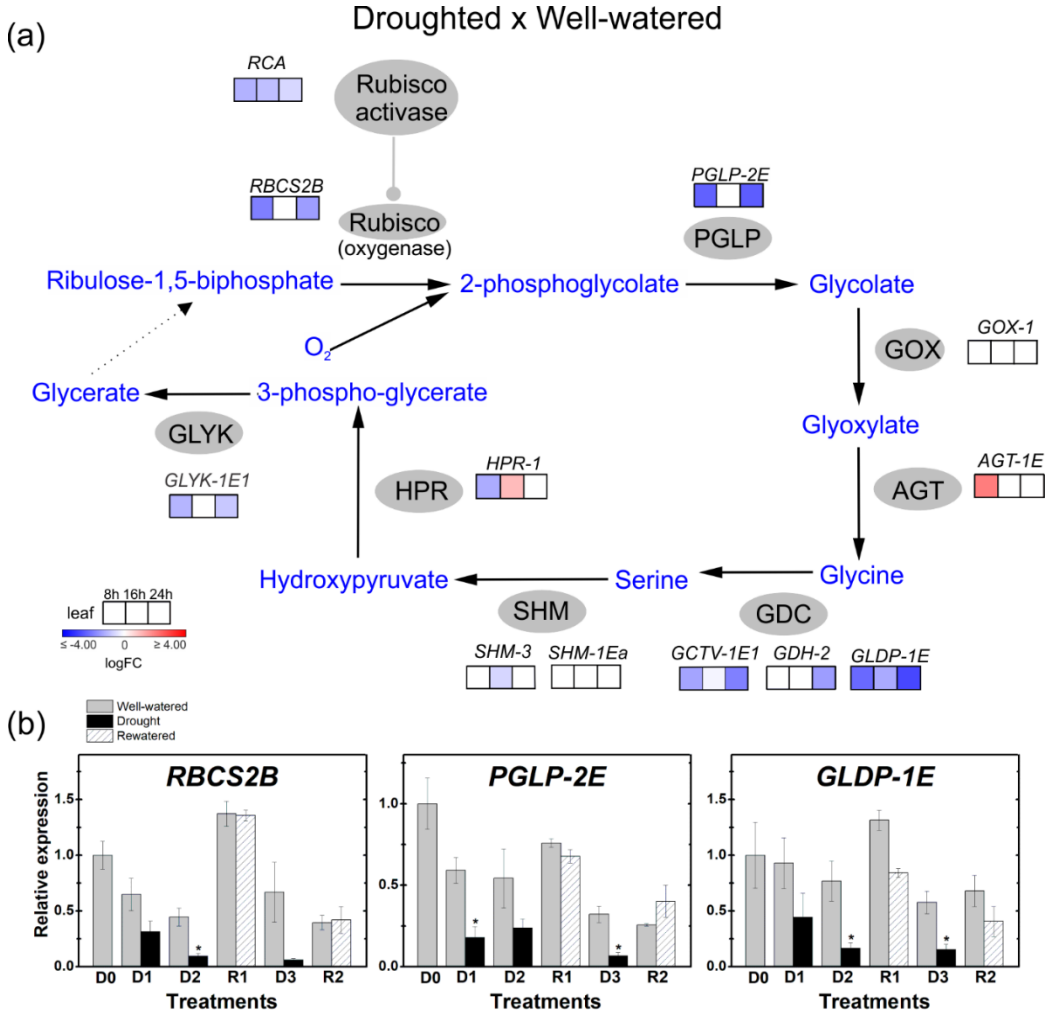

Fig. S10 Relative abundance of genes encoding photorespiration-related enzymes in leaves. Leaf samples were harvested from plants maintained for 34 days under well-watered or drought conditions. (a) Heatmaps indicate log_2-fold change of droughted samples compared to well-watered samples. Black arrows indicate core reactions in photorespiratory pathway whereas gray lines terminated by a closed circle indicate regulatory interactions. Intermediate reactions are omitted. Biosynthetic enzymes and metabolites are represented with gray ovals and blue letters, respectively. TMM and log_2-fold change values for genes shown in the heatmaps (a) are presented in Table S7, and their phylogenetic relationship is presented in Fig. S9. (b) Relative transcript abundance of genes encoding photorespiration-related genes. qPCR data was generated for samples harvested at dawn. Mean relative expression was normalized against D0 leaf samples. Data are means (±SE) of at least three biological replicates. Asterisks indicate significant difference ($P<0.05$). Gene name abbreviations are explained in the text and/ or in Table S7.

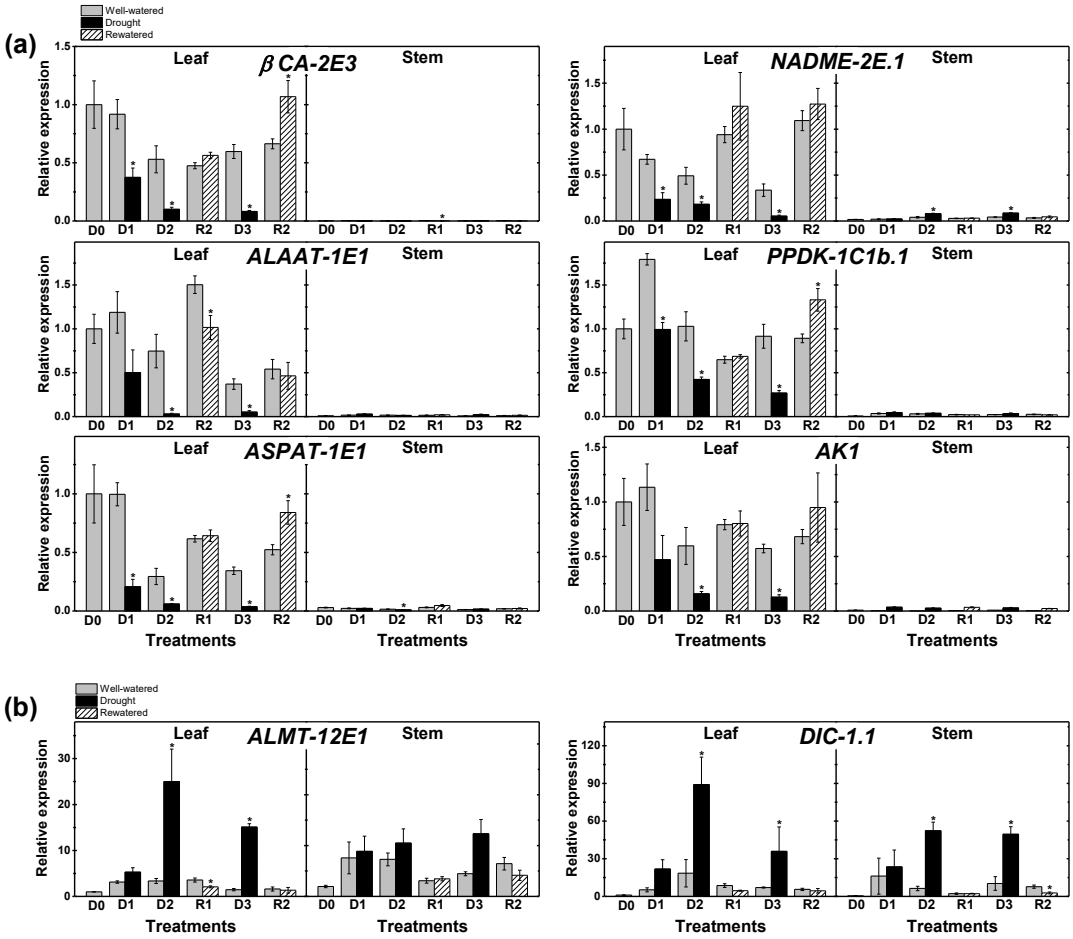

Fig. S11 Transcript abundance of C_4 and CAM marker genes upon drought and rewatering of *P. oleracea* leaves. (a) C_4 marker genes. (b) CAM marker genes. Plants were sampled after 0, 10, 22 and 34 days of drought treatment (D0, D1, D2 and D3, respectively) and during rewatering events initiated after 22 and 34 days of drought (R1 and R2, respectively). Transcript abundance was determined in samples harvested at dawn. Mean relative expression was normalized against D0 leaf samples. Data are means (±SE) of at least three biological replicates. Asterisks indicate significant difference ($P<0.05$). Gene name abbreviations are explained in the text and/ or in Table S6.

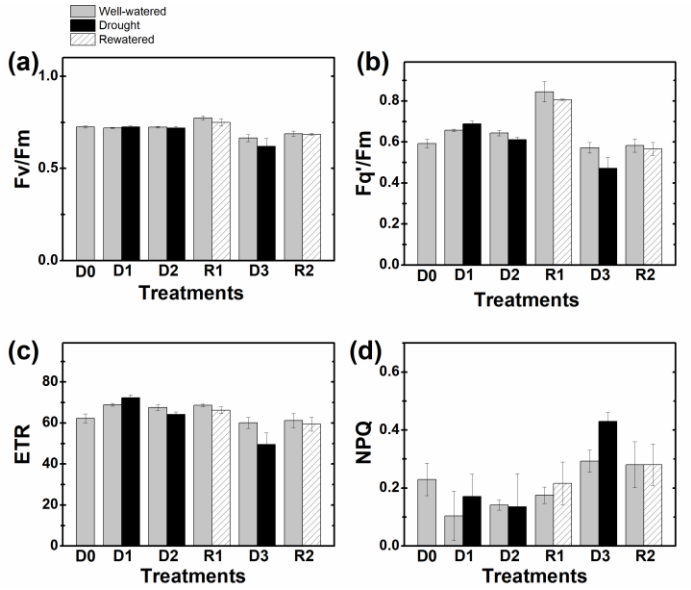

Fig. S12 Chlorophyll *a* fluorescence in leaves of *P. oleracea* in response to drought and rewatering. Plants were sampled after 0, 10, 22 and 34 days of drought treatment (D0, D1, D2 and D3, respectively) and during rewatering events initiated after 22 and 34 days of drought (R1 and R2, respectively). (a) Photochemical efficiency of the PSII (F_v/F_m). (b) PSII effective quantum yield (Fq′/Fm′). (c) Electron transport rate (ETR). (d) Non-photochemical quenching (NPQ). Data are means (±SE) of at least four biological replicates. Differences between treatments were not significant.

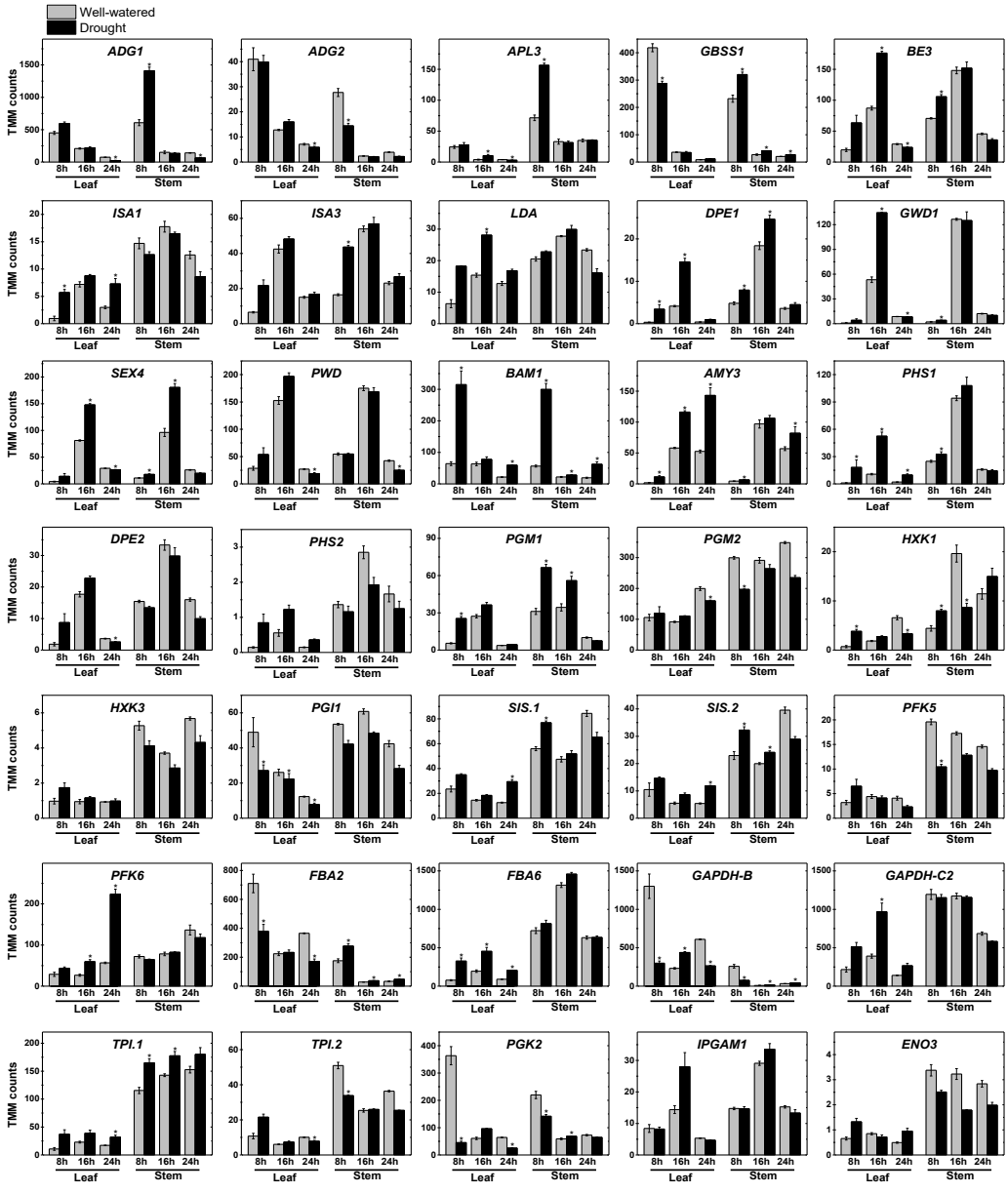

Fig. S13 Mean TMM values for contigs of carbohydrate metabolism genes. Leaf and stem samples were harvested from plants maintained for 34 days under well-watered or drought conditions. TMM values are presented in Table S8. Data are means (±SE) of at least three replicates. Asterisks indicate significant difference (adjusted p-value<0.05) between well-watered and droughted samples. Abbreviations are explained in the text and/ or in Table S8 (see Material and Methods for details).

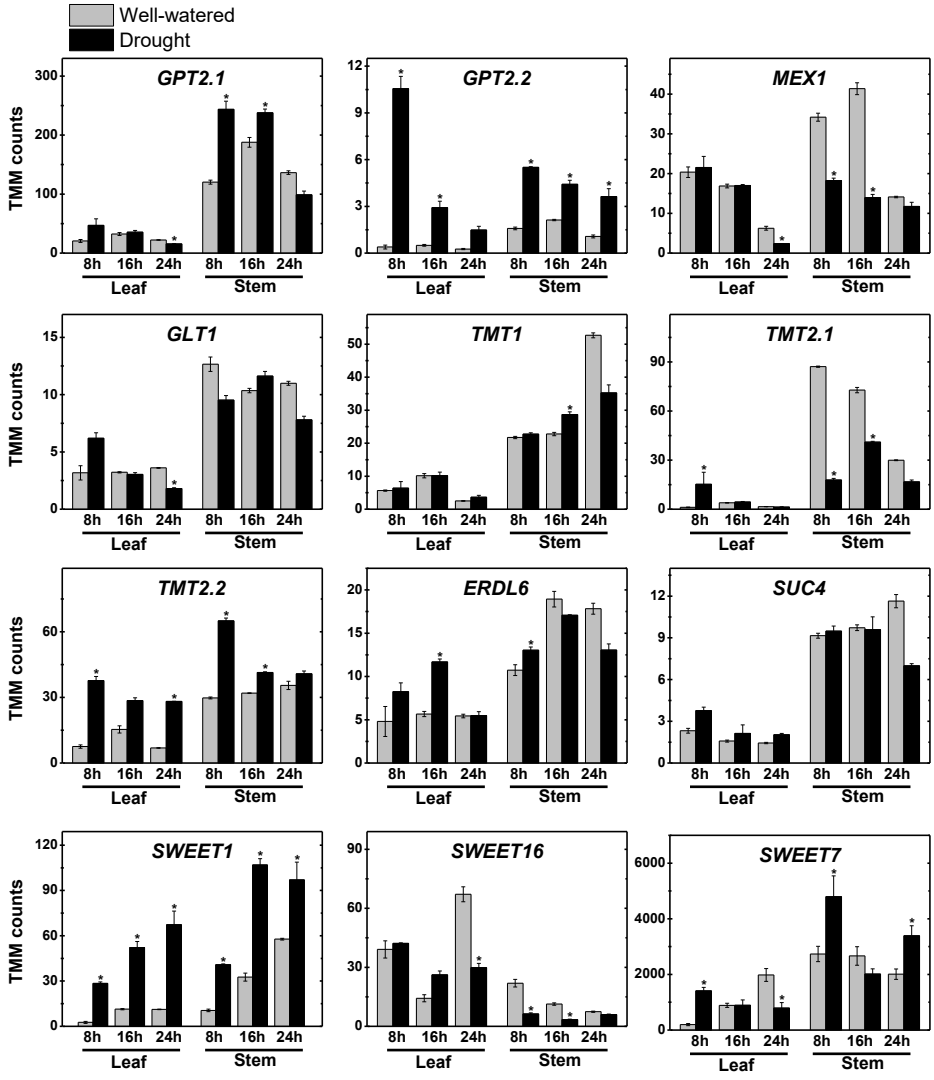

Fig. S14 Mean TMM values for contigs of genes encoding carbohydrate-related transporters. Leaf and stem samples were harvested from plants maintained for 34 days under well-watered or drought conditions. TMM values are presented in Table S8. Data are means (±SE) of at least three replicates. Asterisks indicate significant difference (adjusted p-value<0.05) between well-watered and droughted samples. Abbreviations are explained in the text and/ or in Table S8 (see Material and Methods for details).

Chapter III

Exploring C_4–CAM plasticity within the *Portulaca oleracea* complex

"The spinach is a C_3 plant
It has a Nobel pathway
Its compensation point is high
From early morn till noon-day.
It has carboxy dismutase
But has no malate transferase;
The spinach is a regal plant
But lacks the Hatch-Slack pathway."

F. A. Smith, H. Beevers, and others, sung to the tune of "O Tannenbaum

This chapter is organized as published in the journal Scientific Reports:

Ferrari R.C.; Cruz B.C.; Gastaldi V.D.; Storl T.; Ferrari E.C.; Boxall S.F.; Hartwell J.; Freschi L. Exploring C_4-CAM plasticity within the *Portulaca oleracea* complex. *Scientific Reports* 10, 14237, 2020. Doi:10.1038/s41598-020-71012-y.

Supplementary information is available for this paper at https://www.nature.com/articles/s41598-020-71012-y.

Abstract

Portulaca oleracea is a C_4 herb capable of performing CAM under drought stress. It is distributed worldwide and is either considered a polymorphic species or a complex of subspecies, due to its numerous morphological variations. We evaluated CAM plasticity within *P. oleracea* genotypes since the complexity surrounding this species may be reflected in intraspecific variations in photosynthetic behavior. Eleven subspecies of *P. oleracea* from distant geographical locations and one cultivar were morphologically and physiologically characterized. C_4 and CAM photosynthesis were monitored in plants exposed to well-watered, droughted and rewatered treatments, and data obtained were compared among individual genotypes. All subspecies expressed CAM in a fully-reversible manner. Transcript abundance of C_4-CAM signature genes was shown to be a useful indicator of the C_4-CAM-C_4 switches in all genotypes. C_4-related genes were down-regulated and subsequently fully expressed upon drought and rewatering, respectively. CAM-marker genes followed the opposite pattern. A gradient of morphological traits and drought-induced nighttime malate accumulation was observed across genotypes. Therefore, different combinations of CAM expression levels, plant sizes and shapes are available within the *P. oleracea* complex, which can be a valuable tool in the context of C_4/CAM photosynthesis research.

Keywords: C4 photosynthesis; crassulacean acid metabolism; purslane; photosynthetic plasticity; drought; malate; phospho*enol*pyruvate carboxylase; Caryophyllales; intraspecific variation

Introduction

C_4 photosynthesis and the crassulacean acid metabolism (CAM) are carbon (C) concentrating mechanisms (CCMs), similar in their biochemical pathways, as both use phospho*enol*pyruvate carboxylase (PPC) to perform the primary fixation of CO_2 into 4-C acids[1-2]. These acids are subsequently decarboxylated, regenerating CO_2 in the vicinity of ribulose-1,5-biphosphate carboxylase/oxygenase (Rubisco) to minimize O_2 binding. The oxygenase activity leads to 3-phosphoglycerate (3PGA) and 2-phosphoglycolate (2PG) formation, the latter molecule being toxic, and requiring processing and elimination via photorespiration[3]. Despite the shared similarities between C_4 and CAM, each CCM is usually associated with a specific set of anatomical characteristics and regulatory mechanisms, rendering uncommon the co-occurrence of both syndromes within a single plant[4].

Overall, C_4 acts as a spatial specialization involving the transfer of CO_2 acceptor molecules between a mesophyll and a bundle sheath cell (MC and BSC, respectively)[5]. In contrast, CAM works as a temporal specialization, where acid formation and mobilization occur in a single MC but at different times of the day[6]. Also, CAM has been shown to vary in the degree of diel acid fluctuation and gas exchange patterns, with the contribution of the nocturnal CO_2 primary fixation to total C assimilation varying across species[7]. These features characterize different types of CAM, ranging from strong CAM, where virtually all CO_2 assimilation derives from CAM activity[8] (Nobel 1988), to weak CAM (e.g., CAM cycling), in which atmospheric CO_2 uptake takes place exclusively during the day, and the refixation of respiratory CO_2 leads to a small nighttime accumulation of organic acids[9].

At the weak-CAM end of the spectrum, *Portulaca* species are C_3-C_4 intermediates and C_4 plants capable of performing CAM under drought. Facultative CAM was shown to occur in species belonging to the six phylogenetic clades of *Portulaca*, some of which performing CAM-cycling when water is deprived [10–16]. In addition to this complex scenario, different decarboxylating systems occur in *Portulaca*, with NADP-malic enzyme (ME) and NAD-ME representatives such as *P. grandiflora* and *P. oleracea*, respectively[17,18].

Portulaca oleracea is a promising candidate for a C_4/CAM model species due to its fast growth, efficient seed production, and accumulating literature on CCM-related biochemical and gene expression data[19–26]. The uncommon C_4-to-CAM transition in leaves of *P. oleracea* is associated with the transcriptional induction of specific genes. They include a CAM-specific PPC isoform (*PPC-1E1c*), an aluminum-activated malate transporter (*ALMT-12E.1*) and a dicarboxylate carrier (*DIC-1.1*)[23,27], and their relative transcript abundances have been suggested as a valuable tool to assess CAM induction in this species[27]. ALMT proteins have a role in nocturnal malate uptake into the vacuole[28,29], while DIC transporters mediate C-skeleton transport across mitochondria[30]. Besides, several C_4-related transcripts

were identified to be exclusively expressed in leaves under well-watered conditions in *P. oleracea*, including a C_4-related PPC isoform (*PPC-1E1a'*)[23], a NAD-ME (*NADME-2E.1*) and an aspartate aminotransferase (*ASPAT-1E1*)[27].

Commonly known as purslane, *P. oleracea* can germinate over a wide temperature range (10–40 ºC)[31], thriving in various light intensities, photoperiods, soil types and moisture conditions [32–34], even being considered a noxious weed for agriculture[35]. It also presents a cosmopolitan distribution, occurring in most tropical and subtropical regions[36]. Variations in chromosome number[37], vegetative and reproductive morphology[38–42] are already described between accessions of this species. Because of such high phenotypical plasticity, *P. oleracea* is sometimes referred to as a polymorphic species[33,37], or even subdivided into different subspecies[43,44] or microspecies[45–47] that form a taxonomic aggregate or complex. The most up-to-date phylogeny detailing *Portulaca* infra-familiar relationships still refers to the traditional *P. oleracea* subspecies system to highlight that this clade is paraphyletic and clusters with other species, e.g. *P. molokiniensis*[44,48].

However, comparative information on the physiological performance, particularly in the context of CAM plasticity and CCM-related transcriptional reprogramming, is missing for the *P. oleracea* complex. Understanding CAM plasticity across *P. oleracea* genotypes may be a valuable source of information for future biotechnological applications seeking to explore C_4/CAM compatibility using this species as a model[26,49]. Therefore, we hypothesized that there might be different degrees of CAM expression among members of the *P. oleracea* complex, particularly when comparing genotypes with distinctive morphological traits (e.g., leaf succulence and size) and originally from contrasting environmental conditions.

To this end, we assembled a collection of twelve *P. oleracea* genotypes, composed of eleven subspecies from different geographic regions and one cultivar, to compare physiological variation in CAM response. Subspecies were characterized based on climatic conditions of their place of origin or morphological traits using a clustering approach by principal component and hierarchical clustering analyses (PCA and HCA, respectively). Nighttime malate accumulation (Δ_{malate}) and transcript abundance of CAM- and C_4-signature genes revealed that weakly expressed, facultative CAM is a shared trait among all genotypes analyzed. We also validated the previously published recommendation of specific C_4 and CAM genes[27] by monitoring their relative transcript abundance and detecting similar expression patterns across various genotypes. Finally, our findings indicate that different combinations of drought-induced CAM expression intensities, plant sizes and shapes are available within the *P. oleracea* complex, an array that offers various possibilities for future C_4/CAM photosynthesis research.

Results

Characterizing *P. oleracea* genotypes using clustering approaches

Previously identified *P. oleracea* subspecies and one cultivar genotype (Table 1) were grown side-by-side under greenhouse conditions for three generations before the start of the experiments. Seed attributes were analyzed under scanning electron microscopy (SEM) to confirm subspecies identification and the purity of lots (Supplementary Figure S1). A commercial cultivar was included as a reference genotype for physiological analyses since it was previously used in physio-transcriptomic studies[27]. Additional Brazilian wild accessions were identified via SEM analysis either as subsp. *granulatostellulata* or subsp. *nitida* (Supplementary Figure S1), and were not included in the physiological experiments, as these subspecies were already represented in our collection.

The climatic conditions of the place of origin and morphological attributes were compared for the eleven subspecies, and the cultivar was included in the morphological analysis only. Data obtained was analyzed via principal component analysis (PCA) for cluster identification, and then further evaluated using hierarchical clustering analysis (HCA).

First, 19 climatic variables were retrieved from the World Clim database[50] using the geographic coordinates from the sampling place of each subspecies (Supplementary Table S1, Fig. 1A,C,E). Variables presented > |0.64| correlations to the first 4 PCs, but we focused on PC 1 and 2 since 16 out of the 19 variables were significantly correlated to these PCs. One genotype, *tuberculata*, was isolated from the other subspecies in PC1 by scoring high in winter temperature parameters. On the other hand, precipitation variables reflecting on seasonality contributed to separating the remaining subspecies along PC2. The following groups were formed: 1- consisting of *tuberculata* alone, 2- formed by *edulis, trituberculata, rausii, nitida* and *granulatostellulata*; 3- formed by *sicula, sativa* and *papillatostellulata*; 4- including *oleracea* and *zaffranii* (Fig. 1C,E).

Table 1. Identification and geographical origin of *Portulaca oleracea* genotypes.

Genotype identification	Taxonomic identification [a]	Geographical origin	Ref.
trituberculata	*Portulaca trituberculata* Dani n, Domina & Raimondo	Greece, 38°13'37" N, 25°59'57" E	[1]
sicula	*Portulaca sicula* Danin, Domina & Raimondo	Italy, 43°27'53" N, 11°52'39" E	[1]
oleracea	*Portulaca oleracea* subsp. *oleracea* / *Portulaca trituberculata* [1]	Chile, 36°49' S, 73°03' W	[1]
rausii	*Portulaca rausii* Danin	Greece, 36°50'56" N, 27°04'31" E	[1]
zaffranii	*Portulaca zaffranii* Danin	South Africa, 23°04'04,1" E, 34°02'36,5"S	[1]
nitida	*Portulaca nitida* (Danin & H.G.Baker) Ricceri & Arrigoni	Israel, 31°47'11" N, 34°42'33" E	[2]
edulis	*Portulaca edulis* Danin et Bagella [2]	Greece, 35°05'08" N, 33°16'46" E	[1]
papillatostellulata	*Portulaca papillatostellulata* (Danin & H.G.Baker) Danin	Austria, 48°17'43" N, 16°52'18" E	[1]

sativa	*Portulaca oleracea* subsp. *sativa* (Haw.) Čelak.	Austria, 48°11'33" N, 16°23'04" E	[1]
tuberculata	*Portulaca tuberculata* León	Peru, 12°35'39" S, 69°11'38" W	[1]
granulatostellulata	*Portulaca granulatostellulata* (Poelln.) Ricceri & Arrigoni	Israel, 32°23'60" N, 34°52'58" E	[2]
cultivar	commercial cultivar	Agristar [b]	[3]

[a]Taxonomic identification according to the registry at The Plant List (2013), except for *P. edulis* since it is not listed. [1] Walter et al., 2015. [2] Danin et al., 2012. [3] Ferrari et al. 2020. [b] Seeds bought from Agristar do Brasil Ltda. - São Paulo, Brazil.

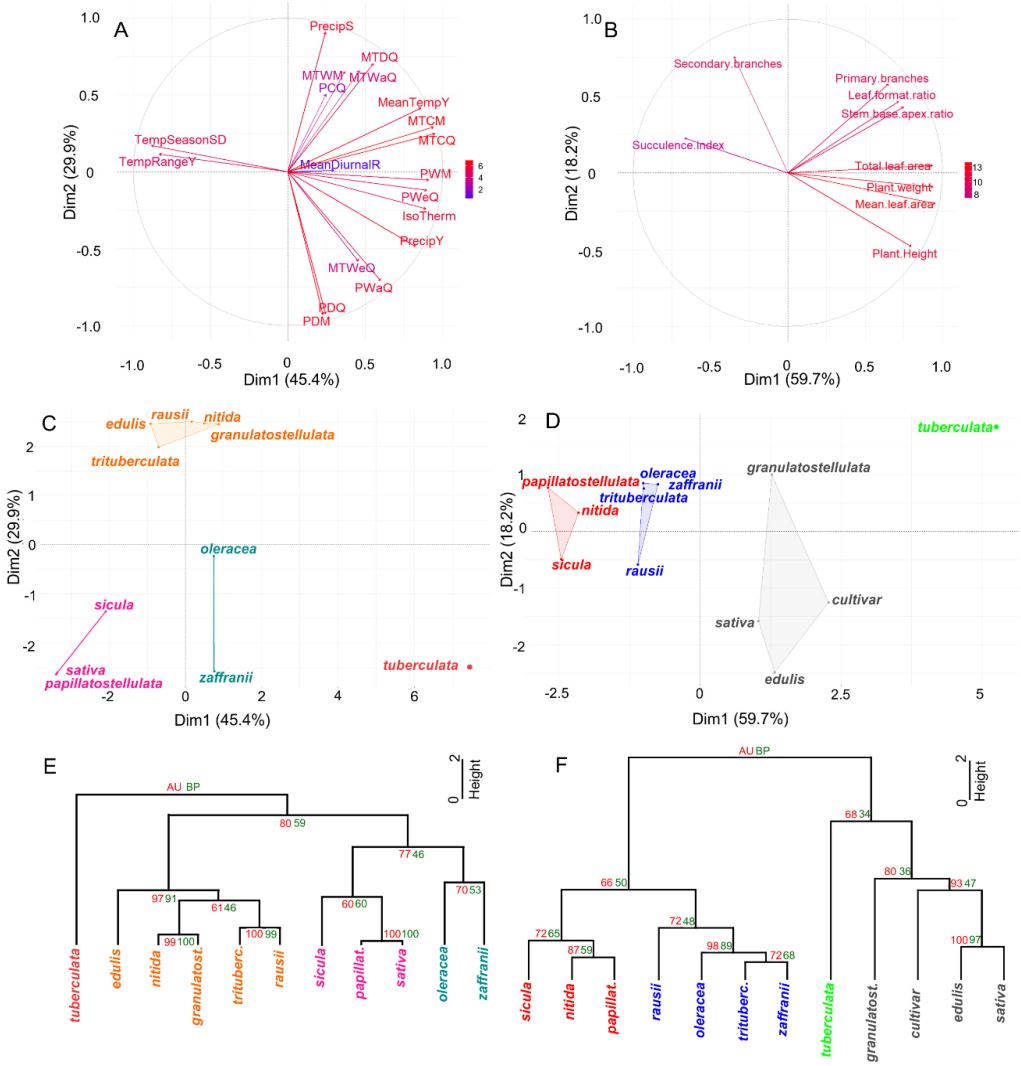

Figure 1. Characterization of the *Portulaca oleracea* complex based on climatic and morphometric variables via principal component analysis (PCA) and hierarchical clustering analysis (HCA). (**A-B**) Variable contribution to each PC. The first two PCs explain 75% and 77% of the variance in A and B, respectively. The color scale indicates the relative variable contribution to each PC. (**C-D**) Groups of subspecies formed - the first two PCs harbor the most significant correlations to the variables. (**E-F**) HCA groups subspecies into clusters and values of approximately unbiased (AU) and bootstrap (BP) are presented in red and green, respectively (see Methods section for details). Data for these analyses are presented in Tables S1 and S2. In (**A, C, E**), the following climatic variables were analyzed: latitude, longitutude, annual mean temperature (MeanTempY), mean diurnal range (MeanDiurnalR), isothermality (IsoTherm, temperature seasonality standard deviation (TempSeasonSD), max. temperature of warmest month (MTWM), min. temperature of coldest month (MTCM), temperature annual range (TempRangeY), mean temperature of wettest quarter (MTWeQ), mean temperature of

driest quarter (MTDQ), mean temperature of warmest quarter (MTWaQ), mean temperature of coldest quarter (MTCQ), annual precipitation (PrecipY), precipitation of wettest month (PWM), precipitation of driest month (PDM), precipitation seasonality (PrecipS), precipitation of wettest quarter (PWeQ), precipitation of driest quarter (PDQ), precipitation of warmest quarter (PWaQ), precipitation of coldest quarter (PCQ).

Second, nine morphometric parameters were measured in the 12 genotypes, using at least 25 well-watered, two-month-old individuals that were grown side-by-side under controlled conditions (Supplementary Table S2, Fig. 1B,D,F). These data were subsequently analyzed by PCA and HCA. The first three principal components explained a total of 90.16% of the variance, but only PCs 1 and 2 (77.83% of the variance) were kept since PC3 showed low correlation coefficients to the variables (< |0.52|). While the number of primary and secondary branches was positively correlated to PC2, succulence was negatively correlated to PC1, and the remaining characteristics were positively correlated to PC1 (Fig. 1B). Considering the contribution of each variable to the PCs, leaf size and stem branching were important factors when separating the four clusters. The groups were composed of: A - containing exclusively *tuberculata*; B- *papillatostellulata, nitida* and *sicula*; C- *oleracea, zaffranii, trituberculata* and *rausii*; and D- *sativa*, *edulis*, and *granulatostellulata* and the cultivar (Fig. 1D,F). We tested if morphological attributes correlated with each other (Supplementary Table S3), and positive correlations ($r > 0.61$, p-value < 0.05) revealed that large plants have large leaves and harbor more primary branches. Succulence was negatively correlated ($r < -0.59$, p-value < 0.05) with plant robustness parameters and leaf area. Overall, taller plants harbored thinner and larger leaves, whereas smaller plants were more branched with smaller, thicker leaves (Supplementary Table S3).

When comparing the clusters formed using either the climate or morphological approaches, *tuberculata* was placed in an isolated cluster, while the following pairs clustered together using both approaches: *sicula* + *papillatostellulata*; *trituberculata* + *rausii*; and *oleracea* + *zaffranii*.

Drought represses C_4 and promotes CAM pathways across genotypes

After characterizing the morpho-climatic traits of our collection, the impacts of water availability on CAM photosynthesis across genotypes was investigated by comparing CAM-related traits. To this goal, one-month-old plants were kept side-by-side under well-watered or droughted conditions for 30 days, or exposed to drought for 30 days followed by two days of complete rewatering (Fig. 2A). To prevent plants from dying, the drought treatment consisted of withholding water for ten consecutive days, followed by a 20 day period in which a small water volume (10 ml) was added to the pots whenever the soil water content reached values close to zero (usually every four days). The drought treatment promoted a

marked reduction in plant size in all genotypes compared to the well-watered counterparts (Fig. 2B).

We monitored continuous net CO_2 exchange in *rausii*, *granulatostellulata*, *nitida* and the cultivar, which are representatives of each of the four morphological clusters identified in this work (Fig. 3). A multi-chamber IRGA system was used to monitor the entire shoot of two-weeks-old plants, revealing a similar behavior for all genotypes monitored (Fig. 3). Well-watered plants displayed CO_2 assimilation throughout the entire light period. In contrast, CO_2 uptake was limited to a brief burst in the early morning at the start of drought treatment, whereas daytime CO_2 uptake was undetectable at the end of the drought period. Daytime CO_2 uptake was recovered within hours after full rewatering of the plants, indicating the activation of C_4 photosynthesis when the water supply returned. Nocturnal net CO_2 uptake was not observed across the genotypes analyzed.

Leaf relative water content (RWC) values were significantly lower under drought compared to well-watered conditions for all genotypes (Fig. 4A). Rewatering recovered leaf RWC to values similar, or almost similar (e.g., *sicula* and *rausii*), to those detected in well-watered plants. To investigate whether all genotypes were able to switch to CAM photosynthesis in response to drought, leaf malate levels were determined at dawn and dusk, and nocturnal malate accumulation (Δ_{malate}) was calculated for each of them (Fig. 4B, Supplementary Table S4). Under well-watered conditions, *papillatostellulata*, *oleracea*, *trituberculata* and *edulis*, the latter at very low levels, displayed accumulation of malate overnight (positive Δ_{malate}), whereas malate levels in the remaining genotypes decreased overnight (negative Δ_{malate}) (Fig. 4B). All genotypes presented positive Δ_{malate} under drought treatment, with the lowest and highest Δ_{malate} values (26.7 and 157.2 μmol malate per g dry weight, respectively) detected in *oleracea* and *trituberculata*, respectively. Nocturnal malate accumulation was consistently reduced following rewatering in all subspecies (Fig. 4B).

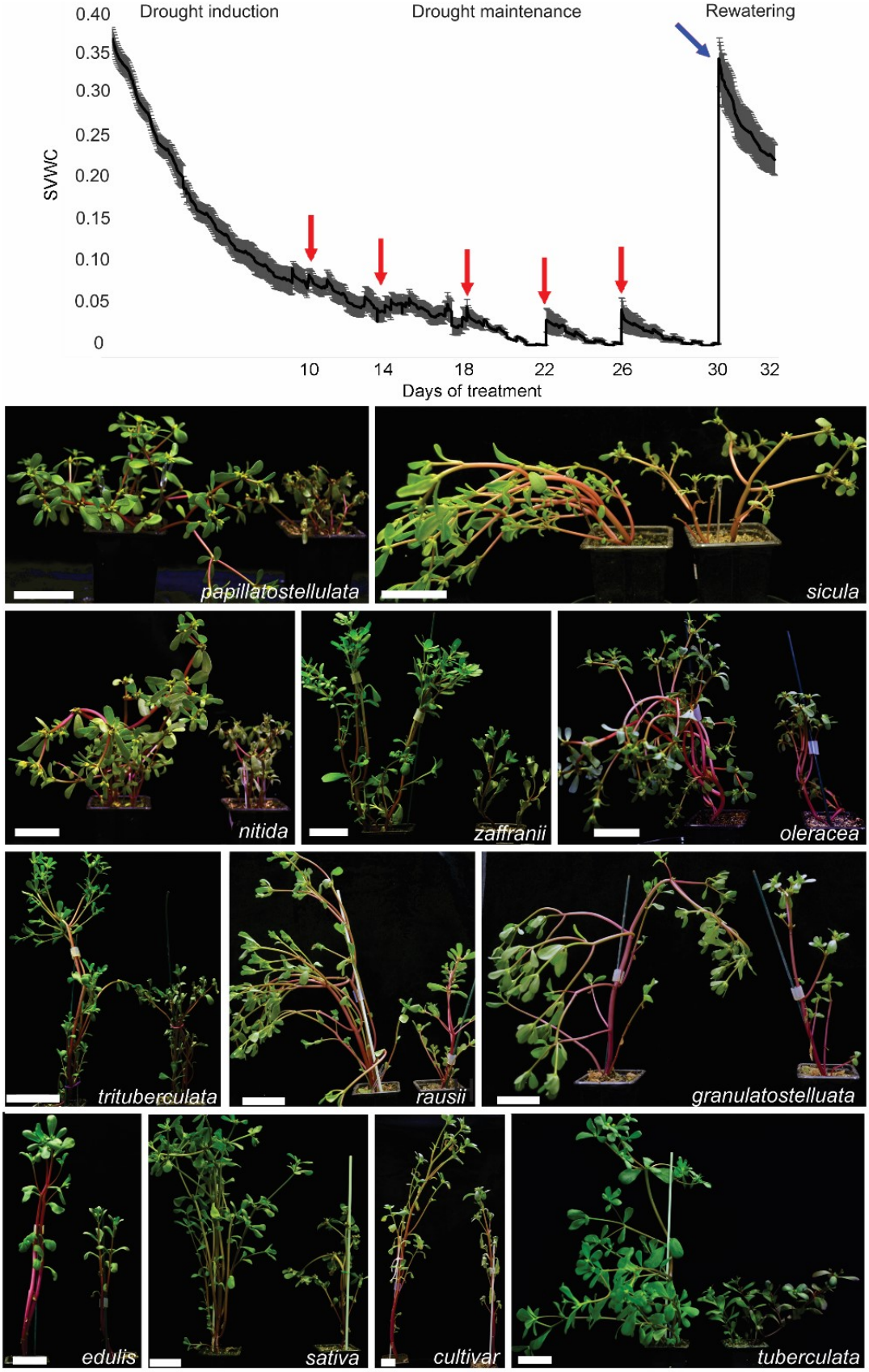

Figure 2. Drought treatment impacts on soil volumetric water content (SVWC) and overall plant morphology. (**A**) Changes in SVWC during drought and rewatering treatments in *P. oleracea*, with red and blue arrows indicating partial (10 ml per pot) and full watering events, respectively (see Methods

for details). Data are means ± SE for monitored genotypes. (**B**) Representative images of two-month-old plants kept under well-watered (left) and droughted (right) conditions.

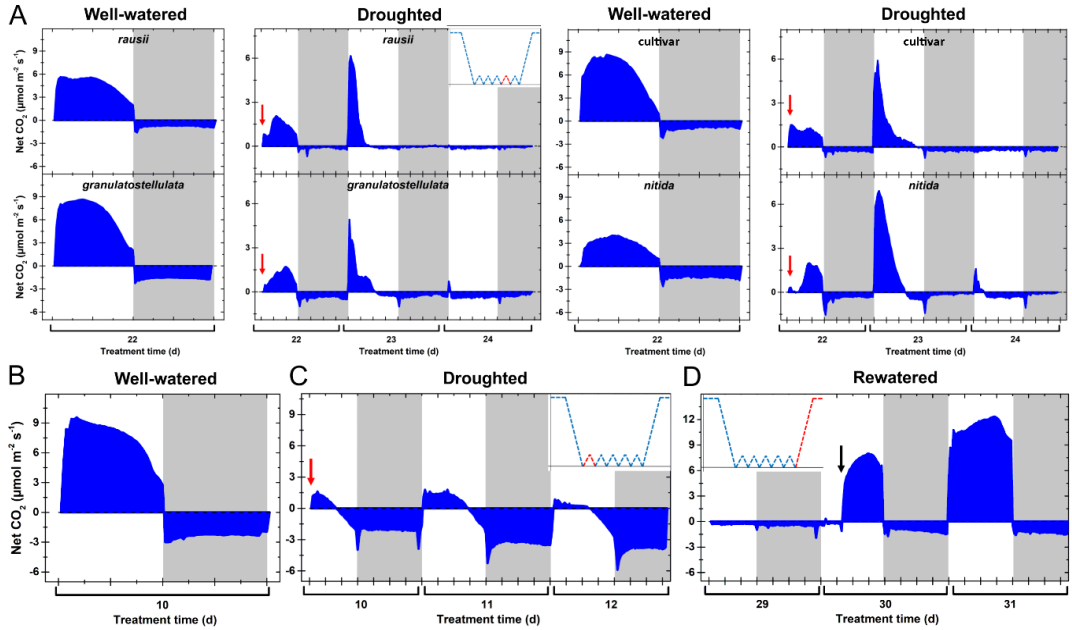

Figure 3. Similar drought-triggered changes in diel gas exchange are shared by *Portulaca oleracea* subspecies. (**A**) Net CO_2 exchange of shoots of representative subspecies after 16 days of drought. (**B-D**) Net CO_2 exchange by shoots of *granulatostellulata* in well-watered conditions (**B**), after the initial 10-day-period of water withholding (**C**), and after 20 days of drought and into rewatering (**D**). In **A-D**, two-week-old individuals were used due to the size restriction of the cuvette. Also, data were normalized against the leaf area. Shaded areas indicate the dark period, red arrows indicate partial watering event (5 ml), and the blue arrow indicates full rewatering. Inserts schematically illustrate soil water content following water deprivation (see Methods for details), and the time points corresponding to the gas exchange measurements are highlighted in red.

We then monitored the transcriptional patterns for CCM-related genes across the studied genotypes. Transcriptional profiling of CAM-related genes under drought, when compared to well-watered conditions, showed increments of up to 165, 123 and 25 times in mRNA levels of *PPC-1E1c*, *ALMT-12E.1* and *DIC-1.1*, respectively (Fig. 5A-C, Supplementary Table S4). Rewatering reduced relative transcript levels for all three CAM-marker genes significantly in most cases, reaching values as low as those detected in well-watered plants.

For C_4-related genes such as *PPC-1E1a'*, *NADME-2E.1* and *ASPAT-1E1*, mRNA levels were between 3 and 48 times lower under drought than in well-watered plants across genotypes (Fig. 5D-F, Table S4). Rewatering resulted in *PPC-1E1a'* mRNA levels relatively higher than those detected in well-watered plants, except for *papillatostellulata*, *granulatostellulata* and the cultivar, which exhibited similar abundance in both rewatered and well-watered plants (Fig. 5F). Upon rewatering, relative transcript abundance of *NADME-*

2E.1 and *ASPAT-1E1* returned to levels as high as those detected in well-watered individuals (Fig. 5D-F, Supplementary Table S4).

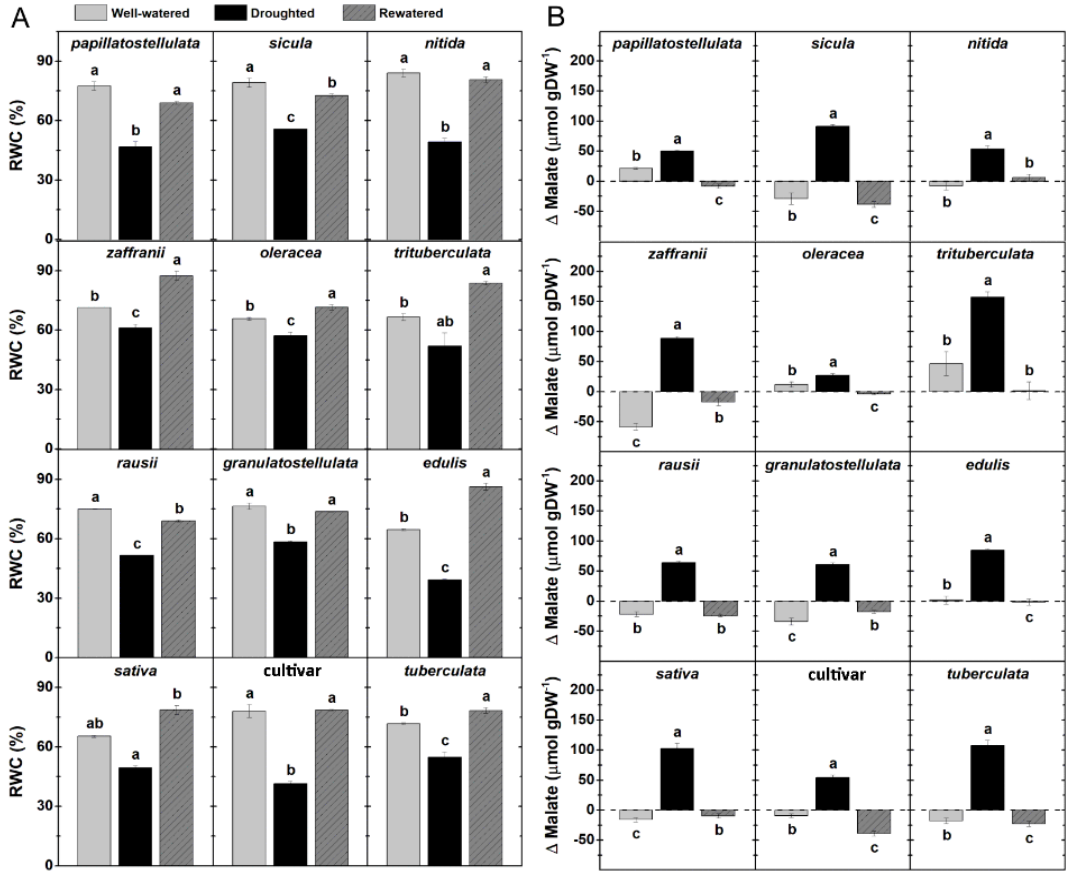

Figure 4. Impacts of water availability *P. oleracea* on relative water content (RWC) and nocturnal malate accumulation. (**A**) Leaf RWC of well-watered, droughted and rewatered plants. (**B**) Nocturnal malate accumulation (Δ malate) in well-watered, droughted and rewatered plants. Data are means ± SE of at least three biological replicates, and different letters indicate statistically significant differences ($p < 0.05$) among the treatments for each subspecies. In **B**, standard error = $\sqrt{((\text{standard error}_{\text{well-watered}})^2 + (\text{standard error}_{\text{droughted}})^2}$.

Lastly, we assessed drought resilience across the genotypes by performing Chl *a* fluorescence imaging in source leaves of plants exposed to long-term, continuous water withholding, i.e., 20 and 35 days (Supplementary Figure S2-4). In all genotypes, PSII operating efficiency (Fq'/Fm') was similar comparing well-watered and droughted plants, and only *trituberculata*, *rausii* and the cultivar exhibited slightly reduced Fq'/Fm' after prolonged droughted (Supplementary Figure S2). Non-photochemical quenching (NPQ) significantly increased after drought only in *tuberculata* (Supplementary Figure S3). The most prominent reduction in maximum quantum efficiency of PSII photochemistry (Fv/Fm) was detected after 34 days of drought stress in *tuberculata*, *papillatostellulata* and the cultivar (Supplementary Figure S4).

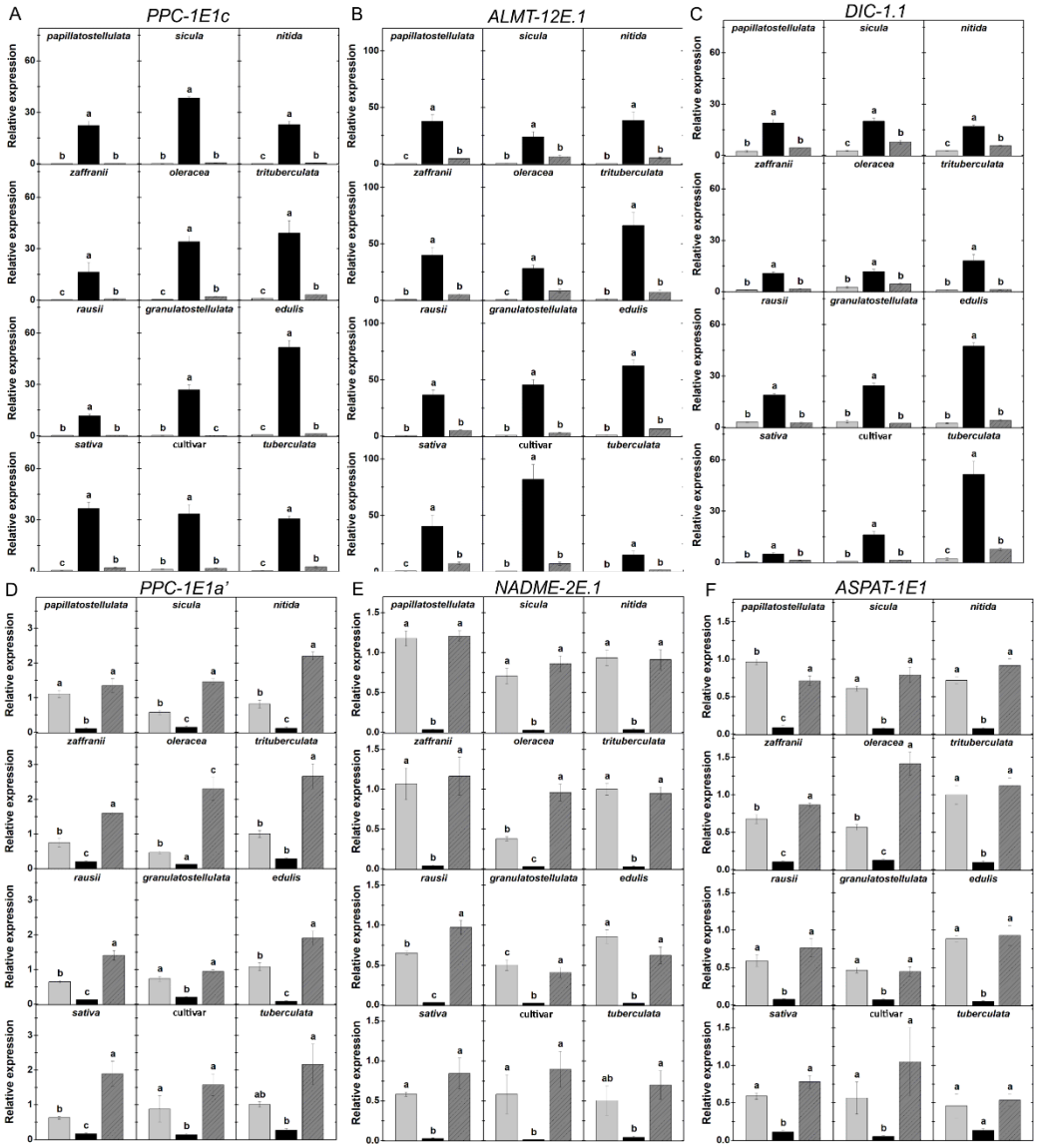

Figure 5. Impacts of water availability on transcript abundance of C_4- and CAM-marker genes. (**A-C**) Relative abundance of CAM-specific transcripts: *PPC1E1c* (**A**), *ALMT-12E.1* (**B**), *DIC-1.1* (**C**). (**D-F**) Relative abundance of CAM-specific transcripts: *PPC1E1a'* (**D**), *NADME-2E.1* (**E**), *ASPAT-1E1* (**F**). Mean relative expression was normalized against well-watered *trituberculata* samples, and mRNA levels were determined in samples harvested at dawn (**A-C**) or dusk (**D-F**). Data are means ± SE of at least three biological replicates, and different letters indicate statistically significant differences ($p < 0.05$) among the treatments for each subspecies.

Comparing CCM-related physio-molecular traits across the genotypes

After characterizing C_4-CAM photosynthesis for *P. oleracea* genotypes individually using malate quantification and transcript abundance of key C_4-CAM-related genes, we compared the genotypes at each water availability condition separately (Supplementary Tables S4, S5). Nighttime malate accumulation was significantly different (p-value < 0.05) across genotypes at all three water availability conditions. However, such a pattern was not statistically supported in terms of CAM-related transcript accumulation. Although *tuberculata* clustered apart from the other genotypes at the initial morpho-climate

characterization, its Δ_{malate} levels and transcript profiles did not stand out compared to the remaining genotypes, except for the lower accumulation of *ALMT-12E.1* mRNA levels under drought. Also, genotype pairs that initially clustered together (*sicula* + *papillatostellulata*; *trituberculata* + *rausii*; and *oleracea* + *zaffranii*) did not show similar trends for any of the CCM-related parameters.

Surprisingly, no significant correlations were observed between Δ_{malate} and CAM-related transcript abundance (including *PPC-1E1c* mRNA levels) under drought. However, a positive correlation ($r > 0.76$, p-value < 0.05) was observed between (1) Fv/Fm and Fq'/Fm', (2) *PPC-1E1a'* mRNA levels and either RWC and Δ_{malate}, and (3) between *NADME-2E.1* and *ASPAT-1E.1* mRNA levels (Supplementary Table S6). Also, *ALMT-12E.1* mRNA abundance was negatively correlated to *ASPAT-1E.1* transcript levels ($r = -0.74$, p-value < 0.05, Supplementary Table S6).

Discussion

CAM has long been described as a highly plastic adaptive syndrome, operating in different modes and magnitudes depending on the lineage[51]. CAM-related literature includes a vast array of studies on interspecific variability in the contribution of nocturnal CO_2 uptake to net daily carbon gain (i.e., weak *versus* strong CAM), the diel pattern of gas exchange, the occurrence of CAM throughout the plant life cycle or as environmental conditions change (i.e., constitutive *versus* facultative CAM), and molecular evolution of CAM-specific gene lineages[1,7,52,53]. Among CAM physiotypes, facultative CAM species, as *P. oleracea*, are recognized as particularly convenient systems for understanding the discrete changes in genetic architecture and gene expression associated with the CAM pathway[54,55].

Different studies have already addressed the pronounced evolutionary changes forming a gradient ranging from C_3 to obligatory CAM species [56–58], but C_4/CAM-performing species comprehend a new and yet little explored scenario[16,23,58,59]. In addition, studies linking CAM intensity, environmental conditions and plant morphoanatomical variations have shown that different trends may occur in different plant lineages[60]. For example, at the plant family level, some Orchidaceae show a correlation between decrescent CAM intensity and increasing altitude[61], whereas Eulophiinae terrestrial orchids evolved higher CAM expression during the transition to drier habitats[62]. Also, tropical Oncidiinae epiphytes that express weak CAM possess thinner leaves, while strong CAM orchids have thicker leaves[63]. However, when comparing morphologically similar C_3-CAM cycling *Talinum* species, differences in nocturnal acidity were more inconspicuous, but still correlated with low humidity coefficients ($r = -0.55$) from each species place of sampling[64]. Although comparing leaf thickness and cell size from C_3 and obligate CAM *Yucca* species showed a positive correlation to nocturnal gas exchange and higher leaf acidification[65], the comparison of 24 genotypes of C_3-CAM *Yucca*

gloriosa showed no correlation between leaf anatomy and CAM intensity[66]. This highlights that among intermediate phenotypes, the evolutionary trends may be more challenging to identify. Therefore, each plant lineage may show specific trends for the group, not necessarily matching the typical CAM trends as traditionally described[67].

In this context, the *P. oleracea* complex represents a valuable system both for exploring the intraspecific variability of CAM and for providing additional biochemical and genetic information about the rare co-occurrence of C_4 and CAM pathways. *P. oleracea* has been considered an aggregate of subspecies or microspecies[43,46,47], also sometimes referred to as different species[68–70]. To our knowledge, taxonomic reports list 19 subspecies/microspecies distinguished according to their seed size and coat ornaments[46]. On the other hand, *P. oleracea* is sometimes considered a polymorphic species, and due to its cosmopolitan distribution and high adaptability, it is somewhat expected to present high variability in morphological traits among populations, even forming a continuum[33,37,38,71]. Such plasticity might also affect seed attributes, making seed morphology and size alone inconclusive to differentiate subspecies, especially considering that hybrid subspecies have already been reported in mixed populations[33,37]. A comprehensive phylogeny including as many accessions of *P. oleracea* as possible will be needed to solve the species paraphyletic scenario, but its cosmopolitan distribution may prove to be a challenge to this goal. In the present study, we selected genotypes sampled from independent populations and identified as different subspecies, and the clustering methods applied here confirmed previously described trends[38], where weedy (small, prostrate and branched) phenotypes were clustered separately from more robust and erect phenotypes, e.g. commercial cultivars.

Regarding the intraspecific metabolic plasticity in *P. oleracea*, CAM was found to be expressed in a completely reversible way in all genotypes analyzed in the present study. Our findings indicate that, although there are significant intraspecific differences in drought-induced Δ_{malate}, these are not directly correlated with the transcript abundances of CAM-specific genes (*PPC-1E1c, ALMT-12E.1* and *DIC-1.1*). Also, there was no correlation between the transcript levels of these CAM-related genes that would suggest a causal relation. Therefore, the widespread occurrence of low-level CAM expression across the *P. oleracea* genotypes seems to be achieved without a strict balance between the expression levels of key CAM-related genes and the intensity of nighttime acidification, which further reflects the complexity behind the CAM syndrome[7,55].

Over the last years, molecular and bioinformatics tools have been progressively applied to characterize the large gradient of expression found in CAM plants[72–77]. Thus, understanding the molecular processes behind CAM photosynthesis has gained further interest as a source of information for bioengineering endeavors seeking to improve crop resistance to extreme drought conditions [49,78,79]. However, a comparative study across

different genotypes using CCM transcript abundances of key genes in C_4-CAM species was missing, despite its potential to provide relevant information for future attempts of engineering CAM into C_4[26,49]. Here we show that, at least at the transcriptional level, major components of C_4 and CAM photosynthesis were regulated in opposite directions by water availability across all *P. oleracea* genotypes analyzed. All three CAM-marker genes (*PPC-1E1c, ALMT-12E.1* and *DIC-1.1*[27]), previously identified exclusively in one genotype (here referred to as cultivar), were expressed at significantly high levels under drought in all genotypes analyzed. This indicates that, in overall terms, the transcriptional control of key components of CAM machinery by water availability is conserved within the *P. oleracea* complex. Similarly, the C_4-related genes *PPC-1E1a'*, *NADME-2E.1* and *ASPAT-1E1* were also clearly down- and up-regulated across subspecies by drought and rewatering, respectively. Still, individual puzzle pieces belonging to different CCMs, such as the significant negative correlation between *ALMT-12E.1* (CAM) and *ASPAT-1E.1* (C_4) mRNA levels under drought, indicates that there is still much room for investigating the intricate connection and concomitant modulation between C_4 down- and CAM up-regulation.

Weak, inducible CAM has been reported for different *Portulaca* species, with the drought-promoted increase in nocturnal acidification either associated with a small nocturnal CO_2 uptake (e.g. *P. cyclophylla* and *P. cryptopela*) or as a result of CAM-cycling (e.g. *P. digyna*)[15,16]. The diel CO_2 uptake patterns observed in the present study support the occurrence of CAM-cycling for all four *P. oleracea* analyzed. Therefore, it is safe to assume that the malate formed overnight in droughted *P. oleracea* genotypes is derived from recycling nocturnal respiratory CO_2[54]. The drought-induced Δ_{malate} values reported here for *P. oleracea* are comparable to previous works detecting malate in the same species[21], and close to the range of acidity detected for other droughted *Portulaca* species (*e.g. P. digyna* and *P. cyclophylla* showed 45.8 and 8.5 µmol H^+ gFW^{-1}, respectively[14]). Overall, when considering a combination of morpho-groups and Δ_{malate} values under drought stress, a small array of combinations was formed, with robust (*sativa* – 102.6 µmol gDW^{-1} and *granulatostellulata* – 60.94 µmol gDW^{-1}) and weedier (*sicula* – 91.15 µmol gDW^{-1} and *papillatostellulata* – 50.13 µmol gDW^{-1}) phenotypes with representatives showing contrasting Δ_{malate} values.

Facultative CAM may provide adaptive advantages other than carbon gain, even for weak cyclers[80]. In this context, the drought-resilient phenotypes of *P. oleracea* reported here, confirmed by the maintenance of photosystem operation throughout prolonged drought (Supplementary Figure S2-S4), and its full and rapid recovery of C_4 upon rewatering (Fig. 3D), may be supported by the persistence of daytime CO_2 assimilation behind closed stomata from the decarboxylation of malate accumulated overnight[80,81]. Also, without undermining the contribution of other traits (e.g., abundant seed production, resistance to abiotic

stresses)[82], the growth rates offered by C_4 photosynthesis when water is available, combined with drought resilience facilitated by CAM expression under drought, can contribute to the weediness of *P. oleracea*. Other morpho-physiological traits as differences in water-capture strategies, cuticle thickness, epicuticular wax, stomatal density, stomatal responsiveness and root architecture, which remains to be determined for the subspecies, may be behind the remarkable drought resilience observed across the *P. oleracea* complex. Moreover, the high antioxidant capacity typically found in *P. oleracea* leaves[24,25], may also be particularly important to maintain photosystem operation and avoid oxidative damage during severe drought spans.

In conclusion, drought was shown to simultaneously down-regulate C_4 and promote CAM in all *P. oleracea* genotypes. The mode of CAM expression (i.e., weak, facultative CAM, CAM-cycling), and the C_4/CAM-marker gene expression profiles were conserved across the genotypes, further emphasizing the occurrence of inducible CAM as a common trait shared by all members of the *Portulaca* genus. As facultative C_4/CAM photosynthesis is found across *P. oleracea* complex, future studies on the tissue organization and molecular regulatory requirements for the occurrence of concomitant C_4/CAM photosynthesis could be performed in genotypes with significant morphological differences. Such studies may provide critical insights for future attempts aiming at incorporating C_4/CAM into crop species. Moreover, from the perspective of photosynthetic plasticity, virtually any of the 12 genotypes of *P. oleracea* analyzed here could serve as model systems for further studies on C_4-CAM transition. Therefore, other aspects, including plant morphology, genome size, ploidy level, and amenability to genetic transformation, could be taken into consideration before the selection of a particular *P. oleracea* genotype to become a genetic model for C_4-CAM research.

Materials and Methods

Studied *Portulaca oleracea* subspecies

To investigate the potential differences in CAM plasticity within the *P. oleracea* complex, a collection of twelve purslane accessions from different geographical locations was assembled (Table 1). Although seed size is not trustworthy for subspecies identification, seed ornamentation is so far considered the best-described structural attribute for subdividing of the *P. oleracea* complex[46], allowing cross-referencing with previous studies in this species. Therefore, at least 15 seeds from each genotype were critical point-dried (Balzers CPD 030), coated with gold (Balzers SCD 050 Sputter Coater), and examined in a scanning electron microscope (Sigma VP - Zeiss, Oberkochen, Germany) to confirm the purity of the lots. The status for each subspecies was checked at The Plant List[83] (Table 1). The genotype here referred to as “cultivar” was previously used in transcriptome studies[27] and was included in

this study as a reference for physiological and molecular data. Seeds from each accession were grown under well-watered conditions for at least three generations before the experiments.

Morphometric analysis

Morphometric measurements were performed in at least 25 individuals of each subspecies grown for 8-10 weeks under well-watered conditions. The following parameters were selected based on existing literature[38] and analyzed: plant height (cm), fresh plant weight (g), number of primary and secondary branches, diameter of stem base and apex (cm, measured at approximately 1cm from plant edges and used to calculate stem base/apex ratio), total and mean leaf area (cm^2), leaf length and width (used to calculate leaf format ratio), and succulence (saturated water content[84]).

Plant material and growth conditions for drought experiments

Plants were grown in 300-mL pots containing a 1:1 mixture of commercial substrate (Plantmax HT, Eucatex, São Paulo, Brazil) and expanded vermiculite supplemented with 1 g L^{-1} NPK 10:10:10, 4 g L^{-1} of dolomite limestone ($MgCO_3$ + $CaCO_3$) and 2 g L^{-1} thermophosphate (Yoorin Master, Brazil). Plants were kept in a growth chamber at approximately 600 µmol m^2 s^{-1} incident to the top of the chamber, 12 h photoperiod, air temperature of around 27 °C day / 22 °C night and air humidity of approximately 60 % day / 80 % night. All plants were watered daily to field capacity until the start of the treatments.

For assessing CAM plasticity, one-month-old plants were separated into three experimental groups subjected to different watering regimes: (1) well-watered, (2) droughted, and (3) rewatered. Well-watered plants were continuously irrigated to field capacity throughout the experiment. Water was withheld from droughted and rewatered groups for 10 days, and subsequently, 10 mL water was added per pot whenever soil humidity reached values close to zero, usually every 4 days, for 20 consecutive days. Plants of the rewatered group were irrigated to field capacity for the next 4 days. From the start of the drought treatment, soil volumetric water content (SVWC) was continuously monitored using Decagon soil moisture meter EC-5 (Fig. 2). At the end of each treatment, samples were harvested 1h after the onset of illumination (dawn samples) and 1h before the end of the light period (dusk samples). For all analyses, four biological replicates, each replicate composed of all fully-expanded and non-senescent leaves of at least three plants, were harvested at each sampling time. Samples were frozen, powdered and stored at -80°C until use. Plants from different genotypes were grown side-by-side, and downstream analyses were performed with samples for all genotypes at the same time to avoid introducing unnecessary variation.

Relative water content (RWC)

Fresh weight (FW) was determined in 10 leaf discs (~0.8 cm diameter) immediately after harvesting. Subsequently, the leaf discs were fully-hydrated by incubation in deionized water for 24 h, followed by measuring the turgid weight (TW). Finally, the samples were dried to a constant weight at 65°C and allowed to cool down before determining the dry weight (DW). RWC was calculated using the formula [(FW-DW)/(TW-FW) x 100][85].

Organic acids quantification

For organic acid profiling, approximately 200 mg FW of frozen leaf samples were extracted in 1 ml of 80 % (v/v) ethanol for 15 min at 80 ºC, and the supernatants were recovered by centrifugation (5,000 *g*, 15 min). Pellets were re-extracted three times, and all supernatants were combined and reduced to dryness under vacuum. Aliquots of 1 mL of the supernatant were dried under vacuum and resuspended in 300 µL ultrapure water. Chromatography was carried out on an Agilent Technologies series 1200 coupled with a diode array detector (DAD) on a reverse-phase column (SupelcoGel C610H - 6% Cross Linked HPLC Column 300 mm x 7.8 mm, 9 microns) and with a guard column (SupelcoGel H Guard Column 50 mm x 4.6 mm, 9 microns) at 30 ºC, using 0.1% (v/v) phosphoric acid as mobile phase running isocratically at 0.5 mL min^{-1}. Eluted compounds were detected at 210 nm and quantified through external calibration. Endogenous metabolite concentrations were obtained by comparing the peak areas of the chromatograms against commercial standards.

Continuous gas exchange

Gas exchange was monitored using a 12-channel, custom-built IRGA system (PP Systems), as described previously[86]. The twelve cuvettes were housed in a growth chamber at approximately 600 µmol m^{-2} s^{-1} incident to the top of the chamber, 12 h photoperiod, air temperature of 28 °C day / 18 °C night and air humidity of 60 % day / 80 % night. Gas exchange was monitored using an infra-red gas exchange system based on a CIRAS-DC analyzer (PP Systems, USA), and calculated using SC-DC software (PP Systems, USA). The contribution of soil respiration and soil moisture to the environment in the cuvette was minimized by wrapping multiple-layers of parafilm around the rim of the pot, with a little hole for the stem. CO_2 exchange rates were based on leaf area, measured using ImageJ 1.50i (NIH, Bethesda, MD, USA).

Chlorophyll *a* fluorescence imaging

The maximum quantum efficiency of PSII photochemistry (Fv/Fm), PSII operating efficiency (Fq'/Fm') and non-photochemical quenching (NPQ) were determined through a non-modulated imaging fluorometer (CF Imager, Technologica, UK), as described by Baker

(2008). All measurements were taken between 2 and 5 h after the start of the light period, and values of minimal (Fo) and maximal (Fm) fluorescence were obtained from dark-adapted leaves for 30 min before receiving a saturating light pulse (~6,000 µmol photons m^{-2} s^{-1} for 1s). Measurements were performed in at least two leaves from three different plants for each treatment.

RNA isolation and quantitative RT-PCR (qPCR) analysis

Total RNA was extracted from approx. 80 mg of frozen leaves using the ReliaPrep RNA Tissue Miniprep System (Promega) for fibrous tissues, with careful homogenization steps. RNA samples were quantified using a microvolume spectrophotometer (NanoDrop ND-1000, Thermo Scientific, USA). Purity was assessed by keeping ratios in between the following intervals: $1.8 < A_{260/280} < 2.3$; $1.6 < A_{260/230} < 2.3$. The extracted RNA was treated with DNase (DNase I Amplification Grade, Thermo Fisher Scientific) for 10 min at room temperature. Complementary DNA (cDNA) synthesis was synthesized using SuperScript IV Reverse Transcriptase kit (Thermo Fisher Scientific) and qPCR reactions were performed in a StepOnePlus Real-Time PCR System (Applied Biosystems), using 10 µl mix reaction composed of 5 µl Power SYBR green 2X (Thermo Fisher Scientific), 2 µl cDNA sample and 300 nM of forward and 300 nM of reverse primers. The amplification program consisted of 10 min initial step at 95°C, followed by 40 cycles with 15 s 95°C, 30 s 60°C and 30 s 72°C. In all cases, the melting curve was analyzed to detect unspecific amplification and primer dimerization. The relative transcript abundance was calculated by applying the $2^{-\Delta\Delta CT}$ method (Livak & Schmittgen, 2001). All primer sequences used are listed in Supplementary Table S7.

Climate space data

Using the coordinates from their places of sampling (Table 1), climate information (19 variables) for all 12 subspecies was retrieved from the WorldClim database (http://www.worldclimorg/bioclim)[50] at a spatial scale of 10 min of a degree, using the raster package[87] in R 3.6.1[88].

Statistical Analysis

All statistical analyses were performed using R (version 3.6.1[88]) via RStudio (version 1.2.1335). The data were checked for normality using the Shapiro-Wilk test, and for homogeneity of variances using the Levene test. When appropriate, two means were compared using: two-sample t-test (normal, homoscedastic), Welch's t-test (normal, heteroscedastic), Mann-Whitney test (non-normal, homoscedastic) or transformed by square root or log and fitted into any of the other descriptions (non-normal, heteroscedastic). For

comparison between three or more means, we used: ANOVA and post-hoc Tukey test (normal, homoscedastic), Welch ANOVA + Games-Howell post-hoc test (standard, heteroscedastic); Kruskal-Wallis + Mann-Whitney U-paired post-hoc test without adjusted p-value (non-normal, homoscedastic) or transformed by square root or log and fitted into any of the other descriptions (non-normal, heteroscedastic).

Morphometric and climate data were normalized using z-scale and analyzed by principal component analysis (PCA) using the pre-installed R function prcomp() (visualized using factoextra package[89]). Hierarchical clustering analysis was done using the pvclust package (version 2.0-0[90]) with Euclidean distance and the Ward's method criterion. For each dendrogram, AU (Approximately Unbiased) and BP (Bootstrap Probability) values were computed using 1000 bootstraps – see pvclust manual (Available at: https://cran.r-project.org/web/packages/pvclust/pvclust.pdf). The AU value is an unbiase p-value, more accurate than BP.

Acknowledgment

We kindly thank Dr. Johannes Walter (Natural History Museum Vienna, Austria), Dr. Avinoam Danin (The Hebrew University of Jerusalem, Israel), Dr. Jose Geraldo de Aquino Assis and MSc. Thaíla Vieira A. Santos (Universidade Federal da Bahia, Brazil) for donating seeds of *P. oleracea* subspecies.

Funding

This work was supported by the São Paulo Research Foundation, Brasil (FAPESP – grant no. 2016/04755-4), by the Royal Society, UK (Newton Advanced Fellowship – grant no. NA140007), and by the Coordenação de Aperfeiçoamento de Pessoal de Nível Superior, Brasil (CAPES – Finance Code 001).

Author Contribution

LF and JH conceived the project and supervised the experiments; RCF conducted most of the experiments; BCC, ECF and SFB conducted part of the experiments; VDG performed the statistical analysis; RCF, LF and JH wrote the article with contributions from other authors.

References

1. Winter, K. & Smith, J. A. C. An introduction to crassulacean acid metabolism. Biochemical principles and ecological diversity. in *Crassulacean Acid Metabolism Biochemistry, Ecophysiology and Evolution* (eds. Winter, K. & Smith, J. A. C.) 1–10 (Springer-Verlag, 1996).
2. Kanai, R., Edwards, G. E. & Introduction, I. *The biochemistry of photosynthesis*. *C_4 Plant Biology* (Woodhead Publishing Limited, 1999). doi:10.1016/B978-012614440-6/50004-5.

3. Bauwe, H., Hagemann, M. & Fernie, A. R. Photorespiration: players, partners and origin. *Trends in Plant Science*, **15**, 330–336 (2010).
4. Sage, R. F. Are crassulacean acid metabolism and C_4 photosynthesis incompatible? *Funct. Plant Biol.* **29**, 775–785 (2002).
5. Hatch, M. D. C_4 photosynthesis: a unique blend of modified biochemistry, anatomy and ultrastructure. *Bioehimica Biophys. Acta* **895**, 81–106 (1987).
6. Osmond, C. Crassulacean acid metabolism: a curiosity in context. *Ann. Rev. Plant Physio* **29**, 379–414 (1978).
7. Winter, K. Ecophysiology of constitutive and facultative CAM photosynthesis. *J. Exp. Bot.* **70**, 6495–6508 (2019).
8. Nobel, P. S. Gas exchange. in *Environmental biology of agaves and cacti* 43–66 (University Press, 1988).
9. Irwin P., T. Crassulacean acid metabolism. *Curr. Biol.* **36**, 595–622 (1985).
10. Koch, K. & Kennedy, R. A. Characteristics of crassulacean acid metabolism in the succulent C_4 dicot, *Portulaca oleracea* L. *Plant Physiol.* **65**, 193–197 (1980).
11. Koch, K. E. & Kennedy, R. A. Crassulacean acid metabolism in the succulent C_4 dicot, *Portulaca oleracea* L. Under Natural Environmental Conditions. *Plant Physiol.* **69**, 757–761 (1982).
12. Ku, S. B., Shieh, Y. J., Reger, B. J. & Black, C. C. Photosynthetic characteristics of *Portulaca grandiflora*, a succulent C_4 dicot. *Plant Physiol.* **68**, 1073–1080 (1981).
13. Guralnick, L. J. & Jackson, M. D. The occurrence and phylogenetics of crassulacean acid metabolism in the Portulacaceae. *Int. J. Plant Sci.* **162**, 257–262 (2001).
14. Holtum, J. A. M., Hancock, L. P., Edwards, E. J. & Winter, K. Optional use of CAM photosynthesis in two C_4 species, *Portulaca cyclophylla* and *Portulaca digyna*. *J. Plant Physiol.* **214**, 91–96 (2017).
15. Winter, K. & Holtum, J. A. M. Facultative crassulacean acid metabolism (CAM) in four small C 3 and C 4 leaf-succulents. *Aust. J. Bot.* **65**, 103–108 (2017).
16. Winter, K., Sage, R. F., Edwards, E. J., Virgo, A. & Holtum, J. A. M. Facultative crassulacean acid metabolism in a C_3–C_4 intermediate. *J. Exp. Bot.* **70**, 6571–6579 (2019).
17. Voznesenskaya, E. V., Koteyeva, N. K., Edwards, G. E. & Ocampo, G. Revealing diversity in structural and biochemical forms of C_4 photosynthesis and a C_3–C_4 intermediate in genus *Portulaca* L. (Portulacaceae). *J. Exp. Bot.* **61**, 3647–3662 (2010).
18. Voznesenskaya, E. V., Koteyeva, N. K., Edwards, G. E. & Ocampo, G. Unique photosynthetic phenotypes in *Portulaca* (Portulacaceae): C_3-C_4 intermediates and NAD-ME C_4 species with Pilosoid-type Kranz anatomy. *J. Exp. Bot.* **68**, 225–239 (2017).
19. Mazen, A. M. A. Changes in levels of phosphoenolpyruvate carboxylase with induction of crassulacean acid metabolism (CAM)-like behavior in the C_4 plant Portulaca oleracea. *Physiol. Plant.* **98**, 111–116 (1996).
20. Mazen, A. M. A. Changes in properties of phosphoenolpyruvate carboxylase with induction of crassulacean acid metabolism (CAM) in the C_4 plant *Portulaca oleracea*. *Photosynthetica* vol. 38 385–391 (2000).
21. Lara, M. V., Disante, K. B., Podestá, F. E., Andreo, C. S. & Drincovich, M. F. Induction of a crassulacean acid like metabolism in the C_4 succulent plant, *Portulaca oleracea* L.: physiological and morphological changes are accompanied by specific modifications in phosphoenolpyruvate carboxylase. *Photosynth. Res.* **77**, 241–254 (2003).
22. Lara, M. V., Drincovich, M. F. & Andreo, C. S. Induction of a crassulacean acid-like metabolism in the C4 succulent plant, *Portulaca oleracea* L.: study of enzymes involved in carbon fixation and carbohydrate metabolism. *Plant Cell Physiol.* **45**, 618–626 (2004).
23. Christin, P. A. *et al.* Shared origins of a key enzyme during the evolution of C_4 and CAM metabolism. *J. Exp. Bot.* **65**, 3609–3621 (2014).

24. D'Andrea, R. M., Andreo, C. S. & Lara, M. V. Deciphering the mechanisms involved in *Portulaca oleracea* (C_4) response to drought: metabolic changes including crassulacean acid-like metabolism induction and reversal upon rewatering. *Physiol. Plant.* **152**, 414–430 (2014).
25. Jin, R. *et al.* Physiological changes of purslane (*Portulaca oleracea* L.) after progressive drought stress and rehydration. *Sci. Hortic. (Amsterdam).* **194**, 215–221 (2015).
26. Ferrari, R. C. & Freschi, L. C_4/CAM as a means to improve plant sustainable productivity under abiotic-stressed conditions: regulatory mechanisms and biotechnological implications in *Plant Signaling Molecules* (eds. Khan, M. I. R., Reddy, P. S., Ferrante, A. & Khan, N. A.) 517–532 (Elsevier Inc., 2019). doi:10.1016/B978-0-12-816451-8.00032-0.
27. Ferrari, R. C. *et al.* C_4 and crassulacean acid metabolism within a single leaf: deciphering key components behind a rare photosynthetic adaptation. *New Phytol.* **225**, 1699–1714 (2020).
28. Kovermann, P. *et al.* The Arabidopsis vacuolar malate channel is a member of the ALMT family. *Plant J.* **52**, 1169–1180 (2007).
29. Borland, A. M., Griffiths, H., Hartwell, J. & Smith, J. A. C. Exploiting the potential of plants with crassulacean acid metabolism for bioenergy production on marginal lands. *J. Exp. Bot.* **60**, 2879–2896 (2009).
30. Palmieri, L. *et al.* Molecular identification of three *Arabidopsis thaliana* mitochondrial dicarboxylate carrier isoforms: organ distribution, bacterial expression, reconstitution into liposomes and functional characterization. *Biochem. J.* **410**, 621–629 (2008).
31. Singh, K. P. Thermoresponse in *Portulaca*. *Curr. Sci.* **17**, 506–507 (1968).
32. Singh, K. P. Effect of different photoperiods on growth and flowering in *Portulaca oleracea* L. *Curr. Sci.* **41**, 573–574 (1972).
33. Matthews, J. F., Ketron, D. W. & Zane, S. F. The biology and taxonomy of the *Portulaca oleracea* L. (Portulacaceae) complex in North America. *Rhodora* **95**, 166–183 (1993).
34. Rahdari, P. & Hoseini, S. M. Effect of different levels of drought stress (peg 6000 concentrations) on seed germination and inorganic elements content in purslane (*Portulaca oleraceae* L.) Leaves. *J. Stress Physiol. Biochem.* **8**, 51–61 (2012).
35. Singh, J. & Singh, K. Contibution to the ecology of ten noxious weeds. *J. Indian Bot. Soc.* **46**, 440–451 (1967).
36. Hernandes-Lopes, J., Oliveira-Neto, M. A. & Melo-de-Pinna, G. F. A. Different ways to build succulent leaves in Portulacineae (Caryophyllales). *Int. J. Plant Sci.* **177**, 198–208 (2016).
37. Walter, J., Vekslyarska, T. & Dobeš, C. Flow cytometric, chromosomal and morphometric analyses challenge current taxonomic concepts in the *Portulaca oleracea* complex (Portulacaeae, Caryophyllales). *Bot. J. Linn. Soc.* **179**, 144–156 (2015).
38. Gorske, S. F., Rhodes, A. M. & Hopen, H. J. A numerical taxonomic study of *Portulaca oleracea*. *Weed Sci.* **27**, 96–102 (1979).
39. Danin, A. & Bagella, S. A new cultivar microspecies of the *Portulaca oleracea* aggregate from the E Mediterranean. *Willdenowia* **42**, 63–65 (2012).
40. Egea-Gilabert, C., Ruiz-Hernández, M. V., Parra, M. Á. & Fernández, J. A. Characterization of purslane (*Portulaca oleracea* L.) accessions: suitability as ready-to-eat product. *Sci. Hortic. (Amsterdam).* **172**, 73–81 (2014).
41. El-Bakatoushi, R. Intra-specific genetic differentiation shaping three *Portulaca oleracea* L. micro-species. *Pakistan J. Bot.* **47**, 2309–2320 (2015).
42. Salah, K. B. H. & Chemli, R. Variabilité phénotypique de quelques populations de Pourpier (*Portulaca oleracea* L.) en Tunisie. *Acta Bot. Gall.* **151**, 111–119 (2004).
43. Danin, A., Baker, I. & Baker, H. G. Cytogeography and taxonomy of the *Portulaca oleracea* L. polyploid complex. *Israel Journal of Botany* vol. 27 177–211 (1978).

44. Ocampo, G. & Columbus, J. T. Molecular phylogenetics, historical biogeography, and chromosome number evolution of *Portulaca* (Portulacaceae). *Mol. Phylogenet. Evol.* **63**, 97–112 (2012).
45. Danin, A., Domina, G. & Raimondo, F. M. Microspecies of the *Portulaca oleracea* aggregate found on major Mediterranean islands (Sicily, Cyprus, Crete, Rhodes). *Flora Mediterr.* **18**, 89–107 (2008).
46. Danin, A. & Raus, T. A key to 19 microspecies of the *Portulaca oleracea* aggregate. in *Caryophyllales: New insights into phylogeny, systematics, and morphological evolution of the order, Proceedings of the Symposium held on 24th–27th* (Timonin, A.K. ed.) 70–83 (Lomonosov State University, 2012).
47. Danin, A., Buldrini, F., Mazzanti, M. B. & Bosi, G. The history of the *Portulaca oleracea* aggregate in the Emilia-Romagna Po Plain (Italy) from the Roman Age to the present. *Plant Biosyst.* **148**, 622–634 (2014).
48. Ocampo, G. *et al.* Evolution of leaf anatomy and photosynthetic pathways in Portulacaceae. *Am. J. Bot.* **100**, 2388–2402 (2013).
49. Yang, X. *et al.* A roadmap for research on crassulacean acid metabolism (CAM) to enhance sustainable food and bioenergy production in a hotter, drier world. *New Phytol.* **207**, 491–504 (2015).
50. Fick, S. E. & Hijmans, R. J. WorldClim 2: new 1-km spatial resolution climate surfaces for global land areas. *Int. J. Climatol.* **37**, 4302–4315 (2017).
51. Dodd, A. N., Borland, A. M., Haslam, R. P., Griffiths, H. & Maxwell, K. Crassulacean acid metabolism: plastic, fantastic. **53**, 569–580 (2002).
52. Lüttge, U. Photosynthetic flexibility and ecophysiological plasticity: questions and lessons from *Clusia*, the only CAM tree, in the neotropics. *New Phytol.* **171**, 7–25 (2006).
53. Heyduk, K., Moreno-Villena, J. J., Gilman, I. S., Christin, P. & Edwards, E. J. The genetics of convergent evolution: insights from plant photosynthesis. *Nat. Rev. Genet.* **20**, 485–493 (2019).
54. Winter, K. & Holtum, J. A. M. Facultative crassulacean acid metabolism (CAM) plants: powerful tools for unravelling the functional elements of CAM photosynthesis. *J. Exp. Bot.* **65**, 3425–3441 (2014).
55. Winter, K., Holtum, J. A. M. & Smith, J. A. C. Crassulacean acid metabolism: a continuous or discrete trait? *New Phytol.* **208**, 73–78 (2015).
56. Winter, K., Garcia, M. & Holtum, J. A. M. On the nature of facultative and constitutive CAM: Environmental and developmental control of CAM expression during early growth of *Clusia*, *Kalanchoë*, and *Opuntia*. in *Journal of Experimental Botany* vol. 59 1829–1840 (2008).
57. Silvera, K. *et al.* Evolution along the crassulacean acid metabolism continuum. *Functional Plant Biology* vol. 37 995–1010 (2010).
58. Hancock, L. & Edwards, E. J. Phylogeny and the inference of evolutionary trajectories. *J. Exp. Bot.* **65**, 3491–3498 (2014).
59. Edwards, E. J. Evolutionary trajectories, accessibility and other metaphors: the case of C_4 and CAM photosynthesis. *New Phytol.* **223**, 1742–1755 (2019).
60. Edwards, E. J. & Ogburn, M. R. Angiosperm responses to a Low-CO_2 World: CAM and C4 photosynthesis as parallel evolutionary trajectories. **173**, 724–733 (2012).
61. Silvera, K., Santiago, L. S., Cushman, J. C. & Winter, K. Crassulacean acid metabolism and epiphytism linked to adaptive radiations in the Orchidaceae. *Plant Physiol.* **149**, 1838–1847 (2009).
62. Bone, R. E., Smith, J. A. C., Arrigo, N. & Buerki, S. A macro-ecological perspective on crassulacean acid metabolism (CAM) photosynthesis evolution in Afro-Madagascan drylands: *Eulophiinae* orchids as a case study. *New Phytol.* **208**, 469–481 (2015).
63. Silvera, K., Winter, K., Rodriguez, B. L., Albion, R. L. & Cushman, J. C. Multiple isoforms of phospho*enol*pyruvate carboxylase in the Orchidaceae (subtribe *Oncidiinae*): implications for the evolution of crassulacean acid metabolism. **65**,

3623–3636 (2014).
64. Harris, F. S. & Martin, C. E. Plasticity in the degree of CAM-cycling and its relationship to drought stress in five species of *Talinum* (Portulacaceae). *Oecologia* 575–584 (1991).
65. Heyduk, K., Burrell, N., Lalani, F. & Leebens-Mack, J. Gas exchange and leaf anatomy of a C_3-CAM hybrid, *Yucca gloriosa* (Asparagaceae). *J. Exp. Bot.* **67**, 1369–1379 (2016).
66. Karolina, H., Ray, J. N. & Leebens-Mack, J. Leaf anatomy is not correlated to CAM function in a C_3+CAM hybrid species, *Yucca gloriosa. bioRxiv* (2019) doi:10.1101/726737.
67. Herrera, A. Are thick leaves, large mesophyll cells and small intercellular air spaces requisites for CAM? *Ann. Bot.* **125**, 859–868 (2020).
68. Ricceri, C. & Arrigoni, P. V. L'aggregato Di *Portulaca Oleracea* L. (Portulacaceae) In Italia. *Parlatorea* **4**, 91–97 (2000).
69. Domina, G. & Raimondo, F. M. A new species in the *Portulaca oleracea* aggregate (Portulacaceae) from the Island of Soqotra (Yemen). *Webbia* **64**, 9–12 (2009).
70. Danin, A. & Reyes Betancort, J. The status of *Portulaca oleracea* in Tenerife, the Canary Islands. *Lagascalia* **26**, 71–81 (2006).
71. El-Bakatoushi, R., Alframawy, A. M., Samer, M., El-Sadek, L. & Botros, W. Evolution of the *Portulaca oleracea* L. aggregate in Egypt on molecular and phenotypic levels revealed by morphology, inter-simple sequence repeat (ISSR) and 18S rDNA gene sequence markers. *Flora Morphol. Distrib. Funct. Ecol. Plants* **208**, 464–477 (2013).
72. Brilhaus, D., Bräutigam, A., Mettler-Altmann, T., Winter, K. & Weber, A. P. M. Reversible burst of transcriptional changes during induction of crassulacean acid metabolism in *Talinum triangulare*. *Plant Physiol.* **170**, 102–122 (2016).
73. Abraham, P. E. *et al.* Transcript, protein and metabolite temporal dynamics in the CAM plant *Agave*. *Nat. Plants* **2**, 1–10 (2016).
74. Yang, X. *et al.* The *Kalanchoë* genome provides insights into convergent evolution and building blocks of crassulacean acid metabolism. *Nat. Commun.* **8**, (2017).
75. Maleckova, E., Brilhaus, D., Wrobel, T. J. & Weber, A. P. M. Transcript and metabolite changes during the early phase of ABA-mediated induction of CAM in *Talinum triangulare*. *J. Exp. Bot.* **70**, 6581–6596 (2019).
76. Wai, C. M. *et al.* Temporal and spatial transcriptomic and microRNA dynamics of CAM photosynthesis in pineapple. 0–3 doi:10.1111/tpj.13630.
77. Boxall, S. F. *et al.* Kalanchoë PPC1 is essential for crassulacean acid metabolism and the regulation of core circadian clock and guard cell signaling genes. *Plant Cell* **32**, 1136–1160 (2020).
78. Borland, A. M. *et al.* Engineering crassulacean acid metabolism to improve water-use efficiency. *Trends in Plant Science* vol. 19 327–338 (2014).
79. Hartwell, J., Dever, L. V & Boxall, S. F. Emerging model systems for functional genomics analysis of crassulacean acid metabolism. *Curr. Opin. Plant Biol.* **31**, 100–108 (2016).
80. Herrera, A. Crassulacean acid metabolism and fitness under water deficit stress: If not for carbon gain, what is facultative CAM good for? *Annals of Botany* vol. 103 645–653 (2009).
81. Adams, W. W. & Osmond, C. B. Internal CO_2 supply during photosynthesis of sun and shade grown cam plants in relation to photoinhibition. *Plant Physiol.* **86**, 117–123 (1988).
82. Zimmerman, C. A. Growth characteristics of weediness in *Portulaca Oleracea* L. *Ecology* **57**, 964–974 (1976).
83. The Plant List. The Plant List - a working list of all plant species. *Version 1.1* http://www.theplantlist.org/ (2013).
84. Ogburn, R. M. & Edwards, E. J. Quantifying succulence: A rapid, physiologically meaningful metric of plant water storage. *Plant, Cell Environ.* **35**, 1533–1542 (2012).

85. Barss, H. D. & Weatherley, P. E. A re-examination of the relative turgidity technique for estimating water deficits in leaves. *Aust. J. Bot.* 413–428 (1962).
86. Dever, L. V, Boxall, S. F., Kneřová, J. & Hartwell, J. Transgenic perturbation of the decarboxylation phase of crassulacean acid metabolism alters physiology and metabolism but has only a small effect on growth. *Plant Physiol.* **167**, 44–59 (2015).
87. Hijmans, R. J. & van Etten, J. raster: Geographic analysis and modeling with raster data. R package version 1.4. (2012).
88. R Core Team. R: A language and environment for statistical computing. (2019) doi:URL https://www.R-project.org/.
89. Kassambara, A. & Mundt, F. factoextra: Extract and Visualize the Results of Multivariate Data Analyses. R package version 1.0.3. (2017).
90. Suzuki, R. & Shimodaira, H. Pvclust: an R package for assessing the uncertainty in hierarchical clustering. *Bioinformatics* **22,** 1540–1542 (2006).

Supporting information

(Supplementary tables can be found at https://www.nature.com/articles/s41598-020-71012-y*)*

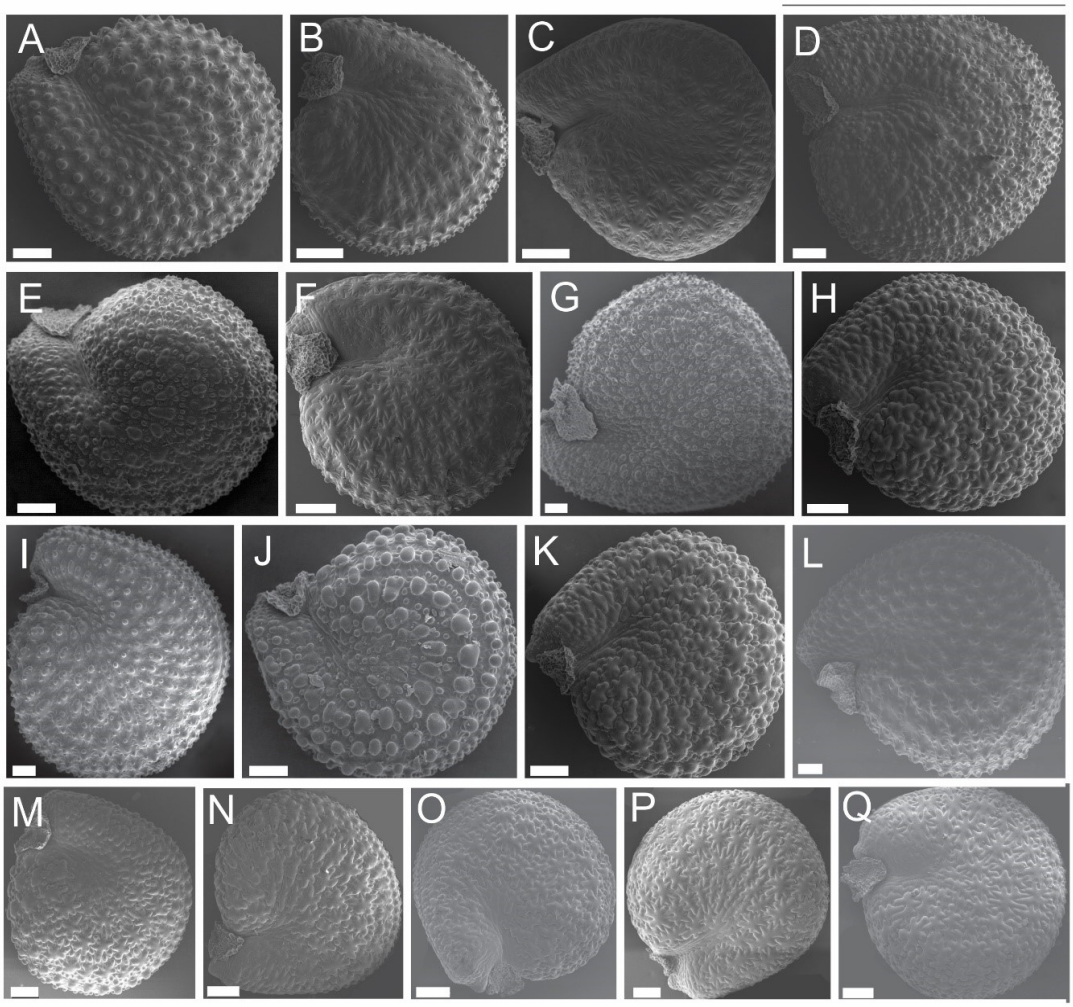

Figure S1. Seed coat ornamentation of *P. oleracea* subspecies studied under scanning electron microscopy (SEM). At least fifteen seeds of each genotype were randomly analyzed. (A) subsp. *trituberculata*. (B) subsp. *sicula*. (C) subsp. *oleracea*. (D) subsp. *rausii*. (E) subsp. *zaffranii*. (F) subsp. *nitida*. (G) subsp. *edulis.* (H) subsp. *papillatostellulata*. (I) subsp. *sativa*. (J) subsp. *tuberculata*. (K) subsp. *granulatostellulata*. (L) commercial *cultivar*. (M-N) Brazilian accessions identified as subsp. *granulatostellulata*. (O-Q) Brazilian accessions identified as subsp. *nitida* . Scale bars = 100 μm.

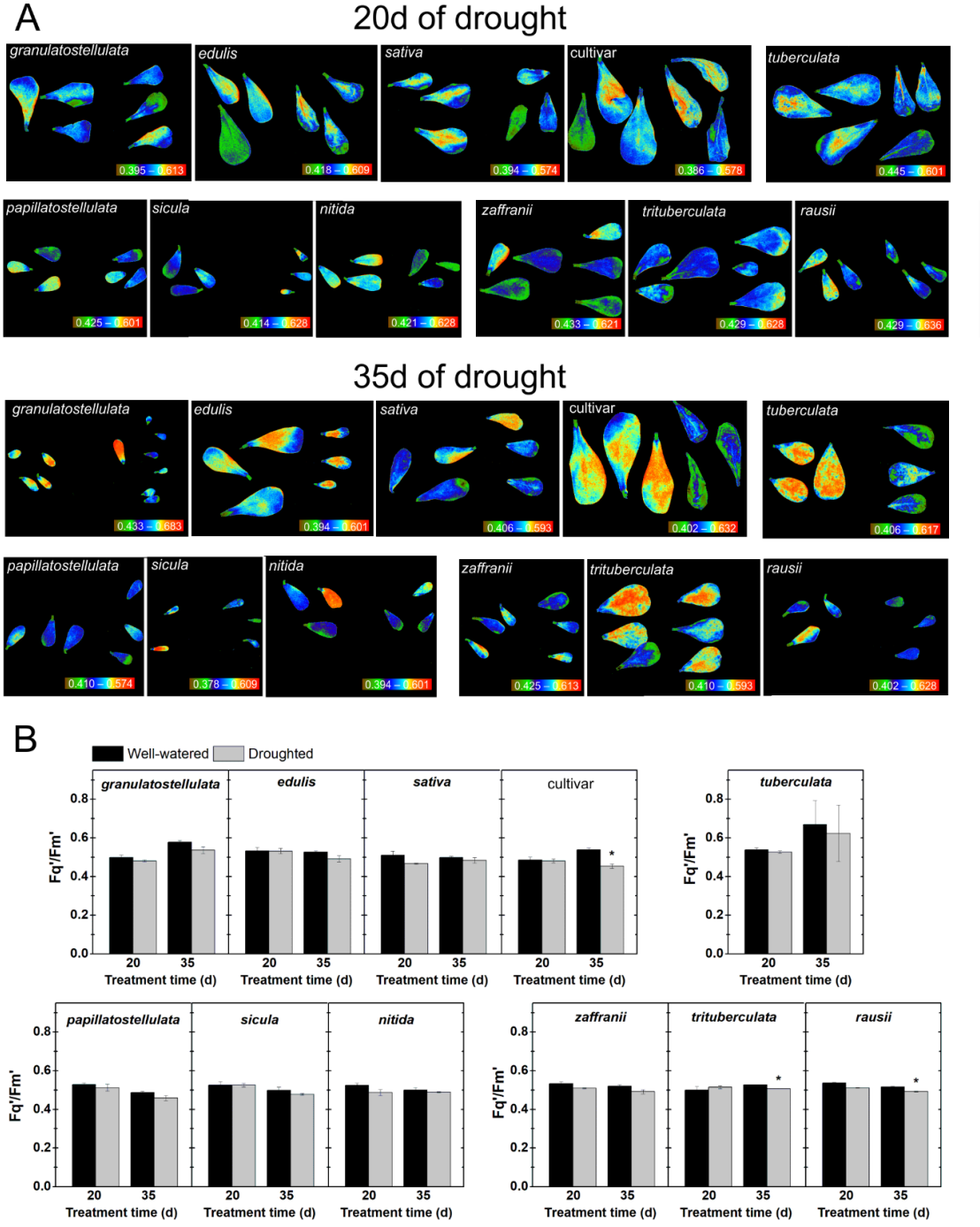

Figure S2. Impacts of drought on PSII operating efficiency (Fq'/Fm') of *P. oleracea* subspecies. One-month-old plants were either kept under well-watered conditions (left) or prolonged, continuous drought (right) for 20 and 34 days. (A) Representative images. (B) Mean Fq'/Fm' values from at least two leaves from three plants. Bars indicate SE and asterisks indicate statistical differences ($p < 0.05$) between treatments for each subspecies.

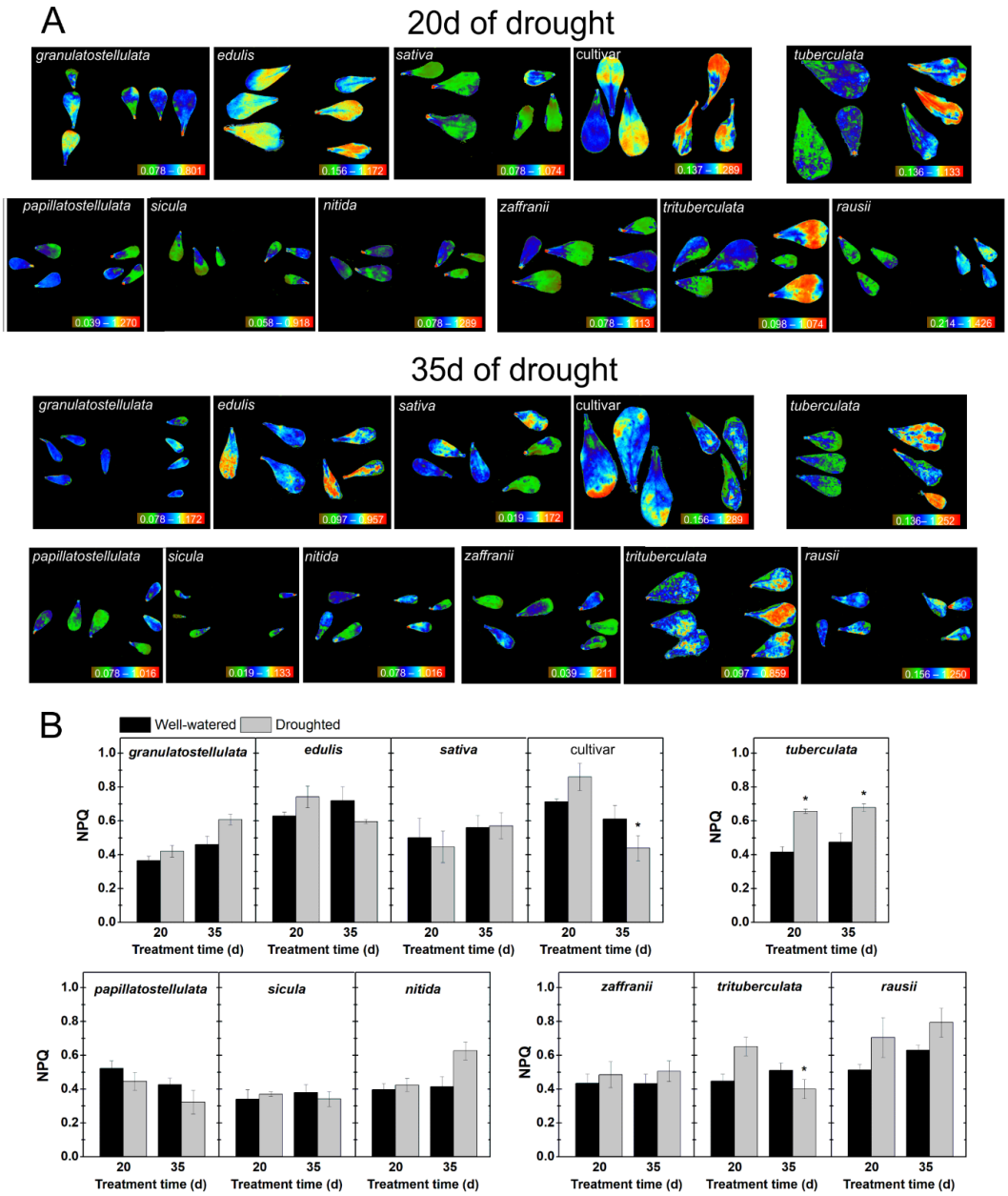

Figure S3. Impacts of drought on non-photochemical quenching (NPQ) in *P. oleracea* subspecies. One-month-old plants were either kept under well-watered conditions (left) or prolonged, continuous drought (right) for 20 and 34 days. (A) Representative images. (B) Mean NPQ values from at least two leaves from three plants. Bars indicate SE and asterisks indicate statistical differences ($p < 0.05$) between treatments for each subspecies.

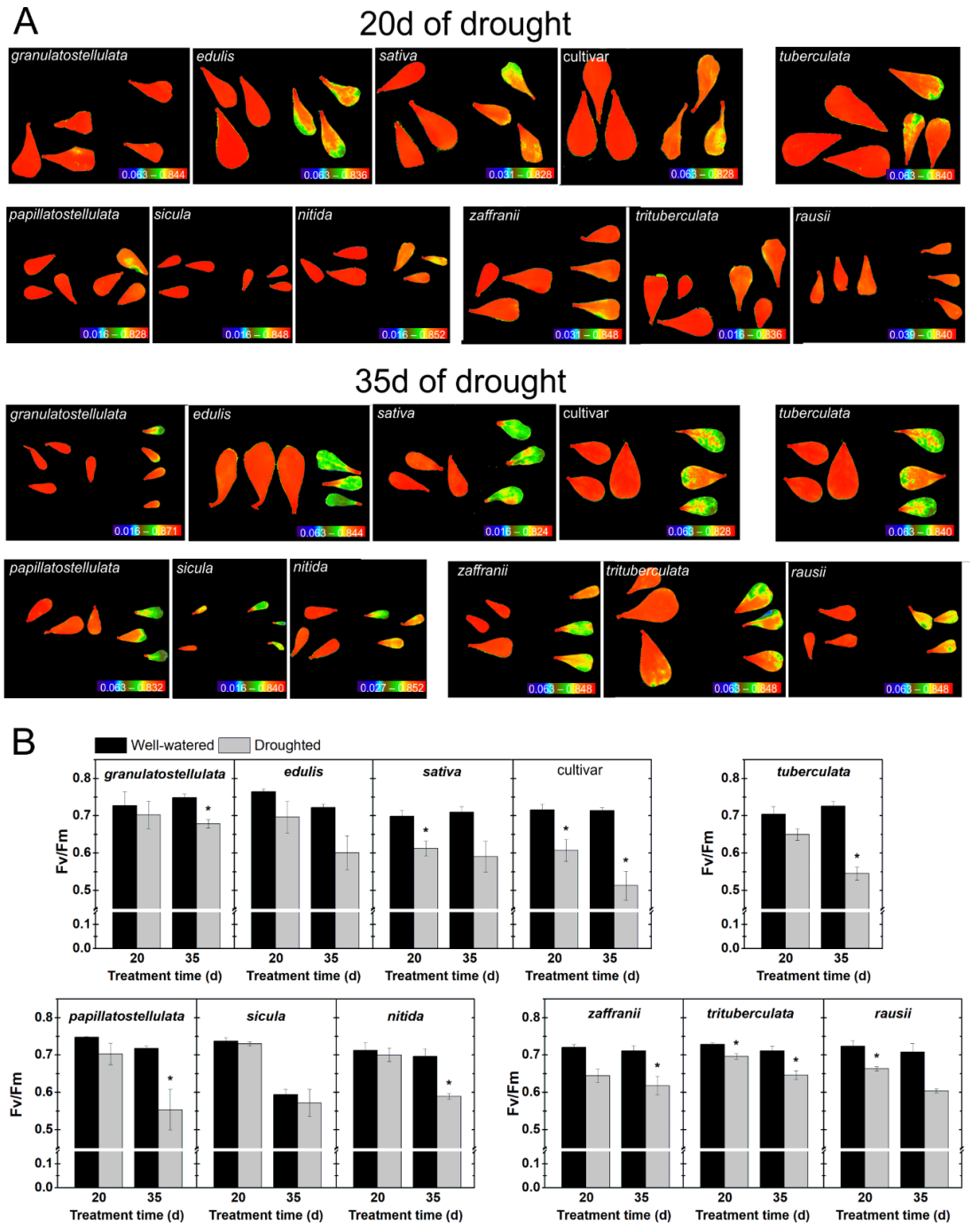

Figure S4. Impacts of drought on maximum quantum efficiency of PSII photochemistry (Fv/Fm) in *P. oleracea* subspecies. One-month-old plants were either kept under well-watered conditions (left) or prolonged, continuous drought (right) for 20 and 34 days. (A) Representative images. (B) Mean NPQ values from at least two leaves from three plants. Bars indicate SE and asterisks indicate statistical differences ($p < 0.05$) between treatments for each subspecies.

Chapter IV

Developing *Portulaca oleracea* as a model species for functional genomics analysis of C_4/CAM photosynthesis

"The force that through the green fuse drives the flower
Drives my green age; that blasts the roots of trees
Is my destroyer.
And I am dumb to tell the crooked rose
My youth is bent by the same wintry fever."
Dylan Thomas

This chapter is organized as published in the journal Functional Plant Biology:

Ferrari, R. C; Bittencourt, P.P.; Nagumo, P.Y.; Oliveira, W.S.; Rodrigues, M.A.; Hartwell, J.; Freschi, L. Developing *Portulaca oleracea* as a model system for functional genomics analysis of C_4/CAM photosynthesis. Functional PlantBiology, 48, 666-682, 2020. Doi: 10.1071/FP20202.

Supplementary information is available for this paper at
https://www.publish.csiro.au/fp/FP20202.

Summary

Formerly regarded as a photosynthetic curiosity, the occurrence of C_4 and Crassulacean acid metabolism (CAM) photosynthesis within a single organism has recently emerged as a source of information for future biotechnological use. Among C_4/CAM facultative species, *Portulaca oleracea* L. has been used as a model for biochemical and gene expression analysis of C_4/CAM under field and laboratory conditions. In the present work, we focussed on developing molecular tools to facilitate functional genomics studies in this species, from the optimisation of RNA isolation protocols to a method for stable genetic transformation. Eleven variations of RNA extraction procedures were tested and compared for RNA quantity and quality. Also, 7 sample sets comprising total RNA from hormonal and abiotic stress treatments, distinct plant organs, leaf developmental stages, and subspecies were used to select, among 12 reference genes, the most stable reference genes for RT-qPCR analysis of each experimental condition. Furthermore, different explant sources, *Agrobacterium tumefaciens* strains, and regeneration and antibiotic selection media were tested in various combinations to optimise a protocol for stable genetic transformation of *P. oleracea*. Altogether, we provide essential tools for functional gene analysis in the context of C_4/CAM photosynthesis, including an efficient RNA isolation method, preferred reference genes for RT-qPCR normalisation for a range of experimental conditions, and a protocol to produce *P. oleracea* stable transformants using *A. tumefaciens*.

Keywords: *Agrobacterium tumefaciens*, CAM, carbon concentration mechanism, crop biotechnology, Crassulacean acid metabolism, C_4 photosynthesis, *Portulaca oleracea*, purslane, reference gene, stable genetic transformation.

Introduction

C_4 and Crassulacean acid metabolism (CAM) are the two major photosynthetic carbon concentrating mechanisms (CCMs) in plants (Keeley and Rundel 2003). Both of these CCMs represent very efficient adaptations to low CO_2 environments, minimising photorespiratory

rates that would otherwise be high under such conditions (Bauwe *et al*. 2010). C_4 predominantly occurs in warm habitats (>30°C), where it performs higher photosynthetic rates and more efficient water and nitrogen use in comparison to C_3 photosynthesis (Sage *et al*. 1999). CAM-performing plants are distributed mostly in semiarid and arid environments, where the higher water use efficiency (WUE) of CAM, as compared with C_3 plants, bestows a selective advantage (Osmond 1978; Winter and Smith 1996). Both CCMs recruited an overlapping set of enzymes and metabolite transporters during their evolution (Winter and Smith 1996; Kanai and Edwards 1999), but differ in regulation and structural arrangements (Sage 2002). Few land plant species can perform both CCMs within a single leaf, the most representative examples belonging to the genus *Portulaca*, a member of the Portulacaceae in the order Caryophyllales. In this genus, C_4 and C_3-C_4 species can perform weak, facultative CAM under water deprivation (Koch and Kennedy 1980, 1982; Ku *et al*. 1981; Holtum *et al*. 2017; Winter and Holtum 2017; Winter *et al*. 2019). Strong CAM (e.g. Cactaceae and Aizoaceae) and facultative/inducible C_3-CAM species (e.g. Talinaceae) are also found in closely related families within the wider Caryophyllales (Winter 2019).

Changes associated with the establishment of C_4 and the drought-induced transition from C_4 to weak CAM have mostly been studied in *P. oleracea* (Mazen 1996, 2000; Guralnick and Jackson 2001; Lara *et al*. 2003, 2004; Christin *et al*. 2014; Ferrari *et al*. 2020*a*). It exhibits a cosmopolitan distribution, being sometimes even classified into different subspecies (Danin and Raus 2012), and is considered one of the most noxious weeds for agriculture (Singh and Singh 1967; Zimmerman 1976). Commonly known as purslane, *P. oleracea* has a wide range of applications. It is edible and highly nutritious, being consumed in salads and soups, to the extent that it is considered a neglected crop (Hernández-Bermejo and León 1994; Gonnella *et al*. 2010). It has also been used as an herbal medicine by traditional cultures, having known neuropharmacological effects and muscle relaxing properties, among others (Habtemariam *et al*. 1993; Radhakrishnan *et al*. 2001; Rashed *et al*. 2003; Karimi *et al*. 2004; Iranshahy *et al*. 2017).

C_4 and CAM, either isolated or co-occurring within a single leaf, are interesting targets for crop improvement due to their ability to outperform C_3 plants in hotter and drier habitats. In the context of the continued growth of the human population, and climate change leading to an increased frequency of extreme weather events and associated heatwaves, droughts and aridification, research initiatives that seek to genetically improve crop species have arisen as an attempt to meet the future demands for food, fuel and renewable feedstocks for platform chemicals for industry (Borland *et al*. 2009; Furbank *et al*. 2015; Yang *et al*. 2015; von Caemmerer and Furbank 2016). Attempts to engineer the C_4 pathway into C_3 crops have mostly focussed on rice, such as the C_4 Rice Initiative (Kajala *et al*. 2011; Covshoff and Hibberd 2012; von Caemmerer *et al*. 2012; von Caemmerer and Furbank 2016). Additionally,

the proposal has been made to transfer CAM into food and bioenergy crops to improve WUE in these plants (Borland *et al*. 2009; DePaoli *et al*. 2014; Yang *et al*. 2015). However, achieving these goals still requires detailed information about the establishment and regulation of both CCMs in existing C_4 and CAM species.

To this end, the establishment of model systems has been instrumental in expanding our understanding of both C_4 and CAM biology. C_4 genetic models include *Zea mays* (Strable and Scanlon 2009), *Flaveria* (Westhoff and Gowik 2004), and more recently *Setaria* (Brutnell *et al*. 2010). In parallel, constitutive CAM species of *Kalanchoë*, particularly *Kalanchoë fedtschenkoi* Raym.-Hamet & H.Perrier and *Kalanchoë laxiflora* Baker, have emerged as the predominant genetic models for CAM research, although the argument has been made that more diverse CAM species must be developed as models because CAM has evolved many times independently (Hartwell *et al*. 2016). Efficient protocols for stable genetic transformation are available for the abovementioned model systems (e.g. Chitty *et al*. 1994; Aida and Shibata 1996; Dever *et al*. 2015; Martins *et al*. 2015), which have offered an unparalleled opportunity to perform functional genomics analysis of C_4 and CAM photosynthesis (von Caemmerer *et al*. 2004; Furumoto *et al*. 2007; Pengelly *et al*. 2012; Dever *et al*. 2015; Boxall *et al*. 2017, 2020). In contrast, efficient and reproducible genetic transformation protocols for facultative CAM species have been missing, although a recent report indicates advances in *Agrobacterium*-mediated transformation of the C_3-CAM species *Mesembryanthemum crystallinum* L. (Agarie *et al*. 2020).

As a facultative C_4-CAM species, *P. oleracea* is an attractive system for the elucidation of CAM-related processes, components and signalling events because they are induced in a reversible fashion according to the environmental conditions (Winter and Holtum 2014). Moreover, there is an enormous potential to be unlocked through monitoring gene transcript levels in order decipher such a complex photosynthetic CCM (Abraham *et al*. 2016; Brilhaus *et al*. 2016; Heyduk *et al*. 2018; Maleckova *et al*. 2019; Boxall *et al*. 2020; Ferrari *et al*. 2020*a*). In this context, the reverse transcription of total RNA coupled to quantitative polymerase chain reaction (RT-qPCR) is a sensitive and efficient method for transcript quantification. It is the gold standard method for analysis of transcript abundance or validation of next generation sequencing (NGS) studies, and has been widely applied in plant research (Gachon 2004; Osuna *et al.* 2007; Usadel *et al.* 2008). Accurate RT-qPCR results require, among other factors, high-quality RNA samples for cDNA production and the selection of adequate reference genes for the normalisation of the measured transcript levels of the target genes of interest (Gutierrez *et al*. 2008).

Reference genes, also referred to as normalising genes, are essential for successful RT-qPCR relative quantification analysis using the $2^{-\Delta\Delta CT}$ method (Livak and Schmittgen 2001). Traditionally, housekeeping genes were assumed to maintain a stable steady-state transcript

abundance between different tissues and conditions due to their roles in cellular homeostasis. However, the transcript level of some of these genes has been shown to vary more than originally assumed, and the selection of the best reference genes for each studied species and set of experimental conditions is required before using the RT-qPCR technique (Thellin *et al*. 1999; Suzuki *et al*. 2000; Brunner *et al*. 2004; Czechowski *et al*. 2005; Gutierrez *et al*. 2008; Guénin *et al*. 2009). Choosing inappropriate normalizers can lead to inaccurate results, introducing variation and leading to errors of interpretation (Gutierrez *et al*. 2008). For these reasons, research efforts over the years have been dedicated to the optimisation of RNA isolation methods and the selection of reliable reference genes for both crop and non-crop species (Czechowski *et al*. 2005; Meisel *et al*. 2005; Reid *et al*. 2006; Hong *et al*. 2008; Elbl *et al*. 2015; Sun *et al*. 2016). However, suitable reference genes for *Portulaca* species have not yet been reported.

Although *P. oleracea* has been progressively emerging as a model species for facultative C_4-CAM photosynthesis research (Lara *et al*. 2003, 2004; Christin *et al*. 2014; Ferrari and Freschi 2019; Ferrari *et al*. 2020*a*, 2020*b*), the development of molecular tools for functional genomics studies using this species is still at its infancy. Hence, in the present work, we compared multiple RNA isolation procedures for a wide range of *P. oleracea* samples and experimental conditions, and subsequently investigated the best normalizers for RT-qPCR considering multiple variables, i.e. leaf development stage, tissue, diel time of sampling, abiotic stresses and hormonal treatments. Finally, we describe efficient and straightforward protocols for *in vitro* regeneration and *Agrobacterium tumefaciens*-mediated stable genetic transformation using hypocotyl fragments from young *P. oleracea* seedlings as explants. Optimised methods are described to facilitate the production of a high frequency of stable transformants. These include the ideal source of explants, the concentration of growth regulators for whole plant regeneration, and the levels of antibiotic selection in the media. Furthermore, the most effective *A. tumefaciens* strains are identified, and the optimal culture conditions for bacterial growth are provided. Altogether, the research tools provided in this study will facilitate the further adoption of *P. oleracea* as a model system for the functional genomics analysis of C_4/CAM photosynthesis in a single species.

Materials and methods

Plant material and growth conditions

Unless otherwise specified, the experiments were conducted with 30-day-old plants of a commercial cultivar of *Portulaca oleracea* L. Seeds were acquired from Agristar do Brasil Ltd, and both morphological and biochemical characterisation of this accession is provided in Ferrari *et al*. (2020*b*). Seeds were grown in 300-mL pots containing a 1 : 1 mixture of

commercial substrate (Plantmax HT, Eucatex), and expanded vermiculite supplemented with 1 g L^{-1} NPK 10:10:10, 4 g L^{-1} of dolomitic limestone ($MgCO_3$ + $CaCO_3$), and 2 g L^{-1} thermophosphate (Yoorin Master). Since germination, potted plants were kept under the following controlled conditions: 600 µmol m^{-2} s^{-1} of photosynthetically active radiation (PAR), 12 h photoperiod, air temperature of 27°C day/22°C night, air humidity of 60% day/80% night and watered daily with tap water.

RNA isolation protocols

Total RNA was extracted using eleven different procedures, each starting with ~100 mg of frozen powdered leaf or stem tissue of drought-stressed samples. Three procedures were based on the use of TRIzol Reagent from Life Technologies as follows: 'TZ1', according to the manufacturer's instructions; 'TZ2', with a 75% ethanol wash before an overnight incubation at –20°C with 45.5 µL of 8 M LiCl, followed by a subsequent pellet wash with 75% ethanol to concentrate RNA (Chang *et al*. 1993); 'TZ3', using cold TRIzol Reagent at the initial extraction step and incubations performed on ice at the lyse and precipitation stages, according to the manufacturer's instructions for samples with high polysaccharide/fat and RNase content. One protocol used the TRIzol Reagent followed by purification using the PureLink RNA Mini Kit ('PL'), as suggested by the manufacturer's instructions for tissues difficult to lyse. Two protocols used the RNeasy Mini Kit from Qiagen: 'RN1', following the manufacturer's instructions for plant samples; and 'RN2', with the addition of 60 µL of polyethylene glycol (PEG) 20000 to the initial extraction step. Three protocols were based on the Concert Plant RNA Reagent kit: 'CC1', according to the manufacturer's instructions; 'CC2': with the modifications described by Porto *et al*. (2010); and 'CC3': with samples constantly kept on ice and all centrifugation steps at 4°C. Moreover, the Spectrum Plant Total RNA Kit by Sigma-Aldrich was tested according to the manufacturer's instructions ('SP'). Finally, the ReliaPrep RNA Tissue Miniprep System from Promega ('RP') was used according to the manufacturer's instructions for fibrous tissue, with the following modifications: (1) vortexing instead of pipetting up and down at the tissue disruption step; (2) careful and slow transfer of lysates; (3) extra homogenisation by pipetting 10 times up and down after adding isopropanol followed by the removal of condensed brown material, if formed; (4) removal of the incubation with DNase before RNA quantification. In all cases, RNA was re-suspended in a final volume of 20 µL of molecular biology grade distilled water. RNA samples were quantified using a microvolume spectrophotometer (NanoDrop ND-1000, Thermo Scientific), and sufficient purity was confirmed $A_{260/280}$ and $A_{260/230}$ ratios between 1.8 and 2.3, or 1.6 and 2.3 respectively. The intactness of the total RNA was also assessed

using the Agilent 2100 Bioanalyser (Agilent Technologies), where an RNA Integrity Number (RIN) ≥ 7 was taken as the cut-off for highly intact RNA samples.

Candidate reference gene selection, statistical evaluation and RT-qPCR analysis

After an extensive literature search, 12 candidate reference genes that have either been used traditionally or reported more recently for the normalisation of plant RT-qPCR data (e.g. Brunner *et al*. 2004; Czechowski *et al*. 2005; Expósito-Rodríguez *et al*. 2008; Elbl *et al*. 2015; Sun *et al*. 2016; Wang *et al*. 2018), were selected for evaluation. In order to design appropriate oligonucleotide primers for each target gene (Table 1), *Arabidopsis* gene index (AGI) numbers and the nucleotide sequences of these genes were retrieved from TAIR (Berardini *et al*. 2015), and the sequences were used as the query in BLASTN searches against the *P. oleracea* transcriptome (Ferrari *et al.* 2020*a*; data deposited at NCBI - BioProject PRJNA576481), using the BLASTN parameters: e-value = 10^{-6}, -max_hsps = 1 (Camacho *et al*. 2009). Multiple transcripts were recovered from the searches and were aligned using T-Coffee software (Notredame *et al*. 2000). When the T-Coffee alignment score was higher than 500, indicating high sequence accuracy between differently annotated transcripts, the counts for these transcripts were summed. The coefficient of variation (CV) was calculated for these transcripts by dividing the standard deviation by the mean of the triplicates at each sampling time for well-watered and drought-stressed leaves and stems.

Table 1. Primers used for qPCR analysis of the selected reference gene candidates

Gene	Transcriptome ID	TAIR Name	AGI #	Sequence
CLAT	DN98678_c3_g1_i5	*Clathrin adaptor complexes medium subunit family protein*/*Adaptor protein-4 mu-adaptin* (*AP4M*)	AT4G24550	F: 5′-GTAGTTCT GGGTCTGGTG-3′ R: 5′-CGGCTTCTT CAATTAGGG-3′
CYP	DN97016_c4_g1_i11	*Cyclophilin*/*Rotamase* (*CYP7*/*ROC7*)	AT5G58710	F: 5′-ATGGGTGG CGAGTCAATC-3′ R: 5′-CTTCCCTC TGCCTCAATCT-3′
EF1A	DN104399_c1_g2_i2	*GTP binding Elongation factor Tu family protein*	AT5G60390	F: 5′-TGTGCCA TCCTCATCATC-3′ R: 5′-CTTGGGA GTGGTAGCATC-3′
GAPDH	DN84125_c0_g3_i5	*Glyceraldehyde-3-phosphate dehydrogenase of plastid 2* (*GAPCP-2*)	AT1G16300	F: 5′-GAGTCTCAT TTGCTTGTTTGG-3′ R: 5′-TCTCAGAAC CTCCAGCG-3′
HEL	DN102928_c0_g2_i1	*Helicase family protein*	AT1G58060	F: 5′-GGTATTCT TGCGGGACAC-3′ R: 5′-TGGACTCGA CAACTTCAT-3′
MADS	DN82809_c3_g5_i17	*K-box region and MADS-box transcription factor family protein* (*SEP3*)	AT1G24260	F: 5′-TCTCCAGCC GAAGAAGAC-3′ R: 5′-AGCATCAT CCAAACCTCTG-3′
PP2A	DN88901_c3_g1_i2	*Protein phosphatase 2A-2* (*PP2A-2*)	AT1G10430	F: 5′-GACAGGACA TAGCAGCTTCA-3′ R: 5′-AGTGGTGTC

				GGGTTCAATCT-3′
SAND	DN102293_c1_g3_i3	*SAND family protein*	AT2G28390	F: 5′-CCTTGTTTG ACCGAAGCG- 3′ R: 5′-CCACT TCCAGCT CCGAAT-3′
THIO	DN92699_c1_g3_i3	*Thioesterase/thiol ester dehydrase-isomerase superfamily protein*	AT5G48370	F: 5′-TATGGACCC TCCTCTGGATG- 3′ R: 5′-CAGTGACAA GCAGCAATGGT-3′
TIP	DN93311_c1_g4_i3	*TIP41-like family protein* (*TIP4*)	AT4G34270	F: 5′-AGTTGACGG CGTGCTTATG-3′ R: 5′-TCTGGCTGA TGACACTCG-3′
UBC10	DN95462_c3_g1_i4	*Ubiquitin-conjugating enzyme 10* (*UBC10*)	AT5G53300	F: 5′-GCTAACAGA CCCGAACCC-3′ R: 5′-CAGTCCTTG CTAGTCCTGG-3′
UBQ	DN104861_c1_g2_i2	*Ubiquitin-protein ligase 7* (*UPL7*)	AT3G53090	F: 5′-GATGGAAGTC GGACAGTGA-3′ R: 5′-TGAAGCTGA GGGAAGTCG-3′

For reference gene testing and selection, the following sample sets were established using four biological replicates: (1) a leaf development series, including 7-day-old cotyledons, and source leaves from 20-, 30-, 42-, 54-, 58- and 62-day-old plants; (2) diel time of sampling, comprising leaf samples from plants harvested every 6 h over a 24-h cycle, starting one hour after light onset; (3) a tissue series, including leaf, stem, and root samples; (4) a drought stress series, comprising well-watered and drought-stressed leaves at 10, 22, and 34 days after water withholding started, as well as plants rewatered for 4 days after the 34-day drought treatment; (5) a salt-stressed group, harvested after one week of incubation in 100 mM NaCl; (6) a hormonal series, with cotyledons and hypocotyls of one-week-old *in vitro*-grown seedlings treated for another week with 50 µM of auxin (indole-3-acetic acid, IAA), abscisic acid (ABA), cytokinin (zeatin), gibberellic acid (GA_3) or 1-aminocyclopropane-1-carboxylic acid (ACC, the ethylene precursor); and (7) a group of three different *P. oleracea* subspecies: subsp. *sicula*, subsp. *rausii* and subsp. *nitida*. The origins of the subspecies seeds are described in Ferrari *et al*. (2020*b*) and the *in vitro* growth conditions for the hormonal treatments were as described in the plant micropropagation section below. After the end of each experimental condition, at least three independent samples were snap-frozen in liquid nitrogen, powdered and stored at –80°C until use for RNA isolations and subsequent RT-qPCR analysis.

DNase treatment of the isolated total RNA, cDNA first-strand synthesis using reverse transcriptase, and subsequent RT-qPCR analysis of the target reference genes and drought-stress responsive genes, were performed as described in Ferrari *et al*. (2020*a*). Steady-state transcript abundance stability for all reference genes in the seven sample sets was evaluated using three statistical approaches available via the following software packages: NormFinder (Andersen *et al*. 2004), geNorm (Vandesompele *et al*. 2014), and BestKeeper (Pfaffl *et al*.

2004). For NormFinder and geNorm analysis, Ct values were transformed using the comparative Ct method ($\Delta Ct = Ct - Ct_{min}$) for each sample group, while raw Ct values were used for BestKeeper. The final output from all three packages was analysed using the RankAggreg approach (Pihur *et al*. 2009), which uses stability values to calculate Spearman distance and obtain the overall ranking among evaluated genes and tools via the Monte Carlo algorithm. Since BestKeeper only compares 10 genes at a time, RankAggreg was also used to select the top 10 candidates from geNorm and NormFinder results, and these were used in BestKeeper analysis.

The reference genes were validated by normalising the relative transcript abundance ($2^{(-\Delta\Delta CT)}$, Livak and Schmittgen 2001) of target genes using the most or least stable reference gene pair selected for each experimental condition. As target genes, we selected the phospho*enol*pyruvate carboxylase (PPC)-encoding genes *PPC-1E1a'* and *PPC-1E1c*, which are critical components of the C_4 and CAM cycles in *P. oleracea* respectively (Christin *et al*. 2014; Ferrari *et al*. 2020*a*). Oligonucleotide primer sequences for *PPC-1E1a'* and *PPC-1E1c* are listed in Table S1, available as Supplementary Material to this paper. Among all samples described above, the following were chosen to validate the selected reference genes: tissue series (root, stem, leaf tissues); diel time of sampling (leaves sampled at 5, 11, 17 h); developmental series (cotyledon and 20-day-old leaf); drought stress series (well-watered, droughted and rewatered leaves); salt stress series (control and salt-treated leaves); subspecies (well-watered leaves from subsp. *rausii* and subsp. *nitida*).

Optimisation of in vitro *plant regeneration*

Seed germination and tissue culture were conducted at 25°C, using a 12 h photoperiod at 50 µmol m^{-2} s^{-1} PAR, unless stated otherwise. *P. oleracea* seeds were surface-sterilised as described in Lindsey *et al*. (2017) before inoculation onto a basal medium composed of half-strength Murashige and Skoog salts (referred to as MS, Murashige and Skoog 1962), 3% (w/v) sucrose, Gamborg's B5 vitamin (Gamborg *et al*. 1968), pH 5.8 and 2% (w/v) Phytagel.

Initially, both hypocotyls and cotyledons isolated from 7-day-old seedlings were evaluated as sources of explants by comparing their shoot induction rates after three months of incubation in basal medium supplemented with 1.25, 2.5, 5, 10, 15, 20, 25 and 30 µM 6-benzylaminopurine (BAP). Shoot regeneration from hypocotyl explants was also analysed after incubation for the same period in basal medium supplemented with 0.125, 0.25, 0.5, 0.75 and 1 µM thidiazuron (TDZ) or 0.5, 1.5, 3, 5, 7.5 and 10 µM zeatin (Z). In a subsequent experiment, hypocotyls were divided into basal, middle and apical regions (one-third of the longitudinal length each) and used as the source of explants for shoot regeneration in basal medium supplemented with 2.5 µM BAP, 0.25 µM TDZ or 5 µM Z for 3 months. The optimal antibiotic concentration for selecting putatively transformed regenerating shoots was

determined by incubating segments of the apical part of hypocotyl in basal medium supplemented with 2.5 µM BAP and different concentrations of hygromycin (2.5, 5, 7.5, 10 and 12.5 mg L^{-1}) or kanamycin (25, 50, 75, 100, 125 and 150 mg L^{-1}).

At least 100 explants were inoculated per treatment. In all cases, the explants were subcultured six times, every 2 weeks. Explant mortality was monitored bi-weekly at each subculture step. The percentage of explants with shoots, the number of shoots per explant, and the fresh weight (FW) of all formed shoots per explant were recorded at the end of the three-month incubation period. Also, the shoot forming capacity (SFC) index was calculated, where the SFC index = (% explants with shoots) × (mean number of shoots per explants)/100 (Cruz-Mendívil *et al*. 2011).

Transformation vectors and A. tumefaciens *culture*

Agrobacterium tumefaciens strains EHA101, EHA105, GV3101 and LBA4404 transformed with the binary vectors pCAMBIA1301 or pCAMBIA2301 (CAMBIA Co., Australia) were used. The pCAMBIA1301 and pCAMBIA2301 contained the *hygromycin phosphotransferase* (*hpt*) and *neomycin phosphotransferase II* (*nptII*) selectable marker genes, respectively. Both plasmids also contained the *gusA* reporter gene driven by the CaMV 35S promoter. Cultures of *A. tumefaciens* were maintained at 28°C in the dark using yeast extract peptone (YEP) medium supplemented with adequate antibiotics for each strain: kanamycin (50 mg L^{-1}), rifampicin (50 mg L^{-1}) and streptomycin (100 mg L^{-1}). Primary *A. tumefaciens* cultures were initiated from single colonies inoculated into 3 mL of YEP liquid medium and incubated at 28°C for 24 h with shaking at 150 rpm. Secondary bacterial cultures were grown overnight (12–16 h) at 28°C with shaking at 150 rpm until they reached an OD_{600} of 1.0, and subsequently centrifuged at 2000*g* for 15 min. The pellets were re-suspended with liquid MS medium supplemented with 3% (w/v) sucrose and Gamborg's B5 vitamins. Fifteen minutes before explant inoculation with *A. tumefaciens* culture, sterile acetosyringone (Sigma-Aldrich) was added to be bacterial suspension to a final concentration of 200 µM.

Plant transformation and validation

Based on the results obtained in the optimisation of *in vitro* plant regeneration previously described, the apical region of hypocotyls from *in vitro*-grown seedlings were fragmented into sections of ~5 mm and used as the source of explants for the *Agrobacterium* transformation trials. Approximately 20 µL of *A. tumefaciens* suspension was applied per explant, followed by incubation for 20 min at room temperature in the dark. The inoculated explants were then briefly blotted dry on a sterile filter paper and transferred onto co-cultivation medium (CC) (half-strength MS salts, 3% (w/v) sucrose, Gamborg's B5 vitamins, 2.5 µM BAP, 200 µM acetosyringone, pH 5.8 and 2% (w/v) Phytagel). After 2 days of co-

cultivation in the dark, the explants were transferred onto shoot induction (SI) medium (half-strength MS salts, 3% (w/v) sucrose, Gamborg's B5 vitamins, 2.5 μM BAP, 25 mg L^{-1} meropenem (Antibióticos do Brasil Ltd), pH 5.8 and 2% (w/v) Phytagel) supplemented with 2.5 mg L^{-1} hygromycin or 50 mg L^{-1} kanamycin, depending on the selectable marker used. The explants were subcultured four times onto SI medium, every 2 weeks, and subsequently transferred to shoot elongation and rooting (SER) medium (half-strength MS salts, 3% (w/v) sucrose, Gamborg's B5 vitamins, 25 mg L^{-1} meropenem, pH 5.8 and 2% (w/v) Phytagel). Shoots were sub-cultured onto SER medium every 2 weeks. Well-developed shoots (2–10 mm in length) were detached from the explant to promote root development. Within 4–5 weeks of incubation on SER medium, T_0 plantlets with roots were removed from the medium, washed thoroughly with distilled water, and transferred immediately to the soil.

Transformants were identified by histochemical β-glucuronidase (GUS) assays and PCR analysis using genomic DNA. Transformation efficiency was calculated by dividing the total number of transgenic plantlets by the total number of explants inoculated and then multiplied by 100. To avoid overestimating the transformation rates, only one plantlet regenerated per explant was used to determine transformation efficiency. The percentage of escapes (i.e. plants that had made it through regeneration and antibiotic selection, but which were not carrying the transgene), was calculated from the number of GUS and PCR positive transgenic plants vs the number of non-transgenic plants.

Histochemical GUS assays were performed as described by Jefferson *et al*. (1987). Briefly, fresh leaf tissue fragments from putative transformants among the regenerants were incubated overnight at 37°C in GUS staining solution (100 mM NaH_2PO_4,10 mM EDTA, 0.5 mM $K_4Fe(CN)_6$, 0.05% (v/v) Triton X-100, and 1 mM 5-bromo-4-chloro-3-indolyl-β-D-glucuronide). Following GUS staining, samples were cleared daily for one week by incubating with 70% (v/v) ethanol at room temperature until chlorophyll removal.

For PCR analysis, ~100 mg of fresh or frozen leaf tissue was used to extract genomic DNA as described by Edwards *et al*. (1991), with the following modifications: samples were left for 30 min at –20°C with isopropanol before centrifugation, and resuspension of DNA was accelerated by heating the samples at 50°C for 20 min. PCR was performed to amplify partial sequences of *hpt*, *nptII* and *gusA* genes, using the primers listed in Table S1, with optimised annealing temperature for ~35–40 cycles. Each PCR (20 μL) contained 20 mM Tris–HCl; 50 mM KCl; 3 mM $MgCl_2$; 125 μM dNTPs; 1 U Taq DNA polymerase; 100 ng plant genomic DNA; and 0.25 μM of each primer. PCR products were loaded for 1% agarose gel electrophoresis, stained with ethidium bromide, and visualised under a gel documentation unit.

Statistical analysis

All statistical analyses were performed using R (ver. 3.6.1, R Core Team 2019) via RStudio (ver. 1.2.1335). Normal distribution of the data was checked using the Shapiro-Wilk test, and homogeneity of variances was checked by the Levene test. According to each condition, three or more means were compared by the following tests at $P \leq 0.05$: ANOVA and *post-hoc* Tukey test (normal, homoscedastic), Welch ANOVA + Games-Howell *post-hoc* test (normal, heteroscedastic); Kruskal–Wallis + Mann–Whitney U-paired *post-hoc* test without adjusted *P*-value (non-normal, homoscedastic); or transformed by square root or log and fitted into any of the other descriptions (non-normal, heteroscedastic).

Results

Optimising the conditions for reliable transcript abundance analysis of P. oleracea *samples*

First, the RNA yield, quality and purity (Table 2, Fig. S1, available as Supplementary Material to this paper), resulting from applying the eleven different RNA isolation protocols, were determined using drought-stressed leaves and stems of *P. oleracea*. Protocols using the Concert reagent (CC1 and CC2) yielded very low amounts of RNA or showed variable purity ratios (CC3), and for these reasons, these samples were excluded from RIN analysis. Protocols using Trizol (TZ1-TZ2), Purelink (PL), and RNeasy (RN1-RN2) did not yield sufficient amounts of RNA for performing subsequent RT-qPCR analysis, although RIN >7 from the Agilent 2100 test for intactness of the rRNA bands. TZ3 showed sufficient RNA yield, but a low purity ratio for stems. The best results were achieved using the Spectrum (SP) and ReliaPrep (RP) methods, but RP presented higher yield, purity and intactness (Table 2, Fig. S1). Therefore, the RP method was selected as the best RNA isolation procedure for *P. oleracea* leaves and stems.

Table 2. Total RNA concentration and purity based on $A_{260/280}$ and $A_{260/230}$ ratios calculated for samples obtained through different extraction procedures[A]

(Different letters next to values indicate statistical differences ($P \leq 0.05$) between all leaf and stem samples using different protocols)

	Leaf			Stem		
	ng μL^{-1}	$A_{260/280}$	$A_{260/230}$	ng μL^{-1}	$A_{260/280}$	$A_{260/230}$
TZ1	147 ± 19abc	1.91a	1.48a	130 ± 16bc	1.99ab	1.35ab
TZ2	84 ± 16abc	2.05ab	1.22ab	76 ± 6abc	2.03ab	0.88ab
TZ3	457 ± 89bc	2.2abc	2.01abc	237 ± 100bc	2.03ab	0.33ab
PL	67 ± 8bc	2.05ab	1.2ab	49 ± 5abc	2.03ab	1.04ab
RN1	77 ± 5bc	2.2abc	1.91abc	207 ± 40abc	2.15abc	2.2abc
RN2	70 ± 8bc	2.17abc	1.11abc	183 ± 37abc	2.11abc	1.82abc
CC1	77 ± 1 bc	2.64a	0.25d	71 ± 31bc	3.67bc	0.17d
CC2	6 ± 3b	2.37abc	–0.18abc	17 ± 6b	2.28abc	0.98abc
CC3	397 ± 278abc	2.29c	0.99c	113 ± 84ac	2.67abc	0.34abc
SP	255 ± 89abc	2.15abc	2.26abc	150 ± 8abc	2.15abc	2.32abc

RP	353 ± 42abc	2.16abc	2.24abc	303 ± 8abc	2.17abc	2.32abc

[A]Sufficient purity was confirmed when rations were between $A_{260/280}$ = 1.8–2.3 and $A_{260/230}$ = 1.6–2.3 respectively.

Statistical evaluation and validation of RT-qPCR reference genes for P. oleracea

The following genes were selected based on previously published reports of reference gene selection and validation in other plant species: *CLAT*, *CYP*, *EF1A*, *GAPDH*, *HEL*, *MADS*, *PP2A*, *SAND*, *THIO*, *TIP*, *UBC10* and *UBQ* (Table 1). Based on previous transcriptomic data for *P. oleracea* well-watered and drought-stressed leaves (Ferrari *et al*. 2020*a*), CV values calculated for all 12 genes were <0.1 (Table S2), and thus these genes were subsequentially tested for their suitability as reference genes for RT-qPCR analysis in *P. oleracea*. All candidates presented a final melt curve with a single peak and satisfactory transcript abundance levels across the RNA samples used (Ct < 30) (Fig. 1), and were tested at three different primer concentrations: 200, 300 and 600 nM (Table S3). Since all primer pairs showed efficiencies >1.8 at all concentrations, we decided to use 300 nM as a standard primer concentration and proceeded to the analysis of all sample sets.

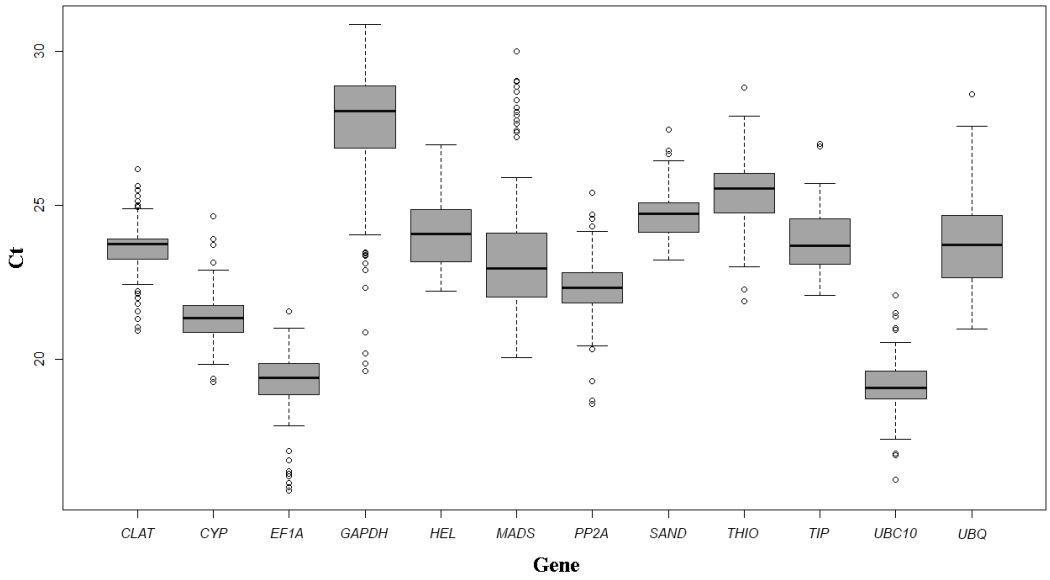

Fig. 1. Box plot representing the Ct range variation of each candidate reference gene. The primer pairs of each gene were used to examine all samples (n = 120; Table S3). Boxes indicate the 25th and 75th percentiles; lines across the box represent the median Ct values; whisker caps represent the minimum and maximum values; and spots represent the outliers.

Ct values for all seven sample sets (i.e. diel time of sampling, different tissues, leaf development, drought stress, salt stress, hormonal treatments and subspecies) (Table S4) were generated and analysed using NormFinder, geNorm and BestKeeper algorithms (Table S5). For each set, the top five candidate genes resulting from RankAggreg analysis of the outputs

from the three software packages are listed in Table 3. geNorm analysis indicated that two reference genes should be used in all sample sets analysed, as $V_{2/3}$ in all sample sets was <1.5 (Fig. S3). When analysing the final selected genes for individual sample sets, *GAPDH* and *THIO* were most frequently selected as the least stable genes (Table S4, including the 12 gene candidates). Also, for individual sample sets, *CLAT*, *TIP*, *UBC10* and *CYP* were among the most stable reference genes (Tables 3, S5). Finally, we analysed candidate gene stability for all samples at the same time using the three algorithms. Although the most stable gene pairs were different for each sample set individually, when increasing sample number and diversity, *CYP* and *CLAT* were selected as the most stable reference gene pair (Tables 3, S5).

Table 3. Consensus ranking by RankAggreg of reference genes evaluated using geNorm, NormFinder and BestKeeper algorithms

Sample set	Five most stable reference genes	Least stable reference genes[A]
Plant tissues	*UBC10*, *CYP*, *EF1A*, *HEL*, *CLAT*	*GAPDH*, *THIO*
Diel time of sampling	*CLAT*, *EF1A*, *TIP*, *CYP*, *SAND*	*GAPDH*, *THIO*
Leaf development	*CLAT*, *TIP*, *PP2A*, *UBC10*, *SAND*	*GAPDH*, *THIO*
Drought stress	*UBC10*, *CYP*, *PP2A*, *CLAT*, *SAND*	*GAPDH*, *THIO*
Salt stress	*CYP*, *CLAT*, *UBQ*, *PP2A*, *UBC10*	*GAPDH*, *THIO*
Hormonal treatments	*TIP*, *PP2A*, *HEL*, *UBQ*, *EF1A*	*GAPDH*, *THIO*
Subspecies	*TIP*, *HEL*, *CYP*, *PP2A*, *CLAT*	*UBC10*, *MADS*
All	*CYP*, *CLAT*, *UBC10*, *TIP*, *SAND*	*UBQ*, *THIO*

[A]Least stable gene pairs were the ones excluded from the BestKeeper analysis.

To validate our selected reference genes, either *PPC-1E1a′* or *PPC-1E1c* (Christin *et al*. 2014; Ferrari *et al*. 2020*a*), were monitored under distinct experimental conditions (Fig. 2). The relative expression was normalised using the most or least stable pair in our reference gene ranking (Tables 2, S5). A reduction in standard error (SE) was observed when the most stable reference gene pairs were employed to normalise *PPC-1E1c* and *PPC-1E1a′* relative expression under drought stress (Fig. 2*d*) and between *P. oleracea* subspecies (Fig. 2*f*) respectively. Moreover, the distinctive peak expression of *PPC-1E1a′* at dawn, which has been consistently detected in previous *P. oleracea* transcriptome studies (Christin *et al*. 2014; Ferrari *et al*. 2020*a*), was significantly attenuated when its transcript abundance was normalised using the least stable normalizer gene pair (*GAPDH* + *THIO*) for this experimental condition (Fig. 2*b*). A significant variation in *PPC-1E1a′* fold change was also observed between *P. oleracea* subsp. *rausii* and subsp. *nitida* (Fig. 2*f*) when the least stable normalizer gene pair (*UBC10* + *MADS*) was employed.

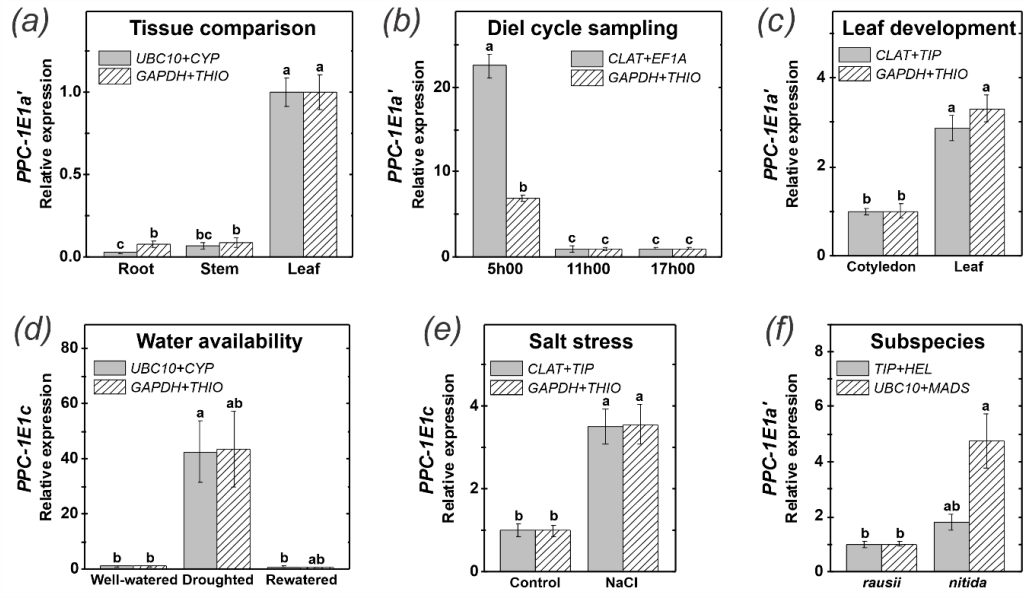

Fig. 2. Validation of selected reference genes in samples from *Portulaca oleracea* harvested at distinct experimental conditions. The relative expression of either the C_4-specific *PPC-1E1a'* (*a*–*c*, *f*) or the CAM-specific *PPC-1E1c* (*d*, *e*) genes was calculated using the most or least stable reference gene pair as ranked in Tables 2 and S5. (*a*) Tissue comparison (root, stem, leaf tissues). (*b*) Day/night sampling (leaves sampled at 5h, 11h, 17h). (*c*) Leaf development series (7-day-old cotyledon and 20-day-old leaf). (*d*) Contrasting water availability conditions (leaves from well-watered, droughted and rewatered plants). (*e*) Salt stress (leaves from control and 100 mM NaCl-treated plants). (*f*) Distinct *P. oleracea* subspecies (well-watered leaves from subsp. *rausii* and subsp. *nitida*). Samples used are described in detail in Methods. Data are means ± s.e., and different letters indicate statistically significant differences between all samples ($P \leq 0.05$).

Optimising in vitro *shoot regeneration*

A prerequisite for successful *Agrobacterium*-mediated transformation of any plant species is the existence of a robust and reproducible *in vitro* regeneration protocol. Thus, before performing the stable genetic transformation trials, a comprehensive optimisation of the *in vitro* conditions for *P. oleracea* regeneration was conducted. Cotyledons and hypocotyls from 1-week-old *P. oleracea* seedlings were compared as explant sources for shoot induction regeneration after inoculation in basal medium supplemented with a range of BAP concentrations (Fig. 3*a*). In the absence of BAP, mortality rates of cotyledon explants (~11%) were significantly lower than those detected for hypocotyl fragments (~45%). When exposed to BAP concentrations ranging from 1.25 to 5 µM, the mortality rate of hypocotyl explants was reduced compared with the basal medium, whereas 15–30 µM BAP promoted necrosis of virtually all hypocotyl explants (Fig. 3*a*). The frequency of explants with shoots and the number of shoots per explants were used to estimate the shoot formation capacity (SFC index). The highest SFC values for hypocotyl explants (0.4) were detected at 2.5–5 µM BAP, exceeding by almost 10 times the maximal SFC values observed for cotyledon explants (0.05 at 15 µM BAP) (Fig. 3*a*). After 3 months of incubation, FW of shoot regenerated from cotyledons (~30 mg per explant at 20 µM BAP) was significantly lower than the FW of

shoots from hypocotyls explants (~190 mg per explant at 2.5 µM BAP) (Fig. 3*a*). The reduced formation of shoots by cotyledon explants (Fig. 3*b*) was associated with a higher proliferation of callus compared with hypocotyl explants (Fig. 3*c*).

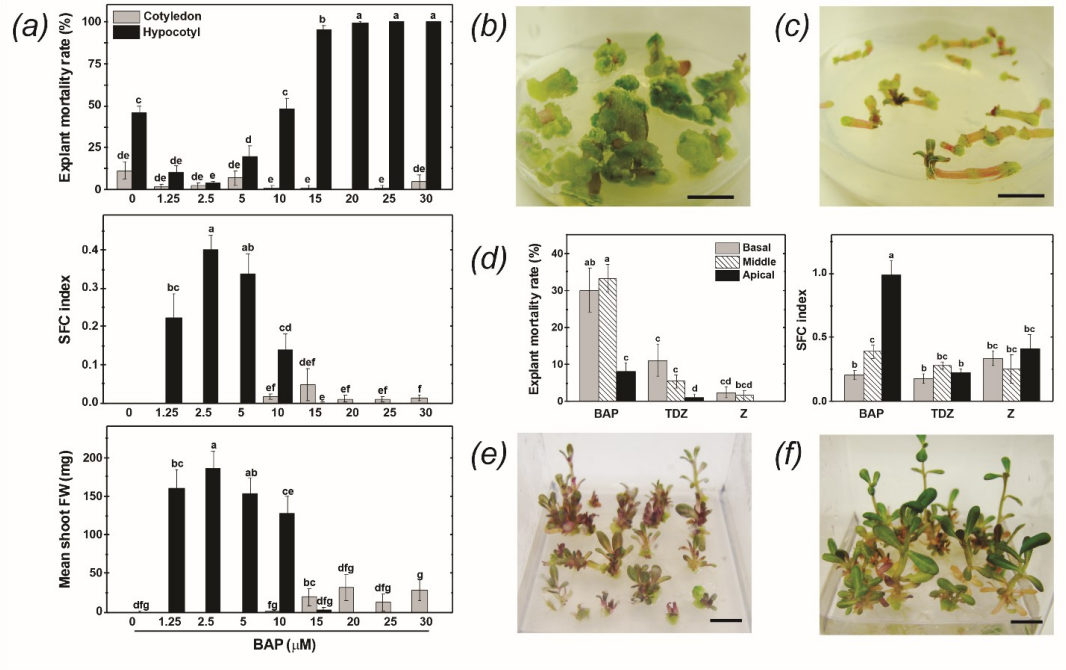

Fig. 3. *In vitro* plant regeneration of *Portulaca oleracea* from cotyledon and hypocotyl explants. (*a*) Explant mortality rate, shoot-forming capacity (SFC) index and mean fresh weight (FW) of shoots formed from cotyledon and hypocotyl explants incubated for three months in basal medium supplemented with different concentrations of benzylaminopurine (BAP). (*b*, *c*) Tissue proliferation from cotyledon (*b*) and hypocotyl (*c*) explants incubated for one month in basal medium supplemented with 2.5 µM BAP. (*d*) Explant mortality rate and SFC index of explants isolated from the apical, middle and basal thirds of hypocotyls and incubated for three months in basal medium supplemented with 2.5 µM BAP, 0.25 µM TDZ or 5 µM Z. (*e*) Shoot isolated from explants and transferred onto shoot elongation and rooting (SER) medium. (*f*) Appearance of plantlets after one-month growth in SER medium. Data are means ± s.e. Distinct letters indicate statistically significant differences ($P \leq 0.05$). Scale bar = 1 cm.

Next, the effectiveness of BAP, TDZ and Z to promote shoot formation from hypocotyl explants was compared (Table S6). For all tested concentrations, explant mortality dropped to zero when using TDZ and was significantly reduced by Z. Analysis of the number of shoots per explant, SFC index and mean shoot FW revealed that optimal on shoot formation was achieved at distinct concentrations for each cytokinin (2.5, 0.25 and 5 µM for BAP, TDZ and Z respectively). BAP was found to be the most effective cytokinin for inducing shoot formation compared with TDZ and Z based both on SFC index and shoot FW, when each was applied at its respective optimal concentration.

When hypocotyls were divided into thirds and analysed separately, the apical section was more responsive to 2.5 µM BAP and displayed significantly lower mortality rates and the highest SFC values compared with the middle and basal regions (Fig. 3*d*). In contrast,

virtually no differences in mortality rates or SFC indexes were observed when the distinct hypocotyl regions were incubated in the presence of 0.25 µM TDZ or 5 µM Z (Fig. 3*d*). Plantlet elongation and rooting were obtained simply by isolating the shoot from the explants and incubating in hormone-free medium (Fig. 3*e*, *f*). The combined use of the apical hypocotyl region as explant source and 2.5 µM BAP supplementation during shoot regeneration resulted in the highest SFC values detected (~1.0). Therefore, this combination was employed for all subsequent parts of this study.

Fine-tuning the transformation: selective agents, A. tumefaciens *strains and inoculation*

The selection of transgenic material is an essential step in the *Agrobacterium*-mediated transformation procedure. Antibiotic and herbicide resistance genes are among the most commonly used selectable markers for the genetic manipulation of plants (Dekeyser *et al*. 1989). When antibiotics were added to the SI medium, either 2.5 mg L^{-1} hygromycin or 50 mg L^{-1} kanamycin were sufficient to inhibit shoot regeneration completely (Table S7). However, hygromycin concentrations higher than 7.5 mg L^{-1} resulted in explant necrosis and death, whereas the explant mortality rate ranged between 60 and 80% at all kanamycin concentrations analysed (Table S7). Therefore, 2.5 mg L^{-1} hygromycin and 50 mg L^{-1} kanamycin were identified as the optimum concentrations to select transformed shoots regenerated from *P. oleracea* hypocotyl explants.

The specific strain of *A. tumefaciens* employed can also impact transformation efficiency significantly depending on the plant species (Gelvin 2003). Thus, strains EHA101, EHA105, GV3101 and LBA4404 harbouring the plasmids pCAMBIA1301 or pCAMBIA2301 were evaluated for their relative efficiency when used for the transformation of *P. oleracea* hypocotyl explants (Table 5). Overall, hygromycin-based selection resulted in higher explant mortality rates compared with kanamycin selection. In all combinations tested, strains GV3101 + pCAMBIA1301 and EHA101 + pCAMBIA2301 exhibited the highest (~55%) and lowest (~10%) percentages of explant mortality respectively (Table 4). The surviving explants developed light green calli and shoots at distinct rates depending on the *A. tumefaciens* strain and plasmid used. EHA101 and EHA105 strains harbouring pCAMBIA2301 displayed the highest percentage of explants with shoots (~40%) and the number of shoots per explant (~0.75 shoots per explant), consequently displaying the highest SFC index (~0.3) among all strains analysed (Table 4). In contrast, GV3101 harbouring pCAMBIA1301 displayed the lowest percentage of explants with shoots (~9%) and SFC values (~0.02) (Table 4).

Table 4. Transformation efficiency of *Agrobacterium tumefaciens* strains and selection markers on *P. oleracea* explants[A]

Strains	Plasmid construct	Explants mortality rate (%)	Explants with shoots (%)	Number of shoots/ explant	SFC index[B]	Transf. efficiency[C] (%)	Escapes (%)
EHA101	pCAMBIA 1301	31.7 ± 3.1b	16.4 ± 3.4de	0.31 ± 0.04cd	0.06 ± 0.01cd	19.3 ± 3.3cd	5.4 ± 2.3c
	pCAMBIA 2301	9.8 ± 2.1d	38 ± 2.5bc	0.72 ± 0.04a	0.28 ± 0.03a	33 ± 1.4ab	10.8 ± 3abc
EHA105	pCAMBIA 1301	26.1 ± 3bc	18.7 ± 3.1e	0.26 ± 0.04cd	0.06 ± 0.01cd	20.2 ± 2.5acd	7.1 ± 4.1abc
	pCAMBIA 2301	15.6 ± 2.7cd	42.7 ± 2.8c	0.81 ± 0.04a	0.34 ± 0.03a	40.1 ± 2.2b	9.4 ± 2.9bc
GV3101	pCAMBIA 1301	54.5 ± 5.7a	9.2 ± 2.7d	0.17 ± 0.05d	0.02 ± 0.01d	12.9 ± 1.9c	3.6 ± 2.8c
	pCAMBIA 2301	25.3 ± 4.2bc	19.9 ± 3.8ae	0.25 ± 0.06cd	0.07 ± 0.02cd	21.7 ± 2.1acd	23.4 ± 4.7a
LBA 4404	pCAMBIA 1301	27.4 ± 3.6bc	26.2 ± 4.2ae	0.34 ± 0.05c	0.1 ± 0.02bc	24 ± 2.6acd	9.2 ± 3.8abc
	pCAMBIA 2301	16.9 ± 3.4bcd	31.5 ± 3.3ab	0.48 ± 0.04b	0.16 ± 0.03b	27.7 ± 3.3abd	15.9 ± 0.8ab

[A]The upper third portion (apical region) of hypocotyls from 7-day-old seedlings were used as explants. The transformation experiments were repeated twice, and at least 100 explants were used in each transformation. Data are means ± s.e. of values from two independent transformation experiments. Distinct letters within the column indicate significant differences ($P \leq 0.05$).
[B]Shoot-forming capacity (SFC) index = (% explants with shoots) × (mean number of shoots per explants) / 100.
[C]Transformation efficiency = (number of transgenic plants)/(number of explants inoculated) × 100. Positive transgenic plants were identified by PCR and histochemical GUS assay, and only one plant regenerated per explant was considered to calculate the transformation efficiency.

Results from two independent co-incubation trials with various *A. tumefaciens* strains harbouring pCAMBIA2301 revealed that the EHA105 strain offered one of the highest transformation rates (40%), followed by EHA101 (33%) and LBA4404 (27%) (Table 4). Conversely, strain GV3101 + pCAMBIA2301 resulted in the lowest transformation efficiency (21%). Except for LBA4404, an overall tendency of lower shoot formation and transformation efficiency was observed when pCAMBIA1301 was used compared with pCAMBIA2301. The percentage of non-transgenic plants (frequency of escapes) regenerated following selection using hygromycin or kanamycin was in the range of 4–9 or 7–23% respectively (Table 4).

Additional experiments employing the EHA105 strain harbouring pCAMBIA2301 were conducted to determine the ideal co-cultivation period and bacterial densities (Table S8). A 4-fold increase in explant mortality rates was observed as the time of co-cultivation and bacterial densities (OD_{600}) increased, as 2 days of co-cultivation with 0.5 OD_{600} showed 18.3% and 4 days with 1.0 OD_{600} was 83.5%. The extension of the co-cultivation period from 2 to 4 days did not significantly influence shoot formation, transformation efficiency, or the number of escapes at both bacterial densities. The lowest transformation efficiency (~13%) was detected after 4 days of co-cultivation with 1.0 OD_{600}, and was less than half of the

transformation rates detected after co-cultivation with 0.5 OD_{600} for 2 or 4 days (37 and 32% respectively).

Discussion

Portulaca oleracea is one of few C_4 species capable of performing CAM when water availability becomes scarce (Winter 2019). As a potential model for C_4/CAM photosynthesis research, *P. oleracea* is known to display rapid growth, abundant seed production, small plant size, and it has been the most widely used *Portulaca* species for biochemical, anatomical, and gene expression studies linked to this unique photosynthetic arrangement (Zimmerman 1976; Koch and Kennedy 1980, 1982; Mazen 1996, 2000; Lara *et al*. 2003, 2004; Voznesenskaya *et al*. 2010; Ocampo and Columbus 2012; D'Andrea *et al*. 2014; Ferrari and Freschi 2019; Ferrari *et al*. 2020*b*). By optimising the conditions for gene expression analysis and developing an efficient *Agrobacterium*-mediated genetic transformation protocol for *P. oleracea*, we offer key molecular tools to accelerate future work to understand the molecular genetics of the fascinating C_4/CAM photosynthetic syndrome found in this species.

A highly viscous polysaccharide matrix is abundant in *P. oleracea* shoot tissues (Wenzel *et al*. 1990), especially under drought conditions, and it has been reported to play a role in maintaining the osmotic balance in plant cells under these stressful conditions (Clifford *et al*. 2002). Mucilage and phenolic substances are known to contaminate nucleic acids extracted from plant samples rich in such compounds (Gehrig *et al*. 2000), which may explain, to some extent, the low RNA yield and purity observed in nine out of the eleven RNA extraction protocols tested for the *P. oleracea* samples. Between the other two protocols (SP and RP), the RP method was found as the most consistent and efficient, allowing RNA yield and purity compatible with downstream molecular procedures (e.g. qPCR, RNAseq) from a relatively small amount of tissue (~100 mg FW).

In a subsequent effort to provide protocols for measuring the mRNA levels of target genes of interest in *P. oleracea* using RT-qPCR, 12 potential reference genes were characterised in order to identify the most stable options across a wide range of samples. The corresponding optimal reference genes were: variation in leaf development – *CLAT* and *TIP*; tissue type and water availability – *UBC10* and *CYP*; day/night sampling time – *CLAT* and *EF1A*; salinity stress – *CYP* and *CLAT*; subspecies – *TIP* and *HEL*; and hormone treatments – *TIP* and *PP2A*. As such, the geometric mean of these gene pairs was found to be optimal for each tissue/ experimental condition and should be used as a normalisation factor when calculating the relative expression of genes of interest under these conditions using RT-qPCR.

The normalisation of RT-qPCR data of *PPC-1E1a′* and *PPC-1E1c* using the most stable and the least stable reference gene pairs confirmed the importance of this optimisation to reduce technical variability and promote the accuracy in estimating the fold-change

induction/ repression of target genes in each treatment condition (Fig. 2). The housekeeping genes used traditionally in other plants (*EF1A*, *GAPDH*, *UBQ* and *UBC10*) were sometimes among the optimal normalizers for *P. oleracea* samples, but most genes identified as the best options in this study corresponded to those recommended more recently (Brunner *et al*. 2004; Czechowski *et al*. 2005). This highlights the importance of the species-specific evaluation of candidate reference genes presented here.

Monitoring the impacts of distinct pairs of reference genes on normalising *PPC-1E1a′* and *PPC-1E1c* relative expression allowed us to compare our findings with previous reports describing the influence of the diel cycle, water availability, plant tissue and genotype on the expression dynamics of these two PPC-encoding genes (Christin *et al*. 2014; Ferrari *et al*. 2020*a*, 2020*b*). Either the most and the least stable normalizer gene pair allowed to corroborate the previously described up- and downregulation of *PPC-1E1c* upon drought and rewatering, respectively (Christin *et al*. 2014; Ferrari *et al*. 2020*a*). However, the conspicuous day/night fluctuation of *PPC-1E1a′* repeatedly observed in well-watered *P. oleracea* leaves (Christin *et al*. 2014; Ferrari *et al*. 2020*a*, 2020*b*) was drastically reduced when the least stable normalizer gene pair was used. In terms of genotypic variation, Ferrari *et al*. (2020*b*) reported no significant differences in *PPC-1E1a′* mRNA levels between the *P. oleracea* subsp. *rausii* and subsp. *nitida*, which was confirmed here only when the most stable normalizer gene pair was employed.

As previously reported in Ferrari *et al*. (2020*a*), *PPC-1E1a′* mRNA levels were more abundantly detected in leaves than in stems. Moreover, data also revealed that *PPC-1E1a′* mRNA levels in stems were as low as those found in root tissues (Fig. 2*a*), which further confirmed that the expression of this C_4-marker gene is restricted to the leaf tissues. In addition, data indicated that *PPC-1E1c* relative transcript abundance was significantly upregulated in leaves from plants exposed to salt stress, suggesting that the C_4-to-CAM transition in *P. oleracea* is also promoted under salinity conditions. Salinity has long been described to promote the C_3-CAM transition in the halophyte *M. crystallinum* (Winter and Holtum 2007), and *P. oleracea* is known to be resistant to high salinity conditions (Rahdari *et al*. 2012), although the influence of this environmental stress alone on *P. oleracea* CCM transition had not been reported before.

In the context of functional genomics, the availability of stable transformation protocols for any given plant model is of paramount importance as a tool to access the function, localisation, interaction, and other relevant information about proteins encoded by genes of interest (Alam *et al*. 2014). *Agrobacterium*-mediated transformation is considered the best overall method for producing stable transgenic plants for many crop and non-crop species (Gelvin 2003). In *P. oleracea*, very few *Agrobacterium*-mediated transformation protocols have been reported. Successful *A. rhizogenes*-mediated hairy root induction has been

employed for the production of noradrenaline and dopamine in *P. oleracea* roots (Pirian and Piri 2012; Moghadam *et al*. 2014). Such methods are regarded as a valid alternative for rapid biomass accumulation and the synthesis of high yields of desirable secondary metabolites (Potrykus 1995; Srivastava and Srivastava 2007; Ream 2009), but *A. rhizogenes* has limited applications with respect to functional genomics studies, especially in terms of understanding the functions of candidate genes in aboveground tissues.

More recently, an *A. tumefaciens*-mediated transformation method using micropropagated *P. oleracea* plantlets obtained from a commercial cultivar was evaluated using kanamycin as the selective agent, two bacterial strains (LBA4404 and GV3101) and both BAP and auxins (indole-3-acetic acid, 1-naphthaleneacetic acid and 2,4-dichlorophenoxyacetic acid (2,4-D)) in the regeneration medium (Sedaghati *et al*. 2019). According to our findings, *in vitro* regeneration of *P. oleracea* was more effective when carried out using the apical region of hypocotyls from very young seedlings as explants, allowing prolific plantlet regeneration in the presence of cytokinins as the exclusive hormonal signal in the regeneration medium. By following these conditions, and avoiding the use of the auxin 2,4-D, which can cause epigenetic and genetic changes (Kubaláková *et al*. 1996; Temel *et al*. 2008), we minimised the formation of calli and were able to obtain healthy plantlets with shoots and roots after a relatively short period (Fig. 4). As auxin supplementation during explant regeneration may inhibit shoot formation and, consequently, shoot development (Kochba and Spiegel-Roy 1977), the removal of this hormonal signal from the micropropagation protocol minimised root formation during the initial phases of plantlet regeneration, without compromising rooting of the shoots after their isolation from the explants.

Although a kanamycin concentration of 250 mg L^{-1} was previously recommended as the optimum for the selection of transgenic *P. oleracea* (Sedaghati *et al*. 2019), under the optimised transformation conditions employed in this study, we demonstrated that 50 mg L^{-1} of this antibiotic was enough to select putatively transformed shoots and facilitate their growth during the regeneration phase. One possible explanation for the success of using a 5-fold lower kanamycin concentration might be that regular subculturing onto fresh selection media (every 2 weeks) allowed 50 mg L^{-1} kanamycin to select successful transformants reliably. As species-specific variation in sensitivity to antibiotics has been described (e.g. Alsheikh *et al*. 2002; Gambhir *et al*. 2017), we compared both kanamycin- and hygromycin-based selection for the transformation of *P. oleracea*, confirming that both selections systems can be used, although kanamycin-based selection resulted in higher transformation rates. In addition, as only two strains of *A. tumefaciens* (LBA4404 and GV3101; Sedaghati *et al*. 2019) were previously tested, here we expanded to four bacterial strains compared side by side, which revealed that EHA105 was comparatively more efficient for the transformation of *P. oleracea* hypocotyl explants relative to LBA4404, GV3101 and EHA101.

After testing multiple combinations of explant sources, bacterial strains, selective agents and growth stimulators, an efficient pipeline for the regeneration of T_0 rooted transgenic *P. oleracea* plants within 10–14 weeks was established (Fig. 4). This duration is in the same range as those described for the *Agrobacterium*-mediated transformation of other species, such as *Flaveria bidentis* (15–19 weeks; Chitty *et al*. 1994), maize (12 weeks; Ishida *et al*. 2007), tomato (7 weeks; Pino *et al*. 2010), *Medicago sativa* L. and *Medicago truncatula* Gaertn. (8–16 weeks; Jiang *et al*. 2019); *Setaria viridis* (L.) P.Beauv. (16 weeks; Nguyen *et al*. 2020). The escape rates (10%) and transformation efficiency rates (up to 38%) achieved here were also comparable, or sometimes superior, to those reported for other species using *A. tumefaciens*-mediated transformation systems (Aida and Shibata 1996; Ishida *et al*. 1996, 2007; Bakhsh *et al*. 2014; Martins *et al*. 2015; Newell *et al*. 2010). For example, using an *A. tumefaciens*-mediated system, a transformation efficiency of 0.6–4.6% was recently reported for *M. crystallinum* (Agarie *et al*. 2020), and 15–65% transformation efficiency and approx. 10% of escapes were reported for tomato (Chetty *et al*. 2013).

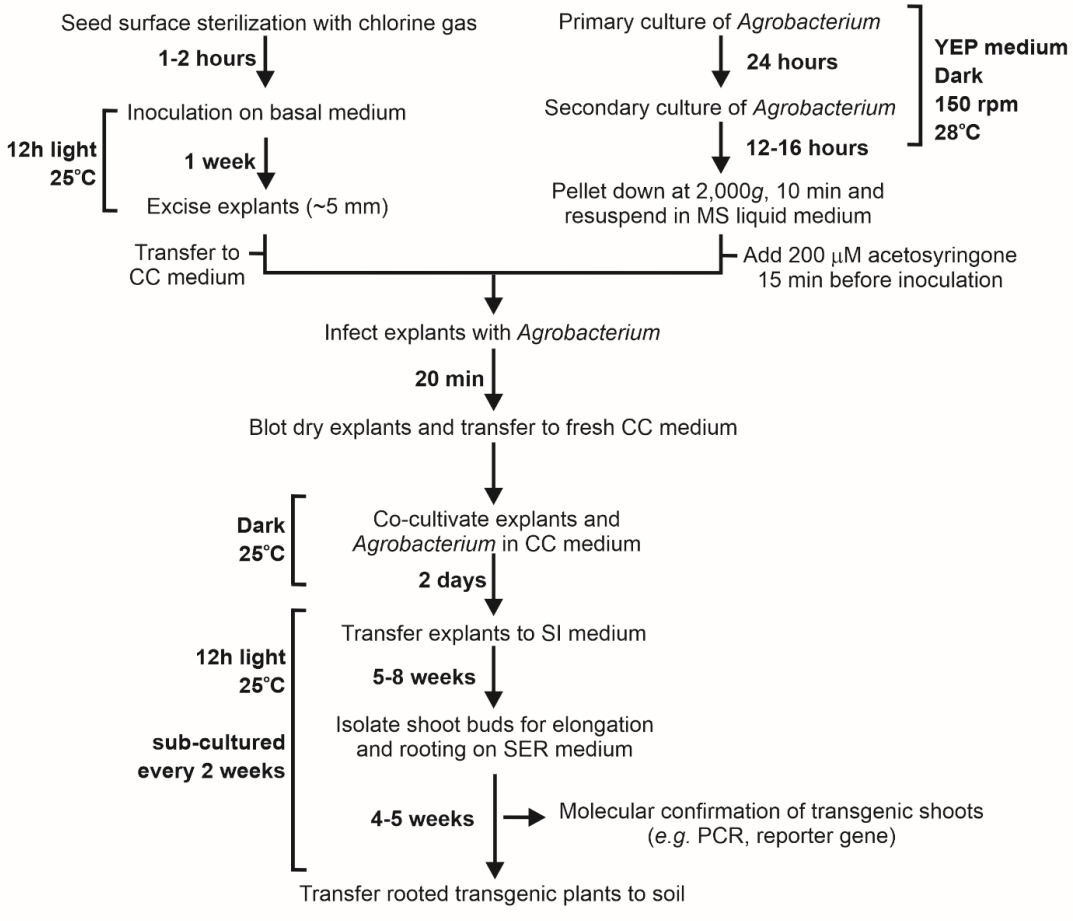

Fig. 4. Schematic diagram depicting the essential steps of *Agrobacterium tumefaciens*-mediated transformation of *Portulaca oleracea*. See 'Material and methods' for details, including the composition of different media, explant isolation procedure and bacteria cultivation.

In conclusion, although much recent progress has been made with the study of C_4 and CAM functional genomics (von Caemmerer *et al*. 2004; Furumoto *et al*. 2007; Pengelly *et al*. 2012; Dever *et al*. 2015; Boxall *et al*. 2017, 2020), similar molecular approaches have not been possible so far in a C_4-CAM facultative species. Other genetic resources are still needed to allow the adoption of *P. oleracea* as a genetic model system, particularly a well annotated genome for the species and more extensive and diverse comprehensive transcriptomic datasets. Nevertheless, the information presented here provides a vital part of the resources required for the further development of *P. oleracea* as an important and valuable molecular-genetic model plant.

As future prospects, reliable RT-qPCR expression profile analysis of candidate genes potentially involved in either or both CCMs can now be performed using the most stable reference genes identified here for a range of experimental conditions. Moreover, the stable genetic transformation protocol described here for *P. oleracea* may also be used to discover and validate the molecular and biochemical functions of target genes using overexpression, RNA interference or CRISPR/Cas9 approaches. Stable *P. oleracea* transgenic lines expressing reporter genes coding for proteins such as β-glucuronidase (GUS), fluorescent protein (e.g. GFP, YFP) or firefly luciferase (LUC) driven by the promoters of CAM-related genes may also provide unparalleled opportunities to determine precisely where the CAM cycle is located within the leaves. Up to now, a single attempt to answer this critical question has been carried out, which was based on the use of anti-*Amaranthus viridis* PPC antibodies to immunolocalise this enzyme within the leaf tissues of well-watered and droughted *P. oleracea* plants (Lara *et al*. 2004). As *P. oleracea* genome encodes both C_4- (*PPC-1E1a'*) and CAM-specific (*PPC-1E1c*) PPCs (Christin *et al*. 2014; Ferrari *et al*. 2020*a*, 2020*b*), the production of transformants expressing either *PPC-1E1a'* or *PPC-1E1c* promoters fused to report genes (e.g. GUS, GFP, YFP, LUC) may provide conclusive information on the tissue localisation of each CCM. In addition, the use of microdissection (Kerk *et al*. 2003; Espina *et al*. 2006) or enzymatic protoplast isolation (Chang *et al*. 2012) to recover cells from mesophyll and bundle sheath separately, followed by subsequent analysis of transcript abundance via RT-qPCR can also help to elucidate CCM-enzyme distribution across different tissues. Overall, the answers to such questions will undoubtedly underpin the future application of these valuable photosynthetic adaptations within crop biotechnology.

Conflicts of interest

The authors declare no conflicts of interest.

Acknowledgements

This work was supported by the São Paulo Research Foundation (FAPESP – grant no. 2016/04755-4 awarded to RCF), by a Newton Advanced Fellowship funded by the Royal Society, UK (grant no. NA140007 awarded to LF and JH), and the Coordenação de Aperfeiçoamento de Pessoal de Nível Superior – Brasil (CAPES) – Finance Code 001. We kindly thank Dr Johannes Walter (Natural History Museum Vienna, Austria) and Dr Avinoam Danin (The Hebrew University of Jerusalem), for donating seeds of *P. oleracea* subspecies.

References

Abraham PE, Yin H, Borland AM, Weighill D, Lim SD, De Paoli HC, Engle N, Jones PC, Agh R, Weston DJ, Wullschleger SD, Tschaplinski T, Jacobson D, Cushman JC, Hettich RL, Tuskan GA, Yang X (2016) Transcript, protein and metabolite temporal dynamics in the CAM plant *Agave. Nature Plants* **2**, 16178 doi:10.1038/nplants.2016.178.

Agarie S, Umemoto M, Sunagawa H, Anai T, Cushman JC (2020) An *Agrobacterium*-mediated transformation via organogenesis regeneration of a facultative CAM plant, the common ice plant *Mesembryanthemum crystallinum* L. *Plant Production Science* **23**, 343–349 doi:10.1080/1343943X.2020.1730700.

Aida R, Shibata M (1996) Transformation of *Kalanchoë blossfeldiana* mediated by *Agrobacterium tumefaciens* and transgene silencing. *Plant Science* **121**, 175–185 doi:10.1016/S0168-9452(96)04524-4.

Alam MA, Juraimi AS, Rafii MY, Hamid AA, Kamal Uddin M, Alam MZ, Latif MA (2014) Genetic improvement of purslane (*Portulaca oleracea* L.) and its future prospects. *Molecular Biology Reports* **41**, 7395–7411 doi:10.1007/s11033-014-3628-1.

Alsheikh M, Suso HP, Robson M, Battey N, Wetten A (2002) Appropriate choice of antibiotic and *Agrobacterium* strain improves transformation of antibiotic-sensitive *Fragaria vesca* and *F.* v. *semperflorens. Plant Cell Reports* **20**, 1173–1180 doi:10.1007/s00299-002-0453-0.

Andersen CL, Jensen JL, Ørntoft TF (2004) Normalization of real-time quantitative reverse transcription-PCR data: a model-based variance estimation approach to identify genes suited for normalization, applied to bladder and colon cancer data sets. *Cancer Research* **64**, 5245–5250. doi:10.1158/0008-5472.CAN-04-0496

Bakhsh A, Anayol E, Ozcan SF (2014) Comparison of transformation efficiency of five *Agrobacterium tumefaciens* strains in *Nicotiana tabacum* L. *Emirates Journal of Food and Agriculture* **26**, 259–264 doi:10.9755/ejfa.v26i3.16437.

Bauwe H, Hagemann M, Fernie AR (2010) Photorespiration: players, partners and origin. *Trends in Plant Science* **15**, 330–336 doi:10.1016/j.tplants.2010.03.006.

Berardini TZ, Reiser L, Li D, Mezheritsky Y, Muller R, Strait E, Huala E (2015) The *Arabidopsis* information resource: making and mining the 'gold standard' annotated reference plant genome. *Genesis* **53**, 474–485 doi:10.1002/dvg.22877.

Borland AM, Griffiths H, Hartwell J, Smith JAC (2009) Exploiting the potential of plants with crassulacean acid metabolism for bioenergy production on marginal lands. *Journal of Experimental Botany* **60**, 2879–2896 doi:10.1093/jxb/erp118.

Boxall SF, Dever LV, Kneřová J, Gould PD (2017) Phosphorylation of Phospho*enol*pyruvate carboxylase is essential for maximal and sustained dark CO_2 fixation and core circadian clock operation in the obligate crassulacean acid metabolism species *Kalanchoë fedtschenkoi. The Plant Cell* **29**, 2519–2536 doi:10.1105/tpc.17.00301.

Boxall SF, Kadu N, Dever LV, Kneřová J, Waller JL, Gould PJD, Hartwell J (2020) *Kalanchoë* PPC1 is essential for crassulacean acid metabolism and the regulation of core circadian clock and guard cell signaling genes. *The Plant Cell* **32**, 1136–1160 doi:10.1105/tpc.19.00481.

Brilhaus D, Bräutigam A, Mettler-Altmann T, Winter K, Weber APM (2016) Reversible burst of transcriptional changes during induction of crassulacean acid metabolism in *Talinum triangulare. Plant Physiology* **170**, 102–122 doi:10.1104/pp.15.01076.

Brunner AM, Yakovlev IA, Strauss SH (2004) Validating internal controls for quantitative plant gene expression studies. *BMC Plant Biology* **4**, 14 doi:10.1186/1471-2229-4-14.

Brutnell TP, Wang L, Swartwood K, Goldschmidt A, Jackson D, Zhu XG, Kellogg E, van Eck J (2010) *Setaria viridis*: a model for C_4 photosynthesis. *The Plant Cell* **22**, 2537–2544 doi:10.1105/tpc.110.075309.

Camacho C, Coulouris G, Avagyan V, Ma N, Papadopoulos J, Bealer K, Madden TL (2009) BLAST+: architecture and applications. *BMC Bioinformatics* **10**, 421 doi:10.1186/1471-2105-10-421.

Chang S, Puryear J, Cairney J (1993) A simple and efficient method for isolating RNA from pine trees. *Plant Molecular Biology Reporter* **11**, 113–116 doi:10.1007/BF02670468.

Chang Y, Liu W, Shih AC, Shen M, Lu C, Lu MJ, Yang H, Wang T, Chen SC, Chen SM, Li WH, Ku MSB (2012) Characterizing regulatory and functional differentiation between maize mesophyll and bundle sheath cells by transcriptomic analysis. *Plant Physiology* **160**, 165–177 doi:10.1104/pp.112.203810.

Chetty VJ, Ceballos N, Garcia D, Narváez-Vásquez J, Lopez W, Orozco-Cárdenas ML (2013) Evaluation of four *Agrobacterium tumefaciens* strains for the genetic transformation of tomato (*Solanum lycopersicum* L.) cultivar micro-tom. *Plant Cell Reports* **32**, 239–247 doi:10.1007/s00299-012-1358-1.

Chitty JA, Furbank RT, Marshall JS, Chen Z, Taylor WC (1994) Genetic transformation of the C_4 plant, *Flaveria bidentis*. *The Plant Journal* **6**, 949–956 doi:10.1046/j.1365-313X.1994.6060949.x.

Christin PA, Arakaki M, Osborne CP, Bräutigam A, Sage RF, Hibberd JM, Kelly S, Covshoff S, Wong GKS, Hancock L, Edwards EJ (2014) Shared origins of a key enzyme during the evolution of C_4 and CAM metabolism. *Journal of Experimental Botany* **65**, 3609–3621 doi:10.1093/jxb/eru087.

Clifford SC, Arndt SK, Popp M, Jones HG (2002) Mucilages and polysaccharides in *Ziziphus* species (Rhamnaceae): localization, composition and physiological roles during drought-stress. *Journal of Experimental Botany* **53**, 131–138 doi:10.1093/jexbot/53.366.131.

Covshoff S, Hibberd JM (2012) Integrating C_4 photosynthesis into C_3 crops to increase yield potential. *Current Opinion in Biotechnology* **23**, 209–214 doi:10.1016/j.copbio.2011.12.011.

Cruz-Mendívil A, Rivera-López J, Germán-Báez LJ, López-Meyer M, Hernández-Verdugo S, López-Valenzuela JA, Reyes-Moreno C, Valdez-Ortizl A (2011) A simple and efficient protocol for plant regeneration and genetic transformation of tomato cv. micro-tom from leaf explants. *HortScience* **46**, 1655–1660 doi:10.21273/HORTSCI.46.12.1655.

Czechowski T, Stitt M, Altmann T, Udvardi MK, Scheible W-R (2005) Genome-wide identification and testing of superior reference genes for transcript normalization in *Arabidopsis*. *Plant Physiology* **139**, 5–17 doi:10.1104/pp.105.063743.

D'Andrea RM, Andreo CS, Lara MV (2014) Deciphering the mechanisms involved in *Portulaca oleracea* (C_4) response to drought: metabolic changes including crassulacean acid-like metabolism induction and reversal upon rewatering. *Physiologia Plantarum* **152**, 414–430 doi:10.1111/ppl.12194.

Danin A, Raus T (2012) 'A key to 19 microspecies of the *Portulaca oleracea* aggregate. Caryophyllales Simposium 70–83.' (Lomonosov State University: Moscow, Russia)

Dekeyser R, Claes B, Marichal M, Van Montagu M, Caplan A (1989) Evaluation of selectable markers for rice transformation. *Plant Physiology* **90**, 217–223 doi:10.1104/pp.90.1.217.

DePaoli HC, Borland AM, Tuskan GA, Cushman JC, Yang X (2014) Synthetic biology as it relates to CAM photosynthesis: challenges and opportunities. *Journal of Experimental Botany* **65**, 3381–3393 doi:10.1093/jxb/eru038.

Dever LV, Boxall SF, Kneřová J, Hartwell J (2015) Transgenic perturbation of the decarboxylation phase of crassulacean acid metabolism alters physiology and metabolism but has only a small effect on growth. *Plant Physiology* **167**, 44–59 doi:10.1104/pp.114.251827.

Edwards K, Johnstone C, Thompson C (1991) A simple and rapid method for the preparation of plant genomic DNA for PCR analysis. *Nucleic Acids Research* **19**, 1349 doi:10.1093/nar/19.6.1349.

Elbl P, Navarro BV, De Oliveira LF, Almeida J, Mosini AC, Dos Santos ALW, Rossi M, Floh EIS (2015) Identification and evaluation of reference genes for quantitative analysis of Brazilian pine (*Araucaria angustifolia* Bertol. Kuntze) gene expression. *PLoS One* **10**, e0136714 doi:10.1371/journal.pone.0136714.

Espina V, Wulfkuhle JD, Calvert VS, VanMeter A, Zhou W, Coukos G, Geho DH, Petricoin EF, 3rd, Liotta LA (2006) Laser-capture microdissection. *Nature Protocols* **1**, 586–603 doi:10.1038/nprot.2006.85.

Expósito-Rodríguez M, Borges AA, Borges-Pérez A, Pérez JA (2008) Selection of internal control genes for quantitative real-time RT-PCR studies during tomato development process. *BMC Plant Biology* **8**, 131 doi:10.1186/1471-2229-8-131.

Ferrari RC, Freschi L (2019) C_4 /CAM as a means to improve plant sustainable productivity under abiotic-stressed conditions: regulatory mechanisms and biotechnological implications. In 'Plant signaling molecules'. (Eds MIR Khan, PS Reddy, A Ferrante, NA Khan) pp. 517–532. (Elsevier Inc.: Amsterdam, Netherlands) doi:10.1016/B978-0-12-816451-8.00032-0

Ferrari RC, Bittencourt PP, Rodrigues MA, Moreno-villena JJ, Frederico RR, Gastaldi D, Boxall SF, Dever LV, Demarco DSC, Edwards EJ, Hartwell J, Freschi L (2020*a*) C_4 and crassulacean acid metabolism within a single leaf: deciphering key components behind a rare photosynthetic adaptation. *New Phytologist* **225**, 1699–1714 doi:10.1111/nph.16265.

Ferrari RC, Cruz BC, Gastaldi VD, Storl T, Ferrari EC, Boxall SF, Hartwell J, Freschi L (2020*b*) Exploring C_4-CAM plasticity within the *Portulaca oleracea* complex. *Scientific Reports* **10**, 14237 doi:10.1038/s41598-020-71012-y.

Furbank RT, Quick WP, Sirault XRR (2015) Improving photosynthesis and yield potential in cereal crops by targeted genetic manipulation: prospects, progress and challenges. *Field Crops Research* **182**, 19–29 doi:10.1016/j.fcr.2015.04.009.

Furumoto T, Izui K, Quinn V, Furbank RT, Von Caemmerer S (2007) Phosphorylation of phospho*enol*pyruvate carboxylase is not essential for high photosynthetic rates in the C_4 species *Flaveria bidentis*. *Plant Physiology* **144**, 1936–1945 doi:10.1104/pp.107.102541.

Gachon C (2004) Real-time PCR: what relevance to plant studies? *Journal of Experimental Botany* **55**, 1445–1454 doi:10.1093/jxb/erh181.

Gambhir G, Kumar P, Srivastava DK (2017) Effect of antibiotic sensitivity on different cultured tissues and its significance in genetic transformation of cabbage *Brassica oleracea*. *Bioscience Biotechnology Research Communications* **10**, 652–661 doi:10.21786/bbrc/10.4/7.

Gamborg OL, Miller RA, Ojima K (1968) Nutrient requirements of suspension cultures of soybean root cells. *Experimental Cell Research* **50**, 151–158 doi:10.1016/0014-4827(68)90403-5.

Gehrig HH, Winter K, Cushman J, Borland A (2000) An improved rna isolation method for succulent plant species rich in polyphenols and polysaccharides. *Plant Molecular Biology Reporter* **18**, 369–376. doi 10.1007/BF02825065.

Gelvin SB (2003) *Agrobacterium*-mediated plant transformation: the biology behind the 'gene-jockeying' tool. *Microbiology and Molecular Biology Reviews* **67**, 16–37 doi:10.1128/MMBR.67.1.16-37.2003.

Gonnella M, Charfeddine M, Conversa G, Santamaria P (2010) Purslane: a review of its potential for health and agricultural aspects. *The European Journal of Plant Science and Biotechnology* **4**, 131–136.

Guénin S, Mauriat M, Pelloux J, Van Wuytswinkel O, Bellini C, Gutierrez L (2009) Normalization of qRT-PCR data: the necessity of adopting a systematic, experimental conditions-specific, validation of references. *Journal of Experimental Botany* **60**, 487–493 doi:10.1093/jxb/ern305.

Guralnick LJ, Jackson MD (2001) The occurrence and phylogenetics of crassulacean acid metabolism in the Portulacaceae. *International Journal of Plant Sciences* **162**, 257–262 doi:10.1086/319569.

Gutierrez L, Mauriat M, Guénin S, Pelloux J, Lefebvre JF, Louvet R, Rusterucci C, Moritz T, Guerineau F, Bellini C, Van Wuytswinkel O (2008) The lack of a systematic validation of reference genes: a serious pitfall undervalued in reverse transcription-polymerase chain reaction (RT-PCR) analysis in plants. *Plant Biotechnology Journal* **6**, 609–618 doi:10.1111/j.1467-7652.2008.00346.x.

Habtemariam S, Harvey AL, Waterman PG (1993) The muscle relaxant properties of *Portulaca oleracea* are associated with high concentrations of potassium ions. *Journal of Ethnopharmacology* **40**, 195–200 doi:10.1016/0378-8741(93)90068-G.

Hartwell J, Dever LV, Boxall SF (2016) Emerging model systems for functional genomics analysis of crassulacean acid metabolism. *Current Opinion in Plant Biology* **31**, 100–108 doi:10.1016/j.pbi.2016.03.019.

Hernández-Bermejo JE, León J (1994) Neglected crops – 1492 from a different perspective. FAO Plant Production and Protection Series No. 26.

Heyduk K, Ray JN, Ayyampalayam S, Leebens-Mack J (2018) Shifts in gene expression profiles are associated with weak and strong crassulacean acid metabolism. *American Journal of Botany* **105**, 587–601 doi:10.1002/ajb2.1017.

Holtum JAM, Hancock LP, Edwards EJ, Winter K (2017) Optional use of CAM photosynthesis in two C_4 species, *Portulaca cyclophylla* and *Portulaca digyna*. *Journal of Plant Physiology* **214**, 91–96 doi:10.1016/j.jplph.2017.01.010.

Hong SY, Seo PJ, Yang MS, Xiang F, Park CM (2008) Exploring valid reference genes for gene expression studies in *Brachypodium distachyon* by real-time PCR. *BMC Plant Biology* **8**, 112 doi:10.1186/1471-2229-8-112.

Iranshahy M, Javadi B, Iranshahi M, Jahanbakhsh SP, Mahyari S, Hassani FV, Karimi G (2017) A review of traditional uses, phytochemistry and pharmacology of *Portulaca oleracea* L. *Journal of Ethnopharmacology* **205**, 158–172 doi:10.1016/j.jep.2017.05.004.

Ishida Y, Saito H, Ohta S, Hiei Y, Komari T, Kumashiro T (1996) High efficiency transformation of maize (*Zea mays* L.) mediated by *Agrobacterium tumefaciens*. *Nature Biotechnology* **14**, 745–750 doi:10.1038/nbt0696-745.

Ishida Y, Hiei Y, Komari T (2007) *Agrobacterium*-mediated transformation of maize. *Nature Protocols* **2**, 1614–1621 doi:10.1038/nprot.2007.241.

Jefferson RA, Kavanagh TA, Bevan MW (1987) GUS fusion: glucuronidase as a sensitive and versatile gene fusion marker in higher plants. *EMBO Journal* **6**, 3901–3907. doi:10.1002/j.1460-2075.1987.tb02730.x

Jiang Q, Fu C, Wang ZY (2019) A unified *Agrobacterium*-mediated transformation protocol for alfalfa (*Medicago sativa* L.) and *Medicago truncatula*. 'Transgenic Plants – Methods and Protocols' (Eds S Kumar, P Barone, M Smith) pp. 153–163. (Humana Press, New York).

Kajala K, Covshoff S, Karki S, Woodfield H, Tolley BJ, Dionora MJA, Mogul RT, Mabilangan AE, Danila FR, Hibberd JM, Quick WP (2011) Strategies for engineering a two-celled C_4 photosynthetic pathway into rice. *Journal of Experimental Botany* **62**, 3001–3010 doi:10.1093/jxb/err022.

Kanai R, Edwards GE (1999) 'The biochemistry of photosynthesis.' (Woodhead Publishing Limited: San Diego, CA).

Karimi G, Hosseinzadeh H, Ettehad N (2004) Evaluation of the gastric antiulcerogenic effects of *Portulaca oleracea* L. extracts in mice. *Phytotherapy Research* **18**, 484–487 doi:10.1002/ptr.1463.

Keeley JE, Rundel PW (2003) Evolution of CAM and C_4 carbon-concentrating mechanisms. *International Journal of Plant Sciences* **164**, S55–S77 doi:10.1086/374192.

Kerk NM, Ceserani T, Tausta SL, Sussex IM, Nelson TM (2003) Laser capture microdissection of cells from plant tissues. *Plant Physiology* **132**, 27–35 doi:10.1104/pp.102.018127.

Koch K, Kennedy RA (1980) Characteristics of crassulacean acid metabolism in the succulent C_4 Dicot, *Portulaca oleracea* L. *Plant Physiology* **65**, 193–197 doi:10.1104/pp.65.2.193.

Koch KE, Kennedy RA (1982) Crassulacean acid metabolism in the succulent C_4 dicot, *Portulaca oleracea* L under natural environmental conditions. *Plant Physiology* **69**, 757–761 doi:10.1104/pp.69.4.757.

Kochba J, Spiegel-Roy P (1977) The effects of auxins, cytokinins and inhibitors on embryogenesis in habituated ovular callus of the 'Shamouti' orange (*Citrus sinensis*). *Zeitschrift für Pflanzenphysiologie* **81**, 283–288 doi:10.1016/S0044-328X(77)80094-9.

Ku S-B, Shieh Y-J, Reger BJ, Black CC (1981) Photosynthetic characteristics of *Portulaca grandiflora*, a succulent C_4 dicot. *Plant Physiology* **68**, 1073–1080 doi:10.1104/pp.68.5.1073.

Kubaláková M, Doležel J, Lebeda A (1996) Ploidy instability of embryogenic cucumber (*Cucumis sativus* L.) callus culture. *Biologia Plantarum* **38**, 475–480 doi:10.1007/BF02896685.

Lara MV, Disante KB, Podestá FE, Andreo CS, Drincovich MF (2003) Induction of a crassulacean acid like metabolism in the C_4 succulent plant, *Portulaca oleracea* L.: physiological and morphological changes are accompanied by specific modifications in phospho*enol*pyruvate carboxylase. *Photosynthesis Research* **77**, 241–254 doi:10.1023/A:1025834120499.

Lara MV, Drincovich MF, Andreo CS (2004) Induction of a crassulacean acid-like metabolism in the C_4 succulent plant, *Portulaca oleracea* L.: study of enzymes involved in carbon fixation and carbohydrate metabolism. *Plant & Cell Physiology* **45**, 618–626 doi:10.1093/pcp/pch073.

Lindsey BE, Rivero L, Calhoun CS, Grotewold E, Brkljacic J (2017) Standardized method for high-throughput sterilization of *Arabidopsis* seeds. *Journal of Visualized Experiments* **2017**, 1–7 doi:10.3791/56587.

Livak KJ, Schmittgen TD (2001) Analysis of relative gene expression data using real-time quantitative PCR and the $2^{-\Delta\Delta CT}$ method. *Methods* **25**, 402–408 doi:10.1006/meth.2001.1262.

Maleckova E, Brilhaus D, Wrobel TJ, Weber APM (2019) Transcript and metabolite changes during the early phase of ABA-mediated induction of CAM in *Talinum triangulare*. *Journal of Experimental Botany* **70**, 6581–6596 doi:10.1093/jxb/erz189.

Martins PK, Ribeiro AP, Da Cunha BADB, Kobayashi AK, Molinari HBC (2015) A simple and highly efficient *Agrobacterium*-mediated transformation protocol for *Setaria viridis*. *Biotechnology Reports (Amsterdam, Netherlands)* **6**, 41–44 doi:10.1016/j.btre.2015.02.002.

Mazen AMA (1996) Changes in levels of phospho*enol*pyruvate carboxylase with induction of crassulacean acid metabolism (CAM)-like behavior in the C_4 plant *Portulaca oleracea*. *Physiologia Plantarum* **98**, 111–116 doi:10.1111/j.1399-3054.1996.tb00681.x.

Mazen AMA (2000) Changes in properties of phospho*enol*pyruvate carboxylase with induction of crassulacean acid metabolism (CAM) in the C_4 plant *Portulaca oleracea*. *Photosynthetica* **38**, 385–391 doi:10.1023/A:1010969419962.

Meisel L, Fonseca B, González S, Baeza-Yates R, Cambiazo V, Campos R, Gonzalez M, Orellana A, Retamales J, Silva H (2005) A rapid and efficient method for purifying high quality total RNA from peaches (*Prunus persica*) for functional genomics analyses. *Biological Research* **38**, 83–88 doi:10.4067/S0716-97602005000100010.

Moghadam YA, Piri K, Bahramnejad B, Ghiasvand T (2014) Dopamine production in hairy root cultures of *Portulaca oleracea* (Purslane) using *Agrobacterium rhizogenes*. *Journal of Agricultural Science and Technology* **16**, 409–420.

Murashige T, Skoog F (1962) A revised medium for rapid growth and bio assays with tobacco tissue cultures. *Physiologia Plantarum* **15**, 473–497. doi:10.1111/j.1399-3054.1962.tb08052.x

Newell CA, Brown NJ, Liu Z, Pflug A, Gowik U, Westhoff P, Hibberd JM (2010) Agrobacterium tumefaciens-mediated transformation of *Cleome gynandra* L., a C_4 dicotyledon that is closely related to *Arabidopsis thaliana*. *Journal of Experimental Botany* **61**, 1311–1319 doi:10.1093/jxb/erq009.

Nguyen DQ, Van Eck J, Eamens AL, Grof CPL (2020) Robust and reproducible *Agrobacterium*-mediated transformation system of the C_4 genetic model species *Setaria viridis*. *Frontiers in Plant Science* **11**, 281 doi:10.3389/fpls.2020.00281.

Notredame C, Higgins DG, Heringa J (2000) T-coffee: a novel method for fast and accurate multiple sequence alignment. *Journal of Molecular Biology* **302**, 205–217 doi:10.1006/jmbi.2000.4042.

Ocampo G, Columbus JT (2012) Molecular phylogenetics, historical biogeography, and chromosome number evolution of *Portulaca* (Portulacaceae). *Molecular Phylogenetics and Evolution* **63**, 97–112 doi:10.1016/j.ympev.2011.12.017.

Osmond CB (1978) Crassulacean acid metabolism: a curiosity in context. *Annual Review of Plant Physiology* **29**, 379–414 doi:10.1146/annurev.pp.29.060178.002115.

Osuna D, Usadel B, Morcuende R, Gibon Y, Bläsing OE, Höhne M, Günter M, Kamlage B, Trethewey R, Scheible W, Stitt M (2007) Temporal responses of transcripts, enzyme activities and metabolites after adding sucrose to carbon-deprived *Arabidopsis* seedlings. *The Plant Journal* **49**, 463–491 doi:10.1111/j.1365-313X.2006.02979.x.

Pengelly JJL, Tan J, Furbank RT, von Caemmerer S (2012) Antisense reduction of NADP-malic enzyme in *Flaveria bidentis* reduces flow of CO_2 through the C_4 cycle. *Plant Physiology* **160**, 1070–1080 doi:10.1104/pp.112.203240.

Pfaffl MW, Tichopad A, Prgomet C, Neuvians T (2004) Determination of most stable housekeeping genes, differentially regulated target genes and sample integrity: BestKeeper. *Biotechnology Letters* **26**, 509–515. doi:10.1023/B:BILE.0000019559.84305.47

Pihur V, Datta S, Datta S (2009) RankAggreg, an R package for weighted rank aggregation. *BMC Bioinformatics* **10**, 62 doi:10.1186/1471-2105-10-62.

Pino LE, Lombardi-Crestana S, Azevedo MS, Scotton DC, Borgo L, Quecini V, Figueira A, Peres LEP (2010) The *Rg1* allele as a valuable tool for genetic transformation of the tomato 'micro-tom' model system. *Plant Methods* **6**, 23 doi:10.1186/1746-4811-6-23.

Pirian K, Piri K (2012) Effect of methyl jasmonate and salicylic acid on noradrenalin accumulation in hairy roots of *Portulaca oleracea* L. *International Research Journal of Applied and Basic Sciences* **3**, 213–218.

Porto BN, Magalhães PC, Campos NA, Alves JD, Magalhães MM (2010) Otimização de protocolos de extração de RNA em diferentes tecidos de milho Brenda. *Revista Brasileira de Milho e Sorgo* **9**, 189–200. doi:10.18512/1980-6477/rbms.v9n2p189-200

Potrykus I (1995) 'Gene transfer to plants.'(Eds I Potrykus, G Spangenberg) (Springer-Verlag: Berlin)

R Core Team (2019) R: a language and environment for statistical computing. (R Foundation for Statistical Computing, Vienna, Austria) Available at https://www.R-project.org/ [Verified 26 October 2020]

Radhakrishnan R, Zakaria MNM, Islam MW, Chen HB, Kamil M, Chan K, Al-Attas A (2001) Neuropharmacological actions of *Portulaca oleraceae* L v. *sativa* (Hawk). *Journal of Ethnopharmacology* **76**, 171–176 doi:10.1016/S0378-8741(01)00230-6.

Rahdari P, Tavakoli S, Hosseini SM (2012) Studying of salinity stress effect on germination, proline, sugar, protein, lipid and chlorophyll content in purslane (*Portulaca oleracea* L.) leaves. *Journal of Stress Physiology & Biochemistry* **8**, 182–193.

Rashed AN, Afifi FU, Disi AM (2003) Simple evaluation of the wound healing activity of a crude extract of *Portulaca oleracea* L. (growing in Jordan) in *Mus musculus* JVI-1. *Journal of Ethnopharmacology* **88**, 131–136 doi:10.1016/S0378-8741(03)00194-6.

Ream W (2009) *Agrobacterium tumefaciens* and *A. rhizogenes* use different proteins to transport bacterial DNA into the plant cell nucleus. *Microbial Biotechnology* **2**, 416–427 doi:10.1111/j.1751-7915.2009.00104.x.

Reid KE, Olsson N, Schlosser J, Peng F, Lund ST (2006) An optimized grapevine RNA isolation procedure and statistical determination of reference genes for real-time RT-PCR during berry development. *BMC Plant Biology* **6**, 27 doi:10.1186/1471-2229-6-27.

Sage RF (2002) Are crassulacean acid metabolism and C4 photosynthesis incompatible? *Functional Plant Biology* **29**, 775–785 doi:10.1071/PP01217.

Sage RF, Li M, Monson RK (1999) The taxonomic distribution of C_4 photosynthesis. In 'C_4 Plant Biology.' pp. 551–584. (Woodhead Publishing Limited, San Diego, CA) doi:10.1016/b978-012614440-6/50017-3

Sedaghati B, Haddad R, Bandehpour M (2019) Efficient plant regeneration and *Agrobacterium*-mediated transformation via somatic embryogenesis in purslane (*Portulaca oleracea* L.): an important medicinal plant. *Plant Cell, Tissue and Organ Culture* **136**, 231–245 doi:10.1007/s11240-018-1509-3.

Singh J, Singh K (1967) Contribution to the ecology of ten noxious weeds. *Journal of the Indian Botanical Society* **46**, 440–451.

Srivastava S, Srivastava AK (2007) Hairy root culture for mass-production of high-value secondary metabolites. *Critical Reviews in Biotechnology* **27**, 29–43 doi:10.1080/07388550601173918.

Strable J, Scanlon MJ (2009) Maize (*Zea mays*): a model organism for basic and applied research in plant biology. *Cold Spring Harbor Protocols* **2009**, doi:10.1101/pdb.emo132.

Sun H-P, Li F, Ruan Q-M, Zhong X-H (2016) Identification and validation of reference genes for quantitative real-time PCR studies in *Hedera helix* L. *Plant Physiology and Biochemistry* **108**, 286–294 doi:10.1016/j.plaphy.2016.07.022.

Suzuki T, Higgins PJ, Crawford DR (2000) Control selection for RNA quantitation. *BioTechniques* **29**, 332–337 doi:10.2144/00292rv02.

Temel A, Kartal G, Gozukirmizi N (2008) Genetic and epigenetic variations in barley calli cultures. *Biotechnology, Biotechnological Equipment* **22**, 911–914 doi:10.1080/13102818.2008.10817577.

Thellin O, Zorzi W, Lakaye B, De Borman B, Coumans B, Hennen G, Grisar T, Igout A, Heinen E (1999) Housekeeping genes as internal standards: use and limits. *Journal of Biotechnology* **75**, 291–295 doi:10.1016/S0168-1656(99)00163-7.

Usadel B, Bläsing OE, Gibon Y, Retzlaff K, Höhne M, Günther M, Stitt M (2008) Global transcript levels respond to small changes of the carbon status during progressive exhaustion of carbohydrates in *Arabidopsis* rosettes. *Plant Physiology* **146**, 1834–1861 doi:10.1104/pp.107.115592.

Vandesompele J, Preter KDP, Pattyn F, Poppe B, Van Roy N, De Paepe A, Speleman F (2002) Accurate normalization of real-time quantitative RT-PCR data by geometric

averaging of multiple internal control genes. *Genome Biology* **3**, 1–12 doi:10.1613/jair.4265

von Caemmerer S, Furbank RT (2016) Strategies for improving C_4 photosynthesis. *Current Opinion in Plant Biology* **31**, 125–134. doi:10.1016/j.pbi.2016.04.003

von Caemmerer S, Quinn V, Hancock NC, Price GD, Furbank RT, Ludwig M (2004) Carbonic anhydrase and C_4 photosynthesis: a transgenic analysis. *Plant, Cell & Environment* **27**, 697–703 doi:10.1111/j.1365-3040.2003.01157.x.

von Caemmerer S, Quick WP, Furbank RT (2012) The development of C_4 rice: current progress and future challenges. *Science* **336**, 1671–1672 doi:10.1126/science.1220177.

Voznesenskaya EV, Koteyeva NK, Edwards GE, Ocampo G (2010) Revealing diversity in structural and biochemical forms of C_4 photosynthesis and a C_3- C_4 intermediate in genus *Portulaca* L. (Portulacaceae). *Journal of Experimental Botany* **61**, 3647–3662 doi:10.1093/jxb/erq178.

Wang L, Wu R, Bo W (2018) Transcriptome profiling of *PeCRY1* transgenic *Populus tomentosa*. *Genes & Genomics* **40**, 349–359 doi:10.1007/s13258-017-0631-7.

Wenzel GE, Fontana JD, Correa JBC (1990) The viscous mucilage from the weed *Portulaca oleracea*, L. *Applied Biochemistry and Biotechnology* **24–25**, 341–353 doi:10.1007/BF02920258.

Westhoff P, Gowik U (2004) Evolution of C_4 phospho*enol*pyruvate carboxylase. Genes and proteins: a case study with the genus *Flaveria*. *Annals of Botany* **93**, 13–23 doi:10.1093/aob/mch003.

Winter K (2019) Ecophysiology of constitutive and facultative CAM photosynthesis. *Journal of Experimental Botany* **70**, 6495–6508 doi:10.1093/jxb/erz002.

Winter K, Holtum JAM (2007) Environment or development? Lifetime net CO_2 exchange and control of the expression of crassulacean acid metabolism in *Mesembryanthemum crystallinum*. *Plant Physiology* **143**, 98–107 doi:10.1104/pp.106.088922.

Winter K, Holtum JAM (2014) Facultative crassulacean acid metabolism (CAM) plants: powerful tools for unravelling the functional elements of CAM photosynthesis. *Journal of Experimental Botany* **65**, 3425–3441 doi:10.1093/jxb/eru063.

Winter K, Holtum JAM (2017) Facultative crassulacean acid metabolism (CAM) in four small C_3 and C_4 leaf-succulents. *Australian Journal of Botany* **65**, 103–108 doi:10.1071/BT16015.

Winter K, Smith JAC (1996) An introduction to crassulacean acid metabolism. In 'Crassulacean acid metabolism – biochemistry, ecology and evolution'. (Eds K Winter, JAC Smith) pp. 1–10. (Springer-Verlag: Heidelberg, Germany)

Winter K, Sage RF, Edwards EJ, Virgo A, Holtum JAM (2019) Facultative crassulacean acid metabolism in a C_3–C_4 intermediate. *Journal of Experimental Botany* **70**, 6571–6579 doi:10.1093/jxb/erz085.

Yang X, Cushman JC, Borland AM, Edwards EJ, Wullschleger SD, Tuskan GA, Owen NA, Griffiths H, Smith JAC, Paoli HC, *et al*. (2015) A roadmap for research on crassulacean acid metabolism (CAM) to enhance sustainable food and bioenergy production in a hotter, drier world. *New Phytologist* **207**, 491–504 doi:10.1111/nph.13393.

Zimmerman CA (1976) Growth characteristics of weediness in *Portulaca oleracea* L. *Ecology* **57**, 964–974 doi:10.2307/1941061.

Supporting Information

Supplementary tables are available at https://doi.org/10.1071/FP20202.

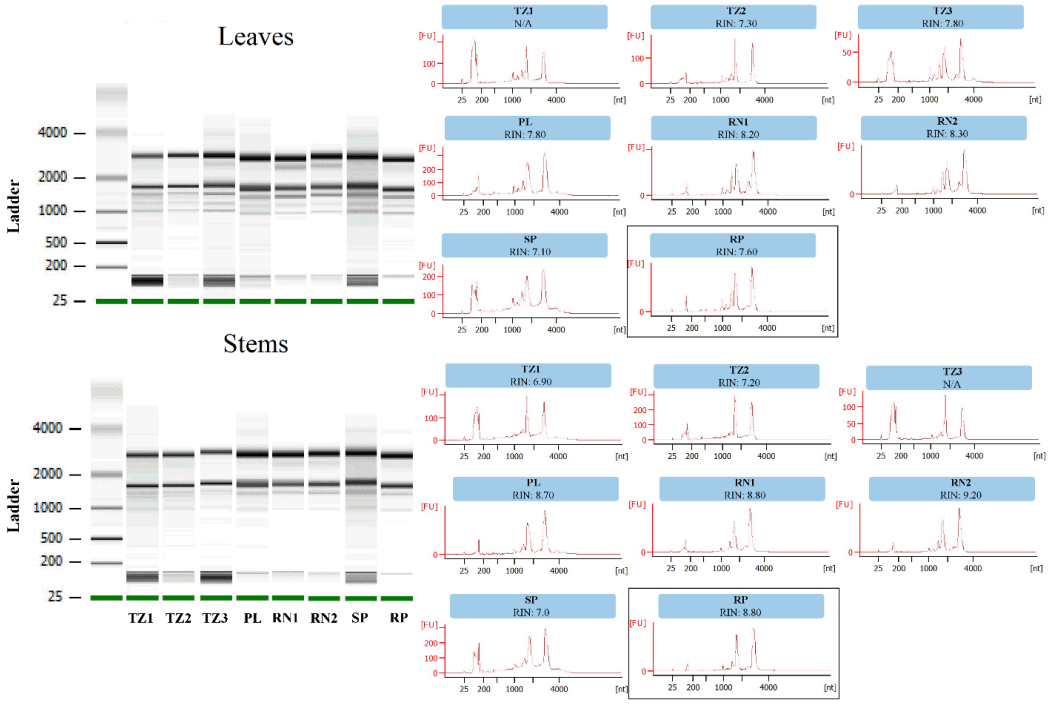

Fig. S1. Representative gel images produced via Bioanalyzer 2100 for *Portulaca oleracea* leaf and stem samples. These images were generated as a result of RNA quality assessment. RNA Integrity Number (RIN) ≥ 7 was considered good.

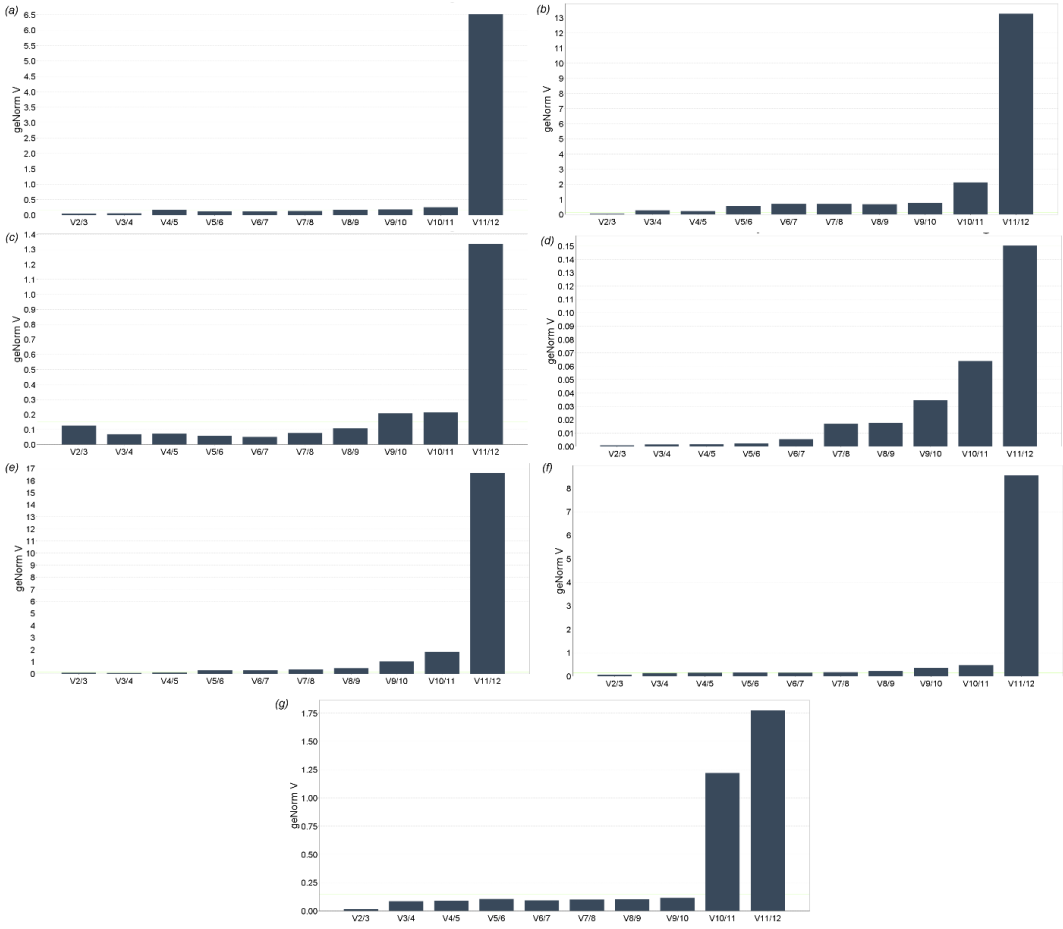

Fig. S2. Pairwise variation (V) analysis of the twelve candidate reference genes in different *Portulaca oleracea* sample sets. Vn/Vn_{+1} was analyzed between the normalization factors Vn and Vn_{+1} by geNorm to determine the optimal number of reference genes required for qPCR data normalization. (a) Leaf development series. (b) Drought stress series. (c) Hormonal treatment series. (d) Salt stress series. (e) Subspecies series. (f) Diel time of sampling series. (g) Tissue series.

Chapter V

A matter of time: regulatory events behind the synchronization of C_4 and crassulacean acid metabolism gene expression in *Portulaca oleracea*

"I went to the woods because I wished to live deliberately, to front only the essential facts of life, and see if I could not learn what it had to teach, and not, when I came to die, discover that I had not lived. I did not wish to live what was not life, living is so dear; nor did I wish to practice resignation, unless it was quite necessary. I wanted to live deep and suck out all the marrow of life, to live so sturdily and Spartan-like as to put to rout all that was not life.

Henry David Thoreau

This chapter is organized as to be submitted to the Journal of Experimental Botany:

Ferrari, RC; Kawabata, AB; Ferreira, SS; Hartwell, J; Freschi, F. A matter of time: regulatory events behind the synchronization of C_4 and crassulacean acid metabolism gene expression in *Portulaca oleracea*.

Supplementary information is available at https://drive.google.com/drive/folders/1lyMZKS_CFHM4jTqeVe3tvb63oK7eaBKK?usp=sharing.

Highlights

A dynamic interplay between phytohormones, transcription factors and the circadian clock provides strict temporal coordination of C_4 and crassulacean acid metabolism gene expression in purslane under changing environmental conditions.

Abstract

Portulaca species can switch between C_4 and crassulacean acid metabolism (CAM) depending on environmental conditions. However, the regulatory mechanisms behind this rare photosynthetic adaptation remain elusive. Using *Portulaca oleracea* as a model system, here we investigated the involvement of the circadian clock, plant hormones and transcription factors in coordinating C_4 and CAM gene expression. Free-running experiments in constant conditions revealed that C_4 and CAM gene expression are intrinsically controlled by the circadian clock. Detailed time-course drought and rewatering experiments revealed distinct timeframes for CAM induction and reversion (days *versus* hours, respectively), which were accompanied by changes in abscisic acid (ABA) and cytokinin metabolism and signaling. Exogenous ABA and cytokinins were shown to promote and repress CAM expression in *P. oleracea*, respectively. Moreover, the drought-induced decline in C_4-transcript levels was completely recovered upon cytokinin treatment. The ABA-regulated transcription factors *HB7*, *NFYA7*, *NFYC9, TT8* and *ARR12* were identified as the most likely candidate regulators of CAM induction, whereas *NFYC4* and *ARR9* were connected to C_4 expression patterns. Therefore, we provided the first insights on the signaling events controlling C_4-CAM transitions in response to water availability and over the day/night cycles, highlighting candidate genes for future functional studies in the context of facultative C_4-CAM photosynthesis.

Keywords

Abscisic acid; Circadian clock; Crassulacean acid metabolism; C_4 photosynthesis; Cytokinin; Drought; Facultative CAM; Portulacaceae; Purslane; Transcription factors.

Introduction

C_4 photosynthesis and the crassulacean acid metabolism (CAM) are two carbon concentrating mechanisms (CCMs) that have evolved multiple times, each of them causing a rewiring of the plant primary metabolism and conferring adaptative advantages for species occupying particularly arid and light-intense environments (Edwards and Ogburn, 2012). In both C_4 and CAM, the cycle starts with a temporary CO_2 fixation step carried out by phospho*enol*pyruvate carboxylase (PPC), leading to the formation of a 4-carbon acid, commonly malate. Subsequently, malate is decarboxylated, generating CO_2 to sustain Rubisco activity (Kanai and Edwards, 1999; Dodd *et al.*, 2002). Similar enzymes are employed, but while C_4 relies on a spatial specialization to concentrate CO_2 in the vicinity of Rubisco, CAM provides temporary CO_2 concentration at night, preceding the daytime Rubisco activity under closed stomata (Winter and Smith, 1996; Sage, 2004). The CAM cycle is highly connected to the plant circadian clock (Hartwell, 2005) and requires multiple regulatory mechanisms to minimize futile cycles of carbon turnover over the diel cycle (Borland and Taybi, 2004; Borland *et al.*, 2016).

Overall, evolutionary, anatomical and physiological constraints contribute to the incompatibility between the two CCMs to simultaneously occur in the same cells and avoid futile cycling (Sage, 2002). As a result, the concomitant occurrence of both C_4 and CAM within a single species is uncommon, and the best example of this exception is the *Portulaca* lineage (Winter *et al.*, 2019). In leaves of *P. oleracea* L., the C_4-CAM transition is triggered by water availability (Koch and Kennedy, 1980, 1982; Winter and Holtum, 2014). Under drought, CAM genes are induced, the diel expression of C_4/CAM-shared genes is rescheduled, and the mRNA levels of many of the key C_4 genes are significantly reduced (Ferrari *et al.*, 2020*b*). This pattern is completely reversed upon rewatering, highlighting the flexibility of this photosynthetic transition (Ferrari *et al.*, 2020*c*). Hence, *P. oleracea* serves as a natural blueprint for how C_4 and CAM are connected inside the same organism, and may facilitate the identification of the regulatory, physiological and biochemical requirements for C_4 and CAM co-occurrence within a single leaf.

Although the first reports of the occurrence of both CCMs in *P. oleracea* date back to the early 1980s (Koch and Kennedy, 1980), only more recently the gene expression reprogramming required for the C_4-to-CAM transition in this species started to be elucidated (Christin *et al.*, 2014; Ferrari *et al.*, 2020*b*). The recruitment of specific *PPC* genes to function in C_4 and CAM (*PPC-1E1a'* and *PPC-1E1c*, respectively) was confirmed across multiple *P. oleracea* accessions and under distinct experimental designs (Ferrari *et al.*, 2020*c*,*a*). Additional C_4-marker genes have also been described for *P. oleracea*, including genes involved in carboxylation (beta-carbonic anhydrase - *βCA-2E3*), acid formation (aspartate aminotransferase - *ASPAT-1E1;* alanine aminotransferase - *ALAAT-1E1*),

decarboxylation (NAD-malate dehydrogenase - *NADME-2E.1*) and PEP regeneration reactions (adenylate kinase protein - *AK-1;* pyruvate, phosphate dikinase - *PPDK-1C1b.1*), as well as intracellular malate transport (aluminum-activated malate transporter - *ALMT-12E.2*) (Christin *et al.*, 2014; Ferrari *et al.*, 2020*b*).

Given the facultative nature of the C_4-CAM transition in *P. oleracea*, a regulatory network fine-tuning the expression of each or both CCMs in response to the environmental cues should be expected. In C_3-CAM facultative species, accumulating evidence indicates abscisic acid (ABA) as a major endogenous signal connecting the plant water status and CAM expression (Taybi *et al.*, 2002). On the other hand, a repressor and still controversial role of cytokinins (CK) on CAM has been described in both facultative and constitutive CAM species (Schmitt and Piepenbrock, 1992; Thomas *et al.*, 1992; Thomas and Bohnert, 1993; Dai *et al.*, 1994; Peters *et al.*, 1997). More recently, transcription factors have been proposed as candidate regulators of CAM induction in facultative species such as *Mesembryanthemum crystallinum* and *Talinum triangulare* (Brilhaus *et al.*, 2016; Amin *et al.*, 2019), though their connections with hormonal signals, including ABA and CKs, are currently unknown.

Whether similar regulatory networks regulate inducible CAM in a C_3 or C_4 background remains elusive. In addition, whether the circadian molecular clock plays equivalent roles in controlling the C_4 and CAM-related gene expression also remains to be elucidated. Given the opposite impacts of water availability on CCM expression in *P. oleracea* (Ferrari *et al.*, 2020*b*,*c*), we hypothesize that drought-induced temporal changes in leaf cell signaling may be as important to promote CAM expression as to limit the transcription of C_4 genes in this species. Here we provide the first insights into the circadian control and the molecular signaling events behind the synchronization of C_4 and CAM pathways in *P. oleracea* plants facing contrasting watering regimes. Moreover, candidate regulators were identified as likely involved in this peculiar photosynthetic transition, ranging from drought- and ABA-regulated transcription factors to ABA-cytokinin crosstalk elements.

Material and methods

Plant material, growth conditions and sampling

Seeds from a commercial cultivar of *Portulaca oleracea* were germinated and grown in 300-ml square pots containing commercial substrate (Plantmax HT) and vermiculite. Comprehensive morphological and biochemical characterization of this *P. oleracea* accession is provided in Ferrari et al. (Ferrari *et al.*, 2020*c*). Unless otherwise specified, plants were grown in a growth chamber at a 12h photoperiod (light period from 06:00 to 18:00), 27 ± 1°C day : 22 ± 1°C night temperature, 65 ± 10 % day : 80 ± 10% night air humidity, and a photosynthetic flux density (PFD) of 400 µmol m^{-2} s^{-1}.

For all analyses and experiments in this work, four biological replicates were sampled, and each replicate was composed of all fully-expanded, non-senescent leaves from three plants. Following sampling, leaves were immediately frozen in liquid nitrogen (N_2) and stored at -80°C until powdered and used in analyses.

Drought and rewatering treatments

To investigate the drought-induced C_4-to-CAM transition, 30-day-old plants were either subjected to complete water withholding (drought-stressed) or watered daily as a control (well-watered). Leaves were sampled after 3, 6, 9, 12, 15, 18, 21 and 22 days of treatment at dawn (07:00, 1 h after the onset of illumination) and dusk (17h:00, 1 h before the end of the light period). To analyze the CAM-to-C_4 transition, plants were induced to CAM after 21 days of drought and subequently rewatered for 0, 0.5, 1, 1.5, 2, 3, 4, 5, 6, 8 and 12 h before sampling. As most CCM genes display a marked diel fluctuation (Ferrari *et al.*, 2020*b*), rewatering was started at distinct moments of the day or night to ensure the simultaneous sampling of all rewatering treatments in a single moment of the diel cycle. For genes with nocturnal peak expression, sampling occurred at 20:00 (two hours after the end of illumination), with rewatering events starting at 19:30, 19:00, 18:30, 18:00, 17:00, 16:00, 15:00, 14:00, 12:00 and 8:00. For genes with diurnal peak expression, sampling took place at 04:00 (two hours before the illumination), with rewatering events starting at 3:30, 3:00, 2:30, 2:00, 1:00, 24:00, 23:00, 22:00, 20:00 and 16:00. Plant and soil water status were monitored as described in Ferrari et al. (Ferrari *et al.*, 2020*b*).

Plant hormone treatments

To examine the role of abscisic acid and cytokinins on the C_4 and CAM machineries, short- and long-term treatments with these hormones were performed at the concentrations specified in each experiment. In all cases, hormones were dissolved in 0.001% (v/v) Tween-20 in water. For the short-term treatments, 60-day-old plants kept well-watered or droughted for 21 days were sprayed with 500 μM ABA or 6-benzylaminopurine (BA) at the start or the end of the light period and sampled approximately 12hs later. For the long-term treatment of well-watered plants, 30-day-old plants were sprayed with 0, 25, 100 and 500 μM ABA for four consecutive days and sampled on the fifth day. For the long-term treatment of droughted plants, 30-day-old plants were sprayed every 5 days with 0, 5, 10, 20 μM of BA or *trans*-zeatin (Z) during the course of 20 days and sampled on 21th day. Sampling for both ABA and CKs long-term treatments occurred at dawn (07:00, 1 h after the onset of illumination) and dusk (17h:00, 1 h before the end of the light period).

Light/dark and free-running circadian time-course experiments

For free-running circadian time-course experiments (LL), 30-day-old plants were grown under the standard 12h-photoperiod conditions (LD) and either subjected to complete water withholding (drought-stressed) or watered daily (well-watered) for 21 days. Two days before sampling, plants were switched to LL after a dark period and kept under constant light, temperature and humidity, or maintained under LD conditions as a control. For LL, the constant conditions were as follows: light 100 µmol m^{-2} s^{-1}, temperature 22 ± 1°C and air humidity 70 ± 10 %. Mature leaves were sampled every three hours for 24h, starting after 48h of the LL treatment.

Titratable acidity analysis

Leaf titratable acidity was determined as described in Ferrari et al. (2020*b*). Briefly, frozen leaf samples (200 mg fresh weight – FW) were extracted in 1 ml 80 % (v/v) methanol for 10 min at 80°C, and the supernatants were recovered by centrifugation (15,000 g, 10 min, 25 ºC). The pellets were re-extracted three times, and all supernatants were combined before the analysis. Aliquots of the supernatant fraction were titrated with 0.2 M NaOH to pH 8.0 using phenolphthalein as an indicator. Dawn and dusk values were subtracted to calculate diel acidity changes (ΔH^+), with positive values indicating nocturnal accumulation. Standard errors were calculated as follows: $SE_{\Delta H+} = \sqrt{((\text{standard error}_{\text{well-watered}})^2 + (\text{standard error}_{\text{droughted}})^2}$ (Popp *et al.*, 2003).

Abscisic acid (ABA) quantification

Endogenous ABA levels were determined by gas chromatography-tandem mass spectrometry-selective ion monitoring. Briefly, frozen leaf samples (~100 mg FW) were extracted with an isopropanol: acetic acid (95:5 v/v) solution containing 0.5 µg of the labeled ABA standard ([$^2H_6$]-ABA, Olchemin Ltd) and maintained under constant shaking for 2 h at 4 °C. The mixture was centrifuged at 13,000 *g,* and the supernatant was recovered and concentrated to 50 µl under nitrogen gas flow. Thereafter, 200 µl of ultrapure water was added, and phase partition was performed with 500 µl of ethyl acetate. The separated organic phase was transferred to a new tube and dried under a nitrogen gas flow. Samples were methylated with trimethylsilyldiazomethane, dried under nitrogen gas flow, and re-suspended in ethyl acetate. The material was analyzed by gas chromatography (model 6890) coupled to mass spectrometry (Shimadzu model: GCMS-QP2010 SE) using an HP-1701 column (30 m, 0.25mm ID, internal film 0.50mm thick). Helium was used as the carrier gas at a flow rate of 4 ml min^{-1} in the following program: 3 min at 150 °C, followed by a ramp by 5 °C min^{-1} to 210 °C and 15 °C min^{-1} to 260 °C. Ions with (m/*z*) 134, 162 and 190 (corresponding to endogenous ABA) and 138, 166 and 194 (corresponding to [$^2H_6$]-ABA) were monitored.

RNA extraction and real-time quantitative polymerase chain reaction (RT-qPCR) analysis

Total RNA was extracted from approx. 80 mg of frozen leaves using the ReliaPrep RNA Tissue Miniprep System (Promega) for fibrous tissues and following the protocol described in Ferrari *et al.* (2020*a*). Complementary DNA synthesis used SuperScript IV Reverse Transcriptase kit (Thermo Fisher Scientific) and RT-qPCR reactions were performed in a QuantStudio Real-Time PCR system (Applied Biosystems, Thermo Fisher Scientific), using 10 µl mix reaction and run conditions as described in Ferrari et al. (2020*b*). The relative transcript abundance was calculated by applying the $2^{-\Delta\Delta CT}$ method (Livak and Schmittgen, 2001). All primer sequences used are listed in Table S1. Reference genes were chosen according to Ferrari *et al.* (2020*a*).

Statistical Analysis

All statistical analyses were performed using R (version 3.6.1; R Core Team, 2021) via RStudio (version 1.2.1335). The data was checked for normality and variance, and appropriate tests were applied (Ferrari *et al.*, 2020*b*). Correlation indexes were generated using R package "corrr".

Bioinformatic analysis: transcriptomic data, co-expression analysis and data mining

Each of the 32,306 contigs identified in Ferrari *et al.* (2020*b*) for leaves of well-watered and droughted *P. oleracea* plants were associated with an *A. thaliana* gene identifier (AGI) based on sequence similarity analysis, and compared to the Arabidopsis transcriptome (Araport11 Official Release dataset) (Berardini *et al.*, 2015) using BLASTX (Camacho *et al.*, 2009) with e-value = 10^{-6} and the -max_hsps = 1 flag. Subsequently, AGI numbers were used to identify genes involved in key steps of ABA and CK metabolism and the molecular circadian clock. For hormone-related genes, the differential expression (DE) analysis data described in Ferrari et al. (2020*b*) was used to filter the most modulated contigs ($\log_2$ fold-change (logFC) > |1.5| with adjusted p-value (false discovery rate - FDR) < 0.05 when comparing well-watered and droughted leaves).

For transcription factor (TF) identification, peptide sequences identified as *A. thaliana* TFs were downloaded from two different online plant transcription factor databases, each on version 3.0 (Jin *et al.*, 2014) and 5.0 (Pérez-Rodríguez *et al.*, 2010), and blasted against the *P. oleracea* transcriptome.

For the co-expression analysis, the low expression transcripts (total TPM < 5) were filtered from well-watered and droughted leaf RNA-seq libraries (Ferrari *et al.*, 2020*b*) and used to construct two co-expression networks, one for each water availability condition, with the WGCNA R-package (Langfelder and Horvath, 2008). The following parameters were used for both sample sets: power = 12, corType = "bicor", networkType = "signed hybrid",

TOMType = "signed", minModuleSize = 30, maxPOutliers = 0.05, reassignThreshold = 0, mergeCutHeight = 0.20, pamRespectsDendro = FALSE, maxBlockSize = 40000. DE data for these genes was retrieved and filtered for TF homologs presenting logFC > |1.5|; FDR < 0.05 when comparing well-watered and droughted leaves.

Results and discussion

Impacts of free-running conditions on clock genes and on diel CAM and C_4 gene expression

Circadian clock-controlled mechanisms affect multiple photosynthesis-related processes in plants, ranging from stomatal aperture and CO_2 assimilation (McClung, 2001) to CAM expression (Hartwell, 2005). To explore the connection between the circadian clock and the CCM functioning in *P. oleracea*, we performed a prolonged free-running experiment in constant light, temperature and air humidity (LL) using C_4 and CAM-performing adult plants. For this, individuals subjected to well-watered and drought conditions for 21 days under light/dark (LD) conditions were kept under LD or transferred to LL conditions, and harvested every three hours for 24h, starting after 48h of the LL treatment (Fig. 1A).

The impacts of the free-running conditions on the circadian clock in *P. oleracea* were monitored by determining the transcript fluctuations of key clock gene components selected based on previous studies with CAM plants (Boxall *et al.*, 2017, 2020) (Table S2). In plants, the basic clock mechanism in the central oscillator works as an interlocked feedback loop, and a typical cycle initiates with *CIRCADIAN CLOCK ASSOCIATED 1 (CCA1), LATE ELONGATED HYPOCOTYL 1 (LHY*) and *REVEILLE 1 (RVE1*) expression peaking at early morning (Alabadi *et al.*, 2002; Rawat *et al.*, 2009). Sequentially, a series of pseudo-response regulators accumulate (*PRR9, PRR7, PRR5*), repressing *CCA1/LHY/REV1* (Pokhilko *et al.*, 2012), which precedes *TIMING OF CAB EXPRESSION* (*TOC1*) nocturnal accumulation (Matsushika *et al.*, 2000). *FLAVIN-BINDING, KELCH REPEAT, F BOX 1 (FKF1*) represses *TOC1* and *PRR5,* and usually peaks 8 h after the start of illumination (Baudry *et al.*, 2010). Finally, *TOC1* peaks early in the dark period, and its own down-regulation at the end of the night leads to the up-regulation of *CCA1/LHY/RVE1*, restarting the cycle (Pokhilko *et al.*, 2010, 2012). *GIGANTEA (GI*) typically peaks 8-10 h after dawn and, alongside *FKF1,* regulates *CO (CONSTANS)* expression (Fowler *et al.*, 1999; Sawa *et al.*, 2007).

Under LD conditions, the diel patterns of *CCA1*, *LHY* and *RVE1* expression in leaves of well-watered *P. oleracea* plants genes were as described for other plant species (Alabadi *et al.*, 2002; Rawat *et al.*, 2009), with mRNA levels accumulating in the late dark period and peaking in the morning (Fig. 1B). After three days entrained in LL, all three genes were drastically down-regulated when compared to LD in both water availability conditions, revealing a clear amortization of these components of the circadian clock. Their mRNA levels were also down-regulated in droughted leaves under LD compared to well-watered

counterparts (Fig. S1A). *GI*, *PRR7* and *FKF1* transcript levels peaked in the late afternoon (16:00) under LD in both well-watered and droughted plants (Fig. 1B). This preceded *TOC1* accumulation at night, which peaked at 22:00 in LD (Fig. 1B). When comparing LL and LD conditions, *GI* and *PRR7* mRNA were kept at higher levels throughout the entire 24 h cycle in LL regardless of water availability treatments, and their transcripts were still abundant when *TOC1* transcripts peaked at 22:00 in LL (Fig. 1B). Under LL, *P. oleracea* plants displayed a rhythm with a greater amplitude for *GI, PRR7* and *FKF1* than LD-treated plants, except for *FKF1* in droughted plants, which collapsed to arrhythmia. *TOC1* was down-regulated in LL compared to LD in both well-watered and droughted leaves, but maintained rhythmicity (Fig. 1B).

The dampening of *CCA1* and *LHY* observed under LL in C_4-performing *P. oleracea* has also been described as a milder phase peak in maize plants under free-running conditions (Wang *et al.*, 2011). Additionally, a decrease in CCA1 level was observed when maize was entrained in LL for more than three days (Ko *et al.*, 2016). When CAM is induced in C_3 systems, the circadian clock is also strictly under the control of the *CCA1/LHY/TOC1* oscillator, as reported in *M. crystallinum* (Boxall *et al.*, 2005). After three days entrained in LL, *TOC1* and *CCA1* still maintained rhythmicity in *K. fedtschenkoi*, although peak phases were slightly changed (Boxall *et al.*, 2017). In addition, robust rhythmicity is sustained under LL for *GI*, *PRR7* and *FKF1* in both *K. fedtschenkoi* and *K. laxiflora*, both obligate CAM plants (Boxall *et al.*, 2017, 2020). However, in *K. laxiflora*, *CCA1* and *FKF1* transcript accumulation rhythms dampened rapidly under LL (Boxall *et al.*, 2020). Comparing the pieces of evidence for C_3 facultative or obligate CAM plants to the C_4-CAM system in *P. oleracea*, the described cycling patterns under well-watered or droughted conditions and the changes observed under LL are within the expected for the *CCA1/LHY/RVE1* and *TOC1* loop.

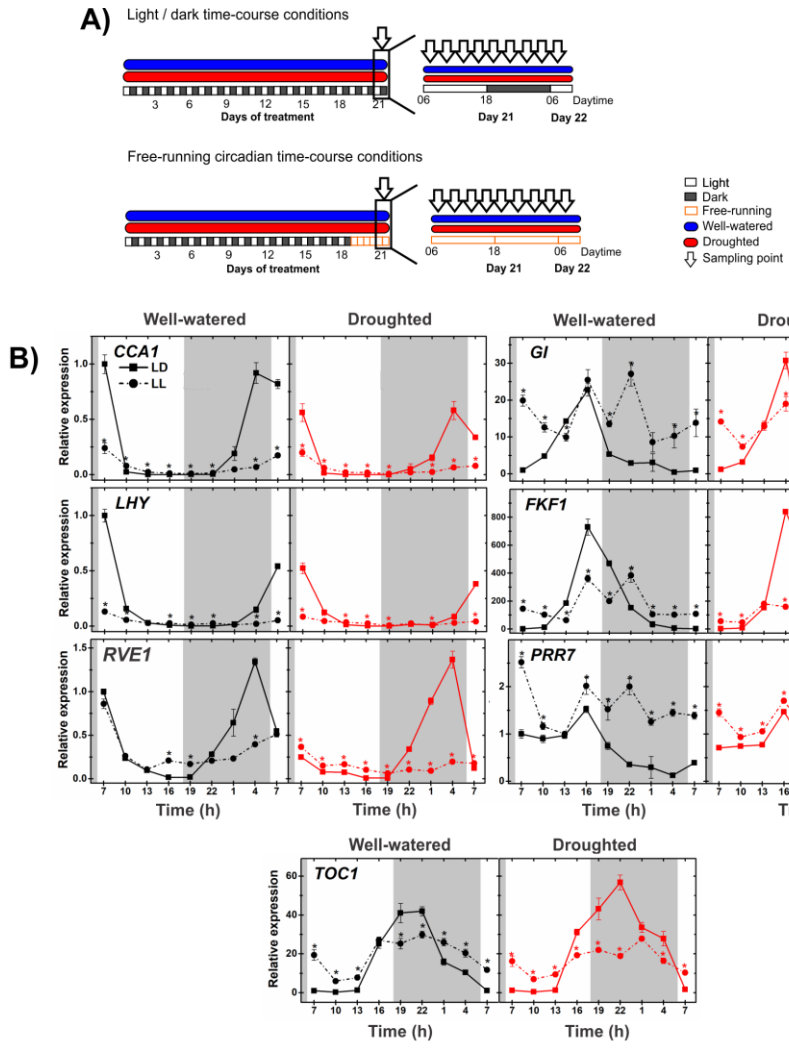
A)
Light / dark time-course conditions
Days of treatment
Day 21
Day 22
Daytime
Free-running circadian time-course conditions
Light
Dark
Free-running
Well-watered
Droughted
Sampling point
B)
Well-watered
Droughted
CCA1
LD
LL
GI
LHY
FKF1
RVE1
PRR7
TOC1
Relative expression
Time (h)
C)
PPC-1E1a'
βCA-2E3
ASPAT-1E1
NADME-2E.1
ALAAT-1E1
PPDK-1C1b.1
AK-1
ALMT-12E.2
PPC-1E1c
PPCK-1E

Fig. 1 Circadian clock-controlled expression of C_4- and CAM-related genes in *Portulaca oleracea*. (A) Schematic representation of the experimental design for the 12 h light / 12 h dark (LD) and constant light and temperature free-running (LL, 100 μmol m^{-2} s^{-1} at 22°C) time-course experiments. Well-watered or droughted plants were kept under LD or transferred to LL conditions, and mature leaves were sampled every three hours for 24h, starting after 48h of the LL treatment. (B) Transcript abundance of central circadian clock genes. (C) Transcript abundance of C_4- and CAM-related genes. Mean relative expression was normalized against the first time point of either well-watered (left) or droughted (right) leaf samples under the LD regime. The shaded areas indicate the dark and subjective dark periods. Data are means (± SE) of at least three replicates. $*P < 0.05$ compared with LD samples at each sampling time. AK, adenylate kinase; ALAAT, ALA aminotransferase; ALMT, aluminum-activated malate transporters; ASPAT, ASP aminotransferase; βCA, beta-carbonic anhydrase; CCA1; circadian clock associated 1; FKF1, flavin-binding kelch repeat F box 1; GI, gigantea; LHY, late elongated hypocotyl 1; NADME, NAD-malic enzyme; PPC, phospho*enol*pyruvate carboxylase; PPCK, phospho*enol*pyruvate carboxylase kinase; PPDK, pyruvate orthophosphate dikinase; PRR, pseudo-response regulator; RVE1, reveille 1; TOC1, timing of CAB expression.

We then monitored C_4- or CAM-marker transcripts under LD and LL to assess whether the free-running conditions affected the CCM expression. In well-watered plants, all eight C_4-markers genes exhibited similar circadian transcript fluctuation patterns under either LD or LL (Fig. 1C). Therefore, the C_4-related transcript accumulation in *P. oleracea* leaves maintained its circadian fluctuation under free-running conditions regardless of the amortization of the *CCA1/LHY/REV1* clock loop. In C_4 species, such as maize and sugarcane, a central molecular oscillator similar to C_3 plants has been described, and 10 to 30% of their transcriptome fluctuates in a circadian clock-controlled fashion (Khan *et al.*, 2010; Hotta *et al.*, 2013). Moreover, photosynthesis-related transcripts in maize oscillate in a circadian manner as in C_3 plants (Khan *et al.*, 2010).

After water was withheld for 21 days under LD conditions, *P. oleracea* leaves displayed significant nocturnal acid accumulation (ΔH^+) (Fig. S1C), and the CAM-marker *PPC-1E1c* gene was up-regulated at least 100-fold at late afternoon and nighttime (Fig. 1C). *PPC-1E1c* gene expression maintained circadian fluctuation in droughted plants under LL conditions (Fig. 1C), which agrees with findings for *PPC* genes in *K. laxiflora* under LL (Boxall *et al.*, 2020). In contrast, compared to LD-treated plants, a less conspicuous accumulation of titratable acidity was observed in *P. oleracea* during the subjective night (Fig. S1C), indicating that CAM functioning was limited under LL, as previously seen in *M. crystallinum* (Dodd *et al.*, 2003; Davies and Griffiths, 2012). Many factors may limit CAM functioning under LL conditions, including the disruption in diel carbon cycles, stomatal movements and CAM-related enzymatic activity (Wyka and Lüttge, 2003).

Additionally, we monitored *PPCK-1E* transcripts, as PPCK is responsible for phosphorylating PPC and plays a pivotal role in coupling the CCM cycles with the plant circadian clock both in C_4 and CAM species (Hartwell, 2005). *PPCK* is regulated by mRNA turnover in both CCMs, but is strongly linked to light in C_4 and the plant circadian clock in

CAM (Hartwell *et al.*, 1996, 1999; Hibberd and Covshoff, 2010). In *P. oleracea*, *PPCK-1E* may represent a bottleneck in the C_4 *versus* CAM differential regulation since it is one of the shared genes between the two CCMs in the species (Ferrari *et al.*, 2020*b*).

PPCK-1E transcripts peaked in the early morning and nighttime in well-watered and droughted plants, respectively (Fig. 1C), which agrees with previous findings under LD conditions (Ferrari et al 2020*b*). In contrast, *PPCK-1E* lost rhythmicity under LL (Figs. 1C, S1B), therefore, resembling the impacts of the free-running conditions on clock gene components (e.g., *GI*, *PRR7*). Although a 6-h delay in *PPCK* transcript abundance peak was observed in the C_3-CAM *M. crystallinum* under LL (Boxall *et al.*, 2005), in obligate CAM *K. fedstchenkoi* and *K. laxiflora,* PPCK transcript rhythms were easily discernible even after prolonged LL conditions (Dever *et al.*, 2015; Boxall *et al.*, 2017). Therefore, within all CCM genes investigated here in *P. oleracea, PPCK* diel expression was identified as the most susceptible to disturbances in the circadian cycling of clock components such as *CCA1/LHY/RVE1, PRR7, GI*, which were particularly affected under free-running conditions.

Temporal synchronization of C_4 and CAM gene expression in P. oleracea *under varying water supply*

After exploring the diel and circadian rhythms of CCM gene expression in C_4- and CAM-performing plants, we focused on dissecting the temporal synchronization of C_4 and CAM gene expression as water becomes scarce and during full rewatering. First, we performed a time-course analysis of ΔH^+ and mRNA levels of key genes of both CCMs in response to the water supply. Over a 22-day period of water withholding (Fig. 2A), soil water content (SVWC) was progressively reduced (Fig. 2B), resulting in a gradual decline in leaf Ψ_S after 12 days (Fig. 2C). However, ΔH^+ and *PPC-1E1c* transcripts revealed that CAM induction occurred after 6 days, thereby preceding any significant change in leaf Ψ_S (Fig. 2D). Therefore, as observed in *M. crystallinum* (Eastmond and Ross, 1997), a reduction in leaf cell turgor does not seem necessary for triggering CAM induction in *P. oleracea*, implicating the involvement of endogenous signals for interconnecting the water deficit perception and the C_4-to-CAM transition.

Maximum CAM expression was achieved within the 22-day period of water withholding, as indicated by the peak in ΔH^+ and *PPC-1E1c* transcript levels between 18 and 21 days, followed by a decline in both parameters on the last day of sampling (Fig. 2D-F). The lowest transcript abundances of C_4-marker genes were also detected after 18 days (Fig. 2E), indicating temporal synchronization in up- and down-regulation of CAM and C_4, respectively.

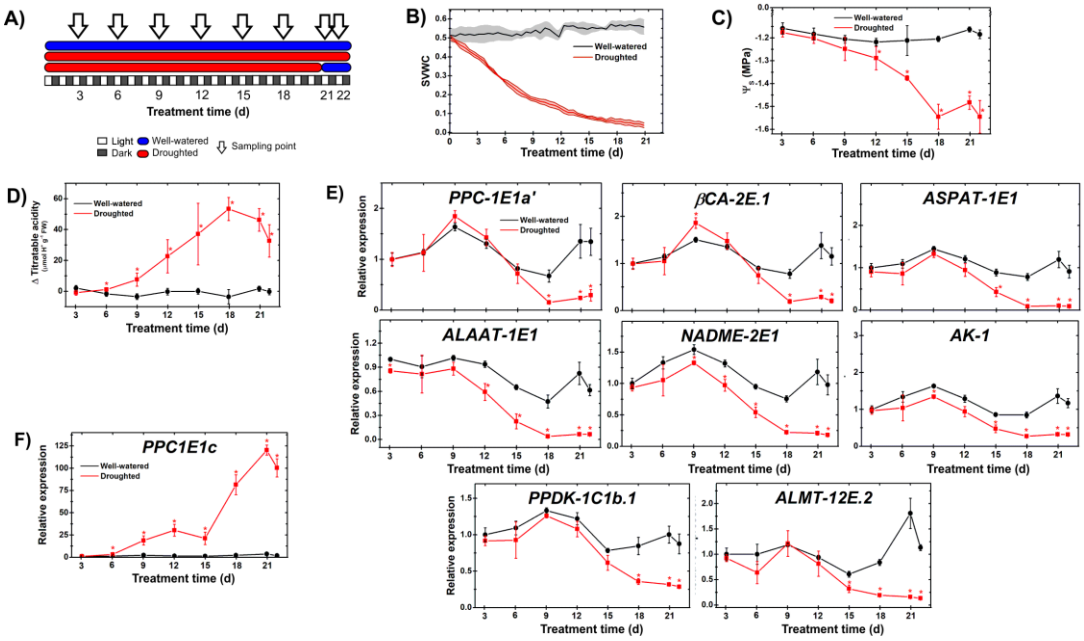

Fig. 2 Drought-induced CAM expression in *Portulaca oleracea* is accompanied by a progressive down-regulation in C_4-related gene expression. (A) Schematic representation of the experimental design for the time-course analysis of CAM induction by drought. Leaves of 30-day old plants were sampled every three days under well-watered or drought conditions at dawn and dusk. (B) Soil volumetric water content (SVWC). (C) Osmotic potential. (D) Nocturnal titratable acid accumulation (ΔH^+). (E) Transcript abundance of C_4-related genes. (F) Transcript abundance of CAM-related *PPC* gene. In D, ΔH^+ indicates dawn-dusk differences and SE of the dawn–dusk difference = $\sqrt{((SE_{dawn})^2 + (SE_{dusk})^2)}$. In E and F, mean relative expression was normalized against well-watered leaves at the start of the treatment. All gene expression data are from samples harvested at dawn, except for *PPC-1E1c,* which was sampled at dusk. Data are means (± SE) of at least three replicates. **P* < 0.05 compared with well-watered samples at each sampling time. AK, adenylate kinase; ALAAT, ALA aminotransferase; ALMT, aluminum-activated malate transporters; ASPAT, ASP aminotransferase; βCA, beta-carbonic anhydrase; NADME, NAD-malic enzyme; PPC, phospho*enol*pyruvate carboxylase; PPDK, pyruvate orthophosphate dikinase.

However, a comparative analysis of the mRNA levels of the two *PPC* genes revealed that after 18 days of water deprivation, *PPC-1E1a'* and *PPC-1E1c* transcripts are still equally abundant in the leaf tissues (Fig. S2). Therefore, C_4 and CAM may co-exist, at least at the transcriptional level, in droughted *P. oleracea* leaves. Since the simultaneous occurrence of C_4 and CAM cycles within the same cells would result in futile carbon cycling (Sage, 2002), these findings further highlight the importance of future attempts to localize both CCMs within the leaf tissues of *P. oleracea* plants under contrasting water conditions.

Our previous findings indicated that rewatering completely abolished CAM and recovered C_4 in *P. oleracea* leaves (Ferrari *et al.*, 2020*b*). Here, we explored the temporal dynamics required for this photosynthetic switch by measuring CCM-related gene expression after 12 and 24 h of rewatering. Nocturnal acid accumulation and C_4 and CAM gene expression were reverted to levels similar to well-watered plants after 24 h (Fig. S3A). Similarly, a 12-h

rewatering period also proved to be sufficient to revert CCM-related gene expression to well-watered levels (Fig. S3), indicating that the CAM to C_4 reversion occurred within 12h of rewatering. In C_3-CAM facultative species, reductions in nocturnal acid accumulation have also been demonstrated to occur within few days after rewatering, e.g. up to five days in *P. cyclophylla* and *P. digyna* (Holtum *et al.*, 2017*a*); one day in *Portulacaria afra* (Guralnick and Ting, 1986); two days for *Talinum triangulare* (Brilhaus *et al.*, 2016); four days in several *Calandrinia* species (Holtum *et al.*, 2017*b*).

Based on these findings, a detailed analysis was performed, focusing on the first hours after rewatering. As *PPC-1E1c* and *PPC-1E1a'* transcripts progressively accumulate at night and daytime, respectively (Ferrari *et al.*, 2020*b*), rewatering events were performed to cover the peak expression of these two CCM-marker genes (Fig. 3A). When comparing the rewatering-triggered transcript abundance changes for the abovementioned *PPC* genes, similar patterns were observed, regardless if water was resupplied either at night or during daytime (Fig. 3B).

Once the water supply was reestablished, gene expression reprogramming leading to CAM-to-C_4 reversion in *P. oleracea* occurred in a fast and remarkably synchronized manner. Limited changes in the transcript abundances of all CCM genes analyzed were observed within the first 4 h of rewatering, followed by a coordinated change in all CCM genes from 5 to 8 h after water resupply (Fig. 3B-C). Significant reductions in CAM-related *PPC* transcripts have also been demonstrated in *M. crystallinum* within 2.5 h after salt stress was interrupted (Vernon *et al.*, 1988). Considering the reduced contribution of weak CAM to overall carbon gain in CAM cycling plants such as *P. oleracea*, a quick reversion back to C_4 would ensure the reestablishment of CO_2 assimilation rates favoring growth (Herrera, 2009). Altogether, our data reveal distinct timeframes for the CAM induction and reversion (days and hours, respectively) in response to changes in soil water availability. Whereas C_4- and CAM-related gene expression co-exist under drought, the complete disappearance of CAM transcripts upon rewatering is fast and synchronized with the recovery of C_4-related gene expression.

ABA-cytokinin antagonism regulates C_4 and CAM expression in P. oleracea

Next, we took advantage of the flexible and fast-responding C_4-CAM system in *P. oleracea* leaves to dissect the regulatory processes allowing C_4-CAM co-existence in a single leaf. Plant hormones, particularly ABA, are crucial players in the signal transduction pathways mediating plant responses to water deficit (Zhang *et al.*, 2006). Based on *P. oleracea* transcriptome data (Ferrari *et al.*, 2020*b*), several ABA-related transcripts were identified as strongly modulated in response to water availability, including critical components of both ABA metabolism and signaling (Table S3). ABA synthesis and conjugation have long been demonstrated to be modulated in response to water deficit, primarily due to transcriptional

changes (Xiong and Zhu, 2003). In the ABA biosynthetic pathway, 9-*cis*-epoxycarotenoid dioxygenase (NCED) is the key rate-limiting enzyme (Tan *et al.*, 2003). Out of the five members of the *NCED* family in the Arabidopsis genome, *AtNCED3* is considered the most critical enzyme for drought-triggered ABA biosynthesis (Iuchi *et al.*, 2001). On the other hand, ABA is catabolized by a group of cytochrome P450 type enzymes, the CYP707As (Okamoto *et al.*, 2011). These enzymes play a crucial role during the prompt ABA inactivation after the water supply is reestablished (Kushiro *et al.*, 2004; Saito *et al.*, 2004). In C_3 species, both *NCED* and *CYP707A* genes display responses ranging from minutes to a few hours (Qin and Zeevaart, 1999; Umezawa *et al.*, 2006).

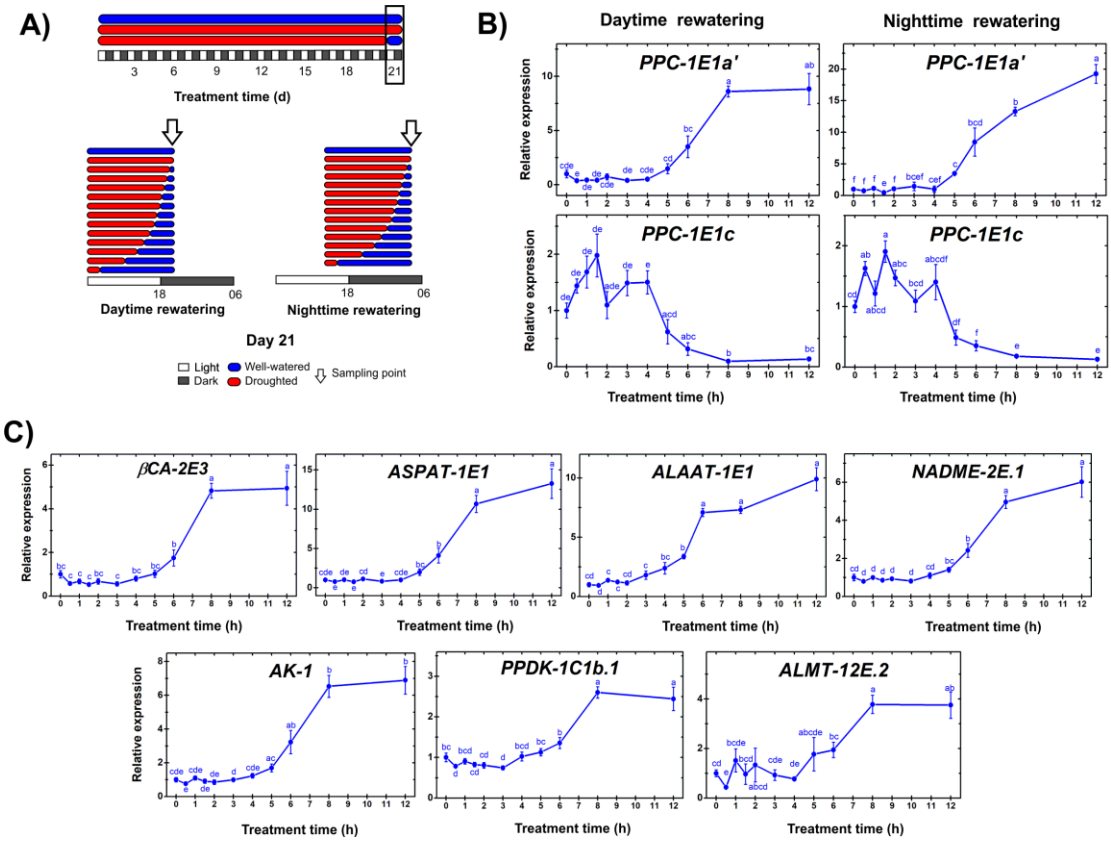

Fig. 3 Rewatering promotes fast and synchronized up- and down-regulation of C_4- and CAM-related genes, respectively. (A) Schematic representation of the experimental design for the time-course analysis of CAM reversion by rewatering. Leaves of 30-day old plants were droughted for 21 days and sampled on day 22 after 0, 0.5, 1, 1.5, 2, 3, 4, 5, 6, 8, 12 hours of rewatering. (B) Transcript abundance of *PPC* genes sampled after distinct rewatering periods followed by harvesting at daytime or nighttime. (C) Transcript abundance of C_4-related genes. Mean relative expression was normalized against the droughted control at time 0. Data are means (± SE) of at least three replicates. Different letters indicate statistically significant differences between time points sampled after different rewatering periods ($P < 0.05$). AK, adenylate kinase; ALAAT, ALA aminotransferase; ALMT, aluminum-activated malate transporters; ASPAT, ASP aminotransferase; βCA, beta-carbonic anhydrase; NADME, NAD-malic enzyme; PPC, phosphoe*nol*pyruvate carboxylase; PPDK, pyruvate orthophosphate dikinase.

Monitoring leaf endogenous ABA content, *NCED3* and *CYP707A1* mRNA levels during the water deprivation and subsequent rewatering in *P. oleracea* revealed a fast response in ABA biosynthesis and degradation depending on the water supply (Figs. 4). ABA accumulation and *NCED3* mRNA levels were significantly promoted as soon as 6 days after water withholding and both parameters displayed fluctuations as water deficit intensified (Fig. 4A). Drought had no impact on *CYP707A1* mRNA abundance, but it was gradually up-regulated in both well-watered and droughted plants after 15 days of treatment (Fig. 4A). Therefore, ABA accumulation in droughted *P. oleracea* seems to rely mainly on *de novo* synthesis rather than a reduction in the degradation of this plant hormone.

At more prolonged periods of rewatering (i.e., 12 – 24 h), endogenous ABA, as well as ABA metabolism and signaling transcripts, returned to levels similar to those detected in well-watered plants (Figs. S4-S5). *NCED3* was drastically down-regulated within the first hour of rewatering, but the most drastic reductions in leaf ABA content were detected between 3 and 8 h after rewatering, coinciding with a transitory peak in *CYP707A1* mRNA levels (Fig. 4B). Members of this specific class of CYP707As have already been regarded as central players in catalyzing the rehydration-triggered ABA degradation in Arabidopsis leaves (Zeevaart, 1980; Umezawa *et al.*, 2006).

As core components of the ABA signaling pathway, Clade A PP2C (PP2CA) phosphatases and ABA-responsive element-binding factors (ABFs) are critically associated with plant responses to drought stress (Kim *et al.*, 2004; Schweighofer *et al.*, 2004), and transcripts for these genes are known to increase in response to water deficit, ABA treatment and CAM induction (Matsui *et al.*, 2008; Brilhaus *et al.*, 2016; Maleckova *et al.*, 2019). In droughted and rewatered *P. oleracea* leaves, the temporal oscillations in *PP2CA* and *ABF2* transcript accumulation patterns mirrored the endogenous ABA levels (Fig. 4A-B).

Our findings clearly indicated that drought-triggered increments in ABA biosynthesis, accumulation and signaling take place as soon as 6 days after water withholding, thereby coinciding with the CAM induction and C_4 down-regulation in *P. oleracea* leaves. Also, a fast down-regulation in ABA biosynthesis (1 hour after rewatering) was followed by a prominent decrease in ABA degradation (3 to 8 hours after rewatering), leading to a decline in leaf ABA levels that temporally coincides with the CAM to full C_4 transition upon rewatering. A temporal coincidence between endogenous ABA levels and CAM up-regulation or induction has also been observed in young *A. comosus* plants (Freschi *et al.*, 2010) and adult *M. crystallinum* individuals (Thomas *et al.*, 1992) exposed to water or salt stress, respectively. In addition, ABA accumulation preceded an increase in *PPC* content in *Kalanchoë blossfeldiana* (Taybi *et al.*, 1995).

Compared to ABA, less is known about the involvement of other plant hormones in the regulation of CAM induction (Taybi *et al.*, 2002). CKs have been considered candidates for

CAM repression, as a decrease in CK content was reported for CAM-induced *M. crystallinum* under salt stress (Schmitt and Piepenbrock, 1992; Peters *et al.*, 1997). In plants, cytokinin metabolism and signaling involves multiple key components including, but not limited to, *LONELY GUY* genes that are involved in CK activation (Kuroha *et al.*, 2009), and *HPT PHOSPHOTRANSMITTER*s (*AHP*s) and *RESPONSE REGULATOR*s *(ARR*s), that are key members of CK signaling transduction (To *et al.*, 2004; Hutchison *et al.*, 2006; Nguyen *et al.*, 2016). Based on *P. oleracea* transcriptome data (Ferrari *et al.*, 2020*b*), *LOG1*, *AHP4*, *ARR9* and *ARR12* were identified as differentially expressed in response to water supply (Table S3). The impacts of water scarcity on *LOG1*, *AHP4*, *ARR9* and *ARR12* transcript abundance were only detected after 15 days of drought treatment (Fig. 4A), thereby taking place after the start of CAM induction and temporally coinciding with the down-regulation of C_4-related genes (Fig. 2E). On the other hand, most of the *LOG1* and *ARR9* up-regulation and *AHP4* and *ARR12* down-regulation in response to rewatering occurred between 4 and 8 h after water was resupplied (Fig. 4B). Whereas *AHP4*, *ARR12* and *ARR9* transcripts were completely recovered to levels similar to well-watered plants after 24h of rewatering, *LOG1* mRNA levels were only slightly recovered after 12h- or 24 h-period rewatering (Fig. S5).

Therefore, compared to the rapid and completely reversible alterations in ABA levels, metabolism and signaling in response to changes in water supply, the impacts of water withholding on CK metabolism and signaling were significantly slower and only partially reverted by rewatering in *P. oleracea*. Endogenous CK levels have been reported to rapidly decrease under drought in C_3 and C_4 species (Pospíšilová *et al.*, 2005), mainly due to restrictions in its biosynthesis, consequently suppressing CK signaling, and thus being quoted as an ABA antagonist (Hare *et al.*, 1999; Oneto *et al.*, 2016).

In order to further elucidate the roles of ABA and CKs on both C_4 and CAM expression in *P. oleracea*, we next conducted a pharmacological approach involving both short- and long-term hormonal treatments (hours *versus* days, respectively). Short-term (i.e., 12 h) treatment with ABA or BA revealed that CK supplementation completely recovered the drought-induced repression of all C_4 genes analyzed (Fig. 5A). Under well-watered conditions, *PPC-1E1c* transcript accumulation was promoted and repressed by ABA and CK supplementation, respectively (Fig. 5A). A small but significant additive effect of ABA on *PPC-1E1c* was also observed in droughted plants (Fig. 5A). In agreement, a dose-response up-regulation of *PPC-1E1c* was observed upon four consecutive days of treatment with ABA under well-watered conditions (Fig. 5B), and several weeks of treatment with different concentrations of either BA or Z under drought confirmed the repressor role of CKs on this CAM-marker gene expression (Fig. 5C).

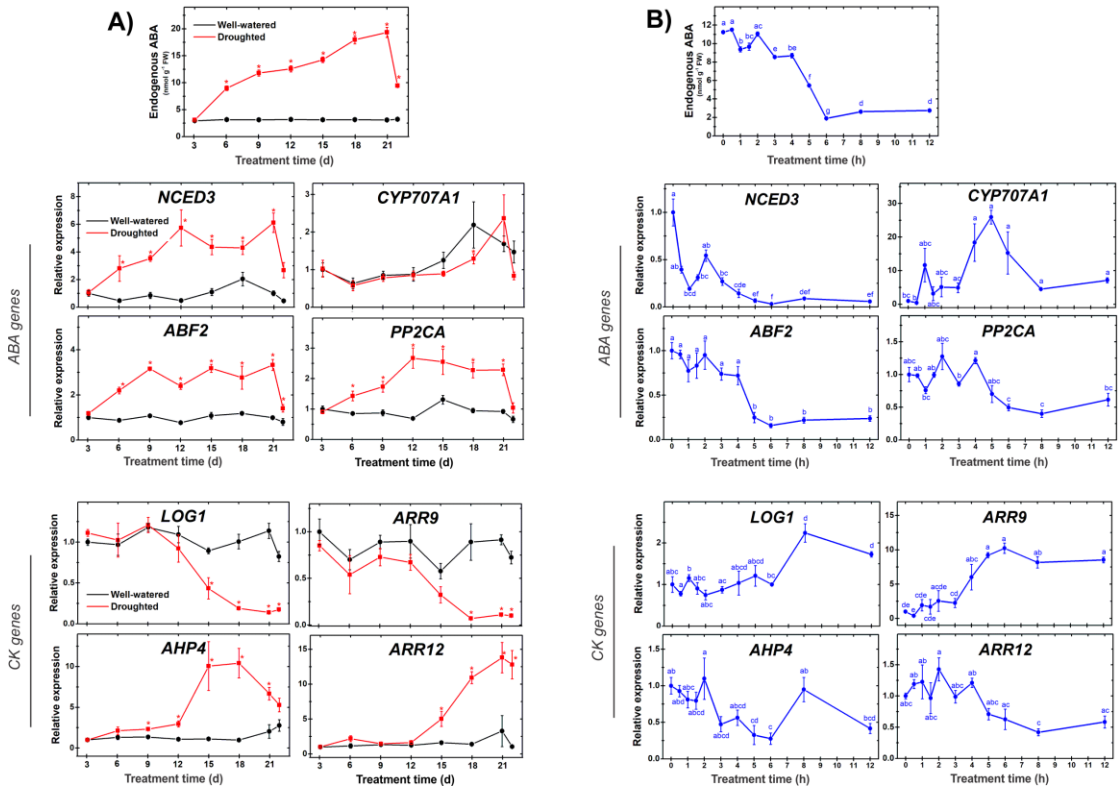

Fig. 4 Changes in hormonal metabolism and signaling during CAM induction and reversion in *Portulaca oleracea*. Treatment details as described in Figs. 2 (drought) and 3 (rewatering). (A) Endogenous abscisic acid (ABA) levels and transcript abundance of ABA- and cytokinin (CK)-related genes under progressive drought. In A, mean relative expression was normalized against well-watered leaves at the start of the treatment. **P* < 0.05 compared with well-watered samples. (B) Endogenous ABA levels and transcript abundance of ABA and CK-related genes under progressive rewatering. In B, mean relative expression was normalized against the droughted control at time 0, and different letters indicate statistically significant differences between time points sampled after different rewatering periods (P < 0.05). In all cases, data are means (± SE) of at least three replicates. All genes were sampled at dawn, except for *NCED3*, *ABF2* and *PP2CA,* which were sampled at dusk. ABF, aba-responsive element-binding factors; AHPT, phosphotransmitter; CYP707A, cytochrome P450 type enzymes; LOG, lonelyguy; ARR, response regulator; NCED, 9-cis-epoxycarotenoid dioxygenase; PP2CA, clade A PP2C phosphatases.

In addition, virtually no changes in C_4 gene expression (Fig. 5B-C) were observed under long-term ABA, BA or Z treatment. In *P. oleracea*, long-term ABA treatment failed to promote significant increments in ΔH^+ (Fig. S6), indicating that ABA alone is not sufficient to induce all the components required to CAM functioning under well-watered conditions. Similarly, although long-term BA or Z treatments restricted the drought-induced *PPC-1E1c* up-regulation (Fig. 5C), they failed in affecting ΔH^+ (Fig. S6).

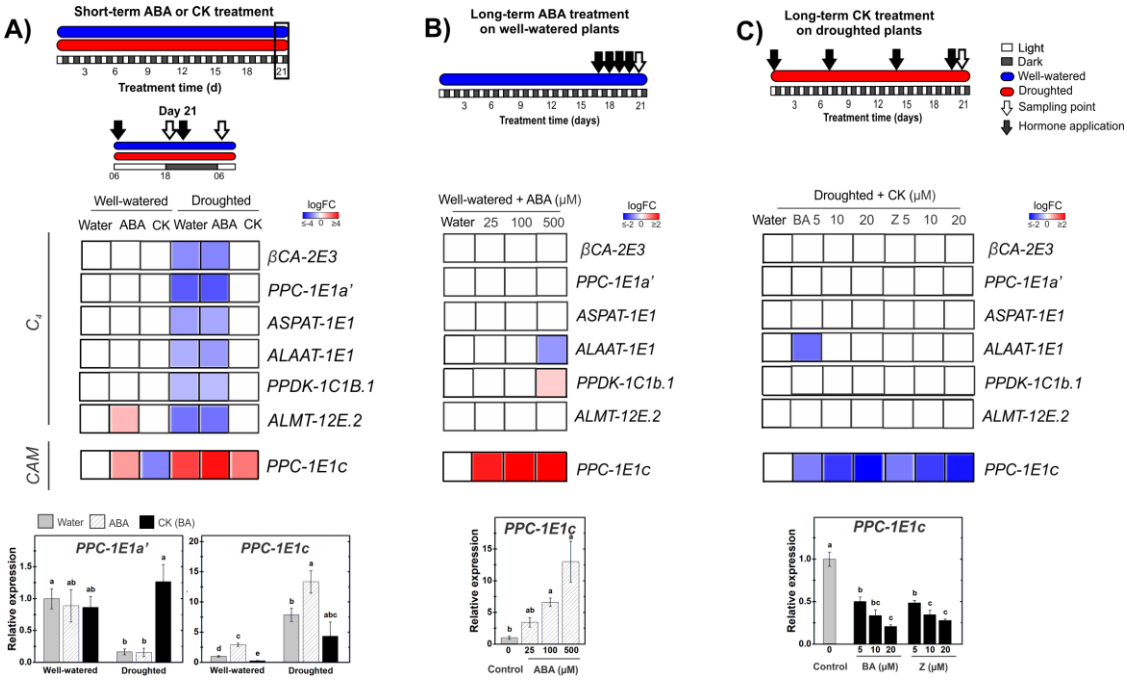

Fig. 5 Impacts of short- and long-term hormonal treatments on C_4- and CAM-related gene expression in *Portulaca oleracea*. (A) Short-term abscisic acid (ABA) and cytokinin (CK) treatment. Well-watered or droughted plants were treated with 500 μM ABA or 6-Benzylaminopurine (BA) for 12h (short-term). (B) Long-term ABA treatment. Well-watered plants were treated with 0, 25, 100 and 500 μM ABA for 4 consecutive days. (C) Long-term CK treatment. Droughted plants were treated with 0, 5, 10, 20 μM BA or *trans*-zeatin (Z) in four applications over 20 days. In all cases, the experimental design schemes are presented on top. Heatmaps indicate $\log_2$(fold-change) of C_4- and CAM-related transcript levels following hormonal treatment, with statistically significant differences in comparison with water-sprayed controls represented as colored squares ($P < 0.05$). Mean relative expression was normalized against water-sprayed controls. Plots represent *PPC* transcript levels under short- or long-term ABA and CK treatment, and different letters indicate statistically significant differences between treatments ($P < 0.05$). Data are means (± SE) of at least three replicates. ALAAT, ALA aminotransferase; ALMT, aluminum-activated malate transporters; ASPAT, ASP aminotransferase; βCA, beta-carbonic anhydrase; NADME, NAD-malic enzyme; PPC, phospho*enol*pyruvate carboxylase; PPDK, pyruvate orthophosphate dikinase.

Therefore, long- and short-term hormonal treatments supported a positive and negative role of ABA and CKs, respectively, on CAM-related gene expression in *P. oleracea*. In line with our findings, exogenous ABA has been repeatedly demonstrated to promote CAM-related gene expression in C_3-CAM facultative species (Chu *et al.*, 1990; Dai *et al.*, 1994; Forsthoefel *et al.*, 1995; Tsiantis *et al.*, 1996). For example, ABA can induce short-term transcriptional increases in core CAM- and carbohydrate-related enzymes in *T. triangulare*, a response coupled to increased ΔH^+ and changes in the transcript abundance of ABA signaling components (Maleckova *et al.*, 2019). Even constitutive CAM species such as *Ananas comosus* and *K. blossfeldiana* can respond to exogenous ABA with increments in characteristics of CAM, such as ΔH^+ and gene expression (Taybi *et al.*, 1995; Freschi *et al.*, 2010). In contrast, very little is known about the influence of ABA on C_4 photosynthesis.

ABA has been shown to induce traits of Kranz anatomy and increase C_4-enzyme activities in the C_3-C_4 intermediate and amphibious species *Eleocharis vivipara* and *E. baldwinii* (Ueno, 2001). Also, leaf disks of *Amaranthus hypochondriacus* treated with ABA showed increased PPC protein and mRNA (Aloor *et al.*, 2017). According to our findings, either short- or long-term ABA supplementation has virtually no effect on C_4 gene expression in well-watered *P. oleracea* plants (Fig. 5).

Compared to ABA, the role of exogenous CKs on CAM induction remains controversial in the literature. Exogenous BA has been predominantly used in CAM signaling studies (Schmitt and Piepenbrock, 1992; Dai *et al.*, 1994; Peters *et al.*, 1997), with few reports comparing different CK types. BA and Z exogenous application has caused opposite effects in *M. crystallinum*, either increasing or repressing the CAM-specific *PPC* transcript abundance (Thomas *et al.*, 1992; Thomas and Bohnert, 1993). In *P. oleracea*, both BA and Z treatment lead to a dose-response *PPC-1E1c* down-regulation, consistently indicating that excess CKs can limit CAM-related gene expression under drought. Also, short-term CK treatment was shown to completely recover the drought-induced transcriptional repression of core C_4 enzymes in *P. oleracea* (Fig. 5A). A similar effect was observed in detached maize leaves, where C_4-*PPC* and *CA* were up-regulated after Z treatment, although this depended on nitrogen availability (Sugiharto *et al.*, 1992; Suzuki *et al.*, 1994; Offermann *et al.*, 2006). In C_3 species such as wheat and rice, exogenous CKs also promoted an increase in PPC and CA enzyme activity, photosynthetic capacity or Rubisco content (Ookawa *et al.*, 2004; Lazova and Yonova, 2010). In addition, Arabidopsis seedlings treated with CK showed increased in *PPDK* and *NADP-ME* transcript abundancies (Brenner *et al.*, 2005). Finally, transgenic maize leaves overexpressing the cytokinin biosynthesis-related gene *ISOPENTENYL TRANSFERASE* (*IPT*) under a senescence-regulated promoter showed increased tolerance to drought and a relatively lower ABA content (Oneto *et al.*, 2016). Therefore, CKs seem to promote C_4 transcript accumulation in *P. oleracea* under drought, which may be a direct action of this hormones or via crosstalk with other signaling molecules.

To gain further insights on the ABA-CK interplay in well-watered and droughted *P. oleracea*, the impacts of the hormonal treatments on the ABA- and CK-related gene expression were also analyzed (Fig. 6). *NCED3* was the only gene identified as repressed by ABA under well-watered conditions. In line with their action downstream to ABA, *PP2CA* and *ABF2* were promoted by exogenous ABA in a dose-dependent manner (Fig. 6A). Similarly, *ABF2* and *PP2CA* were up-regulated by drought and ABA in Arabidopsis (Matsui *et al.*, 2008) and in *T. triangulare* (Brilhaus *et al.*, 2016; Maleckova *et al.*, 2019). Long-term CK treatment significantly promoted *ARR9* but not *ARR12* expression (Fig. 6B), confirming the expected induction patterns for a type-A and type-B RRs (Kiba *et al.*, 1999), and further suggesting a repressor role of water scarcity on CK signaling in *P. oleracea*. As additional ABA-CK

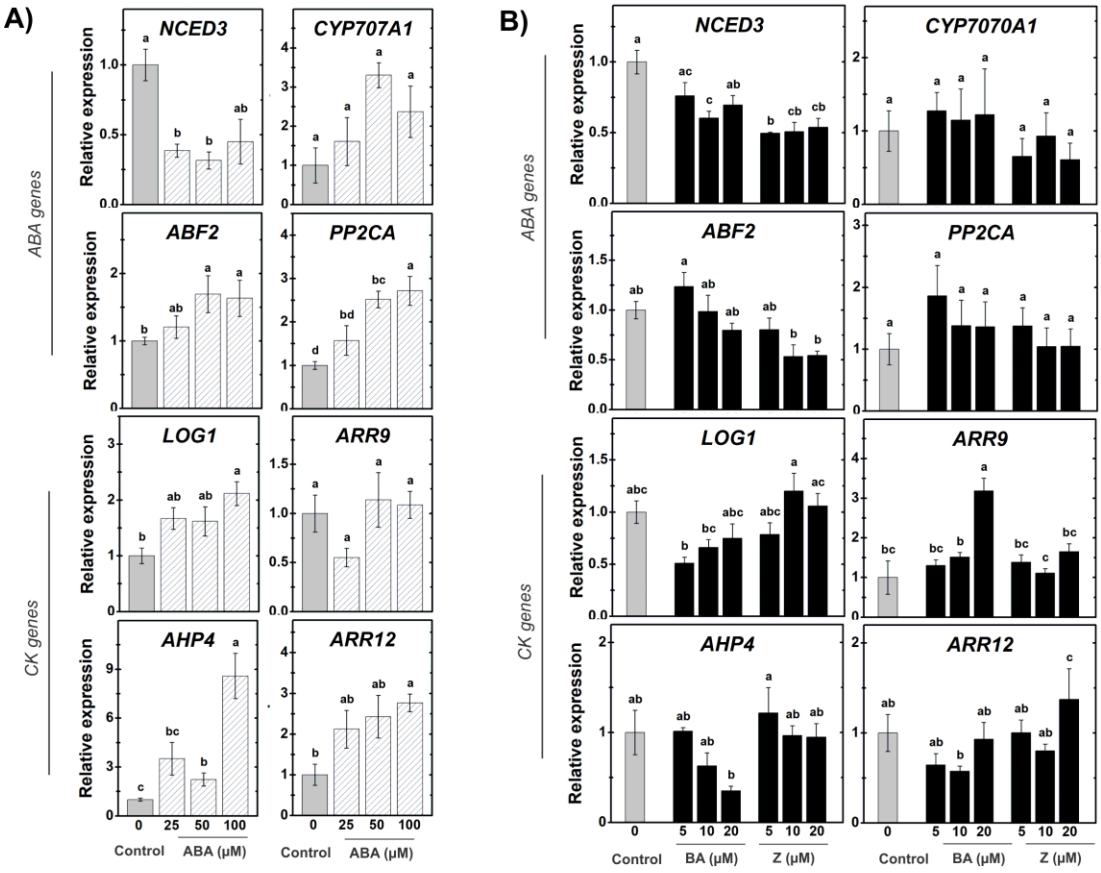

Fig. 6 Hormonal cross-interactions in well-watered and droughted *Portulaca oleracea* plants. Treatment details as described in Fig. 5. (A) Impacts of long-term abscisic acid (ABA) treatment on the transcript abundance of ABA and cytokinin (CK)-related genes in well-watered plants. (B) Impacts of long-term 6-benzylaminopurine (BA) or *trans*-zeatin (Z) treatments on the transcript abundance of ABA- and CK-related genes associated in droughted plants. Different letters indicate statistically significant differences between treatments ($P < 0.05$), and mean relative expression was normalized against control. All genes were analyzed in samples harvested at dawn, except for *NCED3*, *ABF2* and *PP2CA,* which were sampled at dusk. ABF, aba-responsive element-binding factors; AHPT, phosphotransmitter; CYP707A, cytochrome P450 type enzymes; LOG, lonelyguy; ARR, response regulator; NCED, 9-cis-epoxycarotenoid dioxygenase; PP2CA, clade A PP2C phosphatases.

crosstalk points, *ABF2 and NCED3* were repressed by the CK treatment, whereas *LOG1*, *AHP4* and *ARR12* were up-regulated by ABA.

Co-expression network analysis reveals additional candidate regulators of CAM and C_4 gene expression

Plant stress responses commonly involve the action of multiple transcription factors (TFs), many of them responsible for connecting and coordinating several signaling cascades (Li *et al.*, 2004; Abuqamar *et al.*, 2009; Seo and Park, 2010; Kohli *et al.*, 2013). As such, the prospection of non-obvious TFs via bioinformatic approaches has been an important source

of information to clarify the signaling cascades controlling plant stress responses (Mitsuda and Ohme-Takagi, 2009; Wang *et al.*, 2016). Only recently, TFs potentially controlling CAM induction and functioning started to be identified, and a list of candidates presumably fine-tuning CAM responses in *M. crystallinum* and *K. fedtschenkoi* has been published (Amin *et al.*, 2019).

Here, we used previously generated transcriptome data (Ferrari *et al.*, 2020*b*) to screen for non-obvious transcription factors potentially associated with the drought-induced C_4-to-CAM transition in *P. oleracea*. Based on sequence homology, the transcriptome was annotated against available plant transcription factor databases (Pérez-Rodríguez *et al.*, 2010; Jin *et al.*, 2014), retrieving 3,996 hits (Table S4). These were then filtered using the criteria logFC > |1.5| and FDR < 0.05 in at least one of the three-time points sampled (i.e., early morning, late afternoon and nighttime), redeeming a list of 290 hits (Table S5). Co-expression networks were generated, and modules containing key CCM genes (*PPC-1E1a'*, *PPC-1E1c* and *PPCK-1E*) were identified (Fig. S7). Significantly modulated (logFC > |1.5| and FDR < 0.05) TF-encoding genes in these modules were filtered (Table S6), and nine TFs were selected among the most modulated transcripts for detailed expression analysis during the C_4-to-CAM transition and reversion in *P. oleracea*.

Five TFs were present in two modules with opposite expression patterns under contrasting water regimes: *TRANSPARENT TESTA 8 (TT8), FLOWERING MYB PROTEIN* (*EFM*) and *HOMEOBOX 7* (*HB7*); *NAC DOMAIN CONTAINING PROTEIN 21/22* (*NAC22*) and *NUCLEAR FACTOR Y, SUBUNIT C4 (NFYC4*). Four TFs were selected from *PPC* and *PPCK* modules showing a pattern of up-regulation after drought: *NUCLEAR FACTOR Y, SUBUNIT C9 (NFYC9)*; *WRKY TRANSCRIPTION FACTOR FAMILY PROTEIN 44* (*WRKY44*), *NUCLEAR FACTOR Y, SUBUNIT A7 (NFYA7*) and *MYB DOMAIN PROTEIN 82 (MYB82*) (Table S6).

Time-course transcriptional profiling revealed that *EFM*, *HB7, MYB82*, *NFYA7*, *TT8* and *WRKY44* were up-regulated by drought as soon as 6 days of treatment (Fig. 7A), thereby coinciding with the start of CAM expression. In contrast, *NAC22*, *NFYC9* and *NFYC4* transcript abundances were only impacted after 12-15 days of the drought treatment, a moment characterized by the down-regulation of the C_4 genes (Fig. 7A). All these genes recovered their expression levels after 12 h or 24 h of rewatering (Fig. S8). In fact, *EFM, NAC22* and *MYB82* were significantly down-regulated as soon as 2 h of rewatering, and all other TFs reversed their expression pattern after 4 h of water resupplied (Fig. 7B).

In order to understand the possible interconnection between these drought-regulated TFs and the ABA and CKs controlling the C_4 and CAM expression, we next assessed the impacts of hormonal treatment on the transcription abundance of all nine selected TFs. *TT8* presented the same pattern as *PPC-1E1c*, being progressively up- and down-regulated by ABA and CK,

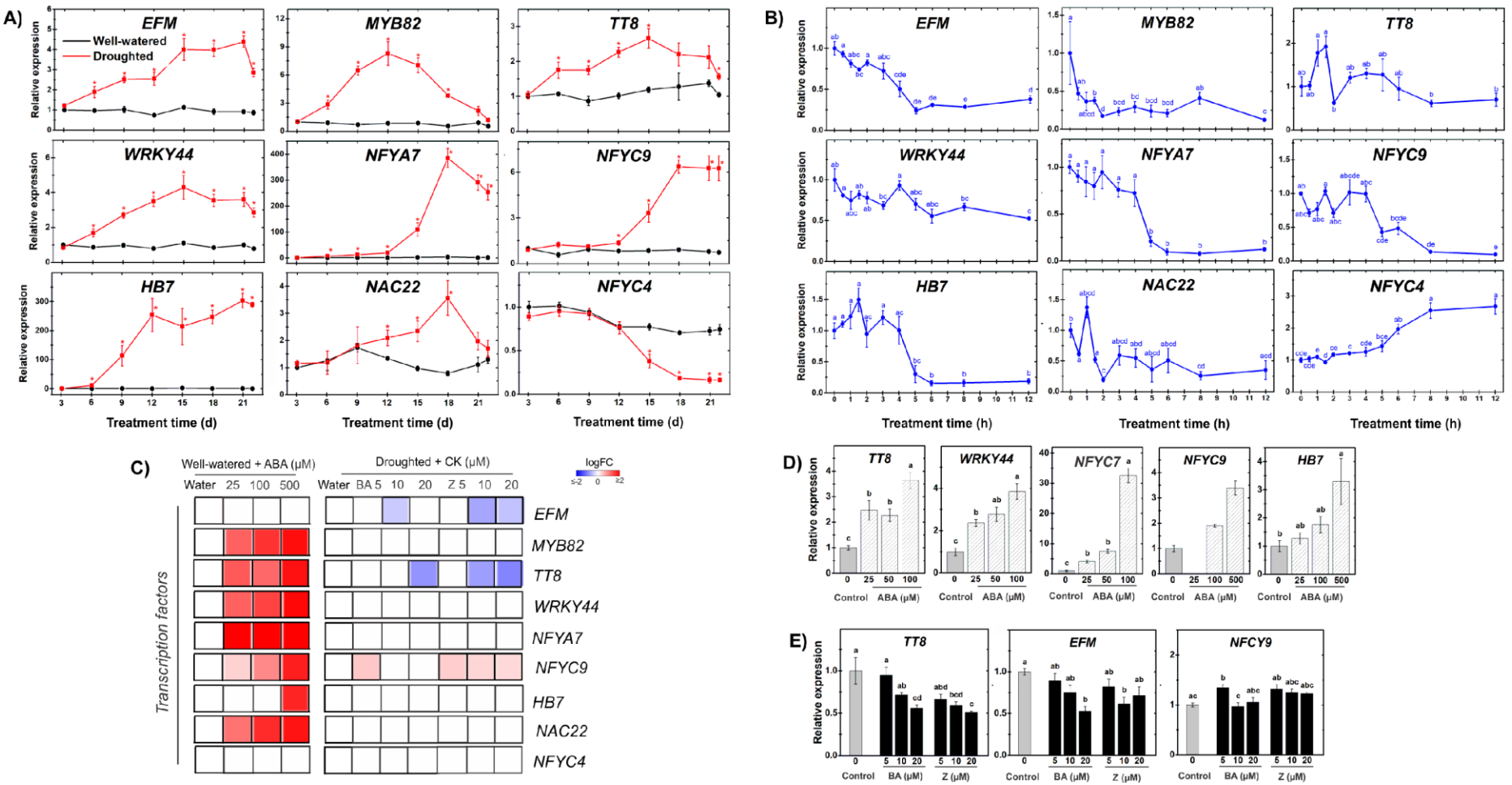
A)
EFM
MYB82
TT8
WRKY44
NFYA7
NFYC9
HB7
NAC22
NFYC4
Well-watered
Droughted
Relative expression
Treatment time (d)
B)
Treatment time (h)
C)
Well-watered + ABA (μM)
Water 25 100 500
Droughted + CK (μM)
Water BA 5 10 20 Z 5 10 20
logFC
≤-2 0 ≥2
Transcription factors
D)
TT8
WRKY44
NFYC7
NFYC9
HB7
Control
ABA (μM)
E)
EFM
NFCY9
BA (μM)
Z (μM)

Fig. 7 Fluctuation in mRNA levels encoding candidate transcription factors (TFs) during CAM induction and reversion in *P. oleracea*. Treatment details as described in Figs. 2 (drought) and 3 (rewatering). (A-B) Transcript abundance of TF-encoding genes under progressive drought (A) and rewatering (B). (C) Heatmaps indicate log_2(fold-change) of TF-encoding genes following hormonal treatment. In the heatmaps, statistically significant differences compared with water-sprayed controls are represented as colored squares ($P < 0.05$). (D-E) Plots represent TF-encoding transcript levels under long-term ABA and CK treatments, and different letters indicate statistically significant differences between treatments ($P < 0.05$), and mean relative expression was normalized against water-sprayed controls. In A, *$P < 0.05$ compared with well-watered samples. In B, different letters indicate statistically significant differences between time points sampled after different rewatering periods ($P < 0.05$). Data are means (± SE) of at least three replicates. All genes were analyzed in samples harvested at dawn, except for *EFM, WRKY44, HB7, MYB82*, and *TT8,* which were analyzed in afternoon/night samples. EFM, flowering MYB protein; HB7, homeobox; MYB, MYB domain protein; NAC, NAC domain-containing protein; NFYC and NFYA, nuclear factor Y, subunits C and A; TT, transparent testa; WRKY, WRKY transcription factor family protein.

respectively (Fig. 7C-E). Other TFs, except *EFM* and *NFYC4*, were up-regulated in response to long-term ABA treatment under well-watered conditions (Fig. 7C-D). Finally, droughted plants exposed to long-term CK treatment displayed up- and down-regulation of *NFYC9* and *EFM*, respectively (Fig. 7C,E).

Correlation analysis based on data collected throughout the water deprivation (Fig. 2), rewatering (Fig. 3) and long-term hormonal treatment experiments (Figs. 4-6) revealed a clear connection between the selected TFs as well as ABA- and CK-related genes with both the CAM- and C_4-specific *PPC* genes (Table S7). Most drought-induced TFs clustered with *PPC-1E1c*, but presented varying correlation levels to this gene, with *NFYA7*, *NFYC9, HB7* and *ARR12* identified as the most strongly correlated to this CAM-marker gene (Fig. 8A). On the other hand, only *ARR9*, *LOG1* and *NFYC4* were shown to be positively correlated to *PPC-1E1a'* (Fig. 8B).

Many TFs possibly involved in CAM induction in *K. fedtschenkoi* and *M. crystallinum* belong to NAC, MYB, Homeobox (HB) and Nuclear factor Y (NFY) families (Amin *et al.*, 2019), which were also identified here as potentially associated with the CCM transition in *P. oleracea*. In addition, *EFM*, *HB7, MYB82*, *WRKY44*, *NAC22*, *NFYC9*, *NFYC4* and *NFYA7* belong to TF families commonly involved in drought responses (Söderman *et al.*, 1996; Nakashima *et al.*, 2007; Li *et al.*, 2008; Tripathi *et al.*, 2014; Baldoni *et al.*, 2015). NF-Ys are known to regulate photosynthesis responses and can be affected by CK and light (Kusnetsov *et al.*, 1999). Moreover, *NFYC9* overexpression in Arabidopsis mutants confers hypersensitivity to ABA (Bi *et al.*, 2017), and here, *NFYC9* was responsive to ABA and CK treatments. Likewise, overexpression of *NFYA7* in Arabidopsis confers resistance to drought stress (Leyva-González *et al.*, 2012), and *NFYA7* was reported to be associated with high temperature and salt stress (Maheshwari *et al.*, 2019).

Among the TFs closely associated with *PPC-1E1c* (Fig. 8A), *HB7* is up-regulated by ABA and drought in the C_3-CAM *T. triangulare* (Brilhaus *et al.*, 2016; Maleckova *et al.*, 2019), and acts positively regulating transcription of *PP2C* genes (Valdés *et al.*, 2012). In *P. oleracea*, MYB-transcription factor-encoding gene *EFM* was up-regulated upon drought (Fig. 6A), as also reported for *T. triangulare* (Brilhaus *et al.*, 2016), and down-regulated by CKs (Fig. 6C) as in Arabidopsis (Bhargava *et al.*, 2013).

Finally, *TT8, NAC22*, and *MYB82* were more distantly correlated to *PPC-1E1c*, but all were up-regulated during long-term ABA treatment (Fig. 8A). *TT8* is a basic helix-loop-helix (bHLH) transcription factor (Nesi *et al.*, 2000) and is also up-regulated during drought induction in *T. triangulare* (Brilhaus *et al.*, 2016). In Arabidopsis, loss-of-function mutants for *TT8* were more sensitive to ABA (Rai *et al.*, 2016). *NAC22*, also referred to as *NAC21/22* or *NAC1*, was induced by ABA in grapevine leaves, and plants overexpressing this gene showed increased tolerance to osmotic, salt and cold stresses (Hénanff *et al.*, 2013). Lastly, *MYB82* can act as a negative regulator of drought-related responses in wheat (Mia *et al.*, 2019).

Although the exact mechanisms connecting water availability and C_4 and CAM gene expression are not completely elucidated, the data obtained here allow us to propose a tentative signaling network (Fig. 8B). Once water becomes scarce, it gradually promotes ABA accumulation by favoring biosynthesis via *NCED3* and repressing *CYP707A1*. This initially induces *TT8* up-regulation, followed by an increase in common ABA-related messengers (e.g. *ABF2*, *PP2CA, HB7*), but also other non-obvious TFs (*NFYA7*, *NFYC9*, *ARR12*). The enrichment in these TFs may lead to the transcriptional activation of CAM-related genes, culminating in the induction of the CAM cycle. Simultaneously, drought represses *LOG1*, probably causing a decrease in CK levels and *ARR9* signaling, also in *NFCY4* expression, leading to an overall down-regulation of the genes encoding C_4-related enzymes. In the C_4-CAM context, *ARR12*, *HB7*, *NFYC9, NFYA7* and *TT8* for CAM, and *NFYC4* and *ARR9* for C_4, displayed striking responsiveness to water availability and hormone treatment, constituting the most promising candidates as regulators of CAM expression in a C_4 background (Fig. 8B).

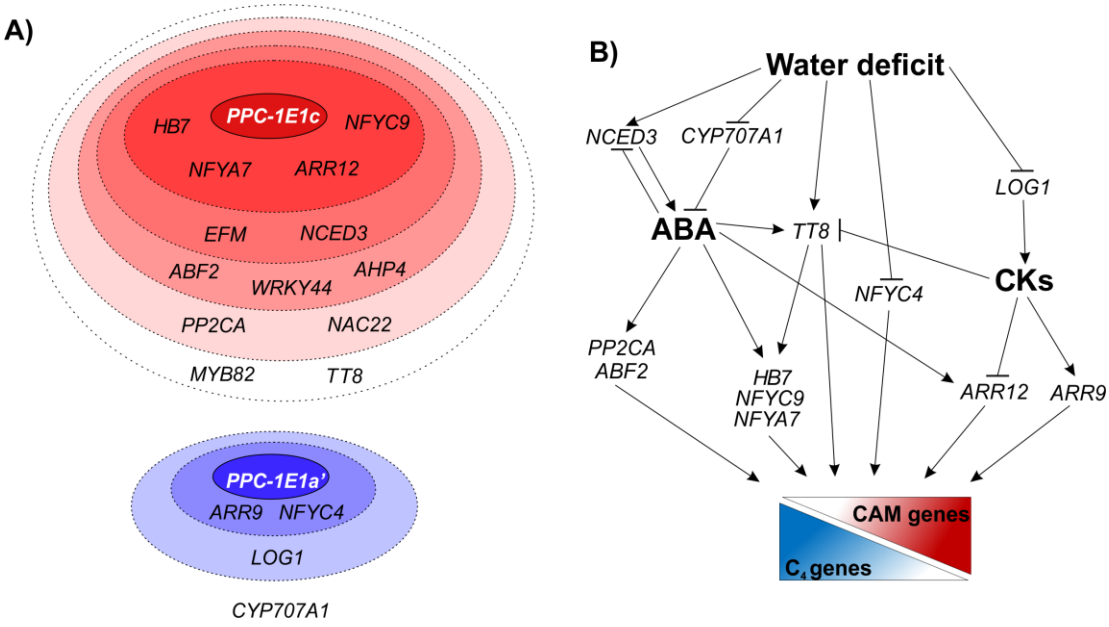

Fig. 8 Regulatory events controlling C_4 and CAM expression in *P. oleracea*. (A) Diagram illustrating (the level of connection between transcription factors (TFs) and the CAM- or C_4-related *PPC* genes according to correlation indexes (correlation indexes listed in Table S7). (B) Schematic representation of signaling events connecting the perception of water deficit and the C_4-to-CAM transition in *P. oleracea*. Water deficit initiates a signaling cascade involving abscisic acid (ABA) accumulation and cytokinin (CK) depletion, leading to the up- or down-regulation of different signaling molecules, which in turn repress C_4-related transcript accumulation and induces CAM photosynthesis. Black arrowheads at the ends of lines indicate stimulatory effects, whereas bars indicate inhibitory effects. Gene abbreviations are described in the text.

Conclusions

Overall, our study reveals that the molecular clock coordinates both the C_4 and CAM diel gene expression in well-watered and droughted leaves, respectively. Among all CCM genes analyzed, *PPCK-1E* was identified as particularly affected by disturbances in the circadian clock. ABA was implicated as major signal interconnecting the plant water status and the C_4 and CAM gene expression, with *NCED3* transcript accumulation quickly responding during drought and rewatering and leading to fast and fully reversible changes in the endogenous levels of this plant hormone. In addition, based on the transcriptional responses of the CAM-marker gene *PPC-1E1c* and various TF-encoding genes to the exogenous ABA and CK treatments, an antagonistic action of these two hormonal classes was implicated in CAM signaling. Moreover, CK treatment recovered the levels of all seven C_4-transcript markers analyzed in droughted plants. Finally, we revealed that *HB7*, *NFYA7*, *NFYC9*, and *ARR12* were particularly correlated with *PPC-1E1c* transcript accumulation responses under drought stress, ABA and CK application, implicating these TFs as the most likely CAM effectors in the C_4-CAM system. In addition, *TT8* seems to act as an early messenger since it responds to ABA and CK stimuli and precedes CAM-related transcript accumulation under drought. On

the other hand, *NFYC4* and *ARR9* are tightly connected to the C_4. Since an efficient, stable *Agrobacterium*-mediated transformation protocol has been recently established for *P. oleracea* (Ferrari *et al.*, 2020*a*), future studies involving loss-of-function and overexpression mutants for the TFs listed here may provide further insights into the signaling networks controlling the coordinated, fast and completely reversible C_4-CAM transition in this species. There is enormous potential in understanding the intricate regulation and connectivity of both C_4 and CAM pathways within a single organism, especially considering biotechnological applications such as engineering crops for more resistant cultivars in a climate change context and creating more sustainable agricultural systems, with higher water use efficiency (Borland *et al.*, 2009; Covshoff and Hibberd, 2012; Yang *et al.*, 2015; Hartwell *et al.*, 2016; FAO 2020).

Author's contributions

LF and JH conceived the project and supervised the experiments; RCF conducted most of the experiments; AKB conducted time-course experiments and analysis together with RCF; SSF conducted the correlation network analysis; RCF, LF and JH wrote the article with contributions from other authors.

Conflict of interest

The authors declare no conflict of interest.

Acknowledgements

This work was supported by the São Paulo Research Foundation (FAPESP – grant no. 2016/04755-4 awarded to RCF), by a Newton Advanced Fellowship funded by the Royal Society, UK (grant no. NA140007 awarded to LF and JH), and in part by the Coordenação de Aperfeiçoamento de Pessoal de Nível Superior – Brasil (CAPES) – Finance Code 001.

References

Abuqamar S, Luo H, Laluk K, Mickelbart M V, Mengiste T. 2009. Crosstalk between biotic and abiotic stress responses in tomato is mediated by the *AIM1* transcription factor. Plant Journal **58**, 347–360.

Alabadi D, Yanovksy MJ, Más P, Harmer SL, Kay SA. 2002. Critical Role for *CCA1* and *LHY* in maintaining circadian rhythmicity in Arabidopsis. Current Biology **12**, 757–761.

Aloor BP, Avasthi UK, Raghavendra AS. 2017. Stimulation by abscisic acid of the activity of phospho*enol*pyruvate carboxylase in leaf disks of Amaranthus hypochondriacus L., C_4 plant: role of pH and protein levels. Protoplasma **254**, 1973–1981.

Amin AB, Rathnayake KN, Yim WC, Garcia TM, Wone B, Cushman JC, Wone BWM. 2019.

Crassulacean acid metabolism abiotic stress-responsive transcription factors: a potential genetic engineering approach for improving crop tolerance to abiotic stress. Frontiers in Plant Science **10**, 1–8.

Baldoni E, Genga A, Cominelli E. 2015. Plant MYB transcription factors : their role in drought response mechanisms. International Journal of Molecular Sciences **16**, 15811–15851.

Baudry A, Ito S, Song YH, *et al.* 2010. F-Box proteins FKF1 and LKP2 act in concert with ZEITLUPE to control Arabidopsis clock progression. Plant Cell **22**, 606–622.

Berardini TZ, Reiser L, Li D, Mezheritsky Y, Muller R, Strait E, Huala E. 2015. The arabidopsis information resource: making and mining the 'gold standard' annotated reference plant genome. Genesis **53**, 474–485.

Bhargava A, Clabaugh I, To JP, Maxwell BB, Chiang YH, Schaller GE, Loraine A, Kieber JJ. 2013. Identification of cytokinin-responsive genes using microarray meta-analysis and RNA-seq in Arabidopsis. Plant Physiology **162**, 272–294.

Bi C, Ma Y, Wang XF, Zhang DP. 2017. Overexpression of the transcription factor *NF-YC9* confers abscisic acid hypersensitivity in Arabidopsis. Plant Molecular Biology **95**, 425–439.

Borland AM, Griffiths H, Hartwell J, Smith JAC. 2009. Exploiting the potential of plants with crassulacean acid metabolism for bioenergy production on marginal lands. Journal of Experimental Botany **60**, 2879–2896.

Borland AM, Guo HB, Yang X, Cushman JC. 2016. Orchestration of carbohydrate processing for crassulacean acid metabolism. Current Opinion in Plant Biology **31**, 118–124.

Borland AM, Taybi T. 2004. Synchronization of metabolic processes in plants with crassulacean acid metabolism. Journal of Experimental Botany.1255–1265.

Boxall SF, Dever L V, Kneřová J, Gould PD. 2017. Phosphorylation of phospho*enol*pyruvate carboxylase is essential for maximal and sustained dark co_2 fixation and core circadian clock operation in the obligate crassulacean acid metabolism species *Kalanchoë fedtschenkoi*. The Plant Cell **29**, 2519–2536.

Boxall SF, Foster JM, Bohnert HJ, Cushman JC, Nimmo HG, Hartwell J. 2005. Conservation and divergence of circadian clock operation in a stress-inducible Crassulacean acid metabolism species reveals clock compensation against stress. Plant Physiology **137**, 969–982.

Boxall SF, Kadu N, Dever L V., Knerová J, Waller JL, Gould PJD, Hartwell J. 2020. *Kalanchoë PPC1* is essential for crassulacean acid metabolism and the regulation of core circadian clock and guard cell signaling genes. Plant Cell **32**, 1136–1160.

Brenner WG, Romanov GA, Köllmer I, Bürkle L, Schmülling T. 2005. Immediate-early and delayed cytokinin response genes of *Arabidopsis thaliana* identified by genome-wide expression profiling reveal novel cytokinin-sensitive processes and suggest cytokinin action through transcriptional cascades. Plant Journal **44**, 314–333.

Brilhaus D, Bräutigam A, Mettler-Altmann T, Winter K, Weber APM. 2016. Reversible burst of transcriptional changes during induction of crassulacean acid metabolism in *Talinum triangulare*. Plant Physiology **170**, 102–122.

Camacho C, Coulouris G, Avagyan V, Ma N, Papadopoulos J, Bealer K, Madden TL. 2009. BLAST+: architecture and applications. BMC Bioinformatics **9**, 1–9.

Christin PA, Arakaki M, Osborne CP, *et al.* 2014. Shared origins of a key enzyme during the evolution of C_4 and CAM metabolism. Journal of Experimental Botany **65**, 3609–3621.

Chu C, Dai Z, Ku MSB, Edwards GE. 1990. Induction of crassulacean acid metabolism in the facultative halophyte *Mesembryanthemum crystallinum* by abscisic acid. Plant Physiology **93**, 1253–1260.

Covshoff S, Hibberd JM. 2012. Integrating C_4 photosynthesis into C_3 crops to increase yield potential. Current Opinion in Biotechnology **23**, 209–214.

Dai Z, Ku MSB, Zhang D, Edwards GE. 1994. Effects of growth regulators on the induction of crassulacean acid metabolism in the facultative halophyte *Mesembryanthemum crystallinum* L. Planta **192**, 287–294.

Davies BN, Griffiths H. 2012. Competing carboxylases: circadian and metabolic regulation of Rubisco in C_3 and CAM *Mesembryanthemum crystallinum* L. Plant, Cell and Environment **35**, 1211–1220.

Dever L V, Boxall SF, Kneřová J, Hartwell J. 2015. Transgenic perturbation of the decarboxylation phase of crassulacean acid metabolism alters physiology and metabolism but has only a small effect on growth. Plant Physiology **167**, 44–59.

Dodd AN, Borland AM, Haslam RP, Griffiths H, Maxwell K. 2002. Crassulacean acid metabolism: plastic, fantastic. Journal of Experimental Botany **53**, 569–580.

Dodd AN, Griffiths H, Taybi T, Cushman JC, Borland AM. 2003. Integrating diel starch metabolism with the circadian and environmental regulation of crassulacean acid metabolism in *Mesembryanthemum crystallinum*. Planta **216**, 789–797.

Eastmond PJ, Ross JD. 1997. Evidence that the induction of crassulacean acid metabolism by water stress in *Mesembryanthemum crystallinum* (L.) involves root signalling. Plant, Cell and Environment **20**, 1559–1565.

Edwards EJ, Ogburn MR. 2012. Angiosperm Responses to a Low-CO_2 World: CAM and C_4 Photosynthesis as Parallel Evolutionary Trajectories. **173**, 724–733.

FAO (The State Of Food And Agriculture). Overcoming water challenges in agriculture. Available at: https://doi.org/10.4060/cb1447en. 2020

Ferrari RC, Bittencourt PP, Nagumo PY, Oliveira WS, Rodrigues MA, Hartwell J, Freschi L. 2020*a*. Developing *Portulaca oleracea* as a model system for functional genomics analysis of C4/CAM photosynthesis. Functional Plant Biology **48**, 666–682.

Ferrari RC, Bittencourt PP, Rodrigues MA, *et al.* 2020*b*. C_4 and crassulacean acid metabolism within a single leaf: deciphering key components behind a rare photosynthetic adaptation. New Phytologist **225**, 1699–1714.

Ferrari RC, Cruz BC, Gastaldi VD, Storl T, Ferrari EC, Boxall SF, Hartwell J, Freschi L. 2020*c*. Exploring C_4–CAM plasticity within the *Portulaca oleracea* complex. Scientific Reports **10**, 1–14.

Forsthoefel NR, Cushman MAF, Cushman JC. 1995. Posttranscriptional and posttranslational control of enolase expression in the facultative crassulacean acid metabolism plant *Mesembryanthemum crystallinum* L. Plant Physiology **108**, 1185–1195.

Fowler S, Lee K, Onouchi H, Samach A, Richardson K, Morris B, Coupland G, Putterill J. 1999.

GIGANTEA: A circadian clock-controlled gene that regulates photoperiodic flowering in Arabidopsis and encodes a protein with several possible membrane-spanning domains. EMBO Journal **18**, 4679–4688.

Freschi L, Rodrigues MA, Domingues DS, Purgatto E, Sluys M Van, Magalhaes JR, Kaiser WM, Mercier H. 2010. Nitric oxide mediates the hormonal control of crassulacean acid metabolism expression in young pineapple plants. Plant Physiology **152**, 1971–1985.

Guralnick LJ, Ting IP. 1986. Seasonal response to drought and rewatering (L.) Jacq. Oecologia **70**, 85–91.

Hare PD, Cress WA, Van Staden J. 1999. Proline synthesis and degradation: a model system for elucidating stress-related signal transduction. Journal of Experimental Botany **50**, 413–434.

Hartwell J. 2005. The co-ordination of central plant metabolism by the circadian clock. Biochemical Society Transactions **33**, 945–948.

Hartwell J, Dever L V, Boxall SF. 2016. Emerging model systems for functional genomics analysis of Crassulacean acid metabolism. Current Opinion in Plant Biology **31**, 100–108.

Hartwell J, Gill A, Nimmo GA, Wilkins MB, Jenkins GI, Nimmo GN. 1999. PEP carboxylase kinase is a novel protein kinase regulated at the level of expression. The Plant Journal.333–342.

Hartwell J, Smith LH, Wilkins MB, Jenkins GI, Nimmo HG. 1996. Higher plant phospho*enol*pyruvate carboxylase kinase is regulated at the level of translatable mRNA in response to light or a circadian rhythm. The Plant Journal **10**, 1071–1078.

Hénanff G Le, Profizi C, Courteaux B, Rabenoelina F, Gérard C, Clément C, Baillieul F, Cordelier S, Dhondt-Cordelier S. 2013. Grapevine *NAC1* transcription factor as a convergent node in developmental processes, abiotic stresses, and necrotrophic/biotrophic pathogen tolerance. Journal of Experimental Botany **64**, 4877–4893.

Herrera A. 2009. Crassulacean acid metabolism and fitness under water deficit stress: if not for carbon gain, what is facultative CAM good for? Annals of Botany **103**, 645–653.

Hibberd JM, Covshoff S. 2010. The regulation of gene expression required for C_4 photosynthesis. Annual Review of Plant Biology **61**, 181–207.

Holtum JAM, Hancock LP, Edwards EJ, Winter K. 2017*a*. Optional use of CAM photosynthesis in two C_4 species, *Portulaca cyclophylla* and *Portulaca digyna*. Journal of Plant Physiology **214**, 91–96.

Holtum JAM, Hancock LP, Edwards EJ, Winter K. 2017*b*. Facultative CAM photosynthesis (crassulacean acid metabolism) in four species of *Calandrinia*, ephemeral succulents of arid Australia. , 17–25.

Hotta CT, Nishiyama MY, Souza GM. 2013. Circadian rhythms of sense and antisense transcription in sugarcane, a highly polyploid crop. PLoS ONE **8**.

Hutchison CE, Li J, Argueso C, *et al.* 2006. The Arabidopsis histidine phosphotransfer proteins are redundant positive regulators of cytokinin signaling. Plant Cell **18**, 3073–3087.

Iuchi S, Kobayashi M, Taji T, Naramoto M, Seki M, Kato T, Tabata S, Kakubari Y, Yamaguchi-Shinozaki K, Shinozaki K. 2001. Regulation of drought tolerance by gene manipulation of 9-cis-epoxycarotenoid dioxygenase, a key enzyme in abscisic acid biosynthesis in Arabidopsis. Plant Journal **27**, 325–333.

Jin J, Zhang H, Kong L, Gao G, Luo J. 2014. PlantTFDB 3.0: a portal for the functional and evolutionary study of plant transcription factors. Nucleic Acids Research **42**, 1182–1187.

Kanai R, Edwards GE. 1999. The Biochemistry of C_4 Photosynthesis. In: Sage RF, Monson RK, eds. C_4 Plant Biology. San Diego: Academic Press, 49–87.

Khan S, Rowe SC, Harmon FG. 2010. Coordination of the maize transcriptome by a conserved circadian clock. BMC Plant Biology **10**.

Kiba T, Taniguchi M, Imamura A, Ueguchi C, Mizuno T, Sugiyama T. 1999. Differential expression of genes for response regulators in response to cytokinins and nitrate in *Arabidopsis thaliana*. Plant and Cell Physiology **40**, 767–771.

Kim S, Kang JY, Cho DI, Park JH, Soo YK. 2004. ABF2, an ABRE-binding bZIP factor, is an essential component of glucose signaling and its overexpression affects multiple stress tolerance. Plant Journal **40**, 75–87.

Ko DK, Rohozinski D, Song Q, Taylor SH, Juenger TE, Harmon FG, Chen ZJ. 2016. Temporal shift of circadian-mediated gene expression and carbon fixation contributes to biomass heterosis in maize hybrids. PLoS Genetics **12**, 1–31.

Koch K, Kennedy RA. 1980. characteristics of crassulacean acid metabolism in the succulent C_4 Dicot, *Portulaca oleracea* L. Plant Physiology **65**, 193–197.

Koch KE, Kennedy RA. 1982. Crassulacean acid metabolism in the succulent C_4 dicot, *Portulaca oleracea* L. under natural environmental conditions. Plant physiology **69**, 757–761.

Kohli A, Sreenivasulu N, Lakshmanan P, Kumar PP. 2013. The phytohormone crosstalk paradigm takes center stage in understanding how plants respond to abiotic stresses. Plant Cell Reports **32**, 945–957.

Kuroha T, Tokunaga H, Kojima M, Ueda N, Ishida T, Nagawa S, Fukuda H, Sugimoto K, Sakakibara H. 2009. Functional analyses of LONELY GUY cytokinin-activating enzymes reveal the importance of the direct activation pathway in Arabidopsis. Plant Cell **21**, 3152–3169.

Kushiro T, Okamoto M, Nakabayashi K, Yamagishi K, Kitamura S, Asami T, Hirai N, Koshiba T, Kamiya Y, Nambara E. 2004. The Arabidopsis cytochrome P450 CYP707A encodes ABA 8′-hydroxylases: key enzymes in ABA catabolism. EMBO Journal **23**, 1647–1656.

Kusnetsov V, Landsberger M, Meurer J, Oelmüller R. 1999. The assembly of the CAAT-box binding complex at a photosynthesis gene promoter is regulated by light, cytokinin, and the stage of the plastids. Journal of Biological Chemistry **274**, 36009–36014.

Langfelder P, Horvath S. 2008. WGCNA: An R package for weighted correlation network analysis. BMC Bioinformatics **9**.

Lazova G, Yonova P. 2010. Photosynthetic parameters were modified in wheat (*Triticum Aestivum* L.) flag leaves by two phenylurea cytokinins. International Journal of Plant Sciences **171**, 809–817.

Leyva-González MA, Ibarra-Laclette E, Cruz-Ramírez A, Herrera-Estrella L. 2012. Functional and transcriptome analysis reveals an acclimatization strategy for abiotic stress tolerance mediated by Arabidopsis NF-YA Family Members. PLoS ONE **7**.

Li J, Brader G, Palva ET. 2004. The *WRKY70* transcription factor: a node of convergence for jasmonate-mediated and salicylate-mediated signals in plant defense. Plant Cell **16**, 319–331.

Li W, Oono Y, Zhu J, He X, Wu J, Iida K, Lu X, Cui X, Jin H, Zhu J. 2008. The Arabidopsis *NFYA5* transcription factor is regulated transcriptionally and posttranscriptionally to promote drought resistance. **20**, 2238–2251.

Livak KJ, Schmittgen TD. 2001. Analysis of relative gene expression data using real-time quantitative PCR and the $2^{-\Delta\Delta CT}$ method. Methods **25**, 402–408.

Maheshwari P, Kummari D, Palakolanu SR, Nagasai Tejaswi U, Nagaraju M, Rajasheker G, Jawahar G, Jalaja N, Rathnagiri P, Kavi Kishor PB. 2019. Genome-wide identification and expression profile analysis of nuclear factor Y family genes in *Sorghum bicolor* L. (Moench). PLoS ONE **14**, 1–27.

Maleckova E, Brilhaus D, Wrobel TJ, Weber APM. 2019. Transcript and metabolite changes during the early phase of abscisic acid-mediated induction of crassulacean acid metabolism in *Talinum triangulare*. Journal of Experimental Botany **70**, 6581–6596.

Matsui A, Ishida J, Morosawa T, *et al.* 2008. Arabidopsis transcriptome analysis under drought, cold, high-salinity and ABA treatment conditions using a tiling array. Plant and Cell Physiology **49**, 1135–1149.

Matsushika A, Makino S, Kojima M, Mizuno T. 2000. Circadian waves of expression of the *APRR1/TOC1* family of pseudo-response regulators in Arabidopsis thaliana: insight into the plant circadian clock. Plant and Cell Physiology **41**, 1002–1012.

McClung CR. 2001. Circadian rhythms in plants. Annual Review of Plant Physiology and Plant Molecular Biology **52**, 139–162.

Mia MS, Liu H, Wang X, Yan G. 2019. Multiple near-isogenic lines targeting a QTL hotspot of drought tolerance showed contrasting performance under post-anthesis water stress. Frontiers in Plant Science **10**, 1–11.

Mitsuda N, Ohme-Takagi M. 2009. Functional analysis of transcription factors in Arabidopsis. Plant and Cell Physiology **50**, 1232–1248.

Nakashima K, Tran LSP, Van Nguyen D, Fujita M, Maruyama K, Todaka D, Ito Y, Hayashi N, Shinozaki K, Yamaguchi-Shinozaki K. 2007. Functional analysis of a *NAC*-type transcription factor *OsNAC6* involved in abiotic and biotic stress-responsive gene expression in rice. Plant Journal **51**, 617–630.

Nesi N, Debeaujon I, Jond C, Pelletier G, Caboche M, Lepiniec L. 2000. The *TT8* gene encodes a basic helix-loop-helix domain protein required for expression of *DFR* and *BAN* genes in Arabidopsis siliques. Plant Cell **12**, 1863–1878.

Nguyen KH, Ha C Van, Nishiyama R, *et al.* 2016. Arabidopsis type B cytokinin response regulators *ARR1*, *ARR10*, and *ARR12* negatively regulate plant responses to drought. Proceedings of the National Academy of Sciences of the United States of America **113**, 3090–3095.

Offermann S, Danker T, Dreymüller D, Kalamajka R, Töpsch S, Weyand K, Peterhänsel C. 2006. Illumination is necessary and sufficient to induce histone acetylation independent of transcriptional activity at the C_4-specific phospho*enol*pyruvate carboxylase promoter in maize. Plant Physiology **141**, 1078–1088.

Okamoto M, Kushiro T, Jikumaru Y, Abrams SR, Kamiya Y, Seki M, Nambara E. 2011. ABA

9′-hydroxylation is catalyzed by CYP707A in Arabidopsis. Phytochemistry **72**, 717–722.

Oneto CD, Otegui ME, Baroli I, Beznec A, Faccio P, Bossio E, Blumwald E, Lewi D. 2016. Water deficit stress tolerance in maize conferred by expression of an *isopentenyltransferase (IPT)* gene driven by a stress- and maturation-induced promoter. Journal of Biotechnology **220**, 66–77.

Ookawa T, Naruoka Y, Sayama A, Hirasawa T. 2004. Cytokinin effects on Ribulose-1,5-bisphosphate carboxylase/oxygenase and nitrogen partitioning in rice during ripening. Crop Science **44**, 2107–2115.

Pérez-Rodríguez P, Riaño-Pachón DM, Corrêa LGG, Rensing SA, Kersten B, Mueller-Roeber B. 2010. PlnTFDB: Updated content and new features of the plant transcription factor database. Nucleic Acids Research **38**, 822–827.

Peters W, Beck E, Piepenbrock M, Lenz B, Schmitt JM. 1997. Cytokinin as a negative effector of phosphoenolpyruvate carboxylase induction in *Mesembryanthemum crystallinum*. Journal of Plant Physiology **151**, 362–367.

Pokhilko A, Fernández AP, Edwards KD, Southern MM, Halliday KJ, Millar AJ. 2012. The clock gene circuit in Arabidopsis includes a repressilator with additional feedback loops. Molecular Systems Biology **8**, 1–13.

Pokhilko A, Hodge SK, Stratford K, Knox K, Edwards KD, Thomson AW, Mizuno T, Millar AJ. 2010. Data assimilation constrains new connections and components in a complex, eukaryotic circadian clock model. Molecular Systems Biology **6**, 1–10.

Popp M, Janett HP, Lüttge U, Medina E. 2003. Metabolite gradients and carbohydrate translocation in rosette leaves of CAM and C_3 bromeliads. New Phytologist **157**, 649–656.

Pospíšilová J, Vágner M, Malbeck J, Trávníčková A, Baťková P. 2005. Interactions between abscisic acid and cytokinins during water stress and subsequent rehydration. Biologia Plantarum **49**, 533–540.

Qin X, Zeevaart JAD. 1999. The 9-cis-epoxycarotenoid cleavage reaction is the key regulatory step of abscisic acid biosynthesis in water-stressed bean. Proceedings of the National Academy of Sciences of the United States of America **96**, 15354–15361.

R Core Team. R: A language and environment for statistical computing. R Foundation for Statistical Computing, Vienna, Austria. Available at: https://www.R-project.org/. (2021)

Rai A, Umashankar S, Rai M, Kiat LB, Bing JAS, Swarup S. 2016. Coordinate regulation of metabolite glycosylation and stress hormone biosynthesis by *TT8* in Arabidopsis. Plant Physiology **171**, 2499–2515.

Rawat R, Schwartz J, Jones MA, Sairanen I, Cheng Y, Andersson CR, Zhao Y, Ljung K, Harmer SL. 2009. The circadian clock and auxin pathways. Forest Genetics **106**, 1–6.

Sage RF. 2002. Are crassulacean acid metabolism and C4 photosynthesis incompatible? Functional Plant Biology **29**, 775–785.

Sage RF. 2004. The evolution of C_4 photosynthesis. New Phytologist **161**, 341–370.

Saito S, Hirai N, Matsumoto C, Ohigashi H, Ohta D, Sakata K, Mizutani M. 2004. Arabidopsis CYP707As encode (+)-abscisic acid 8′-hydroxylase, a key enzyme in the oxidative catabolism of abscisic acid. Plant Physiology **134**, 1439–1449.

Sawa M, Nusinow DA, Kay SA, Imaizumi T. 2007. *FKF1* and *GIGANTEA* complex formation is required for day-length measurement in Arabidopsis. Science **318**, 261–265.

Schmitt JM, Piepenbrock M. 1992. Regulation of phosphoenolpyruvate carboxylase and crassulacean acid metabolism induction in *Mesembryanthemum crystallinum* L. by cytokinin. New Phytologist **99**, 1664–1669.

Schweighofer A, Hirt H, Meskiene I. 2004. Plant PP2C phosphatases: Emerging functions in stress signaling. Trends in Plant Science **9**, 236–243.

Seo PJ, Park CM. 2010. A membrane-bound *NAC* transcription factor as an integrator of biotic and abiotic stress signals. Plant Signaling and Behavior **5**, 481–483.

Söderman E, Mattson J, Engström P. 1996. The Arabidopsis homeobox gene *ATHB-7* is induced by water deficit and by abscisic acid. The Plant Journal **10**, 375–381.

Sugiharto B, Burnell JN, Sugiyama T. 1992. Cytokinin is required to induce the nitrogen-dependent accumulation of mRNAs for phospho*enol*pyruvate carboxylase and carbonic anhydrase in detached maize leaves. Plant Physiology **100**, 153–156.

Suzuki I, Cretin C, Omata T, Sugiyama T. 1994. Transcriptional and posttranscriptional regulation of nitrogen-responding expression of phospho*enol*pyruvate carboxylase gene in maize. Plant Physiology **105**, 1223–1229.

Tan BC, Joseph LM, Deng WT, Liu L, Li QB, Cline K, McCarty DR. 2003. Molecular characterization of the Arabidopsis 9-cis epoxycarotenoid dioxygenase gene family. Plant Journal **35**, 44–56.

Taybi T, Cushman JC, Borland AM. 2002. Environmental, hormonal and circadian regulation of crassulacean acid metabolism expression. Functional Plant Biology.669–678.

Taybi T, Sotta B, Gehrig H, Güçlü S, Kluge M, Brulfert J. 1995. differential effects of abscisic acid on phosphoenolpyruvate carboxylase and CAM operation in *Kalanchoe blossfeldiana*. Botanica Acta **108**, 240–246.

Thomas JC, Bohnert HJ. 1993. Salt stress perception and plant growth regulators in the halophyte mesembryanthemum crystallinum. Plant Physiology **103**, 1299–1304.

Thomas JC, McElwain EF, Bohnert HJ. 1992. Convergent induction of osmotic stress-responses: abscisic acid, cytokinin, and the effects of NaCl. Plant Physiology **100**, 416–423.

To JPC, Haberer G, Ferreira FJ, Deruère J, Mason MG, Schaller GE, Alonso JM, Ecker JR, Kieber JJ. 2004. Type-A Arabidopsis response regulators are partially redundant negative regulators of cytokinin signaling. Plant Cell **16**, 658–671.

Tripathi P, Rabara RC, Rushton PJ. 2014. A systems biology perspective on the role of *WRKY* transcription factors in drought responses in plants. Planta **239**, 255–266.

Tsiantis MS, Bartholomew DM, Smith JAC. 1996. Salt regulation of transcript levels for the C subunit of a leaf vacuolar H+-ATPase in the halophyte *Mesembryanthemum crystallinum*. Plant Journal **9**, 729–736.

Ueno O. 2001. Update on C_4 Photosynthesis Environmental Regulation of C_3 and C_4 differentiation in the amphibious sedge *Eleocharis vivipara*. Plant Physiology **127**, 1524–1532.

Umezawa T, Okamoto M, Kushiro T, Nambara E, Oono Y, Seki M, Kobayashi M, Koshiba T,

Kamiya Y, Shinozaki K. 2006. CYP707A3, a major ABA 8′-hydroxylase involved in dehydration and rehydration response in *Arabidopsis thaliana*. Plant Journal **46**, 171–182.

Valdés AE, Övernäs E, Johansson H, Rada-Iglesias A, Engström P. 2012. The homeodomain-leucine zipper (HD-Zip) class I transcription factors *ATHB7* and *ATHB12* modulate abscisic acid signalling by regulating protein phosphatase 2C and abscisic acid receptor gene activities. Plant Molecular Biology **80**, 405–418.

Vernon DM, Ostrem JA, Schmitt JM, Bohnert HJ. 1988. PEPCase transcript levels in *Mesembryanthemum crystallinum* decline rapidly upon relief from salt stress . Plant Physiology **86**, 1002–1004.

Wang Y, Lu W, Deng D. 2016. Bioinformatic landscapes for plant transcription factor system research. Planta **243**, 297–304.

Wang X, Wu L, Zhang S, Wu L, Ku L, Wei X, Xie L, Chen Y. 2011. Robust expression and association of *ZmCCA1* with circadian rhythms in maize. Plant Cell Reports **30**, 1261–1272.

Winter K, Holtum JAM. 2014. Facultative crassulacean acid metabolism (CAM) plants: powerful tools for unravelling the functional elements of CAM photosynthesis. Journal of Experimental Botany **65**, 3425–3441.

Winter K, Sage RF, Edwards EJ, Virgo A, Holtum JAM. 2019. Facultative crassulacean acid metabolism in a C_3–C_4 intermediate. Journal of Experimental Botany **70**, 6571–6579.

Winter K, Smith JAC. 1996. An introduction to crassulacean acid metabolism. Biochemical Principles and Ecological Diversity. In: Winter K, Smith JAC, eds. Crassulacean Acid Metabolism Biochemistry, Ecophysiology and Evolution. Springer-Verlag, 1–10.

Wyka TP, Lüttge UE. 2003. Contribution of C_3 carboxylation to the circadian rhythm of carbon dioxide uptake in a crassulacean acid metabolism plant *Kalanchoë daigremontiana*. Journal of Experimental Botany **54**, 1471–1479.

Xiong L, Zhu JK. 2003. Regulation of abscisic acid biosynthesis. Plant Physiology **133**, 29–36.

Yang X, Cushman JC, Borland AM, *et al.* 2015. A roadmap for research on crassulacean acid metabolism (CAM) to enhance sustainable food and bioenergy production in a hotter, drier world. New Phytologist **207**, 491–504.

Zeevaart JAD. 1980. Changes in the levels of abscisic acid and its metabolites in excised leaf blades of *Xanthium strumarium* during and after Water Stress. Plant Physiology **66**, 672–678.

Zhang J, Jia W, Yang J, Ismail AM. 2006. Role of ABA in integrating plant responses to drought and salt stresses. Field Crops Research **97**, 111–119.

Supplementary material

(Supplementary tables are available at https://drive.google.com/drive/folders/1lyMZKS_CFHM4jTqeVe3tvb63oK7eaBKK?usp=sharing)

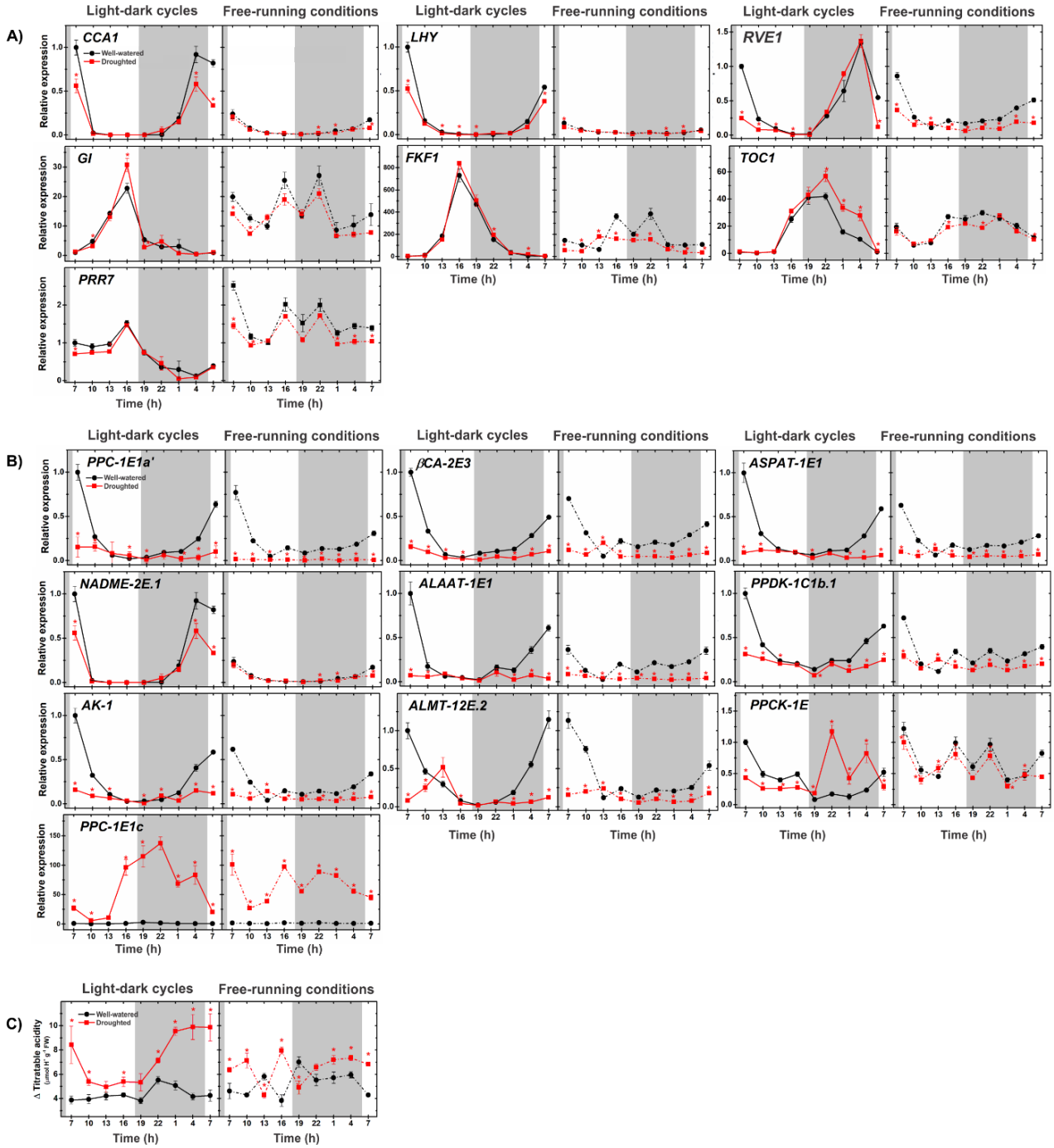

Fig. S1 Metabolic changes according to light treatments in *Portulaca oleracea*. 30-day old plants were either kept well-watered or droughted for 21 days and sampled every three hours for 24h. Both water availability groups were sampled under 12 h light / 12 h dark (LD) and circadian free-running conditions (LL) regimes. (A) Transcript abundance of clock genes. (B) Transcript abundance of CCM-related genes. (C) Titrable acidity over the 24-h cycle. The shaded areas indicate the dark and

subjective dark periods. Data are means (± SE) of at least three replicates. *$P < 0.05$ compared to well-watered samples. AK, adenylate kinase; ALAAT, ALA aminotransferase; ALMT, aluminum-activated malate transporters; ASPAT, ASP aminotransferase; □CA, beta-carbonic anhydrase; CCA1; circadian clock associated 1; FKF1, flavin-binding kelch repeat F box 1; GI, gigantea; LHY, late elongated hypocotyl 1; NADME, NAD-malic enzyme; PPC, phosphoe*nol*pyruvate carboxylase; PPCK, phosphoe*nol*pyruvate carboxylase kinase; PPDK, pyruvate orthophosphate dikinase; PRR, pseudo-response regulator; RVE1, reveille 1; TOC1, timing of CAB expression.

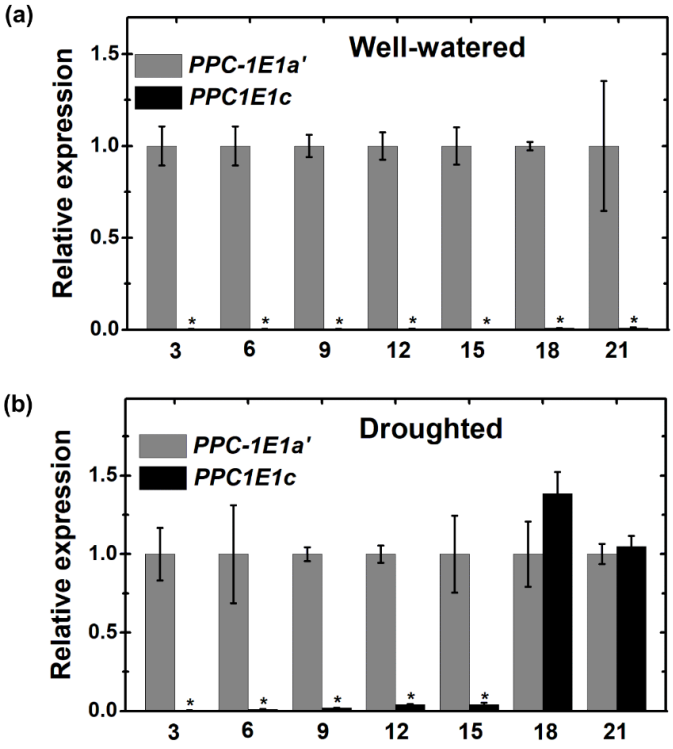

Fig. S2 Relative transcript ratios of C_4- and CAM-related *P. oleracea PPC* genes under drought. Transcript abundance of the *PHOSPHOENOLPYRUVATE CARBOXYLASE* (*PPC*) genes involved in C_4 (*PPC-1E1a'*) and CAM (*PPC-1E1c*). Data are means (± SE) of at least three replicates and are expressed as relative transcript amount compared to *PPC-1E1a'*. **P* < 0.05 between genes at each time point. PPC, phospho*enol*pyruvate carboxylase.

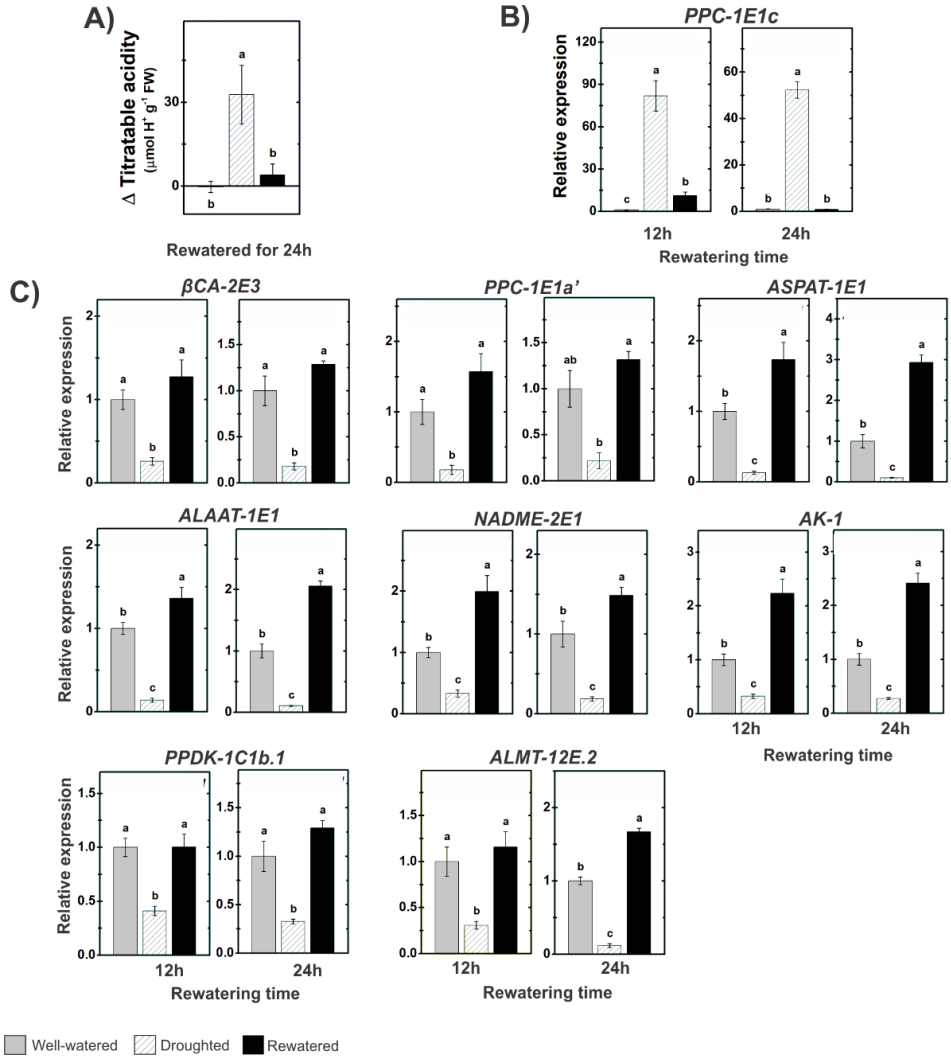

Fig. S3 Nocturnal acidification and CCM-related transcriptional changes upon 12h and 24h of rewatering. One-month-old plants were droughted for 21 days, or kept well-watered, and a third group was sampled on the 22nd day, after 12h and 24h or rewatering. (A) Nocturnal titratable acid accumulation (ΔH^+). (b) Transcript abundance of the CAM-marker gene *PPC-1E1c*. (c) Transcript abundance of the C_4-marker genes. In A, ΔH^+ indicates dawn-dusk differences and SE of the dawn–dusk difference = $\sqrt{((SE_{dawn})^2 + (SE_{dusk})^2)}$. Dawn and dusk samples were harvested one hour after the start of the light and one hour before the end of the light period, respectively. In B and C, mean relative expression was normalized against the well-watered control on day 22 sampled at dawn, except for *PPC-1E1c,* which was sampled at dusk. Different letters indicate statistically significant differences in comparison with the well-watered control (*P-value* < 0.05). Data are means (± SE) of at least three replicates. AK, adenylate kinase; ALAAT, ALA aminotransferase; ALMT, aluminum-activated malate transporters; ASPAT, ASP aminotransferase; □CA, beta-carbonic anhydrase; NAD(P)ME, NAD(P)-malic enzyme; NADMDH, NAD-malate; dehydrogenase; PPC, PEP carboxylase; PPDK, PYR orthophosphate dikinase.

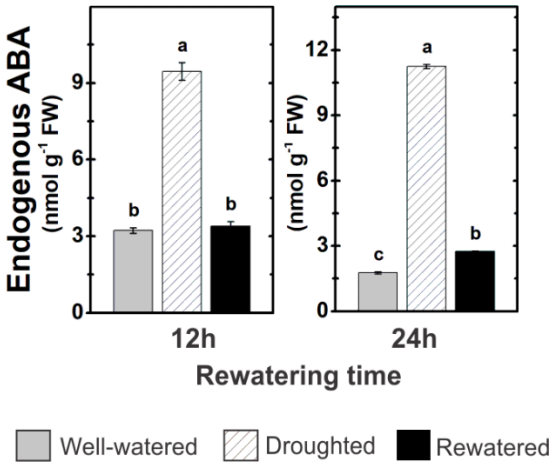

Fig. S4 Impacts of the watering regime on the leaf endogenous abscisic acid (ABA) levels. One-month-old plants were droughted for 21 days, or kept well-watered, and a third group was sampled on the 22nd day, after 12h and 24h of rewatering. Data are means (± SE) of at least three replicates. Different letters indicate statistically significant differences (*P-value* < *0.05*) compared with the well-watered control.

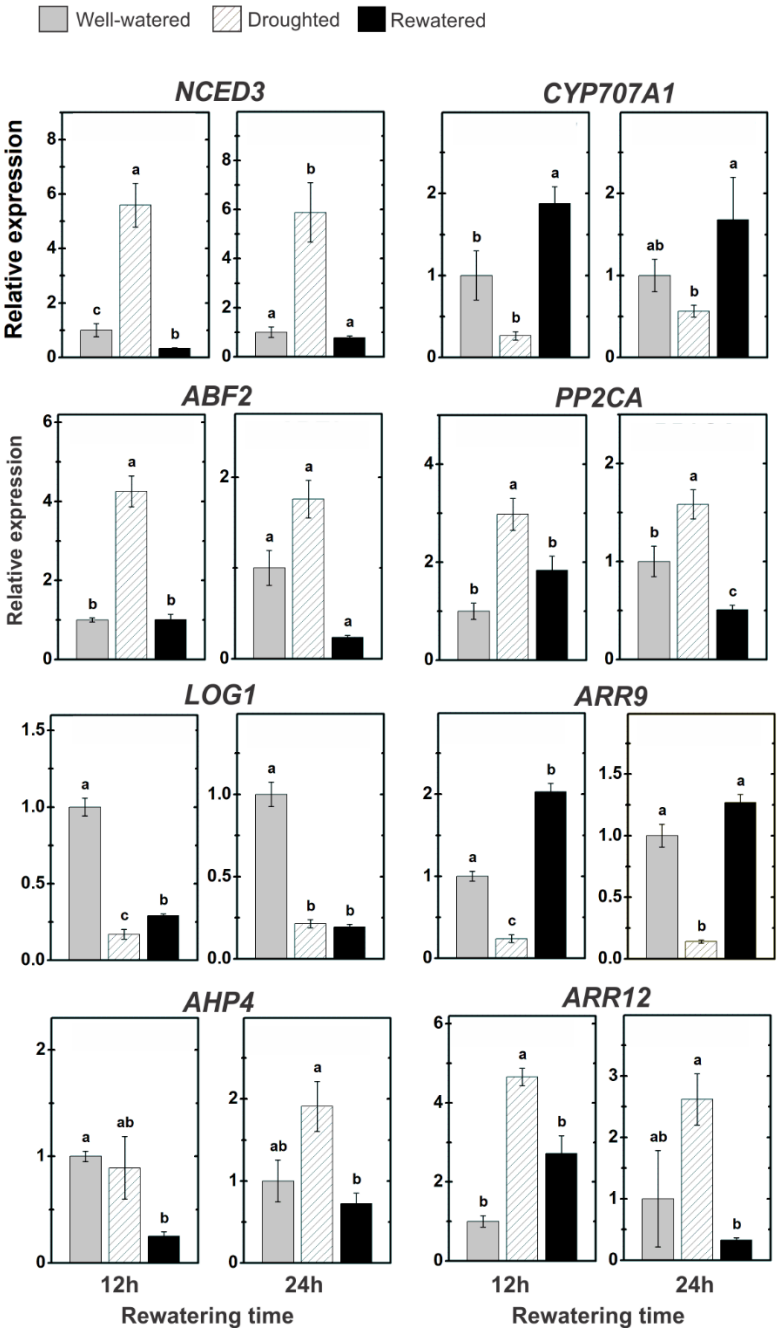

Fig. S5 Impacts of the watering regime on the transcript abundance of hormone-metabolism genes. One-month-old *Portulaca oleracea* plants were droughted for 21 days, or kept well-watered, and a third group was sampled on the 22nd day, after 12h and 24h or rewatering. Data are means (± SE) of at least three replicates measured via RT-qPCR. Different letters indicate statistically significant differences (*P-value* < 0.05) in comparison with the well-watered control. Mean relative expression was normalized against the well-watered control on day 22 at 07:00, except for *PP2CA, ABF2* and *NCED3*, which were analyzed at 20:00. ABF, ABA-responsive element-binding factors; AHPT, phosphotransmitter; CYP707A, cytochrome P450 type enzymes; LOG, lonelyguy; ARR, response regulator; NCED, 9-cis-epoxycarotenoid dioxygenase; PP2CA, clade A PP2C phosphatases.

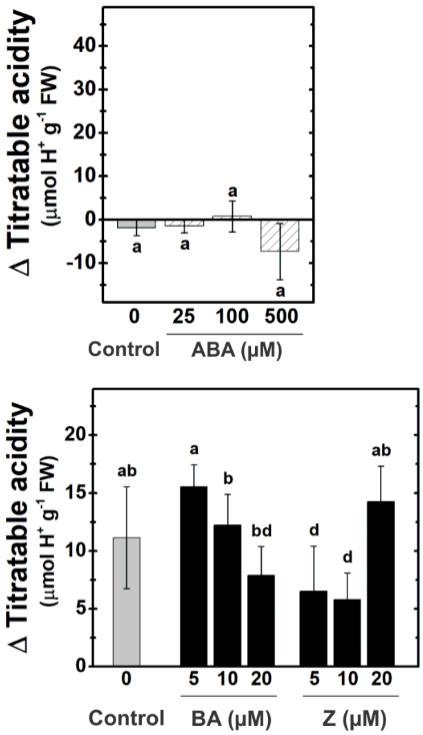

Fig. S6 Leaf nocturnal acid accumulation (ΔH^+) in response to hormonal treatment. Leaves of 30-day-old plants were sampled at dawn (07:00, one hour after the lights were on) and at dusk (17:00, one hour before the lights were off). (A) Well-watered plants sprayed with different abscisic acid (ABA) concentrations every day for four days. (B) Plants droughted for 21 days and sprayed with 6-Benzylaminopurine (BA) or *trans*-zeatin (Z) every five days, totalizing four applications. Data are means (± SE) of at least three replicates. Different letters indicate statistically significant differences (*P-value* < 0.05) in comparison with the water-sprayed control.

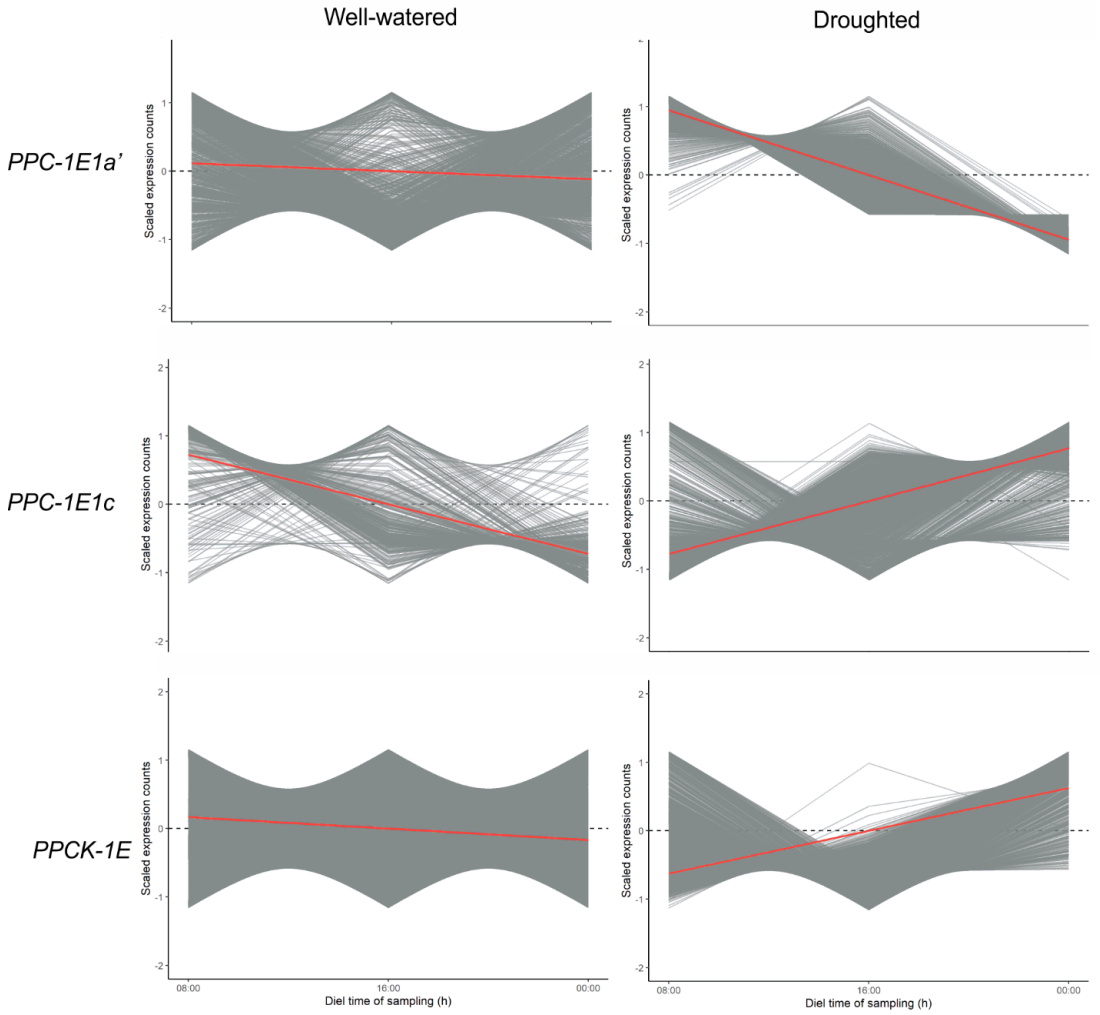

Fig. S7 Selected clusters generated via co-expression analysis for well-watered and droughted plants. Gray lines represent scaled and averaged transcripts per million (TPM) counts for leaves well-watered or droughted for 34 days. Red lines were generated using the *geom_smooth* function from the *ggplot2* library for R, highlighting the overall patterns. See Methods for additional information and source of the transcriptome data used for the analysis. PPC, phospho*enol*pyruvate carboxylase; PPCK, ppc kinase.

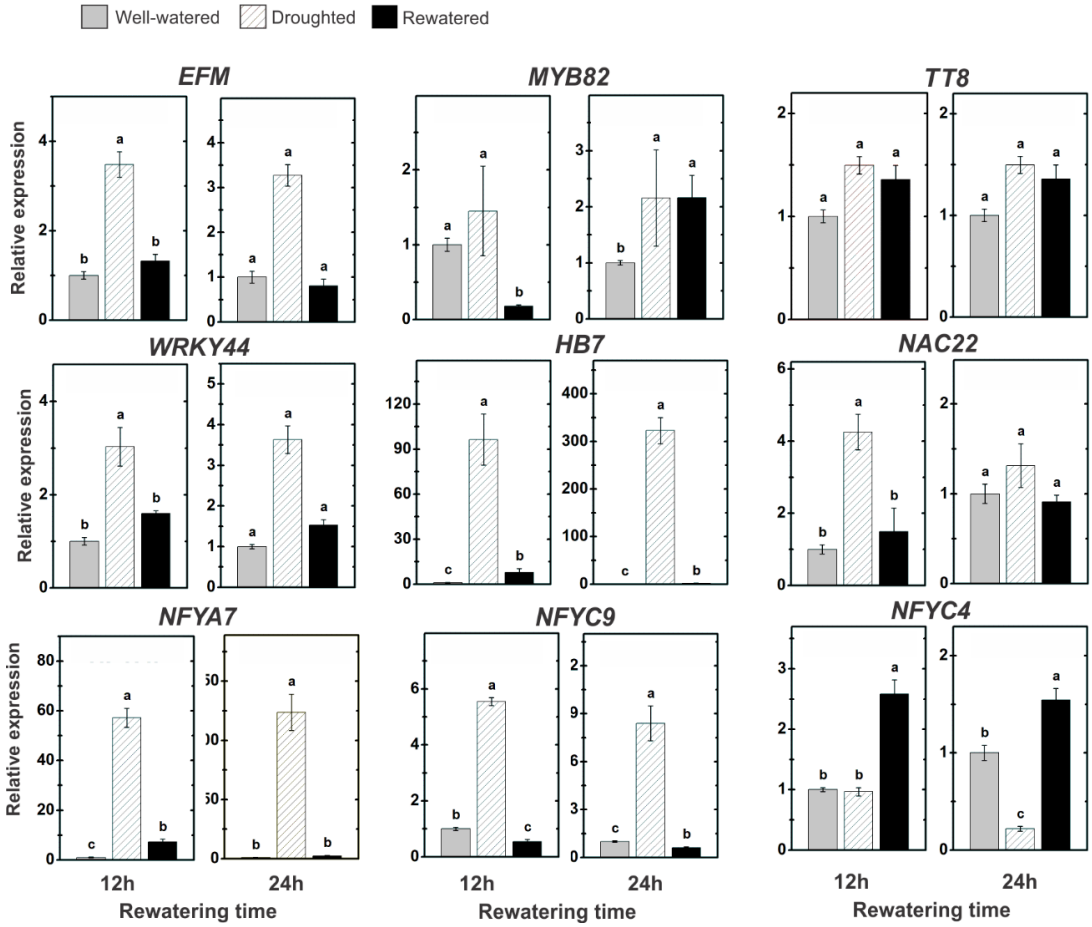

Fig. S8 Transcriptional changes in transcription factors upon different water regimes. Leaves of 30-day old *Portulaca oleracea* plants were either well-watered, droughted for 21 days or rewatered and sampled on day 22 at dwan (07:00, one hour after the lights were on) and at dusk (17:00, one hour before the lights were off). Transcript abudance of genes involved in the carbon-concentrating mechanism (CCM) metabolism and signaling candidates. Data are means (± SE) of at least three replicates. Different letters indicate statistically significant differences ($P < 0.05$) compared with well-watered samples. Mean relative expression was normalized against the well-watered control on day 22 at 07:00, except for *EFM, WRKY44, HB7, MYB82*, and *TT8,* which were analyzed at 17:00. EFM, flowering MYB protein; HB7, homeobox; MYB, MYB domain protein; NAC, NAC domain-containing protein; NFYC and NFYA, nuclear factor Y, subunits C and A; TT, transparent testa; WRKY, WRKY transcription factor family protein.

Final considerations and future perspectives

"Knowledge is like a garden: if it is not cultivated, it cannot be harvested."

African proverb

The overall goal of this Thesis was contributing to elucidating the molecular mechanisms that allow *Portulaca oleracea*, a C_4 weed, to perform the unusual CAM transition when drought-stressed. Our primary motivation was that this species represents a natural blueprint for dissecting how both C_4 and CAM can occur inside a single organism, and such knowlodge may be crucial when seeking to improve stress-resistance in crops, especially in the context of climate change. To pursue this goal, physiological, biochemical, molecular and bioinformatic tools were employed here and yielded a series of significant results.

To provide a global characterization of the gene expression reprogramming required for the C_4-to-CAM transition in *P. oleracea*, we first performed RNA-Seq analysis in well-watered and droughted leaves and stems. We identified shared and exclusive genes in the machinery of each CCM, partially refuting our first hypothesis, since not all genetic components of C_4 were exclusively co-opted for this pathway. Steps as acid decarboxylation and PPCK regulation seem to be shared between the C_4 and CAM cycles. We also generated detailed expression profiles via qPCR for genes involved in each CCM and associated processes (i.e., photorespiration and carbohydrate metabolism), and this revealed the changes in the diel expression of these components in distinct organs (leaves and stems) and conditions (well-watered and drought). In addition, we identified that, although CAM is completely facultative and reversible in leaves, it is also under developmental control in stems. Also, fine adjustments in starch metabolism were shown to be necessary for CAM functioning.

In the second part, we characterized multiple accessions of *P. oleracea* with different geographical origins using morphometric variables, C_4 and CAM marker genes, physiological attributes of CAM (such as acidity and gas exchange), and also monitored chlorophyll *a* fluorescence during water stress treatment. This allowed us to conclude that all accessions performed CAM, and the degree of CAM expression was not directly correlated to the climatic variations of their place of origin and morphometric differences, partially contradicting our second hypothesis. A similar response to drought and rewatering was observed for all CCM genes analyzed, but a continnum of CAM intensity was observed across the genotypes. Therefore, this study identified both morphologically similar genotypes with contrasting degrees of CAM expression and also morphologically distinct accessions performing similar CAM levels, which may be a valuable research material for further studies about the C_4-CAM transition.

In the third part, we compiled a molecular toolkit for *P. oleracea*, including standardization of RNA extraction protocols, selection of reference genes for qPCR under varied conditions, and *in vitro* regeneration and transformation protocols. We believe these

data may facilitate the future development of *P. oleracea* as a model species to the study of the C_4-CAM transition.

Finally, in the last chapter we started elucidating the hormonal and molecular signaling networks controlling the drought-induced transition from C_4 to CAM and its reversion during rewatering. These were the first insights in the literature focused on the signaling mechanisms taking place in this unique system. Abscisic acid was identified as a major signal during CAM induction, whereas exogenous cytokinins were able to recover C_4-related transcripts in droughted plants, possibly playing an antagonistic role on the expression of the CAM machinery. In addition, free-running time-course experiments demonstrated that the circadian expression of specific CCM components (e.g., PPCK) are particularly dependent on the proper functioning of the molecular clock, presumably playing a central role in avoiding futile cycling between the two cycles. In addition, a list of TFs was compiled, and that will be important for functional genomics studies on the species.

When combined, the results from this Thesis lay a strong foundation for future studies on C_4-CAM photosynthesis, since they pinpoint gene modules and signaling events as targets for modulation in bioengineering and synthetic biology approaches. Although combining C_4 and CAM may be yet new and little explored, CCM engineering to produce improved crops has already been the focus of the C_4 Rice and the CAM Biodesign projects. The large-scale 'omics data generation for as many species that express CCMs as possible has been shown to be of utmost importance for both projects, representing one of the early stages of identifying the target genes for manipulation.

This topic is far from being exhausted and the photosynthetic transition in *Portulaca* species, in particular, could still count on analysis of other signaling molecules, such as other classes of plant hormones, nitric oxide (NO) and cytosolic Ca^{2+}, and many other regulatory levels besides the transcriptional regulation of core CCM genes. The findings presented here pave the way for functional genomics studies, which may provide critical information to deepen our current understanding of the C_4/CAM compatibility and its biotechnological potential. One example would be the generation of loss-of-function or overexpression lines for candidate genes identified in chapters 1 and 4 using the standardized molecular biology and transformation protocols for *P. oleracea* described in chapter 3.

Moreover, research seeking to understand the localization of C_4 and CAM inside a single leaf can also benefit from the results produced here. For instance, the production of *P. oleracea* transgenic plants expressing reporter genes fused to the regulatory or coding regions of either C_4- or CAM-marker genes might bring conclusive information on the tissue localization of each CCM, which remains a controversial and poorly understood issue in C_4/CAM hybrid system. In addition, probes can be generated targeting the key C_4-CAM genes described here, which would be helpful to fully explore the spatial configuration of C_4

and CAM cycles within the leaf via *in-situ* hybridization and similar techniques. Yet, another approach that benefits from having the core C_4-CAM genes identified involves microdissection and enzymatic protoplast isolation. These methods combined with monitoring the transcript abundance of the mentioned genes via RT-qPCR could provide key information on the localization of each CCM.

Overall, these approaches are exciting prospects for plant physiologists looking for sustainable and green solutions for tomorrow's problems. In this context, making *P. oleracea* a model C_4-CAM species is an up-to-date and ambitious proposal with yet plenty of room for data generation. It will involve the direct application of cutting-edge technologies and may contribute to generating new tools and methodologies in order to accomplish the goal of expressing multiple or hybrid CCM traits into crops of economic importance.